ESTABLISHING SCALE INHIBITOR RETENTION MECHANISMS IN PURE ADSORPTION AND COUPLED ADSORPTION/PRECIPITATION TREATMENTS

The Thesis by

JAMAL MOHAMAD BIN MOHAMAD IBRAHIM

Submitted for the Degree of

Doctor of Philosophy in Petroleum Engineering

Institute of Petroleum Engineering
Heriot-Watt University
Edinburgh, Scotland, UK

November 2011

ABSTRACT

One of the most common and efficient ways for preventing formation of inorganic solids deposition such as carbonate and sulphate scales in reservoir and near wellbore formation is by applying scale inhibitor (SI) squeeze treatments. The two main mechanisms that govern the scale inhibitor retention and release process in the formation are by **adsorption/desorption** and **precipitation/dissolution**. They are described by different but related modelling approaches, and there is not complete agreement in the literature about when to use one mechanistic description or another. The equilibrium adsorption isotherm determines the general nature and extent of the scale inhibitor return process in the low concentration flow regime. However, the additional SI "loading" within the near wellbore formation may be greatly enhanced by precipitation. The dynamic effects of adsorption and precipitation, also have a strong bearing on a field squeeze treatment and may significantly affect the profile of the inhibitor return curve.

Field observations are not accurate enough to distinguish between different mechanisms and a detailed analysis of a given retention mechanism (e.g. pure adsorption or coupled adsorption/ precipitation) requires carefully designed laboratory experiments at the appropriate "field relevant" conditions. In this study, we present novel experimental techniques systematically from static to dynamic tests, as follows;

1. Static Adsorption/Compatibility Experiments – these experiments were conducted on two phosphonate scale inhibitors; namely DETPMP (a penta-phosphonate) and OMTHP (an hexa-phosphonate) using sand, kaolinite and siderite as the mineral phase. Adsorption experiments were carried out at a range of adsorbent mass/ fluid volume ratios (m/V), since this indicates whether we are in the purely adsorbing or in the coupled adsorption/precipitation regime.
2. Dynamic Sand Pack Experiments – based on the static tests, OMTHP scale inhibitor and sand mineral were selected for dynamic tests as it has the most clearly interpretable results. The experiments were conducted using a sand pack flow apparatus at different flow rates using identical procedures, which demonstrates the non-equilibrium effects which occur in both adsorption and precipitation treatments.

The experimental results from static tests show excellent agreement with the theory in different regions of pure adsorption and coupled adsorption/precipitation. Whereas for dynamic sand pack experiments, the effect on post flush effluent inhibitor concentration is in the same direction for each system under test, i.e. reduced flow rate leads to higher effluent concentrations and vice-versa. These results also show clearly how such laboratory measurements should be carried out to determine both the levels of SI retention and the precise retention mechanism. The generated data from this work will be used as a basis to further develop existing coupled adsorption-precipitation (Γ/Π) models within the Flow Assurance Scale Team (FAST) in Institute of Petroleum Engineering, Heriot-Watt University to improve the future prediction of scale inhibitor squeeze treatments.

ACKNOWLEDGEMENTS

I would like to express my sincere gratitude to my supervisor, Professor Ken Sorbie, for his invaluable guidance, motivation and support throughout the course of my PhD. It would have been difficult for me to have reached this point in my academic journey, without the guidance and technical criticism from him, which is highly appreciated.

My endless gratitude goes to my parents for their prayers and patients through the course of my study. Their sacrifice for providing me with all necessities and education during the early years is immesurable. All assistance and concern from my brother, sisters, relatives, friends, and well wishers is highly appreciated.

I am also grateful to Petroliam Nasional Berhad (PETRONAS) for their sponsorship for funding my PhD at Heriot-Watt University, Edinburgh, UK. My sincere gratitude goes to FAST sponsors (Baker Petrolite, BP, BG Group, BWA Water Additives, Champion Technologies, Chevron, Clariant Oil Services, Conoco-Phillips, Halliburton, MI Swaco, Nalco, PETROBRAS, PETRONAS, PTT, REP, Rhodia, Saudi Aramco, Shell, Statoil Hydro, Talisman Energy, ThermPhos and Total) for their feedback during the steering meeting.

Needless to say to all the members of the Flow Assurance and Scale Team (FAST) for making my stay at Heriot-Watt a memorable one. Prof. Eric Mackay deserves praise for his guidance and provision of motivation, both academic and non-academic issues. I am grateful to Lorraine Boak for her guidance in the laboratory especially with the ICP and the knowledge she shared throughout the years at HWU. I would like to acknowledge Dr. Oscar Vasquez for the modelling work; Dr. Jim Buckman in providing ESEM-EDAX data and images analysis; and Robin Shield for helping in sand pack apparatus and Malvern particle size analyzer. I must mention William Thomas, Ivan Davies, Tom Clark and Thomas McGravie for their assistance in the laboratory. Thanks to Mike Singleton for leading Petronas scale project. Finally, thanks to Heather O'Hara for the administrative help.

Special thanks to Dr. Nicholas Odling of School of Geosciences in Edinburgh University for the XRD analysis.

I am also grateful to Dr. Ping Chen of Champion Technologies, Aberdeen and Prof. Mehran Sohrabi of Institute of Petroleum Engineering, Heriot-Watt University for

agreeing to examine this thesis. Their time invested in reading and evaluation of this thesis was invaluable.

Finally, I am sincerely grateful to my beloved wife Shamila, and my kids, Sabrina, Hazim and Haziq. Their prayers, patience and support throughout the roller-coaster of this PhD is highly appreciated. She made unique contributions at every step during my research period and that really made things a lot much easier.

TABLE OF CONTENTS

LIST OF FIGURES

LIST OF TABLES

NOMENCLATURE

MIC	Minimum Inhibitor Concentration
SI	Scale Inhibitor
SR	Saturation Ratio
K_{sp}	Solubility Product
m/V	Mass Volume Ratio
α, β	Freundlich Constants
Φ	Fraction of the Precipitation
ppm	Parts per million
pH	Negative logarithm of the solution hydrogen ion activity
HEDP	Hexamethylenediamine tetramethylene phosphonic acid
DETPMP	Diethylenetriamine penta (methylene phosphonic acid)
OMTHP	Octa-methylene-tetramine hexa (methylene-phosphonic acid)
Ca^{2+}_DETPMP	Calcium Inhibitor Complex Precipitation
Γ(C)	Rock adsorption isotherm, where C = concentration of inhibitor
Γ_{app}	Apparent adsorption
$[Ca^{2+}]$	Calcium cation concentration
$[Mg^{2+}]$	Magnesium cation concentration
$[Li^{+}]$	Lithium cation concentration
C_o	Initial inhibitor concentration (mg/L)
C_{1f}	Final inhibitor concentration (mg/L)
MW	Molecular weight

SW	Sea water
NSSW	North Sea Sea Water
FW	Formation Water
NFFW	Nelson Forties Formation Water
ICP	Inductively Coupled Plasma
ESEM	Scanning Electron Microscope
EDAX	Energy-dispersive X-ray Spectroscopy
XRD	X-Ray Diffraction
FAST	Flow Assurance and Scale Team
Cm	Mobile-phase inhibitor concentration
ϕ	Porosity
ρ	Density
PV	Pore volume
SW	Sea water

LIST OF PUBLICATIONS

Ibrahim, J., Sorbie, K.S. and Boak, L.S.: "*Coupled Adsorption/Precipitation Experiments: 1.Static Results*", SPE 155109, puplished at the SPE International Conference on Oilfield Scale held in Aberdeen, United Kingdom, 30-31 May 2012.

Ibrahim, J., Sorbie, K.S. and Boak, L.S.: "*Coupled Adsorption/Precipitation Experiments: 1.Non-Equilibrium Sand Pack Treatments*", SPE 155110, puplished at the SPE International Conference on Oilfield Scale held in Aberdeen, United Kingdom, 30-31 May 2012.

CHAPTER 1: INTRODUCTION

1.1 CONTROLLING SCALE PROBLEM IN THE OIL INDUSTRY

In an oilfield production system, one of the main problem affecting productivity is the formation of inorganic mineral scales (Kerver and Heilhecker, 1969; Miles, 1970; Vetter, 1973; Meyers et al., 1985; and King and Warden, 1989). Mineral scale deposition can occur once water –has broken through in producer wells and the type and severity of the scale depends on the water chemistry of the injected and formation brines and the physical conditions (temperature and pressure). Ironically, water injection into the injection well is required in order to maintain reservoir pressure which creates a driving force to push oil towards production wells. The inorganic scale precipitation is mainly due to comingling of injection water (i.e. sea water) and formation water in the case of sulphate scales such as barium sulphate, and due to pressure drops in the system in the case of calcium carbonate scale but other factors such as pH and temperature may also play a role (Boyle and Mitchell, 1979; Cowan, 1976; Johnson, 1983; and Vetter, 1975). There are many type of mineral scales, but 90% or more are likely to be calcium carbonate, calcium sulphate, barium sulphate and strontium sulphate (Goulding, 1987; Pucknell, 1983 and Yuan, 1989). A common feature of all of these inorganic scales is that they have very low solubility and indeed that is why they are deposited as solid.

Scale can deposit in the reservoir, the near wellbore formation, in the production well, in transportation pipelines and in topsides equipment, such as pumps and valves. That is, mineral scale can occur at almost any location within an oilfield water production system. Within the reservoir formation, scale deposition may block pores and reduce formation permeability, and hence cause formation damage. Scale deposition in production tubing and transportation pipelines may cause reduction in the diameter of the tubing and pipelines, sometimes totally blocking it (Carrell, 1987 and Payne, 1987). The replacements of pumps and valves is frequent required due to scale deposition and this can be very expensive. The scale deposit can also intensify corrosion attack on

tubing and pipelines (Carlberg and Matthews, 1975; Charleston, 1968 and Matthews and Carlberg, 1975).

To remediate oilfield scale, a number of techniques (such as chemical, mechanical, electrical and magnetic) have been introduced over the past few decades. However, out of the many techniques which have been proposed and applied, chemical and mechanical approaches are the most commonly used methods applied to remove or prevent scale deposition. However, chemical scale control is usually preferred over mechanical techniques because it is generally cheaper and more applied and is a *preventative* measure, and chemical approaches are especially convenient in offshore and deep water fields.

Chemical scale control is divide into three categories; removal acids, sequestrant or dissolver and scale inhibitors. The first and most common method for removal of calcium carbonate mineral is acidizing, which is also used routinely to restore well productivity. The downside of acidizing is that it does not stop the problem from re-occurring and mineral scale such as barium sulphate is insoluble in acid (Bonnett et al., 1991, Smith et al., 1968 and Vetter, 1975). The second chemical approach is through the use of sequestrants or scale dissolvers, and the most common one used in oilfield operations is EDTA. In few cases, use of EDTA shows some productivity improvement (Charleston, 1968 and Shaughnessy and Kline, 1983); but in the majority of cases, it has failed to show significant improvement. These poor results may be due to EDTA having a poor surface to bulk ratio in tubular environments thus leading to slow rates of dissolution (Carrell, 1987; Mazzolini et al., 1990 and Vetter, 1976). The third chemical approach to mineral scale control is through the use of chemical scale inhibitors. Unlike acids and dissolver chemicals, these acts as crystal distortion reagents at sub-stoichiometric concentration levels. This is achieved by adsorption of the scale inhibitor onto the active growth sites of the scale crystal (or initial scale nucleation), leading to a changes in the crystal morphology and thereby retarding nucleation and crystal growth. As such, use of scale inhibitor has been used widely to control scale formation in oilfield industry; such chemicals may be applied by continual dosing in topside

applications to protect the surface equipment and in downhole operations where the process is known as a inhibitor squeeze treatment.

Although initially downhole squeeze treatments were developed to prevent corrosion problem, the process has been adapted and is now applied more widely for treating/preventing downhole scale formation in oilfield operations. Much experience has been gathered in both the field application of scale inhibitors and in their development by the service sector, although most of the research on developing scale inhibitors has been focused on making new improved chemical which are principally very good at preventing scale formation (i.e. they show very good levels of inhibition efficiency). Much less effort has been put into developing scale inhibitors which are retained very efficiently on to formation rocks. Nevertheless, the success of any inhibitor squeeze treatment depends on both factors; the efficiency of scale inhibitor in preventing scale formation at a low minimum inhibitor concentration (MIC) level, typically at 5 to 15ppm, ***and*** on the ability of the inhibitor must to give a long return curves at or above the MIC during back production after a squeeze treatment. In squeeze treatments, the squeeze lifetime is measured either in terms of the time it takes for the scale inhibitor concentration to drop below MIC or, more commonly, on how many barrels of produced water are "protected" in this period. In terms of time, such treatments may often last from 3 months to 1 year and in terms of protected volume of produced water, they may be from 250Mbbl to 3MMbbl.

Given the background above, this thesis will focus on the inhibitor interaction with the formation minerals through adsorption/desorption and precipitation/dissolution process. That is, our study in principally on the retention mechanisms that govern scale inhibitor squeeze processes.

1.2 OUTLINE

This thesis is focused on understanding the governing mechanism of adsorption/ desorption and precipitation/dissolution that are taking place during scale inhibitor squeeze treatments. The thesis consists of six chapters which are briefly described as follows:

Chapter 1 briefly reviews the importance of scale inhibitor squeeze treatments in the oil industry and explains the main objectives of the study as well as giving a thesis outline.

Chapter 2 presents a detailed literature review of the governing mechanisms of scale inhibitor adsorption and precipitation squeeze processes. This includes a discussion of the theoretical and experimental studies that have been published in the literature which are relevant to this work.

Chapter 3 explains the experimental methodology used to study the governing adsorption and precipitation mechanisms throughout the work. This includes:

(i) beaker tests for static adsorption and compatibility experiments to uncover the pure adsorption and coupled adsorption/precipitation region.

(ii) sand pack test for non-equilibrium experiments to study the influence of flow rate on inhibitor return concentration for both adsorption and precipitation floods.

Chapter 4 presents results from static adsorption and compatibility experiments for two type of phosphonate scale inhibitors in synthetic Nelson Forties Formation Water (NFFW); viz. DETPMP - a penta phosphonate and OMTHP - an hexa phosphonate. The minerals used in these experiments are silica sand, kaolinite and siderite. The chapter defines how to differentiate between pure adsorption and the coupled adsorption/precipitation region. The factors that influence adsorption or precipitation mechanisms have been elucidated.

Chapter 5 present results from a series of non-equilibrium sand pack experiments at different flow rates for both adsorption and precipitation floods. Based on the corresponding static adsorption and precipitation results, scale inhibitor OMTHP, silica sand mineral and NFFW brine was chosen for all the sand pack floods. The conditions maintained in these pack floods were T = 95°C and pH4, throughout the study. The findings explain the influence of flow rate on inhibitor effluent concentrations and reveals the parameters that govern the adsorption or precipitation processes.

Chapter 6 gives the summary and overall conclusions reached during the course of this study and presents recommendations for future research work related to this area.

In the Appendices, the following subjects has been presented in order to support the discussion and findings in the main chapters of this thesis;

- Appendix A: Full derivation of coupled adsorption/precipitation model.
- Appendix B: Materials Safety Data Sheet (MSDS) of the main phosphonate scale inhibitors.
- Appendix C: General equipment and apparatus.

CHAPTER 2: LITERATURE REVIEW

2.1 INTRODUCTION

It has been known for many years that adsorption and/or coupled adsorption/precipitation are the main mechanisms contributing to long term scale inhibitor retention in reservoir formations. Therefore, many experimental and field studies have been carried out to investigate these phenomena. In reviewing this subject matter, the significance of inhibitor adsorption and/or coupled adsorption/precipitation in squeeze treatment is clarified by reassessing the governing mechanisms of the scale inhibitor squeeze process. Previous experimental and field studies of phosphonate and polymeric adsorption onto various minerals are reviewed.

2.2 GENERAL MECHANISM GOVERNING SCALE INHIBITOR RETENTION PROCESSES

It has been perceived that the ***long inhibitor tail*** during the back production stage of an inhibitor squeeze treatment is due to the inhibitor "*desorbing slowly*" over a long period of time after adsorption/desorption squeeze process. However, work carried out by Sorbie et al. (1990 and 1991) has revealed that this view can be further expanded. They have demonstrated that the mechanism of tailing in adsorption/desorption squeeze treatments is a ***propagation phenomenon,*** associated with the profile of the inhibitor adsorption isotherm on the reservoir rock as analyzed using mathematical modelling for both laboratory experiments and field systems. The equilibrium behaviour of adsorption-type inhibitor squeeze treatments is being governed by the adsorption isotherm, although in addition to kinetic (non-equilibrium) effects may be observed in our experiments. The following review is based on their analytical results.

Dispersion and adsorption of a chemical solution flowing through a porous medium can be derived by a mass balance, which can be translated to a chemical transport equation. The 1D (one dimensional) linear form of this equation is as follows:

$$\frac{\partial C_m}{\partial t} = D\frac{\partial^2 C_m}{\partial x^2} - v\frac{\partial C_m}{\partial x} - \frac{1-\phi}{\phi}\frac{\partial \Gamma}{\partial t} \qquad \text{(Eq. 2.1)}$$

The local concentrations in the adsorbed and mobile fluid phases is related to the rate of adsorption, ($\partial\Gamma/\partial t$) through the kinetic rate equation. The linear driving force rate can be expressed as:

$$\frac{\partial \Gamma}{\partial t} = r_2[\Gamma_{eq}(C_m) - \Gamma] \qquad \text{(Eq. 2.2)}$$

where;

C_m = mobile phase inhibitor concentration, (mg/L);

Γ = actual adsorbed level of inhibitor (mg of SI /g of rock or mineral substrate);

$\Gamma_{eq}(C_m)$ = equilibrium adsorption level (mg/g) associated with mobile concentration, C_m (mg/L);

D = dispersion coefficient (cm^2/s);

v = superficial velocity (cm/s); v= q/(Aϕ);

q=fluid volumetric injection rate (cm^3/s);

A = cross sectional core or sand pack area, (cm^2);

ϕ = porosity;

r_2 = inhibitor desorption rate parameter in non-equilibrium model, $seconds^{-1}$ (s^{-1});

t = time, seconds (s);

x = distance, (cm).

Equilibrium theory may be applied when kinetic effects are secondary (i.e. when the adsorption rate is so fast compared with the fluid flow rate, that the system is effectively at equilibrium). At equilibrium, and neglecting dispersion, the inhibitor advancement velocity can then be obtained from Equation (2-1) and is given by;

$$V_c = \frac{V_{fluid}}{\left[1 + \frac{1-\phi}{\phi}\left(\frac{d\Gamma}{dC}\right)\right]} \qquad \text{(Eq. 2.3)}$$

where V_c and V_{ct} are the inhibitor advancement velocities at concentration C and at the threshold concentration value, C_t, respectively; and V_{fluid} is the fluid velocity. The above equation distinctly shows that the inhibitor advancement velocity is governed by the quantity ($\partial\Gamma/\partial C$), the slope of the adsorption isotherm. The velocity for an inhibitor concentration value C (V_c), is inversely proportional to the slope of the isotherm. In the case of a "favourable" adsorption isotherm, the slope is larger for lower concentration values than for higher values and these lower values hence propagate more slowly back to the wellbore as shown in Figure 2.1 (Sorbie, 1991).

In addition, the phenomenon of "front sharpening" in the flow process can give a further demonstration of the effect of the isotherm shape, as illustrated in Figure 2.2. Let us imagine a band of inhibitor solution already on the column, as shown in the figure. When it is subjected to elution, new solvent enters at the top (the 'rear') of the band, and the inhibitor solution emerges from the bottom of the band (the 'front'); as it leaves its concentration will correspond to a point at the high concentration end of the isotherm (Figure 2.2) where the slope is small and the value of inhibitor advancement velocity corresponding large (Gregg, 1965). As the solution moves forward on to clean adsorbent it will begin to lose solute, the concentration C will decrease; this will cause ($\partial\Gamma/\partial C$) to increase and the advancement velocity to fall. Thus, the further forward the point of deposition is, the more slowly it tends to move, and this means that the front of the band will be self sharpening: any portion of the low concentration SI front that tend to get ahead is automatically slowed down. At the rear of the band the converse set of conditions applies; as the solution moves further into the band it becomes more and more concentrated so that $\partial\Gamma/\partial C$ progressively decreases, and the velocity correspondingly increases. Thus the further to the rear point is, the more slowly will it move, so that the rear must become progressively more spread out as a "tail". Therefore, Sorbie et al., (1990) concluded that the squeeze lifetime is essentially the time it takes for the threshold concentration, Ct, to get back to the wellbore and hence an inhibitor having a very steeply rising isotherm at low concentrations will lead to a long lifetime of a squeeze treatment.

Qualitatively, kinetic effects do not introduce any significantly new pattern of behaviour of inhibitor adsorption in terms of the long tail in the SI return curve. However, non-equilibrium effects do play a role in the governing mechanism of scale inhibitor adsorption squeeze processes. For example, if the SI adsorption process with the rock is at equilibrium during the injection period as in Figure 2.3, then the SI slug is retarded as shown. Figure 2.3 shows that the inhibitor is retarded compared to the non-adsorbing tracer in the case of equilibrium inhibitor adsorption (fast adsorption). That is, the inhibitor is closer to the well and this is not ideal considering the distance which the inhibitor must travel back to the wellbore. Figure 2.4 shows the situation of slow inhibitor adsorption (non-equilibrium), where the inhibitor slug is further into the formation and is more like a tracer slug. Thus, on the way back to the wellbore, the threshold concentration velocity for the case of non-equilibrium adsorption is the same as that for equilibrium adsorption but it has farther to travel in the non-equilibrium case thereby extending the squeeze lifetime. In addition to this overall effect on squeeze performance, non-equilibrium effects may appear as "spikes" in SI concentration both in core floods and in the field returns as discussed below.

From the above brief review of the governing mechanism of inhibitor squeeze processes, the key factors influencing an inhibitor squeeze lifetime are the steeply rising isotherm in the low concentration region, the maximum adsorption level at high SI concentration (since higher maximum adsorptions lead to "stripping" of the SI at the front of the SI slug) and non-equilibrium inhibitor adsorption. As such, these key factors should be considered as the basis for choosing the right adsorption/desorption inhibitor for a given field application.

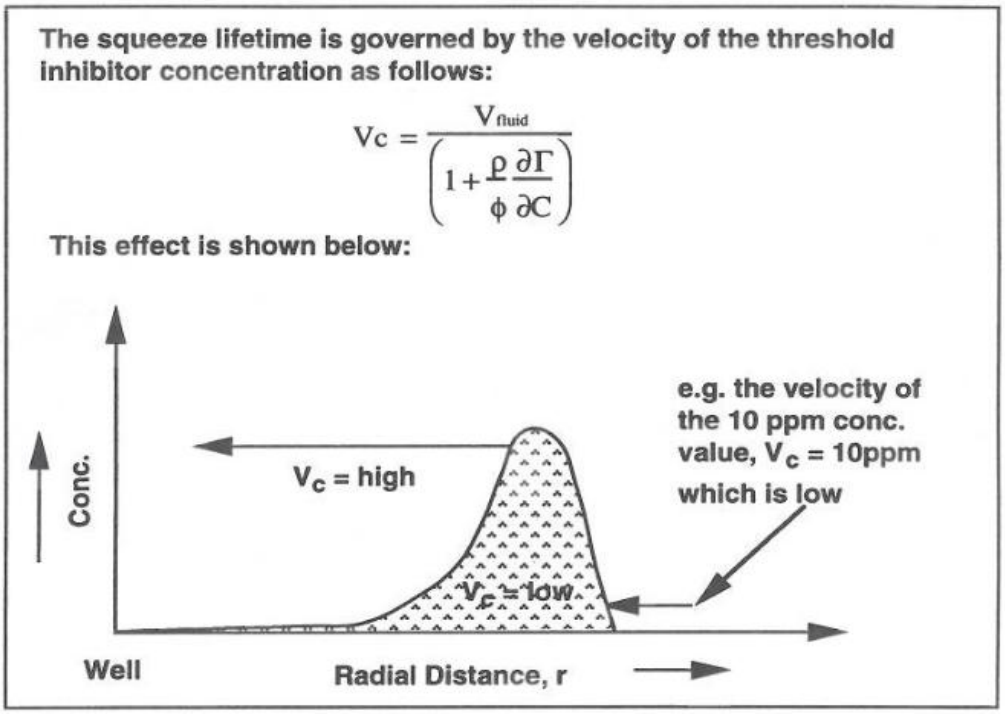

Figure 2.1: The effect of the velocity of threshold inhibitor level on squeeze lifetime (Sorbie, 1991)

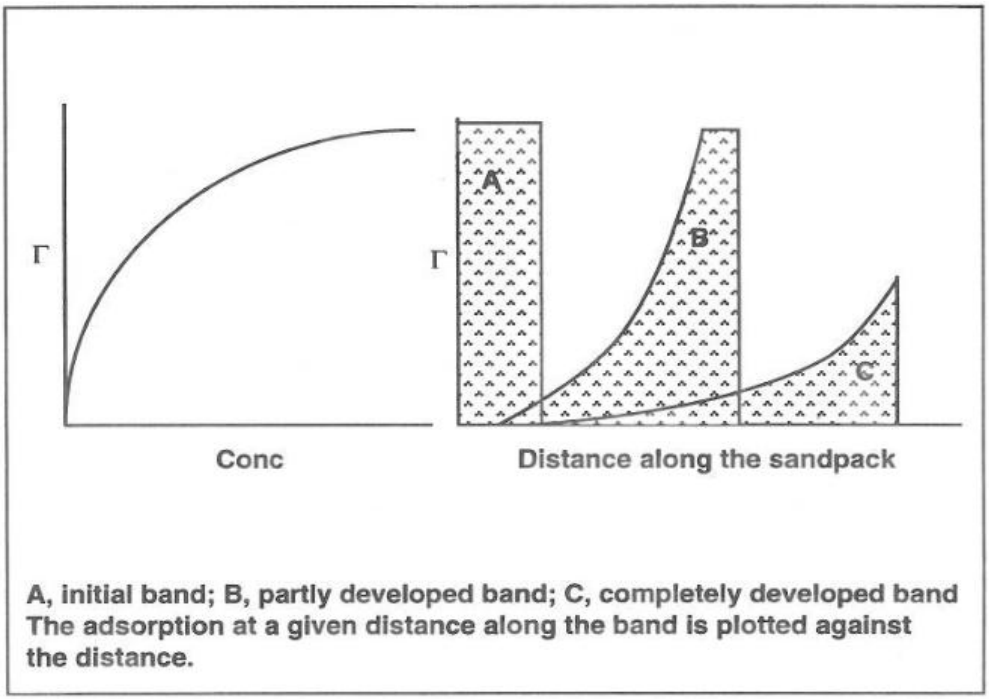

Figure 2.2: The advancement of inhibitor solution along the sandpack showing a relevant adsorption isotherm (Gregg, 1965)

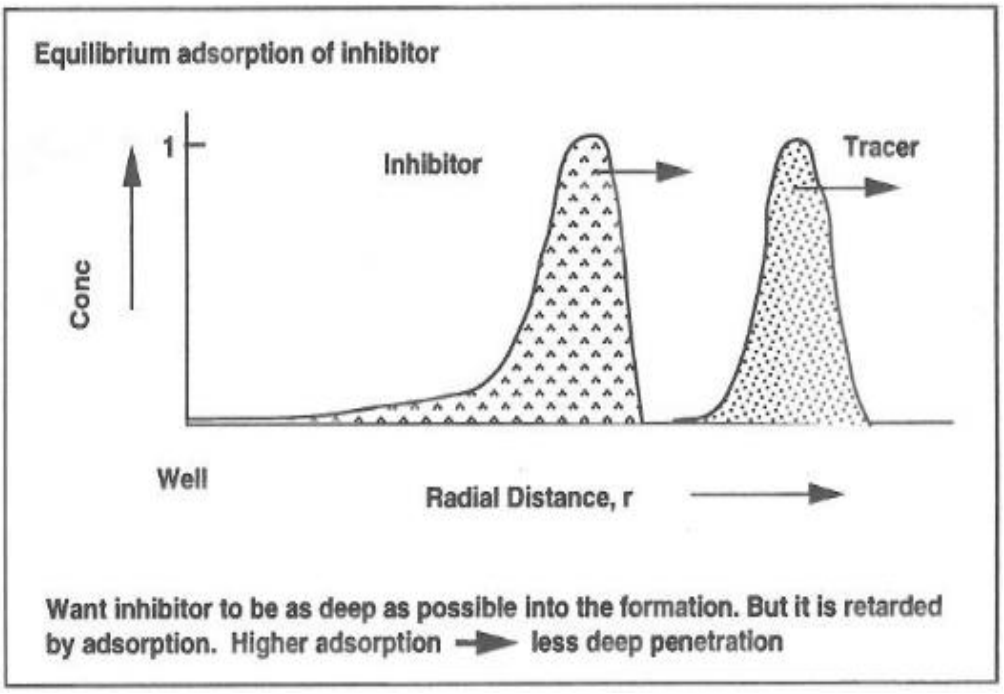

Figure 2.3: Demonstration of how the inhibitor slug is placed in the formation relative to a tracer slug for equilibrium inhibitor adsorption (Sorbie, 1991)

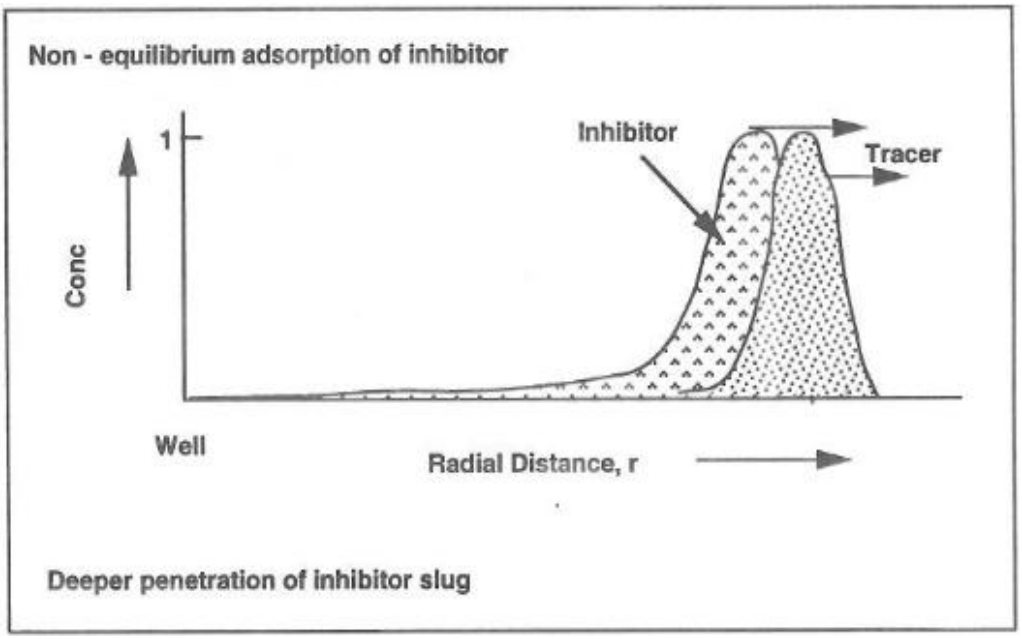

Figure 2.4: Demonstration of how the inhibitor slug is placed in the formation relative to a tracer slug for non-equilibrium inhibitor adsorption (Sorbie, 1991)

2.3 REVIEW OF PREVIOUS EXPERIMENTAL STUDIES

In relation to experimental work on scale inhibitor adsorption and/or coupled adsorption/precipitation, there are two types of experimental methodologies that were engaged to study this phenomenon. These are (i) static adsorption/compatibility tests which are performed using mineral separates (sand, clays etc.) and a volume of SI solution in a beaker or bottle, and (ii) dynamic core flood tests, which utilize sand pack or core displacement apparatus. For static adsorption/compatibility tests, the main factor influencing the inhibitor adsorption/desorption properties are pH, inhibitor type, mineral substrate type, brine composition, time and temperature. For Static Adsorption Tests, the experiments were performed using minerals a fixed volume of SI solution to evaluate the coupled adsorption/precipitation behaviour. In the corresponding Static Compatibility Tests, the *precipitation* behaviour was evaluated, since no mineral was used in these tests, and therefore any loss in concentration of SI from solution must be due to precipitation. Initial stock samples were taken and then small samples of the liquid were withdrawn from the solution at predetermined times. The inhibitor concentration was measured in these samples and the amount of inhibitor adsorbed is calculated (Kerver and Morgan, 1965; Vetter et al., 1979 and 1987). The adsorption isotherm is obtained by plotting the amount of inhibitor adsorbed as a function of the final equilibrium inhibitor concentration in solution. In dynamic tests, the inhibitor adsorption/desorption and/or precipitation/dissolution is evaluated using sand packs or core displacement tests, thus simulating the inhibitor squeeze treatment by flooding through formation porous media. The method involves the injection of an inhibitor slug into a sand pack followed by a post flush slug and then monitoring the effluent composition as a function of time or produced cumulative pore volumes (PV) of fluid. The inhibitor effluent profiles, in particular in the inhibitor desorption region (tail region) have been used by many worker to evaluate the SI squeeze lifetime (Hughes and Whittinghan, 1982; Olson and Moore, 1990; Ray and Fielde, 1988 and Tomson and Rogers, 1986).

Squeeze treatments were first introduced in the 1950s as an adsorption/desorption process in corrosion inhibitors applications (Poetker and Stone, 1956). The use of

inhibitors in such squeeze treatments led further studies to inhibit calcium sulphate in water flooding projects (Smith et al., 1968; Smith, 1978, and Kerver and Heilhecker, 1969). At this stage, little was known about the SI mechanism that was taking place to either inhibit scale formation or indeed to retain the SI in the rock formation. The assumption was that the adsorption/ desorption retention of scale inhibitors was driven by physical processes although there did not exist in the literature a systematic study of the exact mechanisms of inhibitor adsorption/desorption onto rock minerals in the formation. These earlier studies used both static tests for isotherm measurement and core floods for dynamic tests. The results showed that the slope of the adsorption isotherm at low concentrations which implied that the inhibitor would be adsorbed and desorbed gradually, and rather slowly. They also stated that the concentration of the produced fluid could provide sufficient information on the following; (i) adsorptive capacity of the formation, (ii) volume of formation treated, (iii) well production rate and (iv) desorption characteristics of the formation.

The first detailed scale inhibitor squeeze mechanistic study was probably conducted by Vetter (1973 and 1975). His study was designed to examine the feedback mechanisms of liquid scale inhibitor from formation rock. He sought to differentiate between adsorption/desorption, chemical precipitation, and slow feedback mechanisms based on the inhibitor feed from small fractures. He worked with a combination of P32-tagged ortho-phosphoric acids (which do not act as scale inhibitors) and tritium-labelled liquid scale inhibitors such as commercially available phosphonates, organic polymers and organic phosphate esters for all the laboratory and field studies. Adsorption isotherms were determined on sand and dolomite at various temperatures, concentration levels and pH values. The dynamic tests were executed using glass columns packed with sand, limestone, or dolomite. The results from adsorption isotherm determination shows that the adsorption characteristics of the phosphonate and polymer are unusual and complicated. He emphasized that true isotherm exist only between 0 and 100ppm (in solution) and at low concentration. Vetter chose orthophosphoric acid (OPA) for his study because it is a major component of many chemical inhibitors. All the liquid phosphate esters and phosphonates that were checked contained various concentrations of OPA. He also found that the "isotherms" of sand at different pH values at low

temperature are almost identical and there was a very small increase at the higher pH. He assumed that this may be due to the minute clay content of the sand. However, a large difference was found at high temperatures where the adsorption was much smaller at high pH than at low pH. This is due to the neutralized OPA reacting less with the sand than the acid OPA solutions. He indicated that temperature had the (then) expected effect on the isotherm; the adsorption should decrease with increasing temperature because physical adsorption is an exothermic reaction; Note that later this was shown to incorrect for the vast majority of commercial scale inhibitors. With regards to kinetic effects, inhibitor adsorption showed that adsorption increased with time. That is, the equilibrium between mineral concentration on the solid and in the liquid phase is not established instantaneously. Based on dynamic pack floods, he pointed out that the desorption is strongly dependent on the flow velocity and that both adsorption and desorption are highly time dependent. Although Vetter's work showed some early insights, it was wrong in some details regarding commercial scale inhibitors and also he made no attempt to model his results or apply them in a quantitative manner.

Works on the laboratory design and field implementation of scale inhibitor squeeze treatments in Prudhoe Bay field was reported by Meyers et al. (1985). It was found that DETPMP (a penta-phosphonate) was the best inhibitor screened out of five generic phosphonate scale inhibitors for possible application in Prudhoe Bay. It also showed that DETPMP SI exhibits better adsorption values, calcium tolerance and higher solubility in comparison with other scale inhibitors tested. For adsorption/desorption experiments, both crushed and consolidated reservoir formation rock with synthetic NaCl formation brine with no divalent ions was used. The test was meant to study the impact of adsorption/precipitation without the involvement of calcium ions in solution. For static adsorption/desorption tests at 95°C, the scale inhibitor and mineral showed (i) a steep isotherm in the low concentration region, which was consistent with the Langmuir form, (ii) considerable reversible desorption, and (iii) apparent adsorption of inhibitor solution concentration stabilised at less than 25 mg/L.

In dynamic sand pack/core flood tests at 25°C, the results indicated that the inhibitor achieved equilibrium essentially instantaneously at pH of 4.7. This was expected base

on static adsorption tests where it achieved equilibrium in less than one hour. Due to the relatively fast kinetics, it was suggested that long shut-in periods (more than 2 hrs) were not required to maximise the adsorption during squeeze treatments when the inhibitor solution is injected at reservoir conditions.

Meyers et al. also investigated the effects of temperature, pH, divalent cations, salinity and the presence of surfactant on the scale inhibitor adsorption. The main conclusions were that, (i) there was an increase in adsorption by 25% when temperature is increased from 25 to 90°C, which was also confirmed by other workers; (ii) pH plays a major role on inhibitor adsorption. At pH4 and below, the inhibitor adsorption is constant, but decreased steeply between pH5 and 6, and go down to almost zero at pH greater than 7. Thus, to maximise adsorption and to minimise shut-in time, inhibitor slugs near reservoir pH (4.7) were highly recommended. However, why phosphonate adsorption was high at low pH and vice-versa was not proven at that time; (iii) there was no effect on phosphonate adsorption when Ca^{2+} ion concentration is less than that required to precipitate the phosphonate. Only at pH6, was the adsorption enhanced by the presence of calcium. The conclusion was made mainly due to the low pH value they used; (iv) by varying temperature, pH, [SI], [Fe^{3+}] and [Ca^{2+}]; precipitation of Fe^{3+} and Ca^{2+} salts can be induced. But, although such precipitation in the matrix increases inhibitor retention, and thus treatment life, the adverse effect was to reduce near-well bore permeability and possibly cause near well formation damage; (v) a surfactant concentration (0 to 1.5 wt %), salinity (0.5 to 5 % NaCl), and winterizing agents (0 to 15 wt% methanol / 0 to 15 wt% ethylene glycol) had noticeable effects on the adsorption of DETPMP.

Durham stated that adsorption was probably caused by electrostatic attraction between the reservoir formation and scale inhibitors, since most of inhibitors used for squeezing were highly ionic compounds (Durham, 1983). This type of attraction can be readily observed with scale inhibitors as they are anionic in nature, which includes acrylates, phosphates and phosphonates. A hypothesis from King and Warden (1989) stated that: (i) adsorption refers to a plating mechanisms in which a compound at the molecular level, without substantial chemical modification, sticks to the surface of the formation pore or a mineral growth in the pore, by means of electrical or physical forces; (ii) in the

absence of calcium ion, adsorption is the cause of adherence of a scale inhibitor compound onto sandstone formation; (iii) the amount of adsorption is dependent on the amount of active surface area contacted and the thickness to which the inhibitor molecules adsorb.

The adsorption isotherm, Γ(C), is the key characteristics of inhibitor adsorption/desorption behaviour, which quantitatively relates the amount of inhibitor adsorbed on a formation rock surface, Γ (in mg/g or mg/m^2), as a function of inhibitor concentration (C) in the bulk formation fluid. As will be emphasised throughout this work, the behaviour of the adsorption isotherm curve is the most important factor in squeeze treatments. This parameter is measured using static adsorption tests. Two types of experimental approach have been engaged to investigate the scale inhibitors adsorption/desorption for the field applications: (i) static compatibility/adsorption beaker tests and (ii) dynamic sand pack column and/or core displacement tests. Static compatibility/ adsorption beaker tests are conducted using sand, clay (such as illite, kaolinite, siderite, etc.) or crushed core to ascertain bulk adsorption isotherms and to investigate the sensitivities of pH, temperature, time and concentration to adsorption. On the other hand, dynamic sand packed columns or core displacement tests are utilized to simulate scale inhibitor squeeze treatments by flooding through the porous media in the sand packed column or rock core. Dynamic studies involve injection of an inhibitor slug followed by a postflush into a sand pack and then monitoring the effluent composition as a function of produced cumulative fluid or time. The shape of the effluent inhibitor desorption curve (long tail region at the end) have often been used by researches to evaluate the squeeze lifetime.

In a study by Przybylinski, five different inhibitors were investigated using a dynamic sand packed column/core flood displacement technique (Przybylinski, 1989). The five scale inhibitors were (a) phosphonate inhibitor DETPMP; (b) an alkyl phosphonate HEDP; (c) a phosphate ester (TEAPE); (d) a tagged poly acrylic acid (PAA) and (e) a proprietary polymeric phosphonate inhibitor (PPI). The experimental work was conducted using silica sand or limestone packed columns at 40°C and 80°C. A synthetic brine with similar composition to the oilfield brines was used.

The results from Przybylinski led to number of conclusions, as follows;

(i) The experimental results indicated that: (a) the adsorption level of phosphonate on silicate sand is higher than the value which is estimated based on monomolecular layer adsorption; (b) the adsorption of inhibitors increases with increase in temperature and (c) a significant fraction of the adsorbed inhibitor is not readily released to the produced brine. Thus, some of the SI is strongly adsorbed onto the minerals and some is more readily adsorbed just onto the surface. These observations lead to the suggestion that two or more adsorption mechanisms are at work. These may include surface precipitation and strong adsorption.

(ii) Adsorption/desorption very much depends on the partitioning of the SI between the solution and the solid surface which is strongly influenced by the mineral type (sand, kaolinite, siderite, etc.), the nature of the surface (smooth or rough) and the solution. Therefore, using irregular minerals or an inappropriate brine may lead to false conclusions.

(iii) DETPMP phosphonate SI had the highest levels of return on both sand and limestone of all inhibitors tested in this study. These results lead them to conclude DETPMP was the best inhibitor for squeeze applications for their test conditions.

(iv) Precipitation can be induced in the reservoirs due to changes in temperature, resulting in an enhanced squeeze. This conclusion strengthens the findings previously reported by Vetter (1972 and 1976). Caution must be taken as precipitation can also cause formation damage of not studied properly.

Przybylinski's work is in agreement with many workers with regards to the importance of the kinetics of inhibitor adsorption/desorption process. Work by Vetter (1987) also shows that both adsorption/desorption depends on time and desorption is strongly dependent on the flow velocity.

Mathematical modelling was also used to analyse both laboratory experiments and field systems (Sorbie et al., 1990 and 1991). They described that the mechanism of tailing in an adsorption squeeze process is a propagation phenomenon associated with the shape of the inhibitor adsorption isotherm on the reservoir rock. They showed that a steeply

rising isotherm and non-equilibrium inhibitor adsorption are key factors in influencing an inhibitor squeeze.

They studied the effect of pH, temperature and calcium on the adsorption of phosphonate scale inhibitors onto consolidated and crushed sandstone (Sorbie et al., 1993). In summary, (i) SI adsorption onto the crushed rock material increases at higher temperatures under all conditions; (ii) Inhibitor adsorption onto crushed rock is lower at pH4 than at pH2 or pH6; when calcium ions are present (i.e. [Ca^{2+} = 415ppm) at 25°C; (iii) the adsorption of phosphonate inhibitor (DETPMP) decreased predictably as pH increases (at 25°C) in the absence of Ca^{2+} ions, which is due to hydrogen bonding mechanism for adsorption; (iv) at pH6, involvement of Ca^{2+} in the inhibitor/rock interaction was clearly proven (at 25°C); (v) electro kinetic measurements on Clashach rock particles in seawater solution clearly correlate the phosphonate inhibitor adsorption behaviour with the surface charge properties (ζ-potential).

Kan et al. (1991 and 1992) have studied both the equilibrium and the kinetics aspects of phosphonate adsorption in the laboratory using beaker tests and sandstone core floods to understand further DETPMP SI retention in the reservoir after inhibitor squeeze treatment. They reported that there are at least four mechanisms involved in inhibitor retention: (i) acid/base dissolution of the mineral surface; (ii) adsorption to the surface as the result of acid/base dissolution in step (i), (iii) mass-transport molecular diffusion of inhibitor in solution to the solid surface; and (iv) solid phase maturation toward a thermodynamically stable phase, as the solid surface material interacts with the solution. They concluded that the kinetics of the slow reaction governs the phosphonate flow-back trend and the rate-limiting step for the slow adsorption reaction is probably a diffusion-controlled process. Phosphonate contact time and contact area increase the efficiency of inhibitor squeeze treatment.

In a later study by Kan et al. (2004), four oilfield inhibitors (three phosphonates and one poly-acrylate) were investigated to study the inhibitor/rock interaction and factors affecting scale inhibitor retention in carbonate-rich formations during inhibitor squeeze treatments (Kan et al., 2004). They found there are two mechanisms which are central to the SI retention in carbonate-rich formations; (i) SI-Ca^{2+} coating due to reduction of

calcite dissolution and surface poisoning; and (ii) precipitation of SI-Ca^{2+} solid phase due to either low or high calcium ion concentrations. For one of the phosphonate SI, NTMP, an acidic NTMP-Ca^{2+} salt was formed in a low-pH environment. The nature of SI to calcium ion complex might be in a crystalline or an amorphous form depending on the ions present in the formation brine. Quantitative relationships between types of inhibitors, inhibitor acidity and concentration, and kinetics of calcite dissolution and phosphonate-calcium precipitation were developed.

Sources of calcium in a typical field squeeze treatments are; (i) Seawater that contains Ca^{2+} injected along with the scale inhibitor; (ii) Ca^{2+} which is injected as an over-flush; (iii) Ca^{2+} that is dissolved from calcite and solid formation minerals; and (iv) Ca^{2+} that is present in the formation brine itself. Many laboratory experiments and field observations have pointed out the importance of calcium in the various inhibitor retention mechanisms. Like Kan et al., many workers have found that the presence of calcium ions significantly enhance the retention of scale inhibitor within the rock formation which results in an extended squeeze lifetime. However, there is little detailed analysis in the literature of the details of this calcium enhanced retention and it is often described briefly in terms of the formation of an insoluble a Ca-SI complex.

It has been inferred that the formation mineralogy determines how an inhibitor is retained in a formation (Gdanski, 2008). The pill chemistry is also an important factor for retention in carbonate reservoirs. Acidic pills are mostly retained near the well bore whereas more neutralized pills move farther into the formation. Gdanski et al. (2008) found that three calcium nitrilo methylene phosphonate (NTMP) solid phases, an amorphous phase and two crystalline $Ca_{2.5}$HNTMP phases with pKsp = 22.6 and pKsp = 24.2, were particularly important with respect to inhibitor retention. The relative sizes of these solid phases formed are governed by the pill composition and acidity. Nearly all of these field squeezes were done using a common phosphonate inhibitor, NTMP [nitrilotri (methylene phosphonic) acid], although similar results have been observed with several other inhibitors and blends. From these studies and observations, the following conclusions were made; (i) a column apparatus has been developed to simulate inhibitor squeeze and return. (ii) For acidic pill, approximately 78% of injected

phosphonate precipitates in these experiments. The fraction that precipitated is inversely related to the amount of base in the pill. Most of the precipitate is near the injection port. (iii) For partially neutralized pill, approximately 50% of injected phosphonate precipitated at the output end of the column. (iv) A portion of phosphonate was retained as the crystalline phosphonate salt and a portion of the acidic pill was retained as a more soluble calcium phosphonate salt.

Gdanski and Funkhouser (2001, 2005) reported that static adsorption experimental data can be up-scaled to agree with scale inhibitor adsorption/desorption in non-equilibrium sand pack. Their studies showed that static adsorption data has a direct bearing on scale inhibitor adsorption/desorption in dynamic mineral packs (Gdanski and Funkhouser, 2001, 2005). They reported that isotherm fitting with the modified Langmuir equation provided the mathematical framework for an understanding of desorption kinetics, though the Langmuir adsorption isotherm often does not fit experimental data very accurately. In summary, they found that; (i) a wide variety of adsorption data can be fit by using the modified Langmuir equation, (ii) static adsorption isotherms are useful in determining the magnitudes of the kinetic effect on desorption in linear flow tests, (iii) siderite may be responsible for the long-term, low-level inhibitor-return profiles sometimes observed after squeeze treatments, and (iv) the minerals studied can be classified into three groups; (a) strongly adsorbing (siderite), (b) moderately adsorbing silica-like minerals (silica and kaolinite),and (c) weakly adsorbing alumina-like minerals (illite, smectite and alumina).

Many studies have shown that that Ca^{2+} ions play an important role in enhancing inhibitor retention in porous media (Sorbie et al., 1993 and Kahrwad et al., 2008). Almost all of them thought that this was due to phosphonate inhibitor and Ca^{2+} binding to each other and the subsequent formation of a Ca_SI precipitate. No explicit results were reported where adsorption of Ca^{2+} ions on the mineral surface would cause a change in rock surface charge leading to an enhanced inhibitor adsorption. From a series of core floods, Pardue (1991, 1992) reported that the squeeze lifetime using phosphonate SI was reduced by one-half when the calcium in the post flush brine decreases from 5450 to 1000ppm with the same in situ brine. However, the amount of

calcium in the post flush was not significantly seen to affect treatment lifetime. The reason for this was thought to lie in the way the product was precipitating in the core where the connate brine had high calcium and precipitation occurred at the inhibitor slug front during injection. Rogers et al. (1990) carried out column studies with both ground core samples and intact core plugs. The results showed a four-fold enhancement of inhibitor retention as a consequence of using $CaCl_2$. They also stated that packed columns of ground core material were quick and easy to prepare and allowed numerous variables to be examined. Jacobsen et al. (1989) also used Gullfaks sandstone cores to conduct phosphonate and phosphino poly carboxylic acid inhibitor floods. Extended squeeze life was obtained by adding calcium for both inhibitors.

A series of experiments related to static inhibitor adsorption were carried out to determine if it was possible to differentiate between pure adsorption and coupled adsorption/precipitation processes (Kahrwad et al., 2008). The results show that for DETPMP SI with sand mineral at 25°C and 95°C, the experiment was able to distinguish between the two phenomena. It must be noted that the brine used contains only 428ppm of Ca^{2+}, which make it difficult to achieve precipitation. Nonetheless, the work created a pathway for other research and the basis for part of the study which is continued in this thesis.

Dynamic examining the influence of flow rate on inhibitor return concentrations in core flooding of phosphonate scale inhibitors in both adsorption and precipitation flood were previously reported by Zhang, Chen, Sorbie and MacKay at Heriot-Watt University, which was later published by Zhang et al. (2000) and Chen et. al. (2000). This work demonstrated clear non-equilibrium behaviour as the flow rate for the different floods is varied. At the slower flow rate, higher effluent SI concentrations were observed, and vice versa. The direction of the non-equilibrium effect was found to be the same for both adsorption and precipitation floods.

2.4 SUMMARY AND CONCLUSIONS

This survey of the literature on scale inhibitor (SI) retention shows that a significant body of research exists reporting laboratory experiments studying the adsorption and

adsorption/precipitation of scale inhibitors used in squeeze treatments in oilfields. These laboratory experiments are related to adsorption/desorption in static and dynamic conditions. From these various studies, the principal governing mechanisms of inhibitor retention in squeeze processes have been elucidated. The main mechanisms of inhibitor adsorption are understood to depend on; (i) the surface chemistry and roughness of the adsorbing minerals - silica sand, clay, kaolinite, siderite, sandstone, carbonate etc., (ii) experimental or field conditions - pH, temperature, salinity and hardness, and (iii) inhibitor properties - functional group, dissociation degree, polarity, etc. This work shows that the inhibitor adsorption isotherm and associated kinetic properties play important roles in inhibitor adsorption squeeze treatments. Nevertheless, there are conflicting statements and missing links between static and dynamic tests that need to be addressed. For example, there is no comprehensive experimental dataset currently available in the literature to support modelling for better prediction of squeeze treatments for **all** retention processes including pure adsorption and coupled adsorption/precipitation processes. This work will provides such an experimental dataset which has results for both the bulk inhibitor/brine/mineral (sand, kaolinite, siderite) interactions and the corresponding dynamic (sand) pack floods. That is, where the precise system studied in bulk is applied in a dynamic sand pack flood.

Although work has been carried out on static adsorption and precipitation, there has been very little research which has set out to clearly differentiate pure adsorption from coupled adsorption/precipitation. The recent work of Kahrwad et al. (2008) has tackled this issue and has presented initial experimental work on phosphonate SI and silica sand as mineral substrate to distinguish between pure adsorption and coupled adsorption/precipitation. This work presented both the theory showing how this could be achieved and the corresponding experimental verification of this theory. However, the work was of Kahrwad et al. only used a brine that contains only 428ppm of calcium ion. The amount of calcium used prevented them from achieving full precipitation over a wide range of conditions. Work on the theory of coupled adsorption/precipitation in a dynamic context was continued by the work of Sorbie (2008), which is part of the basis of the present work.

CHAPTER 3: EXPERIMENTAL METHODOLOGY

3.1 INTRODUCTION

This chapter gives the detailed description of all the experimental procedures used in the course of this PhD research, they are as follows:

(i) Static Compatibility Tests and Static Coupled Adsorption/Precipitation Tests (between phosphonate scale inhibitors and sand, kaolinite and siderite minerals) where the combination of these two experiments will differentiate between pure adsorption (Γ) and coupled adsorption/precipitation (Γ/Π) behaviour. This will be discussed in detail in Chapter 4;

(ii) Non-equilibrium Sand Pack Flood Experiments using the SI phosphonate OMTHP and sand minerals, which analyze the effluent concentrations of various species (SI, Ca^{2+}, Mg^{2+}, Li^{+}) at various flow rates for both precipitation and adsorption floods. This will be discussed in Chapter 5.

The equipment/apparatus specifications and settings used for the analysis of both the experiments above are fully explained in Appendix C.

3.2 STATIC COMPATIBILITY AND COUPLED ADSORPTION/ PRECIPITATION EXPERIMENTS

Static Compatibility Tests and ***Static Adsorption Tests*** were performed to evaluate both pure adsorption and coupled adsorption/precipitation behaviour of DETPMP (a Penta-Phosphonate) and OMTHP (a Hexa-Phosphonate) scale inhibitors (SI) with synthetic Nelson Forties Formation Water (NFFW). For Static Adsorption Tests, the experiments were performed using different masses of sand, kaolinite and siderite (m = 5g, 10g, 20g and 30g) at a fixed volume of SI solution (V = 0.08L) to evaluate the coupled adsorption/precipitation behaviour. In the corresponding Static Compatibility Tests, the experiments were performed to evaluate the *precipitation* behaviour, since no mineral is

used in these tests. As such, any loss in concentration of SI during the compatibility test must be due to precipitation.

3.2.1 Objective

The objective of one set of experiments was to investigate the apparent adsorption (Γ_{app}) vs. [SI] isotherm behaviour when scale inhibitor (SI) is mixed with formation brine in the presence of selected rock minerals. For such experiment, we must analyse for the concentrations of phosphorous (P), calcium (Ca^{2+}), magnesium (Mg^{2+}), lithium (Li^{+}) and other related cations in the solution before and after heating and filtration. These are analyzed using Inductively Couple Plasma (ICP). ICP measures the concentration of each element under consideration. The difference in concentration of these elements before and after experiment will denote whether any couple adsorption/precipitation has taken place.

3.2.2 Materials

Scale Inhibitors: Two scale inhibitors were used in this work. They are;

a) Di-ethylene Tetra-amine Penta (methylene-phosphonic acid) or DETPMP, a penta-phosphonate

b) Octa-methylene Tetra-amine Hexa (methylene-phosphonic acid) or OMTHP, a hexa-phosphonate

Both of these SIs are from the phosphonate family group. They are commercial products widely used in oilfield applications and the particular products used here were supplied by Rhodia**.** Chapter 4 shows the structure and properties of these products. Appendix B shows the material safety data sheets (MSDS) for both DETPMP and OMTHP. Details of SI commercial name and activity are presented in Table 3.1.

Generic name	Type	Activity%	SI name	Supplier
DETPMP	Penta-phosphonate	45%	Briquest 543-45AS	Rhodia
OMTHP	Hexa-phosphonate	30%	Briquest 684-30S	Rhodia

Table 3.1: Details of phosphonate SI, group and activity

Minerals: Three types of minerals are used in this work, viz. sand, kaolinite and siderite, to study the retention of scale inhibitors onto these mineral substrates.

a. Dry silica sand (BDH GPR, 40 – 100 mesh, purified by acid) was chosen as one of the adsorbent as the majority of sandstone rock is quartz. Silica sand also represents a simple model of a sandstone formation. The chemical compound silicon dioxide, also known as silica, is an oxide of silicon with a chemical formula SiO_2. Refer to Chapter 4 for details of the sand characteristics.
b. Kaolinite is a clay minerals, with the composition $Al_2Si_2O_5(OH)_4$. It is a layered silicate mineral, with one silica tetrahedral sheet linked through oxygen atoms to one octahedral sheet of alumina. Formations that are rich in kaolinite are known as China clays, which is the case for this particular mineral. The structure is rarely as crystals but rather as thin platy or stacked, aggregated into compact, claylike masses. Refer to Chapter 4 for a detailed charaterisation of the kaolinite used in this work.
c. Siderite is a mineral compound of iron carbonate, $FeCO_3$. Generally it has more than 50% iron mineral and contain no sulphur or phosphorous. The sample used in this work also contains ~25% illite and ~20% quartz. Its crystals belong to the hexagonal system, and are rhombohedral in shape, typically with curved and striated faces. Refer to Chapter 4 for details of siderite characterisation.

Brine: Synthetic Nelson Forties Formation Water (NFFW)

All brine solutions are prepared by dissolving appropriate quantities of salts in distilled water. The composition of this NFFW is given in Table 3.2. The brine solution was filtered through a 0.45µmfilter paper which is commonly used by the industry to filter water samples. This gives us an adequate filtration level to remove any suspended solid content in the water.

Ion	Conc. (ppm)	Comp	Mass				
			g/l	g/5L	g/10L	g/15L	g/20L
Na^{+}	31275	NaCl	79.50	397.50	795.00	1192.50	1590.01
Ca^{2+}	2000	$CaCl_26.H_20$	10.93	54.66	109.32	163.98	218.64
Mg^{2+}	739	$MgCl_2.6H_20$	6.18	30.90	61.80	92.69	123.59
K^{+}	654	KCl	1.25	6.23	12.47	18.70	24.94
Ba^{2+}	269	$BaCl_2.2H_2O$	0.48	2.39	4.78	7.18	9.57
Sr^{2+}	771	$SrCl_2.6H_2O$	2.35	11.73	23.46	35.19	46.92
SO_4^{-2}	0	Na_2SO_4	0.00	0.00	0.00	0.00	0.00
Li^{+}	50	LiCl	0.305	1.53	3.05	4.58	6.11
Cl^{-}	50000						
		Actual Cl ppm	55278.64				
		If CaCl2.2H2O is use	7.32	36.62	73.25	109.87	146.49
TDS =	91036.64	ppm					

Table 3.2: Synthetic Nelson Forties formation water brine composition

Notes:

a. 50ppm Li+ has been added as an inert tracer in the brine. This is to check for evaporation (if any) which would directly affect the change in concentration of all elements during the heating process. Since Li^{+} is an inert tracer, it does not react with solutions or adsorb onto any rock minerals. The change in concentration due to evaporation will lead to wrong adsorption and precipitation values and this is corrected for using the Li^{+} results.

b. All prepared brines are filtered using 0.45 µm Whatman filter paper. This is to remove any dirt and physical impurities during preparation.

c. No degassing is required as it does not go through core or sand pack at high temperature. Degassing would be required only for experiments involving core or sand pack at high temperature where the brines flowing through the core/sand pack expands at high temperature and influence the calculation of pore volume, porosity and permeability.

3.2.3 Experimental Methodology

Test Conditions:

Test conditions for the whole cycle of experiment must be set to achieve consistent results. The details are;

Temperature (T)	= 95°C
Pressure(P)	= atmosphere
pH	= 4
Volume of test solution, V	= 80 ml
Mass of substrate, m	= 10g, 20g and 30g minerals (varies)
Mixing ratio	= n/a
Flow rates	= n/a (static)
Flow conditions	= n/a (static)
Coupon material & finish	= n/a
Core properties (including formation mineralogy, permeability, porosity and particle size)	= n/a

Sampling times: 24 hrs after heating at 95°C. Each test is performed in duplicate.

Notes:

a. All stock samples (blank and with inhibitor) are pH adjusted to pH 4 using dilute HCl or NaOH prior to being mixed with the substrate (sand) and heating.

b. The mass of mineral substrate in a given experiment varies and is m = 10, 20 and 30g, while the fluid volume of the inhibitor solution is maintained at V = 80ml = 0.08L. The precise (m/V) ratio used is important since apparent adsorption vs. [SI] results at different (m/V) ratios allow us to differentiate between pure adsorption and coupled adsorption/precipitation behaviour.

Inventories and Preparation:

- Brine: chemicals compound, grade and supplier

Chemicals	Grade	Supplier
Sodium chloride	Analar	VWR
Calcium chloride 6-hydrate	Analar	VWR

Magnesium chloride 6-hydrate	Analar	VWR
Potassium chloride	Analar	VWR
Barium chloride	Analar	VWR
Strontium chloride	Analar	VWR
Sodium Sulphate	Analar	VWR

- pH adjustment: chemicals compound, grade and supplier

Chemicals	Grade	Supplier
HCl	Analar	VWR
NaOH	Analar	VWR

- Standards: chemicals compound, grade and suppliers

Chemicals	Grade	Suppliers
Calcium 1000ppm Standard	Spectrosol	VWR
Magnesium 1000ppm Standard	Spectrosol	VWR
Iron (III) 1000ppm Standard	Spectrosol	VWR
Lithium 1000ppm Standard	Spectrosol	Merck

- Minerals: grade and suppliers

Minerals	Grade	Supplier
Sand	Analar	VWR
Kaolinite	Industry	Northern Geological Supplies
Siderite	Industry	Northern Geological Supplies

Glassware and Apparatus:

a. Apparatus: fan-assisted oven or water bath, balance and : 1000ml, 250ml and 150ml plastic bottles
b. For pH measurement: pH meter, pH 7 & pH 4 buffer solutions for calibration
c. For scale inhibitor dilutions: 1000ml, 500ml, 250ml, 100ml volumetric flasks, and 250ml and 100ml measuring cylinder
d. For diluent solution preparation: 5L volumetric flask, 5L plastic container, 1L beaker and funnel

e. For filtration: filtering equipment (vacuum pump, conical flasks and tubing) and filter papers (0.45µm & 0.20µm).
f. For ICP standard preparation: 250ml volumetric flasks, 10ml and 2.5ml variable and 1ml variable pipettes

Preparation of Bottles and Labelling:

80ml (0.08 L) of brine was used for each static adsorption test. The bottles are numbered to track each concentration used. Experiments at each concentration are carried out in duplicate to assure the consistency of the results.

Bottle No.	[SI], ppm active	Bottle No.	[SI], ppm active
1	Blank	9	500
2	Blank	10	500
3	20	11	1,500
4	20	12	1,500
5	50	13	4,000
6	50	14	4,000
7	100	15	10,000
8	100	16	10,000

Volume of FW Brine required:

For one (1) experiment :

- 10,000ppm stock SI in FW solution was prepared in a 1000ml flask; where 1000ml of FW is required, which can be used for one complete experiment (which consists of four tests). So, for each experiment, 1000/4 = 250ml is required;
- For blank samples and each [SI], 250ml is required each; so for 8 samples = (8X250) ml = 2,000ml.

For four(4) experiments :

- Therefore, for four(4) experiments; 1,000ml of FW is required.
- For blank samples and each [SI]; for all the four (4) tests; 2,000x4 = 8,000ml is required.

Preparation of SI Concentration and Volume:

- To elaborate the procedure, DETPMP SI is chosen for all calculations. The difference in calculation is the activity% involved, where they are 45% and 30% for DETPMP and OMTHP, respectively.
- To prepare 1,000ml of 10,000ppm active SI: use a 1000ml volumetric flask. For the selected scale inhibitor, the amount was prepared to cater for four experiments;

    1. Static Adsorption Test - 10g minerals
    2. Static Adsorption Test - 20g minerals
    3. Static Adsorption Test - 30g minerals
    4. Static Compatibility Test (no mineral)

    Each experiment requires 250ml solution. It is highly recommended that the stock solutions for all these four experiments are prepared together to make sure they are exactly the same and for good consistency in the final results.

- Prepare a 10,000ppm active scale inhibitor stock solution in FW:

    10,000ppm = 10,000 mg/L = 10 g/L as supplied

    @ 45% active (as written on supplier bottle)

    x (g) = 10g / active concentration)

    x (g) = 10 / 0.450 = 22.22 g/l

    So, 22.22 g would be required to prepare 1,000ml of 10,000ppm DETPMP active at 45%.

- Dilute down 10,000ppm active SI stock solution in FW brine to give other concentrations (Table 3.3):

SI Name	SI Activity (%)	Concentration required (ppm)	Volume of SI used (in 1000ml 'FW' brine)
DETPMP	45	Blank	0/10000*1000 = 0 ml
		20	20/10,000*1000 = 2 ml
		50	50/10,000*1000 = 5 ml
		100	100/10,000*1000 = 10 ml
		500	500/10,000*1000 = 50 ml
		1,500	1500/10,000*1000 = 150 ml
		4,000	4000/10,000*1000 = 400 ml
		10,000	10000/10,000*1000 =1000 ml
Total stock SI solution = 0+2+5+10+50+150+400+1000 = <u>1617.0 ml</u>			

Table 3.3: Volume required to make different concentrations

Since the above requirement is more than the prepared bulk volume of 1,000ml at 10,000ppm; another batch of 1,000ml at 10,000ppm is prepared independently to complete the range of concentrations.

Notes :

a. In the above table, instructions for the preparation of 1000 ml of each concentration is given. For one experiment, only 250 ml of each concentration is required. The other 750 ml was then used for the next three experiments using DETPMP SI. The stock sample was prepared once, so that all of the four experiments were using exactly the same stock sample.
b. For one experiment, 250ml of each concentration was taken from the prepared bulk solution of 1000ml. This enables the same solution to be used for duplicate tests; which means 2 bottles i.e. test and a duplicate bottle. Each test at each SI concentration, required 160ml (2x80ml). The remaining 90ml (250-160) was kept in stock, as the initial solutions were analyzed by ICP to find initial concentration, $\mathbf{C_o}$. We must ensure that the stock solution was pH adjusted before using as test samples and ICP analysis.

Preparation of Diluent Solution:

Diluent solution was used to dilute samples taken for ICP analysis. For all the ICP samples, 1% Na^+ is used as its diluent solution because the brine used contains the highest amount of Na^+ (~31,000ppm) compared to other cations in the brine. As such, Na+ as its diluent would provide the closest matrix match when analyzed using ICP. For all the analysis in these experiments, they are diluted 10 times so that they would match the calibrated standards.

1% Na^+ (aq) ≡ 10,000ppm Na^+ (aq) ≡ 25.42g of NaCl (s) in 1 litre of distilled water

So; in 5 litre of distilled water, it requires 25.42g x 5 = <u>127.10g of NaCl</u>

Preparation of Standards used for ICP Analysis:

DETPMP at 45% active is used for all calculation to illustrate the procedures.

- 2,500ppm DETPMP was prepared and used as stock to make all the other concentrations used as standards.

  2,500ppm = 2,500 mg/L = 2.5 g/L as supplied

  @ 45% active (as written on supplier bottle)

  x (g) = 2.5g / active concentration)

  x (g) = 2.5 / 0.45 = 5.56 g/l

  Therefore to prepare 250ml of 2,500ppm active DETPMP;

  (5.56 / (1000/250))g = <u>1.39g is required</u>

- The diluent / matrix used is 1% Na^+ (aq) ≡ 10,000ppm Na^+ (aq). 250ml of each standard was prepared.

Standard number	Constituent(s)	Active concentration(s)	Dilution requirements, in 1% Na^+ (aq), using a 250ml volumetric flask
1	Only 1% Na^+ (aq)	10,000ppm	N / A
2	DETPMP	5ppm	25ml of Standard 3

3	DETPMP	50ppm	25ml of Standard 4
4	DETPMP	500ppm	50ml of Standard 5
5	DETPMP	2500ppm	1.39g of DETPMP SI*
6*	Ca^{2+} Mg^{2+} Li^{+} Fe^{3+}	50ppm Ca^{2+} 25ppm Mg^{2+} 10ppm Fe^{3+} 5ppm Li^{+}	12.5ml of 1000ppm Std Ca^{2+} 6.25ml of 1000ppm Std Mg^{2+} 2.5ml of 1000ppm Std Fe^{3+} 1.25ml of 1000ppm Std Li^{+}
7*	Ca^{2+} Mg^{2+} Li^{+} Fe^{3+}	200ppm Ca^{2+} 100ppm Mg^{2+} 40ppm Fe^{3+} 20ppm Li^{+}	50ml of 1000ppm Std Ca^{2+} 25ml of 1000ppm Std Mg^{2+} 10ml of 1000ppm Std Fe^{3+} 5ml of 1000ppm Std Li^{+}

Notes: The iron is added to standards 6 & 7 because in some analyses, these ions may be present when other substrates are used for this experiment, e.g. siderite. Fe^{3+} should not be present in this experiment using sand.

Experimental Procedure:

1. Prepare FW brine according to the composition as provided in Table 3.2. Stir and leave it for 24 hours so that the brine is homogeneous.
2. Filter the FW brine through 0.45um filter paper. This is to remove any dirt and physical impurities.
3. Use the filtered brine to prepare a 10,000ppm SI stock solution.
4. Use this stock solution to prepare the different SI concentrations for the adsorption test in the test brine. Refer to Table 3.3 for detail calculation.
5. Weight appropriate amount (10g, 20g or 30g) of substrate (sand, kaolinite or siderite) into 150ml plastic bottles.
6. pH adjust all stock solution (blank & SI/FW samples) to the required pH, i.e. pH 4. Record the pH values, before and after adjusted – pH_o @ 20^oC / room temperature.
7. After pH adjusting all the stocks, aliquot 80ml into the appropriately labelled / numbered 150ml plastic bottles.

8. Add the pH adjusted test solutions to the bottles containing the minerals and shake well - ensuring thorough mixing, and transfer into a pre-heated oven at 95^{o}C immediately. Note the time the samples are mixed and put in the oven – t_o
9. After approximately one hour, check the bottle lids are tight, to avoid any evaporation.
10. After 24 hours (t = 24), take out the samples from the oven and filter them under vacuum through a 0.20 µm pore size filter paper. Filtration is carried out at the specific temperature of interest in that experiment. For example, samples from these 95˚C experiments are filtered immediately after they are taken out of the oven. Transfer the filtrate into labelled / numbered 150ml plastic bottles.
11. After the temperature has settled to room temperature, measure the pH of the filtrate samples and record the values – pH_f @ 20^{o}C / room temperature. Be consistent with the timing when the bottles are stabilized and the pH is measured.
12. Prepare some diluent solution (see diluent preparation).
13. Prior to ICP analysis, dilute 1ml samples in 9ml of 1% Na^+ (aq) diluent solution. Use 10ml test tubes. The initial stock solutions of each concentration retained earlier are diluted – to confirm C_o values (initial concentrations), and the filtrate samples are diluted in the same way, to find C_f values (final concentrations after the adsorption process).
14. ALL stocks and samples are analysed by ICP to confirm C_o values, i.e. $[SI]_o$, $[Ca^{2+}]_o$, $[Mg^{2+}]_o$ $[Li^+]_o$ and find $\mathbf{C_f}$ values, ie. $[SI]_f$, $[Ca^{2+}]_f$, $[Mg^{2+}]_f$, $[Li^+]_f$ in order to determine the effect of the adsorption process.
15. The amount of SI retained by the mineral, Γ (in mg SI/ g rock), was calculated using the expression $\Gamma = V\left(c_o - c_f\right)/m$ (where c_o and c_f are the initial and final SI concentrations respectively, V is the SI solution volume and m is the mass of substrate). Figure 3.1 shows the schematic diagram of how coupled adsorption and precipitation occur and this could be interpreted as an "apparent adsorption", $\Gamma_{App.}$

Notes:

The above procedure are applicable for both Static Compatibility Test and Static Coupled Adsorption/Precipitation Test, with a few exception for Static Compatibility Test, as follows;

1. There is no mineral involves, as such no mixing between pH adjusted stock solution and minerals. The pH adjusted stock solutions are to be placed into the pre-heated oven immediately.
2. The filtered precipitates on filter paper are weighted and sent for ESEM-EDAX analysis to quantify the amount of phosphorous, calcium and magnesium.

Notes: Disposal procedure= dilute solution can be washed down the sink with copious amounts of water.

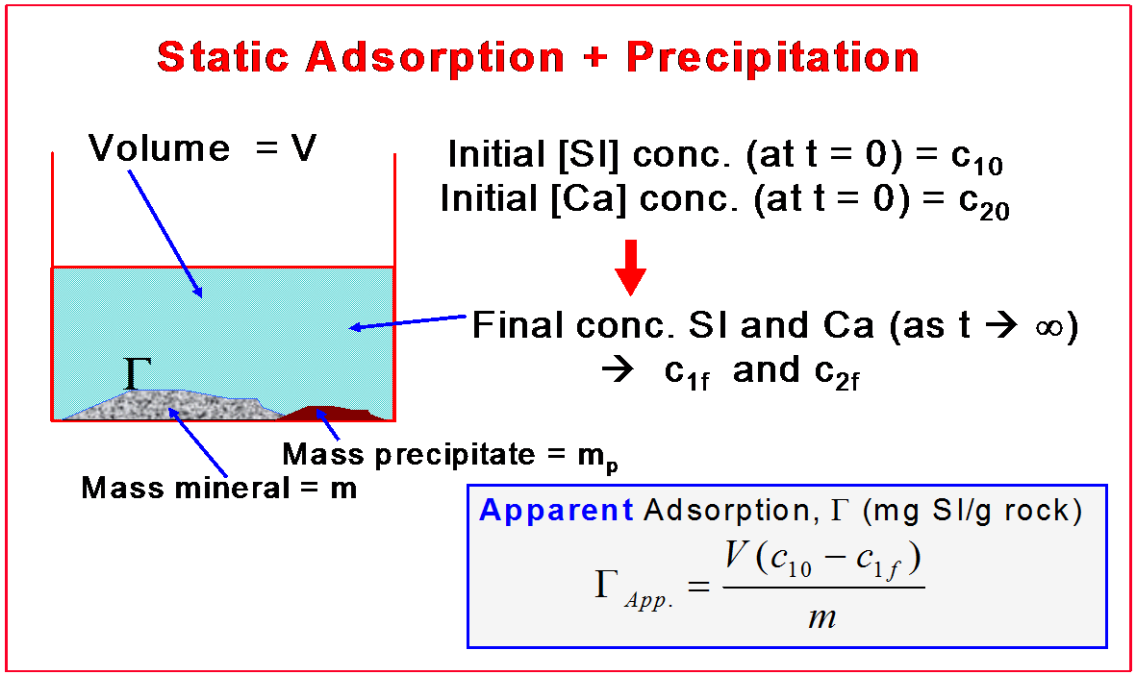

Figure 3.1: Schematic showing how both coupled adsorption and precipitation can occur.

3.3 NON-EQUILIBRIUM SAND PACK EXPERIMENTS

Non-equilibrium experiments are conducted to analyze the effect of both, (i) the adsorption and coupled adsorption/precipitation processes and (ii) the flow rate (non-equilibrium/kinetic effects), on the SI effluent concentrations. Theoretically, the effluent concentration changes as the flow rates changes if the system is not fully at equilibrium. Analysis of the return profile of each flood allows us to make comparisons between precipitation and adsorption floods. The concentrations of calcium and magnesium were also analyzed to investigate their involvement in the retention mechanism.

3.3.1 Objective

The objective of these floods was to investigate the adsorption-desorption and precipitation-dissolution characteristics of pure adsorption and coupled adsorption/precipitation squeezes at various flow rates for OMTHP SI and SAND minerals. The data from these can then be used to validate the various mathematical models which have been proposed for these processes (Sorbie, 2010).

3.3.2 Materials

Scale Inhibitor: The SI used in the non-equilibrium sand pack work is the hexa-phosphonates, OMTHP which is 30% active. This scale inhibitor is one of a range of commercial products used in oilfield applications (Briquest). Refer to Chapter 4 for structure and properties of the OMTHP SI. All inhibitor solutions were prepared in the standard Nelson Forties Formation Water (NFFW), composition in Table 4.1. The postflush or back production stage was carried out with synthetic NFFW degassed under vacuum and pH adjusted to pH= 4. The composition is similar to brine without lithium ion.

For the precipitation floods, 4000ppm OMTHP was introduced into sand pack column; whereas for adsorption floods, in addition to 4000ppm, 500ppm and 2000ppm OMTHP SI was injected.

Minerals: Refer to Chapter 4 for details of the silica sand characterisation. Silica sand was chosen as the solid phase since it represents a simple model of a sandstone formation and the results are also very reproducible. The sand used in these experiments is commercially available (BDH GPR, 40-100mesh) from VWR.

Brine: This brine is Nelson Forties Formation Water (NFFW), similar to the one used for static adsorption and compatibility tests. Refer to Table 3.2 above for composition and details of the brine.

For Static Adsorption and Compatibility Tests, no degassing is required. Whereas, for non-equilibrium sand pack experiments, degassing is required as the fluid passes through the core or sand pack at high temperature, and any degassing may influence the calculation of pore volume, porosity and permeability. Generally, for every litre of brine, it is degassed for an hour. `

Post Flush: There are two types of post flush used in this experiment. The most common case is where a similar postflush composition to the original brine composition is applied but usually without any lithium ion present. It is degassed under vacuum and pH adjusted to pH4. The alternative post flush which is used in this work is 1% Na^+, which is also degassed and adjusted to pH4.

Tracers: Lithium ion is used as a tracer for all the floods in these experiments. Lithium is known as an inert tracer, which does not react with brine, scale inhibitor or sand. Lithium tracer ions are incorporated within the scale inhibitor slug in order to allow direct comparison of the inhibitor and tracer profiles for inhibitor retardation (due to any retention mechanism) and at the end of a particular inhibitor flood.

Iodide ions may be introduced in the synthetic brine as sodium iodide (NaI) where it is used as a tracer to determine the dead volume and pore volume of the sand pack in this study. Iodide tracer analysis is used to characterise the sand packs in term of pore volume prior to an inhibitor flood. The iodide ion can be detected by UV in-line in our floods i.e. it can be analysed directly as the fluid exits the sand pack and we do not need to gather samples and analyse it later (as for Li^+ for example).

3.3.3 Experimental Methodology

Experimental Apparatus

The sand pack experimental set-up consists of the following apparatus:

- High pressure liquid chromatography (HPLC) Pump - Pharmacia Pump P-500
- Pressure transducer (only if permeability is measured)
- High pressure glass column (Pyrex)
- UV spectrophotometer
- Magnetic stirrer
- Auto diluter
- ICP
- Fraction collector -Pharmacia LKB FRAC-100
- Vacuum filter funnel & vacuum pump.

A schematic diagram of the sand pack flooding apparatus is shown in Figure 3.2 and this is essentially a one dimensional (1D) flow experiments. The apparatus was designed to carry out low pressure flooding experiments. The main components are a sand pack column, water bath, pump or a feed unit for injection of fluid into the porous bed, UV spectrophotometer and a sample collector. The column fitting and tubing for the sand pack model were supplied by Anachem. The sand pack column is made from heavy walled borosilicate pyrex glass, which allows a clear view of the packing and provides a metal free environment in which undesirable chemical reaction between the flowing fluid and the conducting media is avoided. Refer to Figure 3.3 for an actual view of the sand packed in the column. The column has an internal diameter of 1.50cm. The associated inlet and outlet fittings have an average dead volume of ~1.36ml. The dead volume determination is very important for accurate effluent profile calculations since a correction factor must be used to allow for this in the effluent profiles. A wet slurry method was adopted for packing the sand in order to prevent the formation of air bubbles in the column and to minimise sagging of the sand. The fluids were injected into the porous pack using a Pharmacia P-500 model HPLC pump. As the fluids exited the sand pack samples were collected in an automatic fraction collector (Pharmacia LKB FRAC-100 model) capable of operating by time intervals. Alternatively, in some

floods the fluids were passed through a UV/Vis Spectrophotometer for in-line iodide tracer analysis.

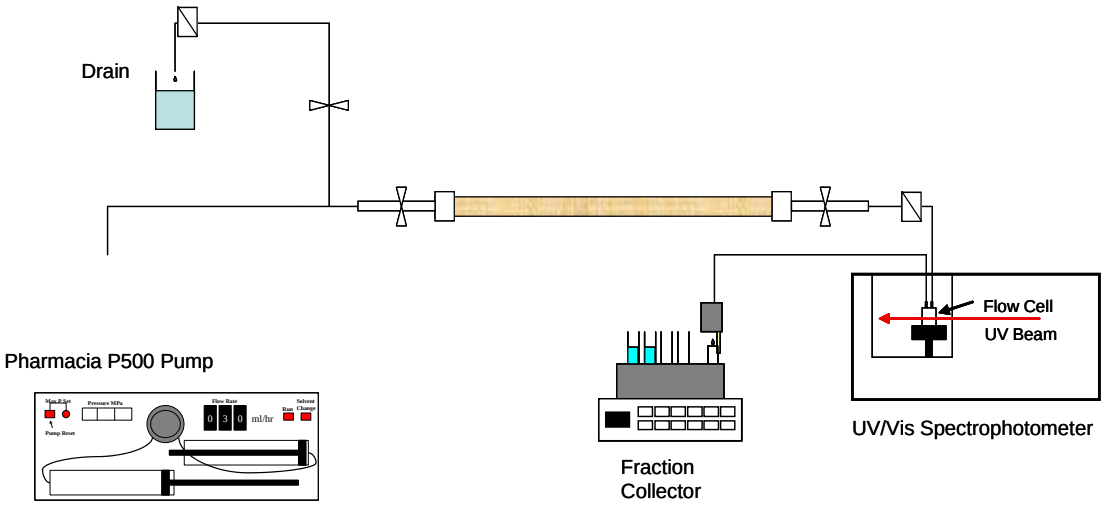

Figure 3.2: Schematic Diagram of the Sand Pack Flooding Apparatus

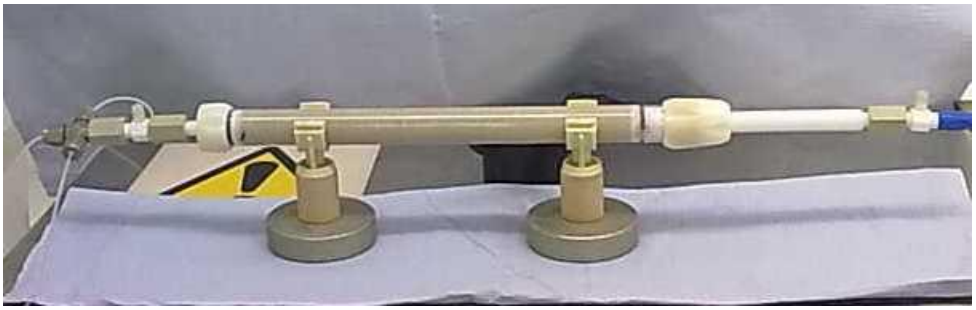

Figure 3.3: Actual view of sand packed in the column

Packing Technique

The column packing method used in this work was the wet slurry packing method. In this method, a very reproducible, air free and homogeneous sand pack can be produced. Care must be taken to ensure that the sand and the model were free from any impurities before and after packing. Figure 3.4 shows the set up of the sand pack in the column with the procedure introduced as follows:

1. Mix a constant mass of sand with 6% NaCl for 1 hour to prevent dusting during dry mixing.
2. One end piece is fitted first and then the 6% NaCl solution is introduced to fill about 1/3 of the column length.
3. Open the valve connected to the bottom end fitting to allow the 6% NaCl solution in the column to flow out slowly to adjust the liquid level.
4. Load the column with sand slurry until it is 1 or 2 cm from the top of the column.
5. Close the valve and take out the excess solution using syringe.
6. The second end piece is fitted once the column has been loaded
7. The column is connected to the pump and the UV Spectrophotometer.

The 6% NaCl solution is used to prepare the slurry because it is the suitable salinity to prevent any precipitation with divalent cation if it is to be prepared with formation water brine. The 6% NaCl is also suitable as to prevent early swelling effect on the sand.

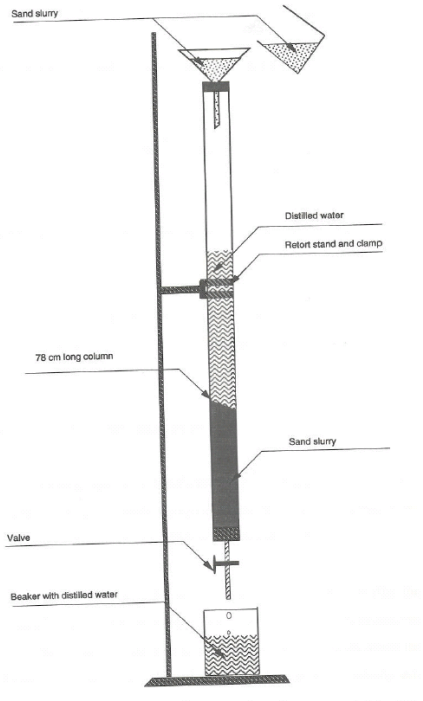

Figure 3.4: Schematic diagram of sand pack "packing" technique

Sand Pack Characterization

Dead Volume Measurement: The dead volume determination is carried out by connecting two end pieces of an empty column (without sand packed in the column) as shown in Figure 3.5. The solutions that were required for this test are the synthetic NFFW with the composition as in Table 3.2 or any base brine used to make scale inhibitor solutions for a particular experiment, and 10ppm sodium iodide in NFFW. Sodium Iodide is an inert tracers which is used in the in-line tracer experiments to determine dead volumes, pore volume etc.

For the dead volume determination using iodide tracer, the pump is first flushed (solvent changed) with the synthetic formation brine to purge out the previously used brine in the pump. The column is then flushed with the same formation brine to get the UV/Vis baseline level. The column is then injected with the iodide tracer solution. The UV/Vis Spectrophotometer is automatically started and logs the iodide tracer that passes through the exit cell using UV light. The system was allowed to reach the full input concentrations before the test was stopped. The tracer brine is then displaced by the non-tracer brine and a second dead volume calculation is made. The average of the two values is taken as the final dead volume measurement.

For dead volume characterisation using lithium tracer (Li^+), the analysis is done using Inductively Couple Plasma Optical Emission Spectroscopy (ICP-OES). Lithium tracer is used to investigate the true dead volume of the tubing that flows to the fraction collection as the remainder of the experiment will use the fraction collection line. The shape of the Li^+ or iodide tracer profiles can also be used to diagnose heterogeneity within the sand packs.

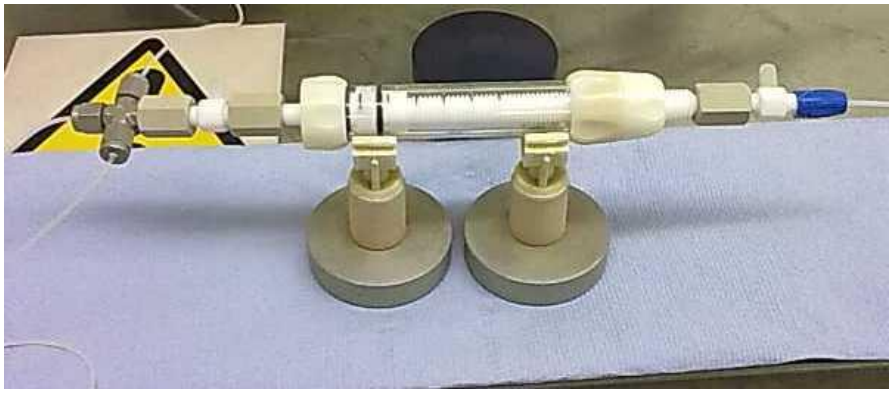

Figure 3.5: Column without sand for dead volume measurement

Pore Volume and Porosity Measurement

The iodide tracer flood was carried out to determine the pore volume and porosity of the sand pack. The pore volume determination is done by using the same method as described above with sand pack placed in the system. For each sand pack, the pore volume characterisation is done by flowing in the iodide tracer into the pack and measuring the effluent profile using the UV Vis Spectrophotometer. The remaining procedure for pore volume characterisation follows the same procedure as in dead volume characterisation using the iodide tracer. The porosity can then be calculated from the pore volume value obtained from the experiment by determining the fraction of the sand pack volume available for fluid flow.

The values of dead volume and pore volume are important to determine the total volume that needs to be injected during the main treatment and post flush of the squeeze experiment. The dead volume determination is measured at room temperature ($T=20^0C$) while the pore volume determination is carried out at 95^0C. Table 3.3 shows results for the the dead volume, pore volume and porosity of all the sand packs used in this study. In all the experiments reported later in this thesis, the pore volume at room temperature will be used for all calculation.

Sand Pack ID	A	C	D	E	F	G
Length (cm)	20.05	20.50	20.40	20.40	20.70	20.9
Diameter (cm)	1.5	1.5	1.5	1.5	1.5	1.5
Dead Volume (ml)	1.54	1.54	1.24	1.34	1.34	1.34
Pore Volume (ml)	13.64	14.69	14.73	14.60	14.66	14.11
Porosity (%)	38.49	40.52	40.85	40.87	40.06	38.21
Sand Wt. (g)	93.58	95.68	95.21	95.21	96.61	97.87

Table 3.4: Example of Sand Pack Characterization Results

Chemical Preparation:

a. Brine: Synthetic Nelson Forties Formation Water (NFFW)

- Weigh out the correct amount of the salt compounds based on the composition given in Table 3.2.
- Dissolve the salt in the required amount of distilled water.
- Mix and stir the solution for 4-5 hours to allow for adequate mixing.
- Leave the brine for 24 hours before use if 20L brine prepared.
- Filter through 0.45μm filter paper prior to use.
- Degas the brine prior to use. Degas for one (1) hour for every litre of brine.
- Do the pH adjustment to 4 after the pH meter has been calibrated.

b. Tracer: 10ppm Sodium Iodide

- 0.29 gram of Sodium Iodide is weighed out using a 3 figure balance.
- Dissolve the salt in 250ml with formation water brine. This will give 1000ppm of Sodium Iodide solution.
- Pipette 10ml of 1000ppm Sodium Iodide solution and make up to 1000ml with formation water.
- This will give the required 10ppm Sodium Iodide solution.
- Filter the solution with 0.45μm filter paper.
- Degas the solution for 1 hours.
- Do the pH adjustment to 4 after the pH meter has been calibrated.

c. Tracer: 50ppm Lithium Ion

- 3.06 gram Lithium Chloride is weighed out using a 3 figure balance
- Dissolve the salt in 500ml formation water brine. This will give 1000ppm of Lithium Chloride solution
- Pipette 50ml of 1000ppm Lithium Chloride solution and make up to 1000ml with formation water to give 50ppm Lithium Chloride solution
- Filter the solution with 0.45μm filter paper
- Degas the solution for 1 hours
- Do the pH adjustment to 4 after the pH meter has been calibrated.

d. 1% Na^+ Diluents Solution

- 1% Na^+ (aq) ≡ 10,000ppm Na^+ (aq) ≡ 25.42g of NaCl (s) / 1L H_2O (l) ≡ 127.10g of NaCl (s) / 5L H_2O (l)
- Dissolve 127.10g of NaCl (s) in 5L of distilled water.

e. 4000ppm active SI Solution with 50ppm Lithium ion in NFFW

- Determination of the amount of scale inhibitor needed:

  4000ppm = 4000mg/L = 4 g/L as supplied @30% active

  X (g) = 4 x (4000/active concentration)

  X (g) = 4 x (4000/1200)

  = 13.33 g/L

- Weigh out 13.33g OMTHP SI, commercial name = Briquest 684-30S
- Dissolve the scale inhibitor in 1000ml formation water brine that contains 50ppm Lithium for inert tracer and scale inhibitor adsorption comparison
- Filter the solution with 0.45μm filter paper
- Degas the solution for at least 1 hour
- Do the pH adjustment to 4 after the pH meter has been calibrated.

f. Preparation of Standards used for Diluted Samples for ICP analysis

OMTHP at 30% active is used for all calculation to elaborate the procedure.

2,500ppm = 2,500 mg/L = 2.5 g/L as supplied

@ 30% active (as written on supplier bottle)

x (g) = 2.5g x (2500/active concentration)

x (g) = 2.5 x (2500/750) = 8.3333 g/l

Therefore to prepare 250ml of 2,500ppm active OMTHP, (8.3333/4)g = <u>2.08 g</u> is required.

The diluent / matrix used is 1% Na^+ (aq) ≡ 10,000ppm Na^+ (aq). 250ml of each standard will be prepared.

Standard Number	Constituent(s)	Active Concentration(s)	Dilution requirements, in 1% Na^+ (aq), using a 250ml volumetric flask
1	Only 1% Na^+ (aq)	N/A	N / A
2	OMTHP	5ppm	25ml of Standard 3
3	OMTHP	50ppm	25ml of Standard 4
4	OMTHP	500ppm	50ml of Standard 5
5	OMTHP	2500ppm	* 2.08g of OMTHP SI
6**	Ca^{2+}	50ppm Ca^{2+}	12.5ml of 1000ppm Std Ca^{2+}
	Mg^{2+}	25ppm Mg^{2+}	6.25ml of 1000ppm Std Mg^{2+}
	Li^+	10ppm Fe^{3+}	2.5ml of 1000ppm Std Fe^{3+}
	Fe^{3+}	5ppm Li^+	1.25ml of 1000ppm Std Li^+
7**	Ca^{2+}	200ppm Ca^{2+}	50ml of 1000ppm Std Ca^{2+}
	Mg^{2+}	100ppm Mg^{2+}	25ml of 1000ppm Std Mg^{2+}
	Li^+	40ppm Fe^{3+}	10ml of 1000ppm Std Fe^{3+}
	Fe^{3+}	20ppm Li^+	5ml of 1000ppm Std Li^+

Notes: **The Iron is added to standards 6 & 7 because in some analyses, this ion may be present when other substrates are used for this experiment, e.g. siderite. Fe^{3+} should not be present in this experiments using sand.

g. Preparation of Standards used for Neat Samples for ICP analysis in NFFW.

Use Main Treatment at 2000ppm active as initial stock

The diluent / matrix used is NFFW. 250ml of each standard will be prepared.

Standard Number	Constituent(s)	Active Concentration(s)	Volume required in 250ml volumetric flask
1	NFFW	n/a	n/a
2 (Stock)	OMTHP	2000ppm active	Use prepared stock
3	OMTHP	500ppm	62.5 of Std-2
4	OMTHP	50ppm	25 ml of Std-3
5	OMTHP	5ppm	25 ml of Std-4

6	OMTHP	0ppm	n/a

Notes:

Referring to the (g) preparation of standards used for neat samples for ICP analysis in NFFW; it is advisable to make 2500ppm again from neat to check that the solution is diluted first from Sand Pack stock correctly.

Sand Pack SI Flood - Experimental Procedure

The procedure comprises the injection of a scale inhibitor (SI) slug into the pre-conditioned substrate (in this case, the sand pack), followed by a shut-in for a certain period of time to allow the adsorption/precipitation to take place. For all the sand packs in these experiments, the shut in took place at 95°C. This is followed by post flushing with a synthetic NFFW brine (with various compositions as specified) where desorption/dissolution will then take place.

The procedure applied in the sand pack study replicates to some extent the squeeze treatment process carried out in the actual production well. The test was started by pre-flushing the sand pack to pre-condition it with synthetic NFFW brine (or any base brine used to make scale inhibitor concentrations) solution at a flow rate of 20ml/hr**.** Pre-flushing is carried out at room temperature in order to prevent any precipitation in the pack. This is followed by a main treatment, i.e. injecting the scale inhibitor into the pack at 20ml/hr, which is also carried out at room temperature. The total volume of scale inhibitor to be injected is approximately 10PV, where the objective is to inject the scale inhibitor into the pack until maximum concentration is reached i.e. the pack is fully saturated with SI at input concentration. The effluent samples were collected every 2ml for the duration of the injection stage. All these samples were collected in a fraction collector and analysed later by the ICP.

After the main treatment, the sand pack is shut-in for at least 20 hours in the water bath which is then set at 95^{o}C. At this stage all the injected scale inhibitor solutions are expected to have reached maximum equilibrium adsorption or precipitation on the mineral sand.

After the shut-in, the system is post-flushed by injecting the synthetic NFFW brine into the system at various rate (refer to Table 3.5) at reservoir temperature of 95°C. At this stage a large volume of post flush must be injected into the pack (typically 11+PV). The idea is to continuously flush out all the adsorbed/retained scale inhibitor in the pack until a low [SI] in the effluent is reached; this low concentration is equivalent to a nominal "minimum inhibitor concentration" (MIC) of about 1ppm or until the concentration stabilizes. Over all of this postflush period, effluent samples were collected as shown in Table 3.5. All of these samples were collected in a fraction collector and diluted 1 in 10 for the first 60 samples (1ml of sample in 9ml of 1%Na^+ solution = 10ml per sample). All the samples were analysed by ICP for calcium, lithium, magnesium, and phosphorus (SI) concentrations.

Step-by-Step General Experimental Procedure:

Dead Volume Measurement

1. To calculate dead volume; connect the end pieces without sand pack and perform in-line trace in/out with 10ppm iodide in NFFW.
2. The pump must first be flushed with the synthetic formation water brine (NFFW) to purge out the previously used brine in the pump.
3. Flush with NFFW to get the UV/Vis spectrophotometer baseline level.
4. Solvent change the pump with the iodide tracer solution to condition the pump with the solvent required for the test.
5. Inject the pack with the iodide tracer solution. Switch on the UV/Vis spectrophotometer as soon as the first drop appears at the outlet end of the tubing.
6. Stop the pump and UV-Vis when the system reaches the plateau. Save the UV file.
7. Solvent change to non-dosed FW. Repeat steps 5-6 for the trace out.
8. Repeat the dead volume determination with lithium tracer by using the same procedure as the iodide tracer.
9. Send the effluent samples collected by fraction collector to ICP for analysis of lithium ion to determine the dead volume.

Pore Volume and Porosity Measurement

10. After loading the column with minerals equilibrate the column with NFFW (pH4) at flow rates of (30-250) ml/hr for 1hr until steady ΔP.
11. (Trace in) Pump several pore volumes of 10ppm iodide in NFFW (pH4) at 150 ml/hr and analyze for iodide using the in-line UV spectrophotometer to calculate the pore volume.
12. (Trace out) inject NFFW (pH4) at flow rate of 150 ml/hr.
13. Place Pack in water bath at 95'C.
14. Repeat stages 10-12 at 95'C.
15. Remove pack from water bath.
16. Repeat stages 10-12 at room temperature.

Main Treatment and Post Flush

17. Preflush to precondition the column with NFFW (pH4) at 150 ml/hr at room temperature.
18. Main treatment: Introduce the prepared scale inhibitor and (50ppm Li^+) lithium tracer in NFFW (pH4) at a flow rate of 30 ml/hr and collect every 2 ml of the effluent (2ml sample/4min) for 160 min (48 samples) at room temperature.
19. The inhibitor flow is stopped after (3PV to 5PV) pore volumes when 100% injected inhibitor concentration is recorded in the effluent.
20. Place the pack back into the water bath at 95'C. Shut-in overnight (24 hrs). The remainder of the experiment will now take place in the water bath at 95'C
21. Post-flush treatment: Collect every 2ml of the effluent in the first 2PV (32 samples); 5ml for 5PV (32 samples) and 10 for 10PV (32 samples) (i.e. Post-flush the packed column with NFFW (pH4) until the [effluent] drops below minimum inhibitor (active) concentration).
22. The collected samples for the main treatment and initial post flush are diluted 10 times (1ml of sample in 9ml of 1% Na^+ solution = 10ml total) and analyzed (using ICP) for calcium, lithium, magnesium, inhibitor (Phosphonate based inhibitors) and pH is monitored.

23. Late post-flush samples are analyzed 'neat' (i.e. no dilution) using the FW standards prepared in (f) to determine the [SI].

Sand Pack ID	Flood Type	Main Treatment					Shut-In		Post Flush		
		[SI] (ppm)	[Ca] (ppm)	pH	T (°C)	Q (ml/hr)	T (°C)	T (hrs)	T (°C)	Q (ml/hr)	[Ca] (ppm)
SP-A	Pptn	4000	2000	4	20	20	95	>20	95	20	2000
SP-C	Pptn	4000	2000	4	20	20	95	>20	95	20 10 5 5 2	2000 2000 2000 2000 2000
SP-D	Pptn	4000	2000	4	20	20	95	>20	95	20 20 10 5 2	2000 0 0 0 0
SP-E	Ads	500	2000	4	20	20	95	>20	95	20 10 5 2	2000 2000 2000 2000
SP-F	Ads	4000	428	4	20	20	95	>20	95	20 10 5 2	428 428 428 428
SP-G	Ads	2000	428	4	20	20	95	>20	95	20 10 5 2	428 428 428 428

Table 3.5: Summary of Experimental Details of Adsorption and Precipitation Flood

Notes: Between each flow rate, shut-in took place for more than at least 20 hrs

CHAPTER 4: ESTABLISHING RETENTION MECHANISMS THROUGH STATIC COMPATIBILITY AND COUPLED ADSORPTION / PRECIPITATION EXPERIMENTS SAMPLES

4.1 INTRODUCTION

The retention of the scale inhibitor (SI) within the formation is central to a squeeze treatment having a long lifetime (Kerver and Heilhecker, 1969; Miles, 1970; Vetter, 1973; King *et al*., 1985, 1989; Yuan *et al*., 1993; Boreng *et al*., 1994 and Sorbie *et al*., 1994). Scale inhibitors are retained within porous media by the two main mechanisms of "***adsorption***" (Γ) and "***precipitation***" (Π) . There is not complete agreement in the literature about when we should use one mechanistic description or another and three "schools" of thought on the retention issue have emerged, as follows:

(i) Heriot-Watt University (HWU) – where adsorption is described by a generalised adsorption isotherm, Γ(C), and precipitation is described by a solubility function, Π(C), and a dissolution rate constant (denoted, r_2);

(ii) Halliburton – Gdanski and Funkhouser(2001) describe retention through an adsorption mechanism based on the specific mineralogy of the (sandstone) rock;

(iii) Rice University – describe SI retention by a precipitation/dissolution mechanism based on the precipitation and solubility of the various Ca-SI salts that are formed.

Field SI squeeze treatments have been modelled quite successfully using all three of the above approaches, but often the field observations are not accurate enough to distinguish clearly between different models. A detailed analysis of a given retention mechanism – for example pure adsorption or coupled adsorption and precipitation – requires careful laboratory experiments at the appropriate "field relevant" conditions. A central objective of current research within the FAST group at Heriot-Watt University is to (i) provide data for the development of a fully consistent generalised model that can describe both coupled* adsorption and precipitation, and (ii) devise experiments which can test this model experimentally. (*By "coupled" here, we mean that the SI species

may be involved in *both* adsorption and precipitation and hence these processes are not independent. This feature must consistently and correctly described by any mathematical model of the coupled processes).

In this chapter, we present the results on static compatibility and coupled adsorption/precipitation experiments using a range of phosphonate scale inhibitors and several minerals. Scale inhibitors DETPMP (a penta-phosphonate) and OMTHP (an hexa-phosphonate) are used to study this behaviour. These experiments were carried out at a range of fluid volume/adsorbent mass ratio, since, as we will show below, this indicates whether we are in the purely adsorbing or in the coupled adsorption/precipitation regime. For the static adsorption tests; m = 10g, 20g and 30g sand, kaolinite and siderite were used (with a fixed volume of SI solution; V= 80ml)) as minerals to analyse the adsorption behaviour. On the other hand, static compatibility test were conducted with no minerals present, and these are used to determine whether or not any pure precipitation is observed. The experimental results for phosphonate scale inhibitors show excellent agreement with the theory in different regions of pure adsorption and coupled adsorption/precipitation. These results show clearly how such laboratory measurements should be carried out to determine both the levels of SI retention and the precise retention mechanism.

4.2 BACKGROUND AND NOMENCLATURE

Chemical scale inhibitors (SI) are applied routinely in downhole "squeeze" treatments to prevent mineral scale formation (Kerver and Heilhecker, 1969; Miles, 1970; Vetter, 1973 and King *et al*., 1985, 1989). One of the most important issues in this process is how long the squeeze lifetime will last where this lifetime is defined as the time until the returned SI concentration drops below the MIC (Minimum Inhibitor Concentration) to prevent/delay scale formation. The squeeze lifetime in turn depends very strongly on precisely how – i.e. through which *mechanism* - the SI is "retained" within the porous medium. To assist the discussion on this chapter we clarify the terms we use in the following terminology:

4.2.1 Retention

"***Retention***" refers to ***any*** mechanism whereby the scale inhibitor (SI) is held back or "retained" in the porous medium relative to an inert non-interacting tracer species e.g. by adsorption, precipitation, etc. The SI may be released in various ways related to the actual retention mechanism (see below);

4.2.2 Adsorption/Desorption

"***Adsorption/Desorption***" or pure adsorption refers to the retention mechanism where SI is physically or chemically adsorbed onto the mineral surface of the porous medium. It is normally described by an **adsorption isotherm**, $\Gamma(C)$ (King *et al*., 1985; Boreng *et al*., 1994; Sorbie *et al*., 1991, 1992 and Hong and Shuler, 1998), although this adsorption level may be a function of several variables e.g. $\Gamma=\Gamma(C, [Ca^{2+}], pH, \text{and } T)$ (Sorbie *et al*., 1993, 1993, 2005; Zhang *et al*., 2000 and Gdanski and Funkhouser, 2001). The adsorption process may be kinetic in that it is described by a rate law (Sorbie, *et al*., 1992, 2005; Zhang *et al*., 2000 and Gdanski and Funkhouser, 2001). The SI is released by "desorption" which may again occur (practically) at equilibrium – i.e. in a manner fully consistent with the equilibrium adsorption isotherm. Alternatively, desorption may be kinetic in that it is described by a desorption rate law which after sufficient time will come to equilibrium consistent with the isotherm. There are no distinct objects known as "adsorption isotherms" and "desorption isotherms" as we will explain here: There are only adsorption and desorption "rate laws" which – under full equilibrium conditions – give rise to a single adsorption isotherm. Various assumptions can be made about the mathematical form of the adsorption isotherm e.g. Freundlich, Langmuir etc. Here, we assume the Freundlich form in the following developments, but this does not affect the generality of our later conclusions.

4.2.3 Precipitation

"Precipitation" refers to the mechanism where the SI actually precipitates (becomes insoluble) or "phase separates" and this particulate or flocculated "precipitate" is hence retained within the porous medium. In a precipitation process, we envisage the precipitation occurs by the formation of the calcium salt of the SI. Assuming a

precipitation reaction such as $SI + n_2.Ca \rightleftarrows SI\_Ca_{n_2}$, where n_2 Ca ions may bind to a single SI molecule. The solubility of this sparingly soluble salt would be described by an equilibrium solubility product, K_{sp}, of the form: $K_{sp} = [SI].[Ca]^{n_2}$. However, a more complex form of this precipitation law may be formulated but again this derives from the steady-state form of the various rate laws for deposition and re-dissolution, as explained in detail in this chapter.

4.3 THEORY OF COUPLED ADSORPTION AND PRECIPITATION

The discussion of when SI "adsorption" and/or "precipitation" are occurring in a given system provides much confusion to the oil industry. Hence, detailed and clear description of these processes will be put forward since it is straightforward to establish experimentally when adsorption or adsorption/precipitation is taking place for a given porous medium (or a mineral separate), SI, brine composition, pH and temperature (T).

4.3.1 Static Adsorption

A schematic diagram of a static adsorption experiment is shown in Figure 4.1, which is the basic concepts of scale inhibitor adsorption. A SI of initial concentration, c_0 (ppm or mg/L), in a volume, V (L), is allowed to come to equilibrium with a mass, m (g), of mineral. At equilibrium concentration of the SI, c_{eq}, then by material balance the adsorption level is as follows:

$$\Gamma = \frac{V(c_0 - c_{eq})}{m} \tag{5.1}$$

where in the units used, then Γ is in mg of SI/g of rock. The apparent adsorption isotherm may depend on the mass/volume (m/V) ratio if a coupled adsorption/precipitation process occurs. However if the pure adsorption is the main mechanism of the bulk inhibitor then the adsorption results at different m/V ratio will change along the isotherm curve. In this case it is clearly observed that the apparent adsorption is not a function of the m/V ratios. Therefore plotting adsorption Γ vs. inhibitor concentrations C and doubling the mass/volume ratios (m/V) would appear to reduce the results to the half values for the apparent adsorption which is coupled inhibitor adsorption/precipitation, but we know that at low inhibitor concentrations

region the pure adsorption isotherm is responsible.

Figure 4.2 shows measured experimental static adsorption isotherms, Γ (C), for DETPMP on crushed core material. At various pH values, 2, 4 and 6 at T = 25^{o}C (Yuan *et al*, 1994). It is quite clear from these results that the level of SI adsorption is also strongly dependent on pH as well as on [SI] and hence we should strictly write, $\Gamma = \Gamma$ (C, pH) or $\Gamma = \Gamma$ (C, [H^{+}]). However, for the moment, we will persist with simpler assumption that Γ is a function of C = [SI] only.

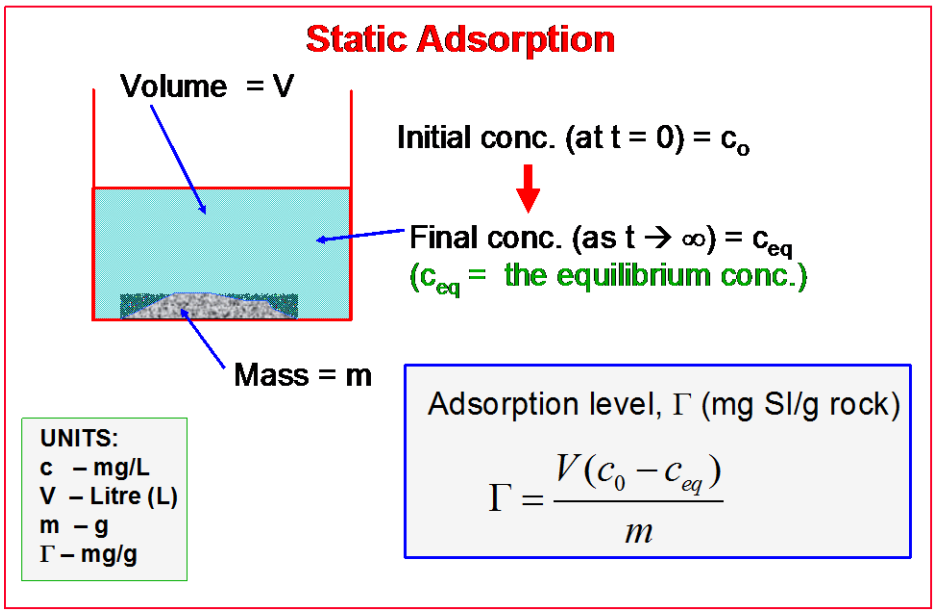

Figure 4.1: Shows the process of simple static adsorption on a porous medium comprising a mineral separate, of mass m e.g. sand, kaolinite, siderite etc. See units.

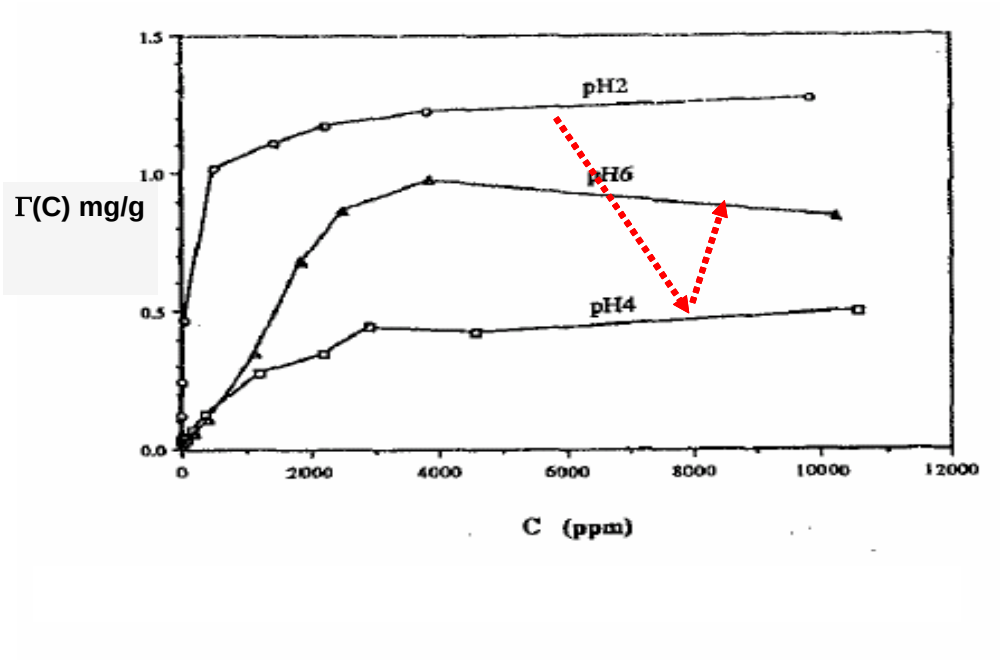

Figure 4.2: Experimental static adsorption isotherms, Γ(C), for DETPMP on crushed core material. At various pH values, 2, 4 and 6 at T = 25°C (Yuan *et al*., 1994).

4.3.2 Coupled Adsorption/Precipitation

The analysis for pure adsorption can be extended to the case where both adsorption and precipitation can occur simultaneously. This is shown schematically in Figure 4.3, where we envisage that precipitation occurs by the formation of the calcium salt of the SI, SI_Ca_n, as follows:

$$SI + n.Ca \rightleftarrows SI\_Ca_n \tag{5.2}$$

where n Ca^{2+} ions may bind to a single SI molecule. The solubility of this sparingly soluble salt would be described by an equilibrium solubility product, K_{sp}, of the form:

$$K_{sp} = [SI].[Ca]^n \tag{5.3}$$

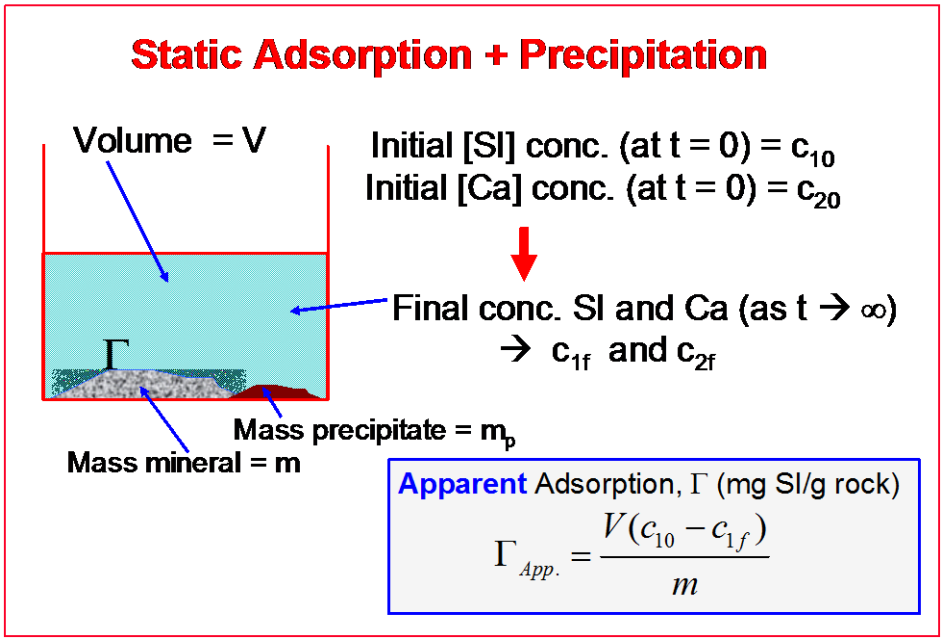

Figure 4.3: Schematic showing how both coupled adsorption and precipitation can occur showing how this could be interpreted as an "apparent adsorption", $\Gamma_{App.}$

The following additional notation is introduced in Figure 4.3:

- c_{10} and c_{1f} - initial (t = 0) and final equilibrium (t→ ∞) Sl Molar concs. (M);
- c_{20} and c_{2f} - initial (t = 0) and final equilibrium (t→ ∞) Ca Molar concs. (M);
- Γ is the adsorption which depends on c_{1f}, $\Gamma = \Gamma(c_{1f})$ (mg/g);
- the precipitation process depends on both c_{1f} (Sl conc.) and c_{2f} (Ca conc.) through K_{sp} as follows: $K_{sp} = (c_{1f}).(c_{2f})^n$ in this notation when the system is at equilibrium; units of K_{sp} → M^{n+1};
- m_p is the actual mass of precipitate which forms.

Note that the initial and final values of Sl concentration are c_{10} and c_{1f}. Some of this Sl which is "missing" from the bulk solution is adsorbed and the remainder of it is part of the precipitate. However, if we assumed that *all* of this "missing" Sl is adsorbed, then we would calculate an "apparent adsorption", $\Gamma_{App.}$, as follows:

$$\Gamma_{App.} = \frac{V(c_{10} - c_{1f})}{m} \tag{5.4}$$

which would clearly be an *over*-estimate of the actual adsorption (since some of this

would be precipitate) but it is what would be measured in an actual experiment if the above formula were applied.

In Appendix A, a full derivation of the equations is presented describing coupled adsorption/precipitation based on the view of the process shown schematically in Figure 4.3 (Kahrwad, M et al., 2008). Using the notation above, the final working equation for c_{1f} (the equilibrium [SI]) is given by:

$$c_{10} = c_{1f} + \left(\frac{m}{V.M_{SI}1000}\right).\Gamma\left(c_{1f}\right) + \left(\frac{1}{n}\right)\left(c_{20} - \left(\frac{K_{sp}}{c_{1f}}\right)^{1/n}\right) \tag{5.5}$$

and this equation can be rewritten in the final working form as:

$$F(c_{1f}) = c_{1f} + \left(\frac{m}{V.M_{SI}1000}\right).\Gamma\left(c_{1f}\right) + \left(\frac{1}{n}\right)\left(c_{20} - \left(\frac{K_{sp}}{c_{1f}}\right)^{1/n}\right) - c_{10} \tag{5.6}$$

Where, at equilibrium adsorption/precipitation, we must solve this equation for c_{1f} i.e. find the root of $F(c_{1f}) = 0$. Note that Eq. 5.6 applies *if* (and only if) there is definitely a precipitate i.e. $\left(c_{1f}\right).\left(c_{2f}\right)^n$ > K_{sp}. If there is no precipitate, then the substitution, $c_{2f} = \left(K_{sp}/c_{1f}\right)^{1/n}$, does not apply and the quantity $\left(c_{20} - \left(K_{sp}/c_{1f}\right)^{1/n}\right)$ < 0 which is unphysical. Hence in solving the main working Eq. 5.6, we can use it for all cases of adsorption only or coupled adsorption/precipitation by setting the quantity $\left(c_{20} - \left(K_{sp}/c_{1f}\right)^{1/n}\right)$ to its actual value if it is ≥ 0, or to zero otherwise.

4.4 EXPERIMENTAL DETAILS

Static Adsorption Tests and Static Compatibility Tests were performed to evaluate pure adsorption and coupled adsorption/precipitation behaviour of DETPMP (a Penta-Phosphonate) and OMTHP (an Hexa-Phosphonate) scale inhibitors (SI) with synthetic Nelson Forties Formation Water (NFFW). For static adsorption tests, the experiments were performed using different masses of sand, kaolinite and siderite (m = 5g, 10g, 20g

and 30g) to evaluate the coupled adsorption/precipitation behaviour. In the corresponding static compatibility tests, the experiments were performed to evaluate the *precipitation* behaviour, since no mineral was used in these tests. As such, any lost in concentration of SI during compatibility test must be due to precipitation.

The following experiments were conducted to study the adsorption and coupled adsorption/precipitation phenomena.

1. DETPMP-Sand Static Adsorption/Compatibility at 95°C
2. OMTHP-Sand Static Adsorption/Compatibility at 95°C
3. DETPMP-Kaolinite Static Adsorption/Compatibility at 95°C
4. OMTHP-Kaolinite Static Adsorption/Compatibility at 95°C
5. DETPMP-Siderite Static Adsorption/Compatibility at 95°C

4.4.1 Materials

Scale Inhibitors (SI): Two scale inhibitors were used in this work. They are;

a) Di-ethylene Tetra-amine Penta (methylene-phosphonic acid) or DETPMP, a penta-phosphonate

b) Octa-methylene Tetra-amine Hexa (methylene-phosphonic acid) or OMTHP, a hexa-phosphonate

Both SIs are from the phosphonate family group. They are commercial products widely used in oilfield applications. Figure 4.4 and Figure 4.5 show the structure and properties of DETPMP and OMTHP, respectively. Appendix B table shows a table of the material safety data sheet (MSDS). All SI concentration with lithium tracers were prepared in standard synthetic NFFW and were pH adjusted to any suitable value chosen for these experiments. Inductive Coupled Plasma (ICP) analytical method (Water Analysis Handbook, 1989) was used in this study for many of the elements e.g. P, Ca, Mg, Li etc., and we are able to assay down to <1ppm (±0.2ppm) for all of these species. Results for different SI concentrations using phosphonate inhibitors with sand mineral were conducted earlier by Kahrwad *et al*. (2008).

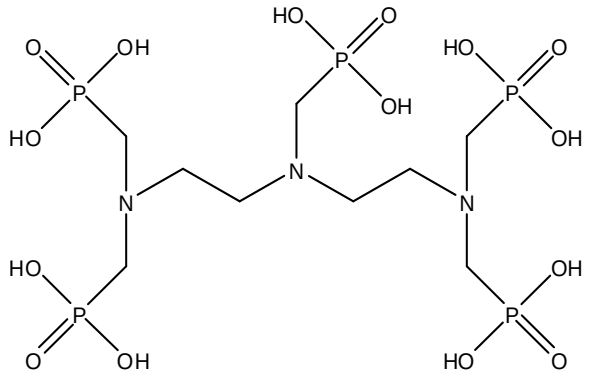

Properties	
Appearance	- Brown liquid
Iron (as Fe)	- 100ppm max
Chloride (as Cl)	- 6% w/w max
Active Solids (as acids)	- 45% w/w
pH (1% w/v soln, 20 C)	- 2 max
SG (20 C)	- 1.20 – 1.26
MWt.	- 573.25 g/mol

Figure 4.4: DETPMP SI structure and properties

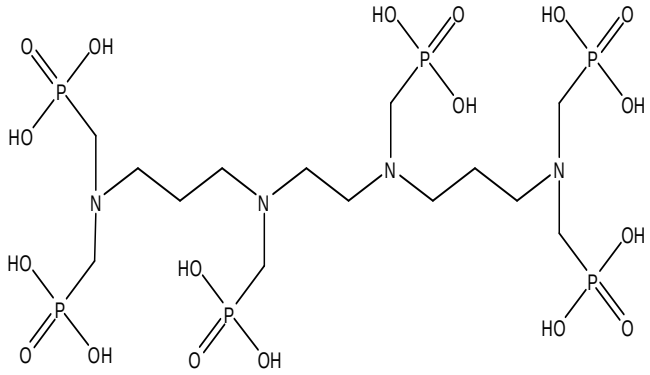

Properties	
Appearance	- Amber liquid
Iron (as Fe)	- < 30ppm
Chloride (as Cl)	- < 6%
Active Solids (as acids)	- 30% w/w
pH (1% w/v soln, 20 C)	- 2
SG (20 C)	- 1.34
MWt.	- 738.40 g/mol

Figure 4.5: OMTHP SI structure and properties

Minerals: Three types of minerals were used in the work, viz. sand, kaolinite and siderite, to study the retention of scale inhibitor onto these minerals.

Dry silica sand (BDH GPR, 40 – 100 mesh, purified by acid) was chosen as one of the adsorbent as the majority of sandstone rock is quartz and hence silica sand represents a simple model of a sandstone formation. The chemical compound silicon dioxide, also known as silica, is an oxide of silicon with the chemical formula SiO_2. Analysis by X-Ray Diffraction shows this sand has a composition of ~80 to 90% quartz. Analysis by particle size analyzer instrument shows that the particle size is around 80 to 400 um with a distribution mode of 180 um. The size and distribution is about the same from other workers who has performed similar work. The shapes are quite round and square which agrees well with the size of the particles. Refer to Figure 4.6 for details of sand characteristic.

•Industrial sand.

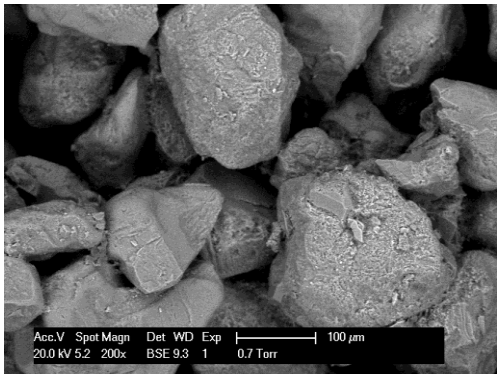

•Sand particles analyzed using SEM.

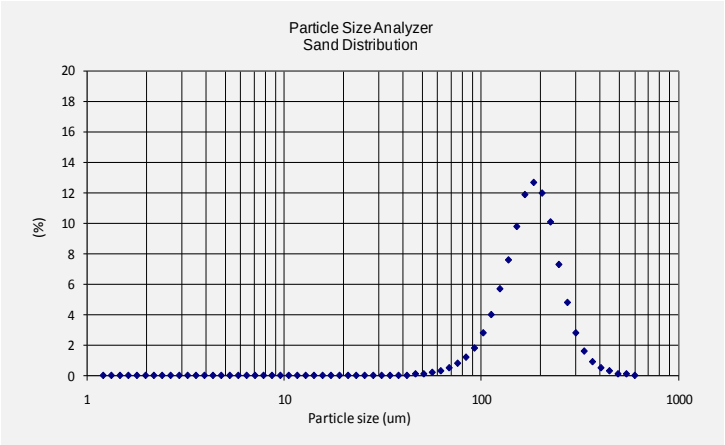

•Sand distribution analyzed using Particle Size Analyzer.

Sample : SAND			
No	1	2	3
Quartz	89.7	85.1	80.4
Kaolinite	0.7	0.5	0.6
Illite	0	11.8	14.4
Calcite	0	0	0.2
Rutile	0.5	0.1	0.1
Orthoclase	6.3	0.9	2.1
Microcline	2.8	1.6	2.2
Total	100	100	100

•Elements in sand analyzed using X-Ray Diffraction.

Figure 4.6: Sand distribution, elements and SEM

Figure 4.7 shows the characteristic of kaolinite minerals. Kaolinite is a clay minerals, with the composition $Al_2Si_2O_5(OH)_4$. It is a layered silicate mineral, with one tetrahedral sheet linked through oxygen atoms to one octahedral sheet of alumina octahedral. Formations that are rich in kaolinite are known as China clay, which is the case for this particular mineral. It has a low shrink-swell capacity and a low cation exchange capacity (1 to 15 meq/100g), produced by the chemical weathering of aluminium silicate minerals like feldspar. The structure is rarely as crystals but tend to be thin platy or stacked, or aggregated into compact, clay-like masses, as shown in the SEM picture in Figure 4.7. X-Ray Diffraction analysis shows that the kaolinite sample has about 75% kaolinite with 21% illite and 4% quartz. It has a wide distribution size

from 0.5 to 60 µm, which is why it has a large surface area. The distribution mode is ~10 µm.

•Kaolinite, from China clay

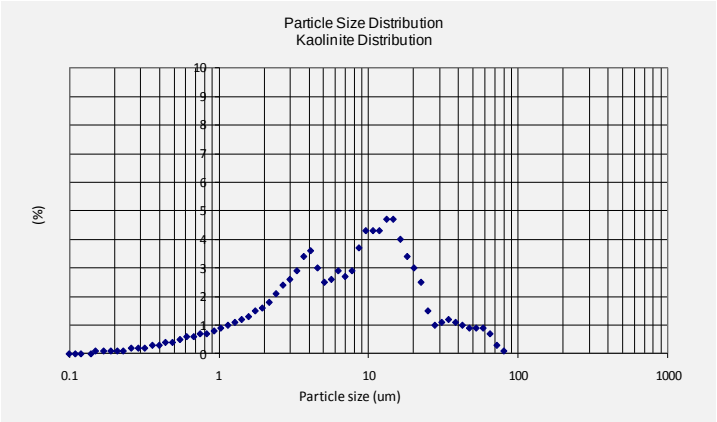

•Kaolinite distribution analyzed using Particle Size Analyzer.

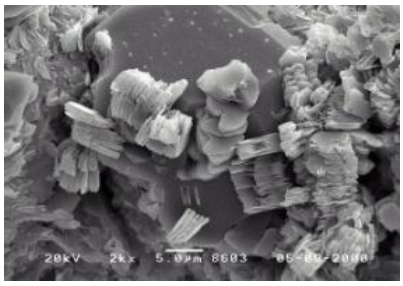

•Kaolinite analyzed using SEM.

Sample : KAOLINITE

No.	1	2	3	4	5	6	7	8
Quartz	3.70	3.20	4.10	4.20	4.20	4.20	3.70	4.00
Kaolinite	74.30	75.60	76.00	75.70	75.70	75.60	75.80	76.20
Illite	22.00	21.20	19.90	20.10	20.10	20.20	20.50	19.80
Total	100.00	100.00	100.00	100.00	100.00	100.00	100.00	100.00

•Elements in kaolinite analyzed using X-Ray Diffraction.

Figure 4.7: Kaolinite distribution, elements and SEM

Figure 4.8 shows the characteristic of siderite minerals. Siderite is a mineral compound of iron carbonate, $FeCO_3$. Generally it has more than 50% iron mineral and contain no sulphur or phosphorous. It also contains 25% illite and 20% quartz. Its crystals belong to the hexagonal system, and are rhombohedral in shape, typically with curved and striated faces. In sedimentary rocks, siderite commonly forms at shallow burial depths and its elemental composition is often related to the depositional environment of the enclosing sediments. It has a very wide distribution from 0.2 to 60 µm, with an average mode of 20 µm. This produces a large surface area similar to kaolinite.

•Siderite, from Lancashire

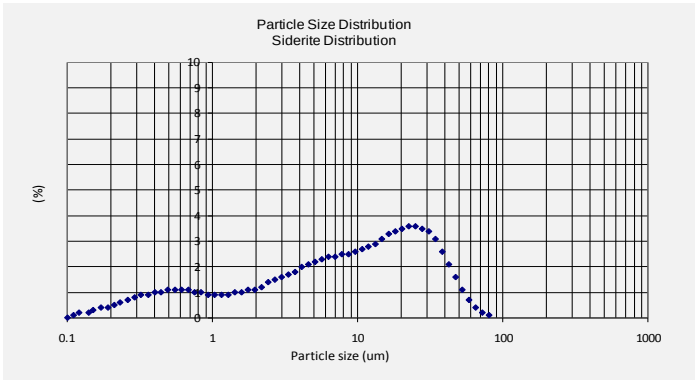

•Kaolinite distribution analyzed using Particle Size Analyzer.

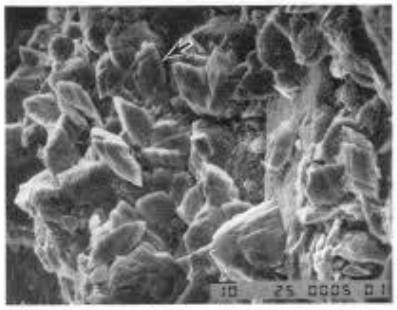

•Siderite analyzed using SEM.

Sample : SIDERITE

No.	1	2	3	4	5	6	7	8
Quartz	23.20	20.70	22.90	18.50	14.30	17.00	15.00	16.80
Kaolinite	3.90	3.70	3.50	3.70	2.70	3.30	2.90	2.80
Illite	25.10	22.90	24.70	21.00	19.80	21.20	17.80	21.11
Siderite	47.80	52.70	48.90	56.80	63.20	58.50	64.30	59.29
Total	100.00	100.00	100.00	100.00	100.00	100.00	100.00	100.00

•Elements in siderite analyzed using X-Ray Diffraction.

Figure 4.8: Siderite distribution, elements and SEM

Brine: The brine solution used in this study is synthetic brine, where the composition is similar to Nelson Forties Formation Water (NFFW). The composition is given in Table 4.1. The brine used in this study is sulphate free formation water, to avoid any precipitation due sulphate scale. The calcium level in the brine also has been increased to 2000ppm to induce precipitation at 95°C for some cases. Lithium has been added as an inert tracer to observe if there any evaporation took place in the static compatibility and adsorption/precipitation experiments.

Ion	Conc. (ppm)	Comp	Mass				
			g/l	g/5L	g/10L	g/15L	g/20L
Na^+	31275	NaCl	79.50	397.50	795.00	1192.50	1590.01
Ca^{2+}	2000	$CaCl_2 6.H_20$	10.93	54.66	109.32	163.98	218.64
Mg^{2+}	739	$MgCl_2.6H_20$	6.18	30.90	61.80	92.69	123.59
K^+	654	KCl	1.25	6.23	12.47	18.70	24.94
Ba^{2+}	269	$BaCl_2.2H_2O$	0.48	2.39	4.78	7.18	9.57
Sr^{2+}	771	$SrCl_2.6H_2O$	2.35	11.73	23.46	35.19	46.92
SO_4^{-2}	0	Na_2SO_4	0.00	0.00	0.00	0.00	0.00
Li^+	50	LiCl	0.305	1.53	3.05	4.58	6.11
Cl^-	50000						
		Actual Cl ppm	55278.64				
		If CaCl2.2H2O is used	7.32	36.62	73.25	109.87	146.49
TDS =	91036.64 ppm						

Table 4.1: Synthetic Nelson Forties Formation Water Composition (NFFW)

4.4.2 Experimental Procedure

Both experiments were performed at a "reservoir-like" temperature of 95˚C and the pH was adjusted to 4 in all cases. Stock solutions of DETPMP and OMTHP SI were prepared using synthetic NFFW as in Table 4.1. Experiments were conducted at various concentrations, as follows – Blank (0) , 10, 20, 50, 100, 300, 500, 800, 1000, 1500, 2000, 4000 and 10000ppm. After 24hrs at 95°C, the solutions were filtered through a 0.20µm filter paper and then analysed for phosphorus, calcium, magnesium, lithium and the pH values were measured. Inductively Coupled Plasma (ICP) was used to analyse the ions in the solution before and after filtration. The amount of SI retained by the mineral, Γ (in mg SI/ g rock), was calculated using the expression $\Gamma = V\left(c_o - c_f\right)/m$ (where c_o and c_f are the initial and final SI concentrations respectively, V is the SI solution volume and m is the mass of substrate). For static compatibility tests, the filter papers were weighed and sent for ESEM-EDAX analysis to quantify the amount of phosphorous, calcium and magnesium. Refer to Chapter 4 for details.

4.5 EXPERIMENTAL RESULTS AND DISCUSSION

In this section, we present the results on the coupled (static) adsorption/precipitation experiments using a range of phosphonate scale inhibitors. Scale inhibitors DETPMP (a penta-phosphonate), OMTHP (an hexa-phosphonate) and HMDP (a tetra-phosphonate) were used to study this behaviour. These experiments were carried out at a range of adsorbent mass/ fluid volume ratios, (m/V), since this indicates whether we are in the purely adsorbing or in the coupled adsorption/precipitation regime (Kahrwad *et al*, 2008). For the static adsorption tests, m = 10g, 20g and 30g sand, kaolinite and siderite were used (with a fixed volume of SI solution, V = 80ml = 0.08L) as minerals to analyse the coupled adsorption/precipitation behaviour.

4.5.1 DETPMP-SAND Adsorption/Compatibility Test

Figure 4.9 shows DETPMP SI in NFFW at 10,000ppm. This is the stock concentration used to prepare the various concentrations used in the experiments. At this concentration, DETPMP SI is fully dissolved, completely clear and slightly yellowish in colour. No precipitation is observed even after the solution was left for 24 hours. It was then diluted to attain lower concentrations of 10, 20, 50, 100, 300, 500, 800, 1000, 2000 and 4000ppm which were used for all the experiments. pH was measured for all the stock solutions and was later adjusted to pH4. At pH4, most of the particles dissolved in the solutions at the various concentrations at which they were prepared. No precipitation was seen even after the solutions were left for 24 hours at pH 4. The observation of precipitation is important as this will indicate whether only adsorption or precipitation is taking place in the later adsorption/precipitation experiments. Table 4.2 and Figure 4.10 shows the initial pH of these SI solutions at various concentrations before adjustment (to pH 4). The blank sample has a pH value of 4.93 and this decreases gradually to pH 1.96 at 4000 ppm of DETPMP SI. The decreasing trend of pH is due to the acidic nature of the DETPMP scale inhibitor as the concentration increases.

Figure 4.9: DETPMP in NFFW at 10,000ppm active. It is soluble at this concentration and yellowish in colour.

Conc.	pH (Initial)	pH (Final)				
DETPMP (ppm)		Compatibility Test	Adsorption (5g Sand)	Adsorption (10g Sand)	Adsorption (20g Sand)	Adsorption (30g Sand)
0	4	4.03	4.24	4.35	4.61	4.59
10	4	4.01	4.30	4.45	4.67	4.78
20	4	4.00	4.31	4.48	4.72	4.80
50	4	4.00	4.27	4.37	4.54	4.74
100	4	4.00	4.22	4.31	4.39	4.51
300	4	4.00	4.19	4.25	4.24	4.30
500	4	3.99	4.16	4.18	4.17	4.23
800	4	3.99	4.11	4.10	4.10	4.14
1000	4	3.96	4.05	4.04	4.00	4.09
2000	4	3.81	3.84	3.84	3.82	3.86
4000	4	3.70	3.70	3.70	3.66	3.69

Table 4.2: **:** DETPMP-Sand Static Adsorption/Compatibility Test. pH measurement of Initial, Adjusted and Final

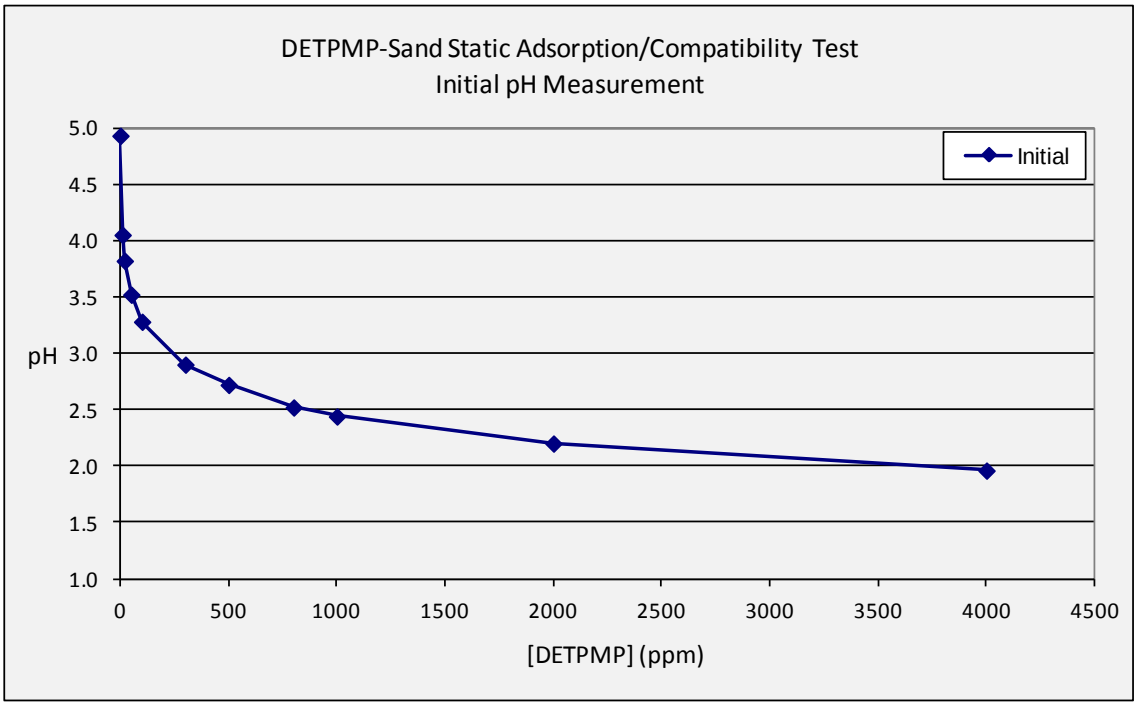

Figure 4.10: DETPMP-Sand Static Adsorption/Compatibility Test. Initial pH measurement of stock solutions vs. SI concentrations before pH adjustment.

Figure 4.11 and 4.12 show the adsorption ("apparent" or actual) level of scale inhibitor (DETPMP in mg SI / g rock) for different masses of sand as a function of the scale inhibitor concentration in synthetic NFFW at pH 4 at 95°C. The adsorption (or apparent adsorption), Γ (in mg SI/ g rock), was calculated using the expression $\Gamma = V\left(c_o - c_f\right)/m$ (where c_o and c_f are the initial and final SI concentrations respectively, V is the SI solution volume and m is the mass of substrate). The main observation from these figures is whether pure adsorption or coupled adsorption/precipitation is taking place. The figures clearly indicate that both pure adsorption and coupled adsorption/precipitation took place in different concentration regimes. Only pure adsorption is seen for [SI] up to ~750ppm, before the different (m/V) curves starts to deviate due to coupled adsorption/precipitation behaviour occurring. This is evident since, if pure adsorption occurred, then this curve would plateau at a level of up to ~0.20 – 0.25 mg/g – in fact, we see that level of "coupled adsorption/precipitation" of ~1.0 – 5.0 mg/g are observed. This indicates that the mixture of DETPMP and NFFW onto sand shows both "pure adsorption" up to ~750ppm and coupled adsorption/precipitation above ~750ppm. From these figure, at

~750ppm, the coupled adsorption/precipitation starts to be noticeable as the curve deviates from pure adsorption (plateau) behaviour.

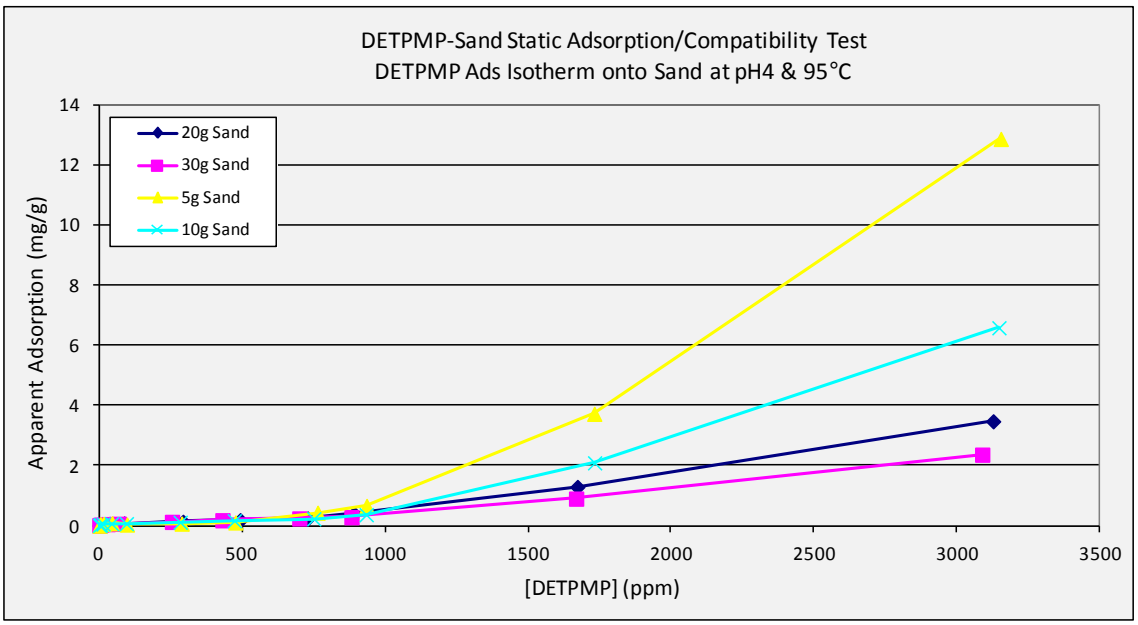

Figure 4.11: DETPMP-Sand Static Adsorption/Compatibility Test. DETPMP Adsorption Isotherm onto different masses of sand at pH4 & 95°C.

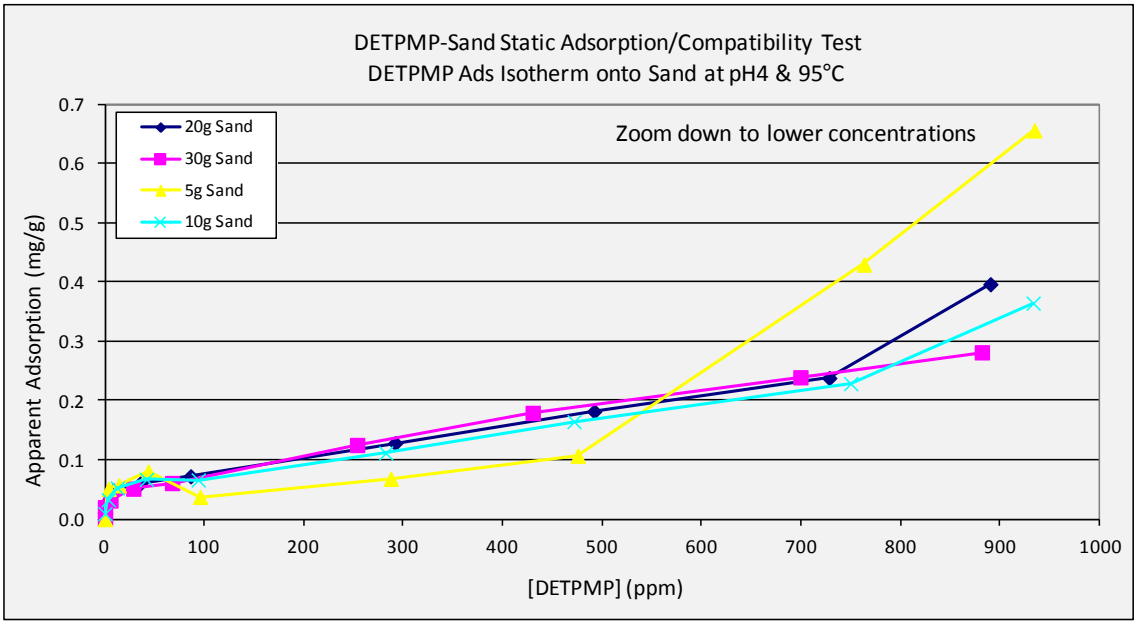

Figure 4.12: DETPMP-Sand Static Adsorption/Compatibility Test. DETPMP Adsorption Isotherm onto different masses of sand at pH4 & 95°C; zoomed down to lower concentrations.

In summary, the results in Figure 4.11 and Figure 4.12 show the "apparent adsorption" vs. [SI] (strictly this is the final [SI] after the adsorption/precipitation process, cf – see above). The region of "pure adsorption" is seen up to [SI] ~750ppm since all the (m/V) curves collapse onto one cure, the static adsorption isotherm. Above [SI] ~750, "coupled adsorption/precipitation" is observed since the various apparent adsorption curves for different (m/V) separate i.e. follow different curves. Thus, the regions of "pure adsorption" and "coupled adsorption/ precipitation" behaviour are strictly established by the results shown.

To further establish the pure adsorption and coupled adsorption/precipitation behaviour, changes of [phosphorous], [Ca^{2+}] and [Mg^{2+}] concentration before and after the experiments in the mixture of SI and NFFW solution in both adsorption and compatibility test were measured. Any divalent ion levels above stock solution concentration are not expected or must be within its analytical error of less than 5%. The decrease in the solution divalent ion levels are due to either precipitation of M-DETPMP complex or because of involvement of the divalent ions in the pure adsorption process (e.g. by cation bridging). Any changes in [Li+] were also noted in order to check whether there was any evaporation taking place. There should not be any changes in [Li^{+}] as it is an inert tracer ion which does not adsorb onto sand or react with DETPMP SI. The estimated amount of evaporation (as measured by Li^{+} increase) was used to correct the concentration for all the other elements.

Figure 4.13, Figure 4.14 and Figure 4.15 show the differences in [phosphorous], [Ca^{2+}] and [Mg^{2+}] amount for both compatibility and adsorption test. The differences in the amounts show that there is definitely pure adsorption and coupled adsorption/precipitation taking place. It is known that Ca^{2+} and Mg^{2+} ions do not significantly adsorb* onto sand, so the differences are due to cation bridging between the SI and the Ca^{2+} and Mg^{2+} ions onto the sand. [*NB however, there may be some ion exchange of Ca^{2+} and Mg^{2+} ions onto the rock/mineral surface but this is not a large effect for such pure quartz sand – it is much larger in clays]. It is also noted that in almost all cases, there is a small increase in [Ca^{2+}] and [Mg^{2+}] ions, which is not expected, but they are all within its analytical error of less than 5%. Even changes in

[Li^+] ions are observed for all the cases, but again, they are within its analytical error of less than 5%. The increase in Li+ also shows slight evaporation was taking place. The % increase was used to correct the concentrations for all the other elements.

Figure 4.13 shows the changes in phosphorous ion concentrations for both compatibility and adsorption test. Referring to adsorption test at 5g to 30g sand; the figure shows that phosphorous starts adsorbing onto sand even at a lower concentration of 10ppm for the different masses of sand used, where the difference between the stock solution and the filtrate is about 3 to 8ppm as the mass of sand increases from 5g to 30g sand. As the concentration of DETPMP SI increases from 10ppm to 4000ppm, the changes in phosphorous (i.e. SI) concentration are also increased. Two things can be observed from this figure; firstly, phosphorous starts adsorbing or precipitating even at a lower concentration of 10ppm and increases as the DETPMP concentration increases; secondly, as the mass of sand increases from 5g to 30g, increase in phosphorous concentration is also observed. Whereas, in the precipitation case (referring to compatibility test) where there was no sand present, reduction in phosphorous concentration can only be observed at 2000ppm, where 180ppm was left as precipitates, and increases to 650ppm (left as precipitates) as the DETPMP concentration increases to 4000ppm. The figure indicates pure adsorption of phosphorous onto sand until ~1000ppm and coupled adsorption/precipitation from 2000ppm onward.

Figure 4.14 shows the change in Ca^{2+} ion concentrations for both compatibility and adsorption test. Referring to adsorption test at 5g to 30g sand; the figure shows that Ca^{2+} ions starts to show a significant reduction from 2000ppm and are even further reduced at 4000ppm. The reduction in Ca^{2+} ions increases as the mass of sand increases from 5g to 30g. Whereas, for the compatibility tests, reduction in Ca^{2+} is observed only at 4000 ppm. The difference of Ca^{2+} ion in both experiments shows that Ca^{2+} some must have precipitated to some extent from 2000ppm onwards due to M-DETPMP complex precipitation. At 4000ppm DETPMP, 115 to 135ppm of Ca^{2+} precipitated out of solution depending on the mass of sand tested.

Figure 4.15 shows the change in Mg^{2+} ions concentration for both compatibility and

adsorption test. Referring to adsorption test at 5g to 30g sand; the figure shows that the changes in Mg^{2+} ion concentrations can only be seen clearly at 4000ppm although the measured adsorption level appears to fluctuate at 2000ppm as well. For compatibility tests with no minerals, significant reduction in Mg^{2+} is observed at only 4000ppm. Again, the difference in Mg^{2+} ion concentration proves that Mg^{2+} some have precipitated from 2000ppm onward due to M-DETPMP complex precipitation. At 4000ppm DETPMP, 10 to 20ppm Mg^{2+} precipitated out of solution at different mass of sand tested. Comparing phosphorous to Ca^{2+} and Mg^{2+} binding, Ca^{2+} has much more affinity to DETPMP SI as shown from the amount of concentration change observed on precipitation.

Figure 4.16 shows the change in Li^{+} ions concentration. The figure shows there is no change in Li^{+} concentration. Li^{+} as an inert tracer ion does not adsorb or precipitate onto sand mineral. It clearly shows that there is no adsorption or precipitation. It is analysed to see if there was any evaporation. Base on the figure, there is an increase of 1% to 3% in Li^{+} concentration, which shows slight evaporation taking place apart from analytical error. This factor was taken into account for all the calculation made for all the elements.

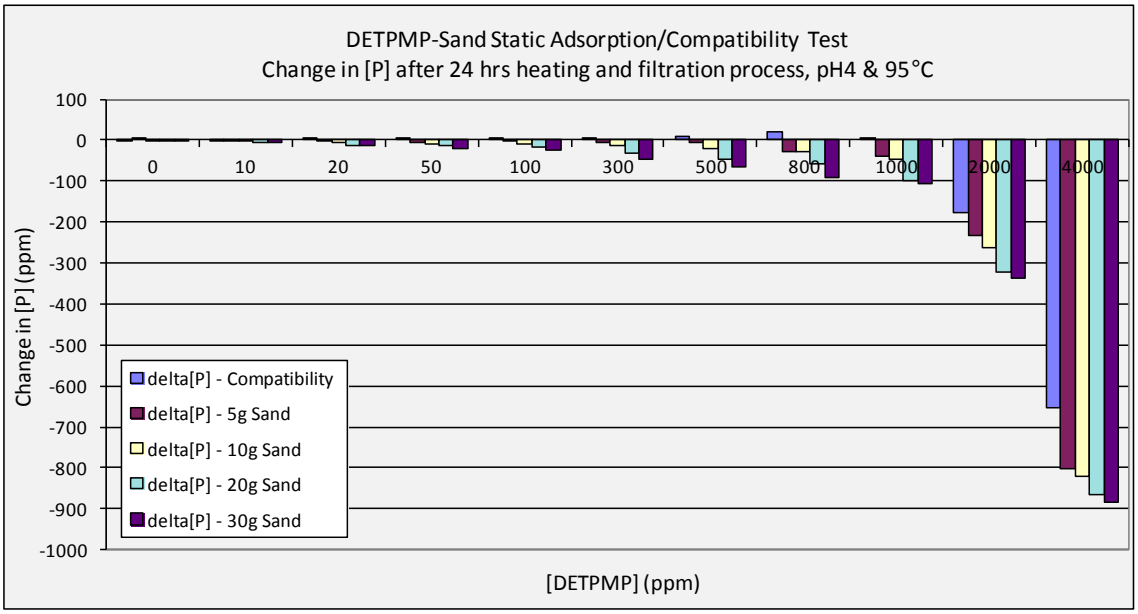

Figure 4.13: DETPMP-Sand Static Adsorption/Compatibility Test (5g, 10g, 20g & 30g Sand). Change in [P] vs [DETPMP].

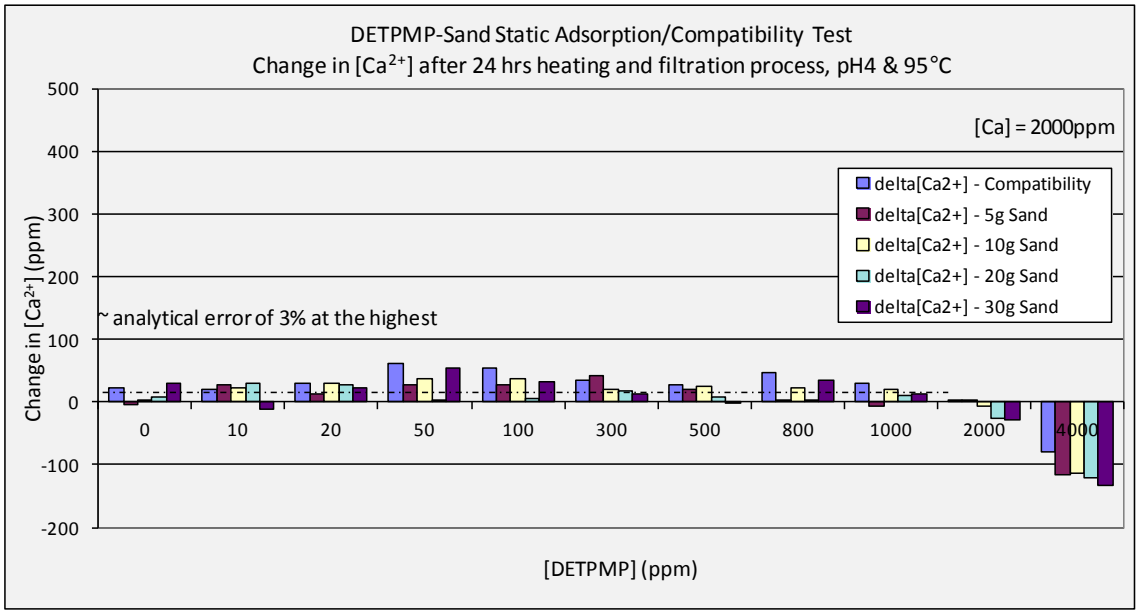

Figure 4.14: DETPMP-Sand Static Adsorption/Compatibility Test (5g, 10g, 20g & 30g Sand). Change in $[Ca^{2+}]$ vs [DETPMP].

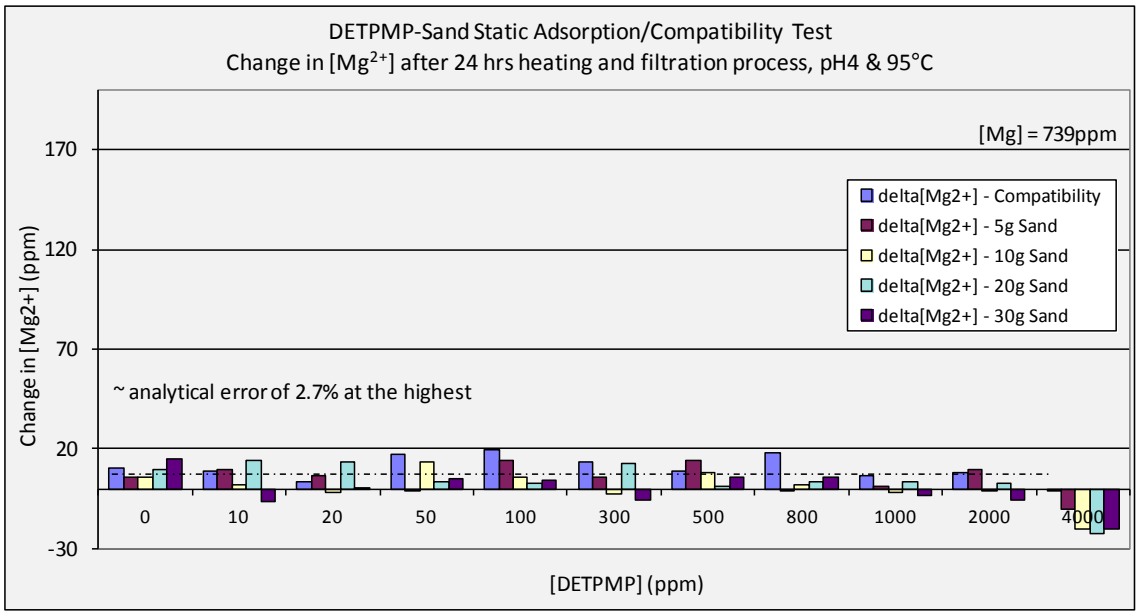

Figure 4.15: DETPMP-Sand Static Adsorption/Compatibility Test (5g, 10g, 20g & 30g Sand). Change in $[Mg^{2+}]$ vs [DETPMP].

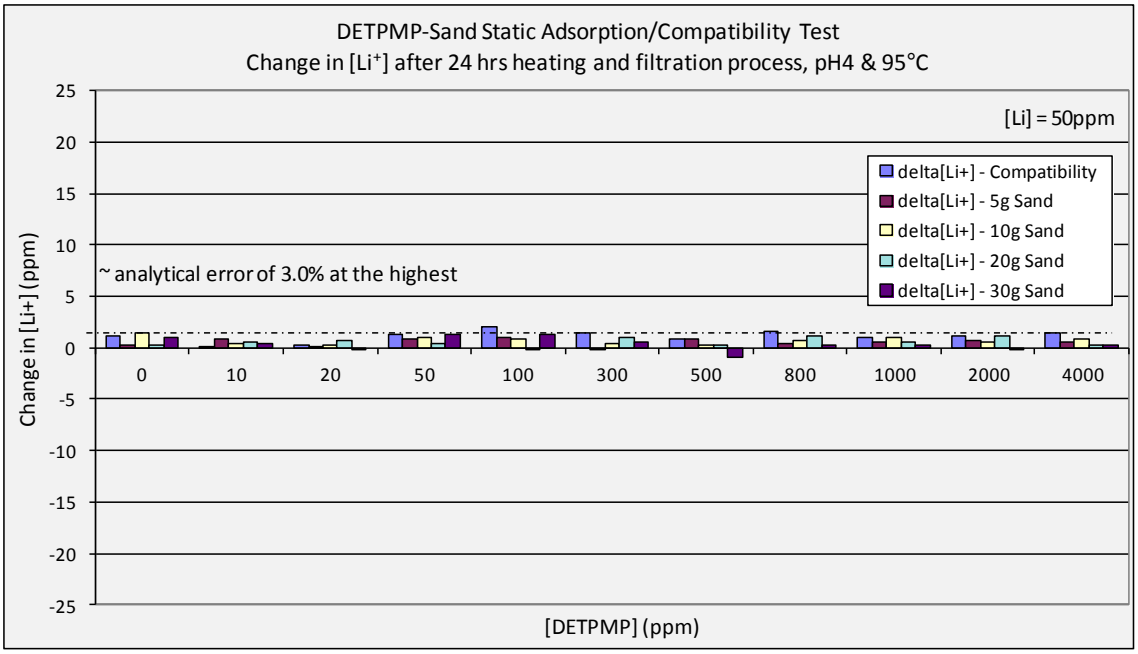

Figure 4.16: DETPMP-Sand Static Adsorption/Compatibility Test (5g, 10g, 20g & 30g Sand). Change in [Li^+] vs [DETPMP].

After the filtration, all the filter papers were dried, weighed, photographed and sent for ESEM-EDAX analysis. The sample solutions were measured for pH. The weight of the samples that precipitated out of the solutions are given in Table 4.3 and the corresponding photographed filter papers after filtration are shown in Figure 4.17. Only at 2000ppm do we clearly see clear differences in both the weight and the appearance of precipitate, although there is some tracers of precipitate seen on the filter paper at 1000ppm. As the concentration increases, the weight increases as expected and more significant amounts of precipitate can be seen clearly on the filter paper. These results are very consistent with observations (above) on the amount of phosphorous, Ca^{2+} ions and Mg^{2+} ions that were measure in solution, which was less than in the stock solutions. The results prove that precipitation took place from 2000ppm onward, with some indication it starts as early as 1000ppm.

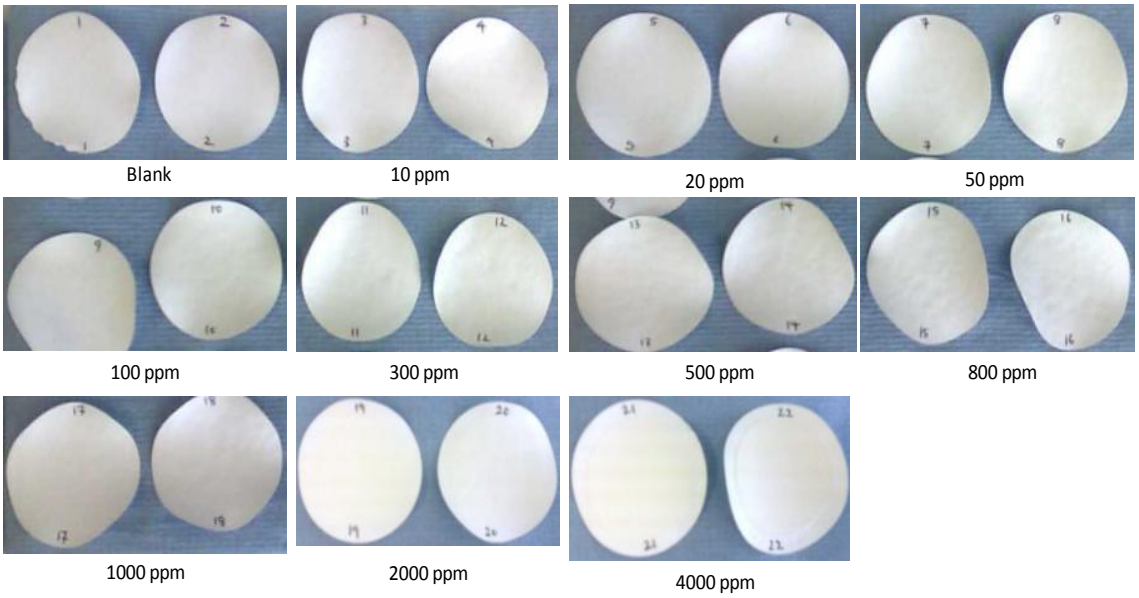

Figure 4.17: DETPMP-Sand Static Adsorption/Compatibility Test. Precipitates on filter papers at different concentration of DETPMP. Traces of precipitates can be observed at 2000ppm and clear precipitates at 4000ppm.

DETPMP Conc. (ppm)	Weight of Ppt (g)
0	0.02
10	0.02
20	0.02
50	0.02
100	0.02
300	0.02
500	0.02
800	0.02
1000	0.02
2000	0.04
4000	0.12

Table 4.3: DETPMP-Sand Static Adsorption/Compatibility Test. It shows the weight of precipitate on filter papers after filtration.

Table 4.4 and Figure 4.18 show ESEM-EDAX atomic and weight percentage and photographed samples of phosphorous, Ca^{2+}, Mg^{2+} and other ions presents on the filter papers. For each concentration, two points were taken for analysis. The hazy black background was identified to be the filter paper itself, the solid white marks are the salts

and the hazy white background is the compound of phosphorous (SI), Ca^{2+} and Mg^{2+} ions. The blank samples without any SI shows only filter paper and some salts. Based on the atomic% from ESEM-EDAX, there is no phosphorous, Ca^{2+} and Mg^{2+} compound identified below 500ppm. It must be noted that the EDAX signals are localized and inconsistent values are expected since they depend on precisely which point has been analyzed. Only when it reaches 800ppm and above, can a clear hazy white background be seen on the filter paper samples, which is identified to be phosphorous, Ca^{2+} and Mg^{2+} ions base on EDAX signal. Above 800ppm concentration, based on the atomic%, phosphorous, Ca^{2+} and Mg^{2+} are seen consistently. Atomic% of phosphorous ranges from 4 to 14; Ca^{2+} from 2 to 6 and Mg^{2+} from 1 to 2. Although the values are not accurate, the presence of phosphorous, Ca^{2+} and Mg^{2+} as precipitates above 800ppm is clearly proven.

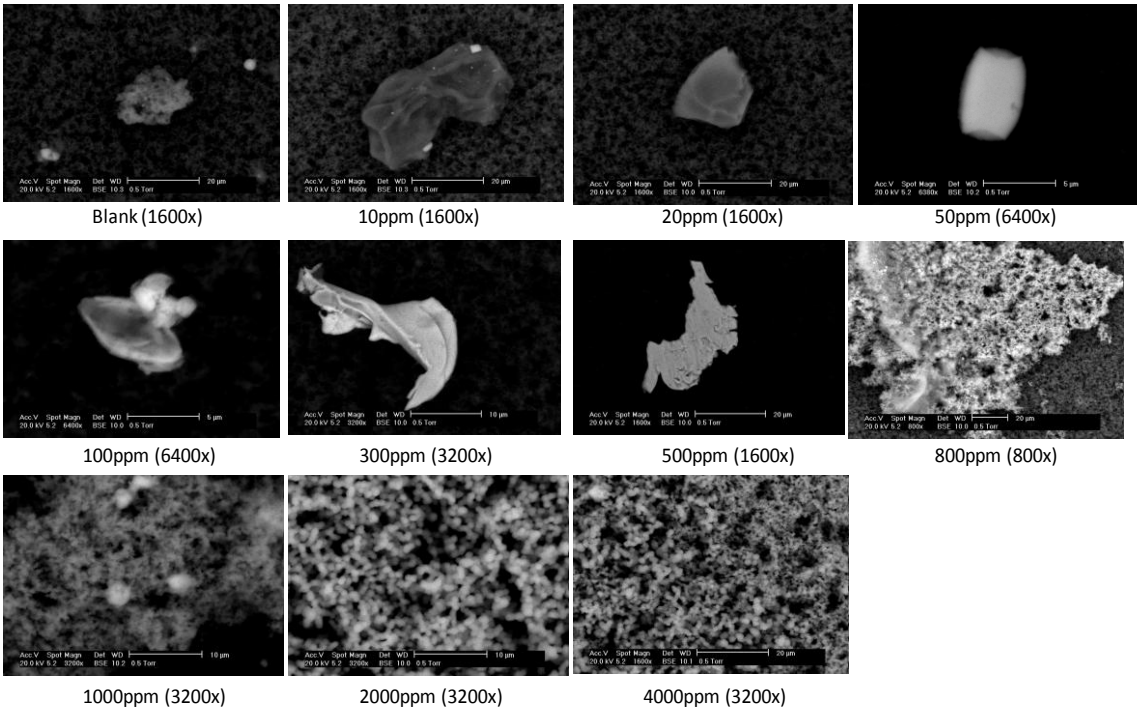

Figure 4.18: DETPMP-Sand Static Adsorption/Compatibility Test. Morphology of precipitates on ESEM photographed samples.

	Blank		10 ppm		20 ppm		50 ppm		100 ppm		300 ppm		500 ppm		800 ppm		1000 ppm		2000 ppm	
Element	Wt %	At %	Wt %	At %	Wt %	At %	Wt %	At %	Wt %	At %	Wt %	At %	Wt %	At %	Wt %	At %	Wt %	At %	Wt %	At %
C K	55.06	66.83	37.72	53.05	21.98	41.23	21.98	41.23	28.27	48.95	11.19	35.64	14.87	39.4	39.35	51.57	30.74	43.3	25.72	38.92
N K			4.27	5.15													7.48	9.04	4.92	6.38
O K	28.92	26.35	32.46	34.27	32.17	45.3	32.17	45.3	24.82	32.27	1.12	2.68	7.63	15.18	39.01	38.38	29.2	30.88	29.62	33.64
NaK	1.66	1.06	1.12	0.82	1.01	0.99	1.01	0.99	0.87	0.79					0.8	0.55	4.11	3.02	1.19	0.94
MgK	0.27	0.16	0.61	0.42											1.61	1.04	1.82	1.27	2.2	1.64
AlK	0.47	0.25							1.3	1.01										
SiK	0.77	0.4							0.7	0.51	1.01	1.37	1.05	1.19						
SrL			1.26	0.24	1.03	0.26	1.03	0.26							1.08	0.19	2.07	0.4	2.64	0.55
P K															8.2	4.17	10.58	5.78	17.95	10.53
S K			3.51	1.85	8.23	5.78	8.23	5.78	1.03	0.67										
ClK	9.26	3.81	4.02	1.91	0.92	0.58	0.92	0.58	1.53	0.9	1.04	1.13	0.86	0.77	3.86	1.71	7.57	3.61	4.1	2.1
CrK											15.74	11.58	13.83	8.47						
K K			0.4	0.17	0.42	0.24	0.42	0.24												
CaK	0.71	0.26	1.07	0.45					0.58	0.3					6.1	2.39	6.43	2.71	11.67	5.29
BaL			13.57	1.67	34.25	5.62	34.25	5.62	1.92	0.29										
FeK									34.4	12.81	61.57	42.17	53.96	30.76						
NiK											8.33	5.43	7.82	4.24						
CuK									4.58	1.5										
TiK	2.87	0.87																		
Total	100	100	100	100	100	100	100	100	100	100	100	100	100	100	100	100	100	100	100	100

Table 4.4: DETPMP-Sand Static Adsorption/Compatibility Test. EDAX signals on the precipitates from ESEM.

Table 4.2 and Figure 4.19 show the pH values of the adjusted and filtered samples. All the stock solutions were adjusted to a pH value of 4. At pH4, it had been proven that the solutions do not precipitate at room condition. After 24 hrs heating and filtration, the pH values were measured again. For compatibility test with no minerals, the pH values stays around pH4 until 800ppm, and they reduce to 3.96, 3.81 and 3.70 at 1000, 2000 and 4000ppm, respectively. It shows that the pH value starts to reduce when significant P, Ca^{2+} and Mg^{2+} are missing due to precipitation during filtration. Thus, significant precipitation of P, Ca^{2+} and Mg^{2+} on the filter paper has caused reduction of pH. For adsorption tests at different masses of sand; 5g, 10g, 20g and 30g sand, the pH value increases for blank sample, and increases further up to 50ppm before it then reduces until 4000ppm. Although different masses of sand result in different values of pH, they all decrease gradually. At 4000ppm, the pH value converges at pH ~3.7 for all the different masses of sand. The hypothesis that can be made from pH behaviour alone is, there must be only P (slight Ca^{2+} and Mg^{2+}) ions missing due to adsorption onto sand from blank up to 4000ppm. pH reduces significantly at 2000 and 4000ppm due to all three component; P, Ca^{2+} and Mg^{2+} missing due to precipitation.

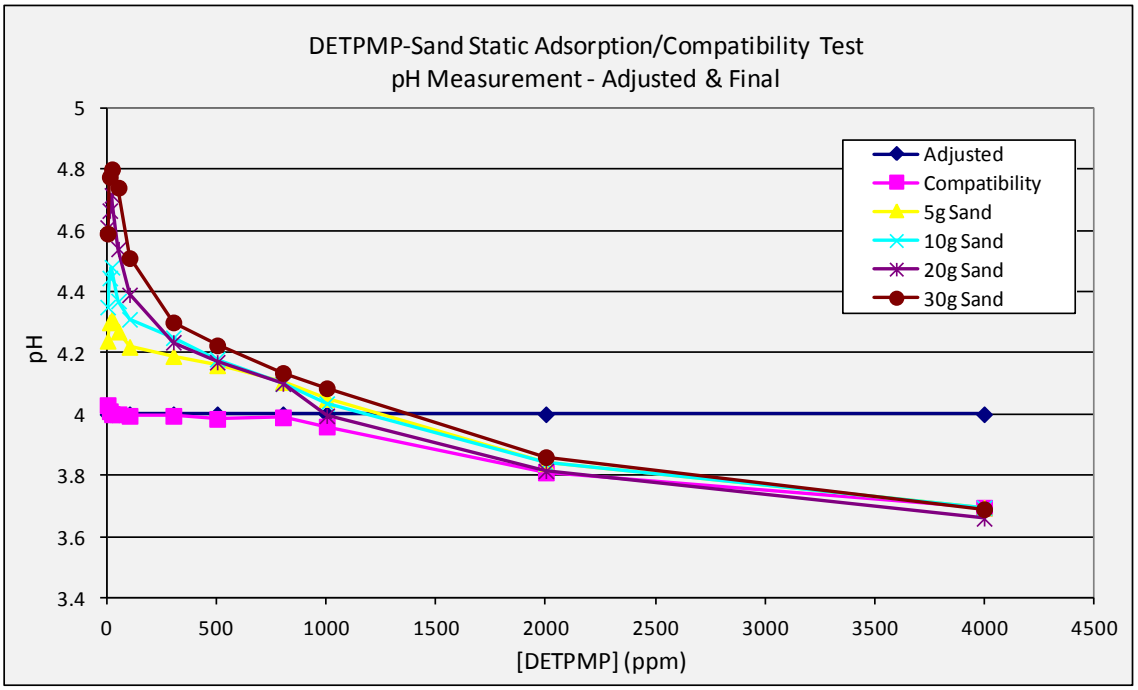

Figure 4.19: DETPMP-Sand Static Adsorption/Compatibility Test. pH Measurement – Adjusted and Final

4.5.2 OMTHP-SAND Adsorption/Compatibility Test

Figure 4.20 shows OMTHP in NFFW at 10,000ppm. At this concentration, OMTHP SI is not fully dissolved and is whitish and opaque in appearance. After it is left for about two hours, the solution starts to precipitate. This is the stock solution which was used for all the experiments in this particular set. This preparation was then diluted to attain the lower concentration levels, 10, 20, 50, 100, 300, 500, 800, 1000, 2000 and 4000ppm which were used for all the experiments. pH was measured for all the stock solutions and was later adjusted to pH 4. At pH4, the particles dissolved in the solutions at the different concentrations at which they were prepared. Table 4.5 and Figure 4.21 shows the initial pH values of the various stock solutions before adjustment. The blank sample has a pH value of 4.91 and this decrease gradually to pH 4.52 at 4000ppm. The decreasing trend of pH indicates the acidic nature of the OMTHP scale inhibitor as the concentration increases. OMTHP is less acidic than DETPMP (DETPMP has pH 1.93 at 4000ppm). At this point, it is assured that no precipitation occurs for all the concentration up to 4000ppm at pH4 which is important before the 24 hours of heating at 95°C in the compatibility tests.

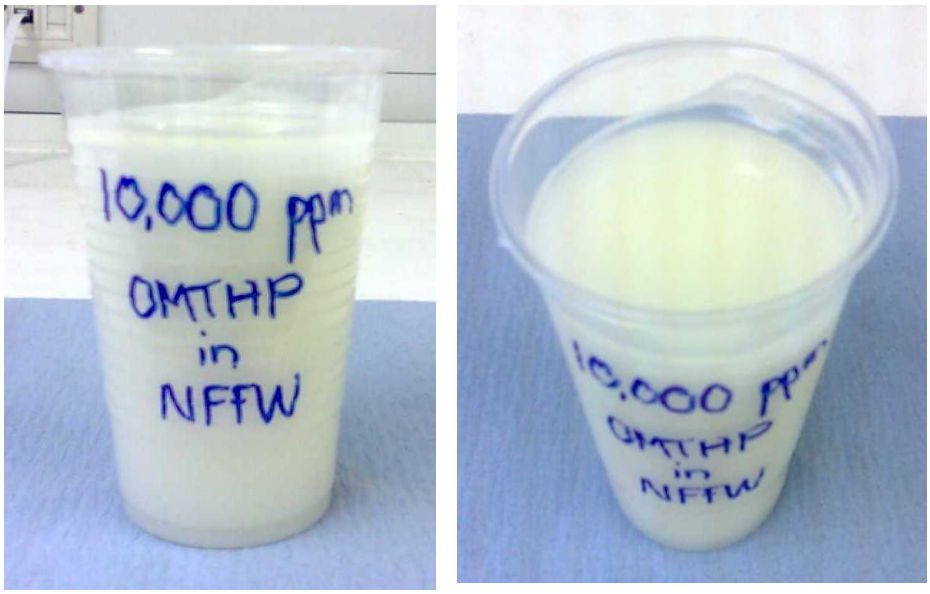

Figure 4.20: OMTHP SI in NFFW at 10,000ppm active. It is whitish in colour and insoluble at this concentration. It precipitates when left for a few hours.

Conc. OMTHP (ppm)	pH (Initial)	pH (Adjusted)	pH (Final)			
			Compatibility Test	Adsorption (10g Sand)	Adsorption (20g Sand)	Adsorption (30g Sand)
0	4.91	4	3.97	4.37	4.47	4.69
10	4.77	4	3.96	4.53	4.73	4.88
20	4.73	4	3.97	4.47	4.77	4.98
50	4.68	4	3.96	4.37	4.62	4.90
100	4.66	4	3.95	4.23	4.30	4.45
300	4.65	4	3.97	3.98	3.93	4.02
500	4.64	4	3.96	3.95	3.88	3.93
800	4.61	4	3.90	3.90	3.84	3.88
1000	4.59	4	3.86	3.84	3.80	3.82
2000	4.54	4	3.72	3.69	3.63	3.64
4000	4.52	4	3.65	3.63	3.59	3.59

Table 4.5: OMTHP-Sand Static Adsorption/Compatibility Test. pH measurement – Initial, Adjusted and Final

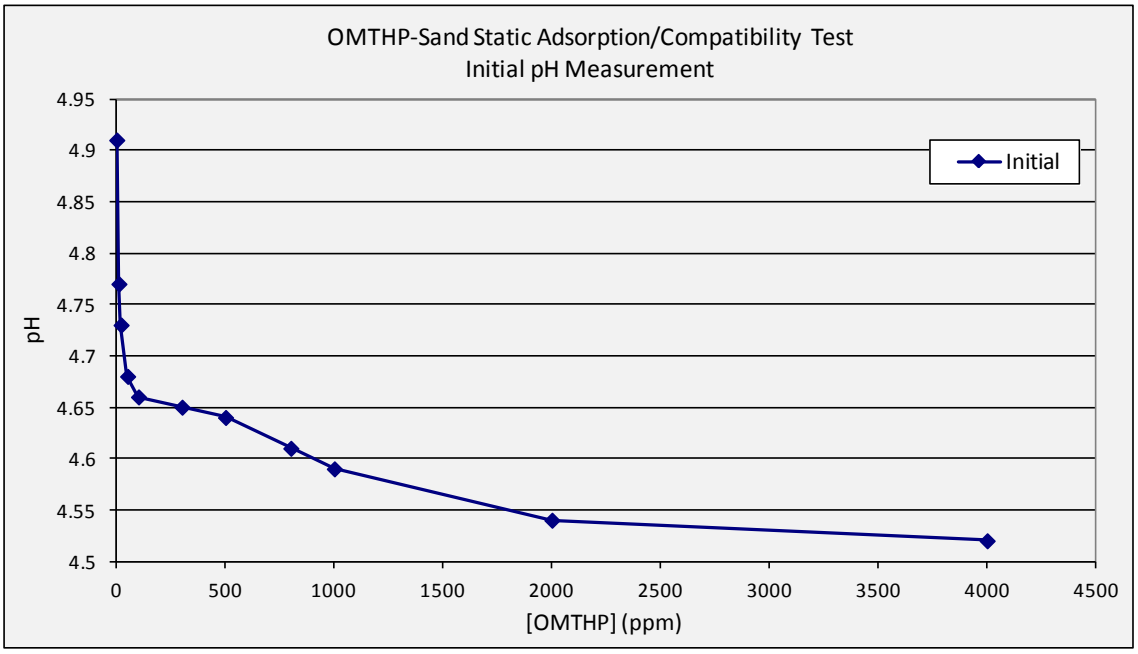

Figure 4.21: OMTHP SI initial pH measurement of each stock solutions before adjustment. The decreasing trend of the pH indicates acidic nature of OMTHP SI.

Figure 4.22 and Figure 4.23 show the adsorption ("apparent" or actual) level of scale inhibitor (OMTHP in mg SI / g rock) on different masses of sand (i.e. at varying m/V ratios) as a function of the scale inhibitor concentration in synthetic NFFW at pH 4 and 95°C. These figures clearly indicate that both pure adsorption and coupled adsorption/precipitation took place at this set of conditions. Clearly, pure adsorption is seen for SI concentrations up to ~700ppm since the data for the different (m/V) ratios collapse onto the same curve. Above [SI] ~700ppm, the different (m/V) curves starts to deviate thus indication that coupled adsorption/precipitation occurring (since apparent adsorption becomes a function of m/V ratio). These types of behaviour are also evidenced by the actual values of the apparent adsorption itself. In the pure adsorption region, then Γ ~0.35mg/g which is a reasonable level for pure adsorption. However, in the "couple adsorption/precipitation" regime at [SI] > 700ppm, the Γ_{app} ~4.0 – 11.0 mg/g and this is far too high to be pur adsorption. Thus, in summary, like the DETPMP/NFFW/sand system, the OMTHP/NFFW/sand system shows both "pure adsorption" up to ~700ppm and coupled adsorption/precipitation above ~700ppm.

To further establish the pure adsorption and coupled adsorption/precipitation regimes in

the OMTHP/NFFW/sand system, changes of [phosphorous], [Ca^{2+}] and [Mg^{2+}] concentration in the mixture of SI and NFFW solution in both adsorption and compatibility tests were observed. Any divalent ion level above stock solution concentration is not expected or must be within its analytical error of less than 5%. The decrease in the solution divalent ion levels are due to either precipitation of M-OMTHP complex or involvement of the divalent ions in the pure adsorption process (e.g. by cation bridging). The change in [Li^+] is also observed to establish if any evaporation has taken place. There should not be any changes in [Li^+] as it is an inert tracer ion which does not react with OMTHP SI or adsorb onto sand.

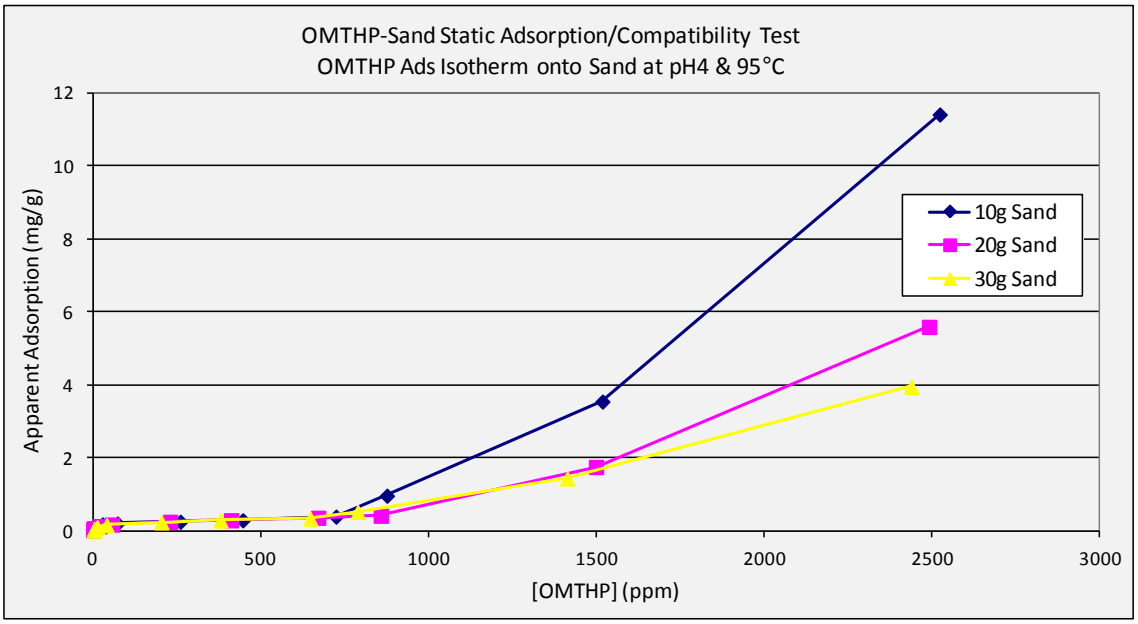

Figure 4.22: OMTHP-Sand Static Adsorption/Compatibility Test. OMTHP Adsorption Isotherm onto different masses of sand at pH4 & 95°C.

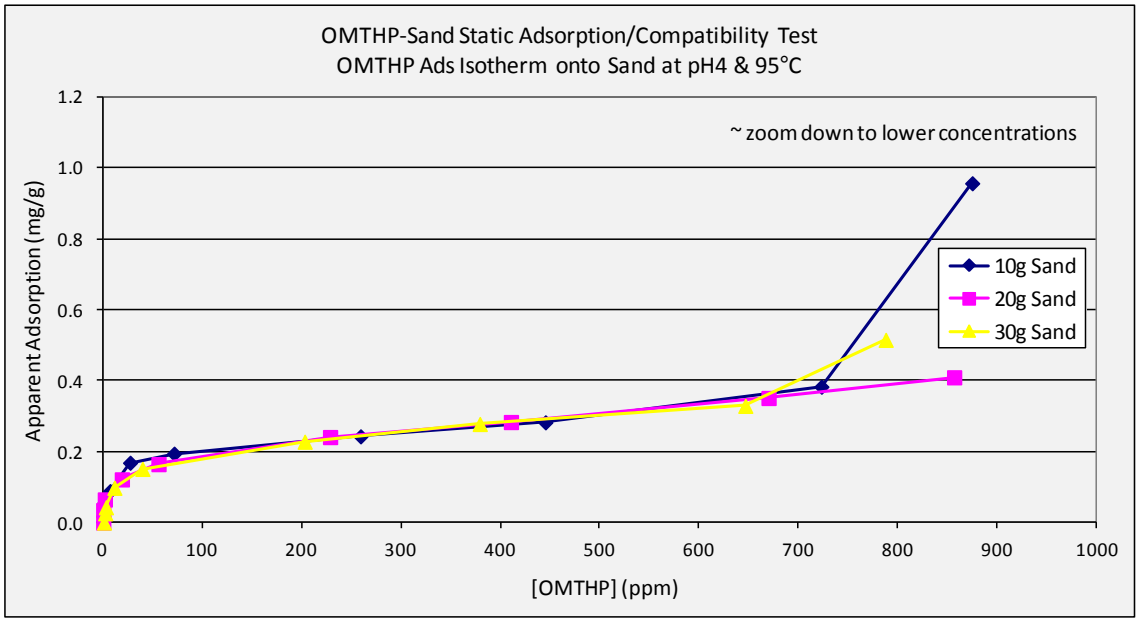

Figure 4.23: OMTHP-Sand Static Adsorption/Compatibility Test. OMTHP Adsorption Isotherm onto different masses of sand at 95°C and pH4; zoomed down to lower concentration.

Figure 4.24, Figure 4.25 and Figure 4.26 show the differences in the solution levels of [phosphorous], [Ca^{2+}] and [Mg^{2+}] for both static compatibility and adsorption tests for the OMTHP/NFFW/sand system. The differences in the amounts in each test show that there is definitely pure adsorption and coupled adsorption/precipitation taking place in different concentration regions. It is known that Ca^{2+} and Mg^{2+} ions do not significantly adsorb* onto sand, so the differences are probably due to cation bridging of phosphorous to Ca^{2+} and Mg^{2+} ions onto the sand or to precipitation. [*NB however, there may be some ion exchange of Ca^{2+} and Mg^{2+} ions onto the rock/mineral surface but this is not a large effect for such pure quartz sand – it is much larger in clays]. It is also noted that in almost all cases, there is a small increase in [Ca^{2+}] and [Mg^{2+}] ions, which is not expected, but they are all within its analytical error of less than 5%. Even changes in [Li^{+}] are observed for all the cases, but again, they are within its analytical error of less than 5%. The increase in Li^{+} also shows slight evaporation was taking place. The %increase was used to correct the concentrations for all the other elements involved.

Figure 4.24 shows the change in phosphorous ions concentration for both compatibility and adsorption test. Referring to adsorption tests at 10g to 30g sand; the figure shows that phosphorous starts adsorbing onto sand even at a lower concentration of 10ppm OMTHP for the different masses of sand used, where the difference between the stock solution and the filtrate is about 5 to 10 ppm as the mass of sand increases from 10g, 20g and 30g sand. As the concentration of OMTHP SI increases from 10ppm to 4000ppm, the changes in phosphorous ions also increase. Two important points can be made from the results in this figure; firstly, phosphorous starts adsorbing even at a lower concentration of 10ppm and increases as the DETPMP concentration increases; secondly, as the mass of sand increases from 5g to 30g, an increase in phosphorous concentration change is also observed. Whereas, in the precipitation case where there is no sand present, reduction in phosphorous can only be observed at ~800ppm, where 40ppm was left as precipitates, and increases to 1450ppm (left as precipitates) as the DETPMP concentration increases to 4000ppm. The figure indicates pure adsorption of phosphorous onto sand until 500ppm and coupled adsorption/precipitation from 800ppm onward.

Figure 4.25 shows the change in Ca^{2+} ions concentration for both compatibility and adsorption tests. Referring to adsorption test at 10g to 30g sand; the figure shows that Ca^{2+} ions starts to show a significant reduction from 2000ppm and is further reduced at 4000ppm, in the adsorption test. There was some indication of Ca^{2+} ion reduction at 1000ppm based on the fluctuation in Ca^{2+} concentration. For the compatibility tests, reduction in Ca^{2+} is also observed starting at 2000 ppm. The difference of Ca^{2+} ion in both experiments shows that some must have precipitated and some must have adsorbed, probably the Ca^{2+} is bridged along with phosphorous onto the mineral surface. At 4000ppm OMTHP, between 150 and 180ppm of Ca^{2+} was lost from solution at different mass of sand tested.

Figure 4.26 shows the change in Mg^{2+} ion concentrations for both compatibility and adsorption tests. Referring to adsorption tests at 10g to 30g sand; the figure shows that significant changes can only be seen at 4000ppm though some adsorption can be seen at 30g sand at 2000ppm. For compatibility test with no minerals, significant reduction is

observed at only 4000ppm. Again, the difference in these experiments only proves that some precipitated and some adsorbed, bridged along with phosphorous divalent ions. At 4000ppm OMTHP, only about 30ppm Mg^{2+} was lost from solution at different masses of sand tested. Comparing phosphorous to Ca^{2+} and Mg^{2+} binding, again Ca^{2+} has more affinity to OMTHP SI as shown from the amount of concentration lost in these tests.

Figure 4.27 shows the change in Li^{+} ion concentration. The figure shows that there is virtually no change in Li^{+} concentration. Li^{+} is an inert tracer ion and is not expected to show any adsorption or precipitation. It is analysed to determine whether there was any evaporation. Base on the figures, there is an increase of 1% to 2% in Li+ concentration, which shows slight evaporation taking place apart from analytical error. This factor was taken into account for all the calculation made for all the other elements (P, Ca and Mg).

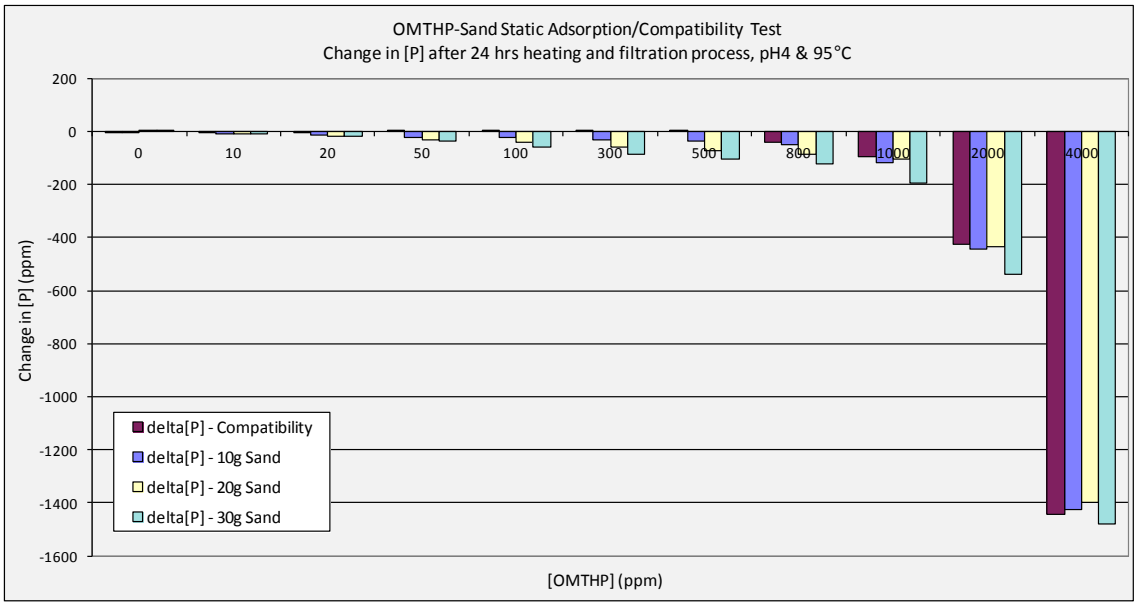

Figure 4.24: OMTHP-Sand Static Adsorption/Compatibility Test (10g, 20g & 30g Sand). Change in [P] vs [OMTHP].

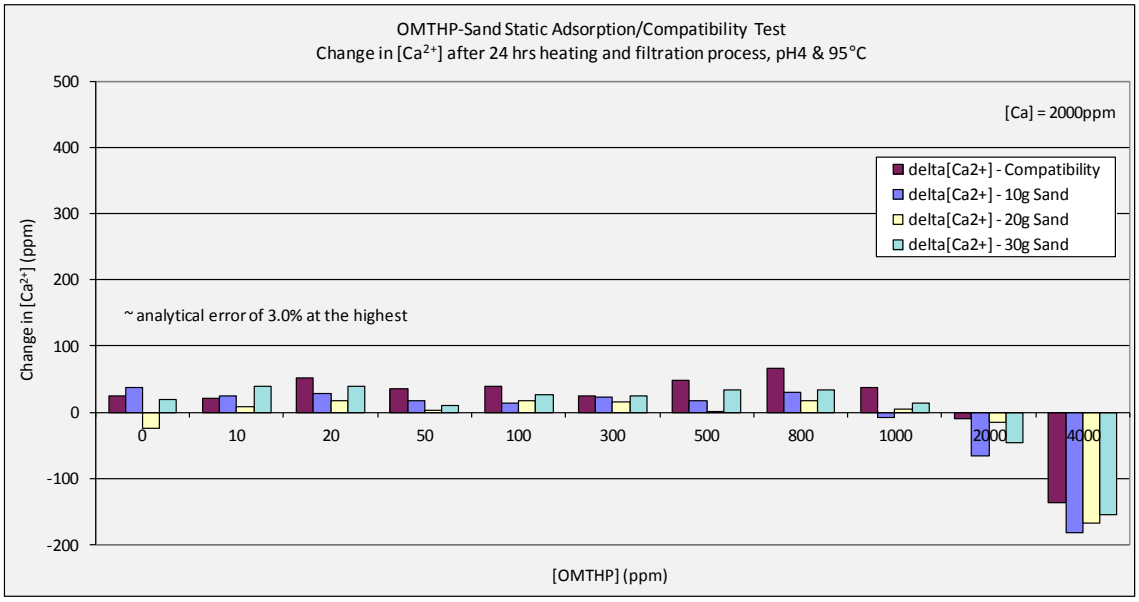

Figure 4.25: OMTHP-Sand Static Adsorption/Compatibility Test (10g, 20g & 30g Sand). Change in [Ca^{2+}] vs [OMTHP].

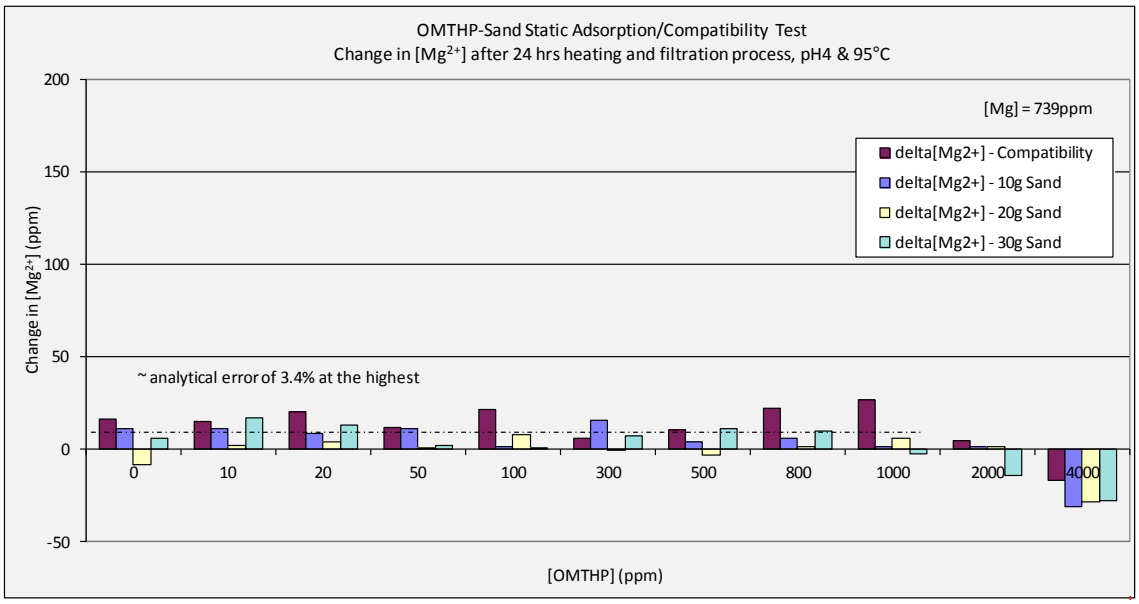

Figure 4.26: OMTHP-Sand Static Adsorption/Compatibility Test (10g, 20g & 30g Sand). Change in [Mg^{2+}] vs [OMTHP].

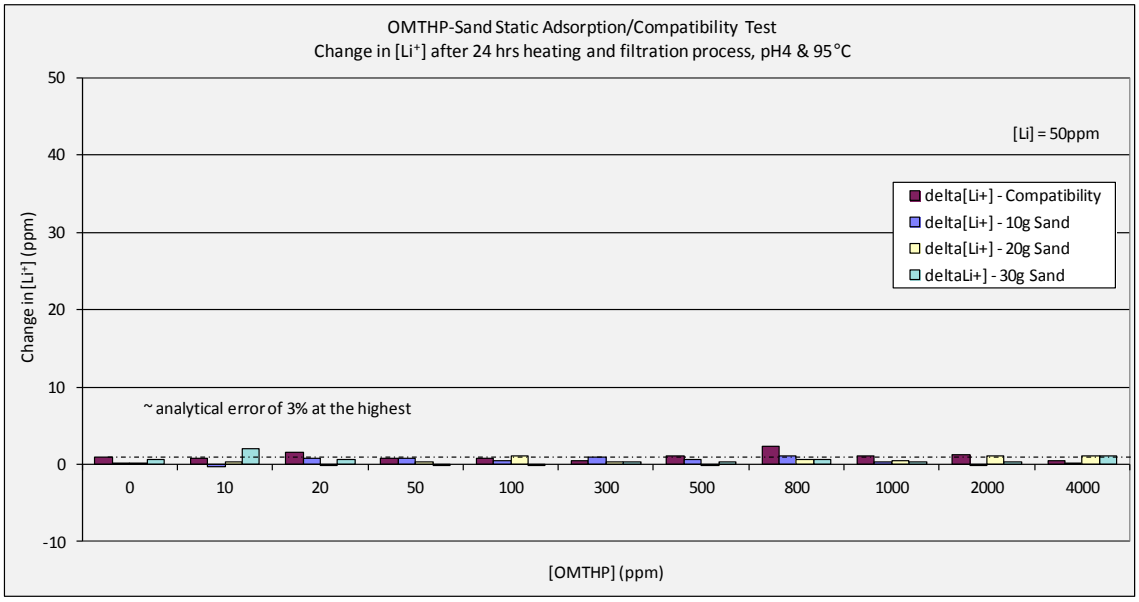

Figure 4.27: OMTHP-Sand Static Adsorption/Compatibility Test (10g, 20g & 30g Sand). Change in [Li^+] vs [OMTHP].

After filtration, all the filter papers were dried, weighed, photographed and sent for ESEM-EDAX analysis. The sample solutions were measured for pH. The weight of the samples that precipitated out of the solutions is presented in Table 4.6 and the corresponding photographed filter papers after filtration are shown in Figure 4.28. Only at 2000ppm and 4000ppm do we clearly see differences in both the weight and the appearance of precipitate, though traces of precipitate can be seen on filter paper along with very slight increases in weight. These results are very consistent with observations (above) on the amount of phosphorous, Ca^{2+} ions and Mg^{2+} ions that were measure in the filtered samples, which is less than in the stock solutions. The results prove that precipitation took place from 1000ppm onward.

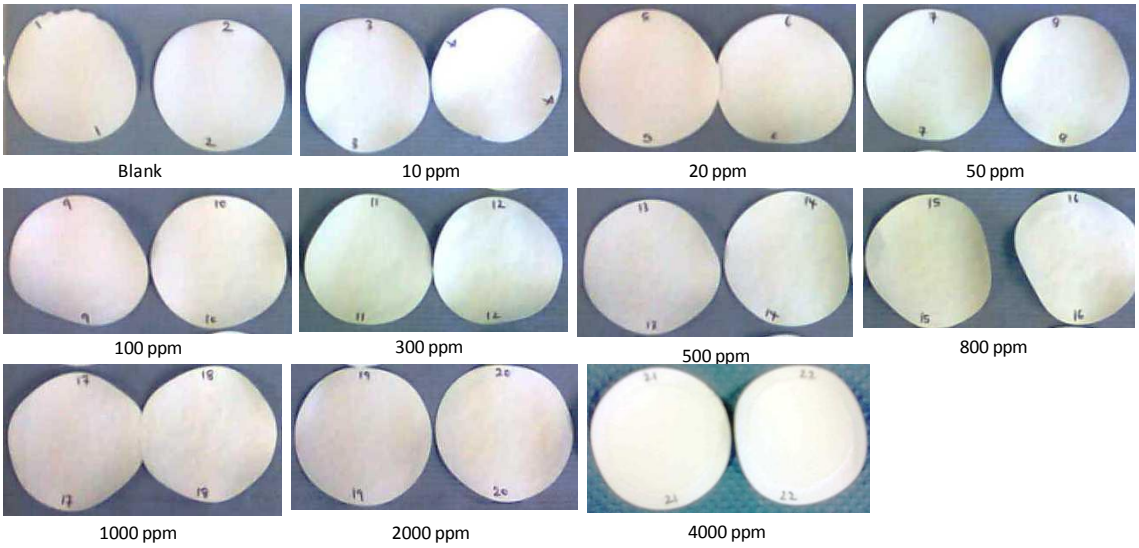

Figure 4.28: OMTHP-Sand Static Adsorption/Compatibility Test. Precipitates on filter papers at different concentrations of OMTHP.

OMTHP Conc. (ppm)	Weight of Ppt (g)
0	0.02
10	0.02
20	0.02
50	0.02
100	0.02
300	0.02
500	0.02
800	0.02
1000	0.03
2000	0.08
4000	0.21

Table 4.6: OMTHP-Sand Static Adsorption/Compatibility Test. Weight of precipitates on filter paper after filtration.

Table 4.7 and Figure 4.29 show ESEM-EDAX atomic and weight percentage, and photographed samples of phosphorous, Ca^{2+}, Mg^{2+} and other ions presents on the filter papers. For each concentration, two points were taken for analysis. The hazy black background was identified as being the filter paper itself, the solid white marks are the salts and the hazy white background is the compound of phosphorous, Ca^{2+} and Mg^{2+} ions. The blank samples without any SI show only filter paper and some salts on them. Base on the atomic% from ESEM-EDAX, there is no phosphorous compound identified

below 500ppm, but very small variable levels of Ca^{2+} and Mg^{2+} ions are identified. It must be noted that the EDAX signals are localized and values are not expected to be very accurate. Only when it reaches 800ppm and above, is clear hazy white background seen on the filter paper samples, which is identified to be phosphorous, Ca^{2+} and Mg^{2+} ions. Above 800ppm concentration, base on the atomic %, phosphorous, Ca^{2+} and Mg^{2+} are seen consistently, although the atomic % values are quite variable. Atomic% of phosphorous ranges from 7 to 12; Ca^{2+} from 3 to 6 and Mg^{2+} about 1. Although the values are rather variable, the presence of phosphorous, Ca^{2+} and Mg^{2+} as precipitates above 800ppm is clearly proven.

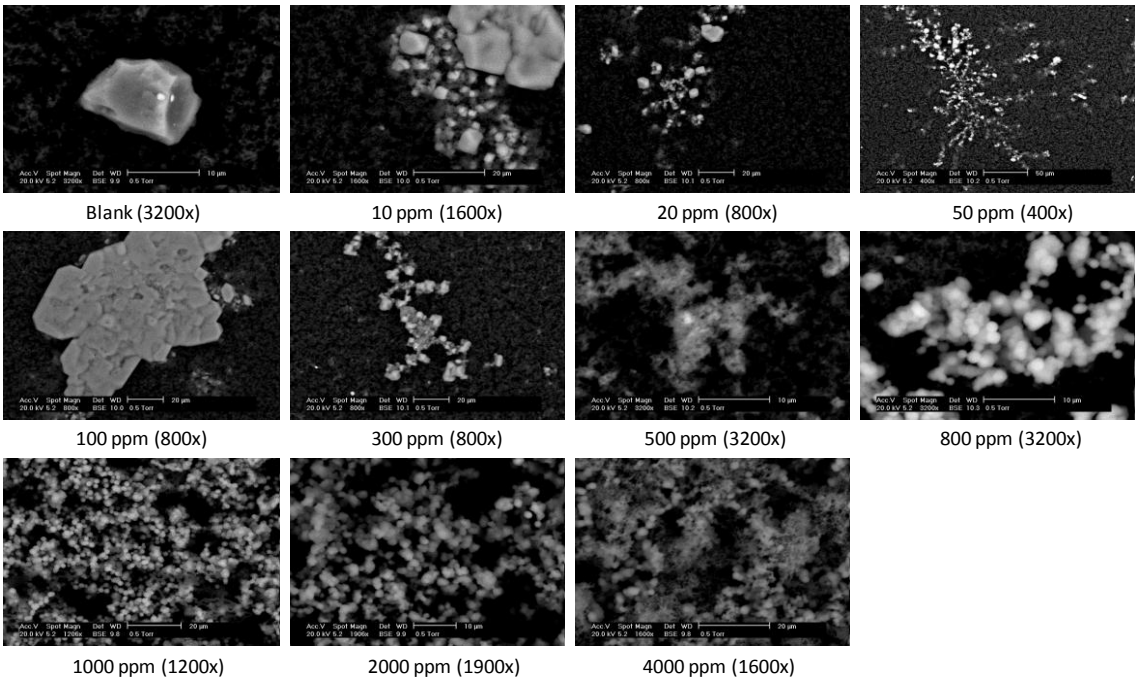

Figure 4.29: OMTHP-Sand Static Adsorption/Compatibility Test. Morphology of precipitates on ESEM photographed samples.

	Blank		10ppm		20ppm		50ppm		100ppm		300ppm	
Element	Wt %	At %	Wt %	At %	Wt %	At %	Wt %	At %	Wt %	At %	Wt %	At %
C K			48.73	61.32	43.91	52.85	45.28	54.37	44.34	59.88	42.35	57.27
N K			4.59	4.96	10.63	10.98	9.88	10.18			4.37	5.06
O K	39.44	53.34	22.43	21.19	34.56	31.23	33.58	30.27	20.62	20.9	17.04	17.3
NaK			9.05	5.95	2.76	1.74	2.58	1.62	12.95	9.13	15.27	10.79
MgK			0.45	0.28			0.24	0.14				
AlK			0.39	0.22								
SiK	60.56	46.66	0.85	0.46			0.23	0.12				
SrL					0.35	0.06						
P K												
S K			0.23	0.11								
Cl K			11.41	4.87	7.32	2.99	7.71	3.14	21.54	9.85	20.41	9.35
K K												
Ca K			1.3	0.49	0.46	0.17	0.5	0.18	0.56	0.22	0.56	0.23
Fe K			0.55	0.15								
Total	100	100	100	100	100	100	100	100	100	100	100	100

	500ppm		800ppm		1000ppm		2000ppm		4000ppm	
Element	Wt %	At %	Wt %	At %	Wt %	At %	Wt %	At %	Wt %	At %
C K	43.11	53.31	40.17	53.51	29.96	44.41	31.5	45	32.28	46.64
N K	7.57	8.03			3.16	4.02	6.08	7.44	0	0
O K	34.13	31.68	34.21	34.22	28.33	31.53	28.38	30.44	32.54	35.29
NaK	2.36	1.52	1.12	0.78	0.95	0.74	1.08	0.81	1.63	1.23
MgK	0.95	0.58	1.46	0.96	1.61	1.18	1.47	1.04	1.7	1.22
AlK										
SiK										
SrL	0.69	0.12	1.13	0.21	2.34	0.47	2.2	0.43	2.44	0.48
P K	3.43	1.65	11.85	6.12	18.51	10.64	16.64	9.22	17.15	9.61
S K	0.17	0.08								
Cl K	4.69	1.96	3.58	1.62	5.06	2.54	3.76	1.82	4.1	2.01
K K	0.26	0.1								
Ca K	2.64	0.98	6.48	2.59	10.08	4.48	8.9	3.81	8.16	3.53
Fe K										
Total	100	100	100	100	100	100	100	100	100	100

Table 4.7: OMTHP-Sand Static Adsorption/Compatibility Test. EDAX signals on the precipitates from ESEM.

Table 4.5 and Figure 4.30 show the pH values of the adjusted and filtered samples. All the stock solutions were adjusted to pH 4 to make sure it does not precipitate at room condition. After 24 hrs at 95^{o}C and filtration, the pH values were measured. For compatibility test with no minerals, the pH value is retained at ~4 until 500ppm; and reduces to 3.90, 3.86, 3.72 and 3.65 at 800, 1000, 2000 and 4000ppm, respectively. It shows that the pH value starts reducing when significant P, Ca^{2+} and Mg^{2+} are missing due to precipitation during filtration. Thus, significant precipitation of P, Ca^{2+} and Mg^{2+} on the filter paper has caused a reduction of pH. For adsorption tests at different masses

of sand, the pH value increases for the blank sample, and increases further up to 50ppm before pH reduces at 4000ppm. Although different masses of sand lead to different final pH values, they behave similarly in a reducing trend. At 4000ppm, the pH value converges to ~3.6 for all the different masses of sand. The observation here is similar to that seen in the DETPMP/NFFW/sand experiments; i.e. as more phosphorous, Ca^{2+} and Mg^{2+} are lost from the solution due to adsorption and precipitation, the lower is the pH value.

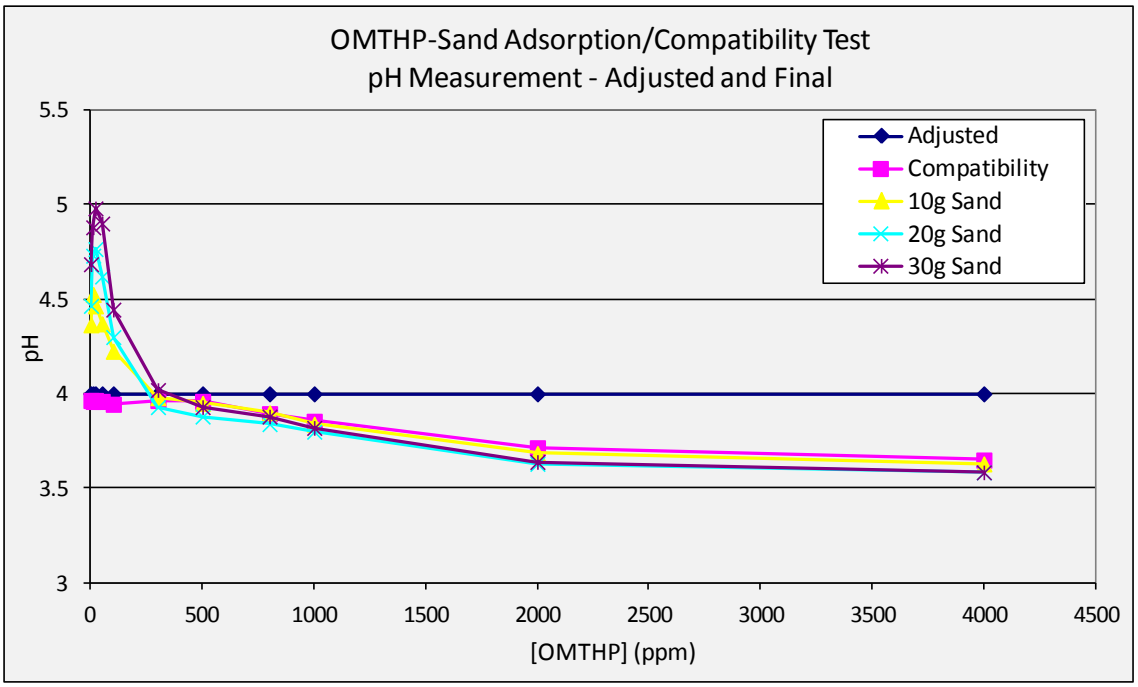

Figure 4.30: OMTHP-Sand Static Adsorption/Compatibility Test. pH Measurement – Adjusted and Final

4.5.3 DETPMP-KAOLINITE Adsorption/Compatibility Test

A stock solution of 10,000ppm DETPMP in NFFW was prepared for this experiment. At this concentration, DETPMP SI is fully dissolved and yellowish in colour. It was then diluted to attain lower concentrations of 10, 20, 50, 100, 500, 800, 1000, 1500, 2000, 3000 and 4000ppm which were used for all the experiments. In addition to that, additional DETPMP solutions at concentrations 15000 and 25000ppm in NFFW were

prepared to complete the total concentrations used for the experiment. pH was measured for all the stock solutions and was later adjusted to pH 4. At pH 4, the particles (if any) dissolved in the solutions at the various concentrations at which they were prepared. Figure 4.31 shows the initial and adjusted pH values of these SI solutions at various concentrations. The blank sample has pH 4.95 and this decreases gradually to pH 1.44 at 25000ppm of DETPMP SI. The decreasing trend of pH indicates the acidic nature of the DETPMP scale inhibitor as the concentration increases. The figure also shows some fluctuation in pH readings which is due to the fact that measurements were taken from two different experiments.

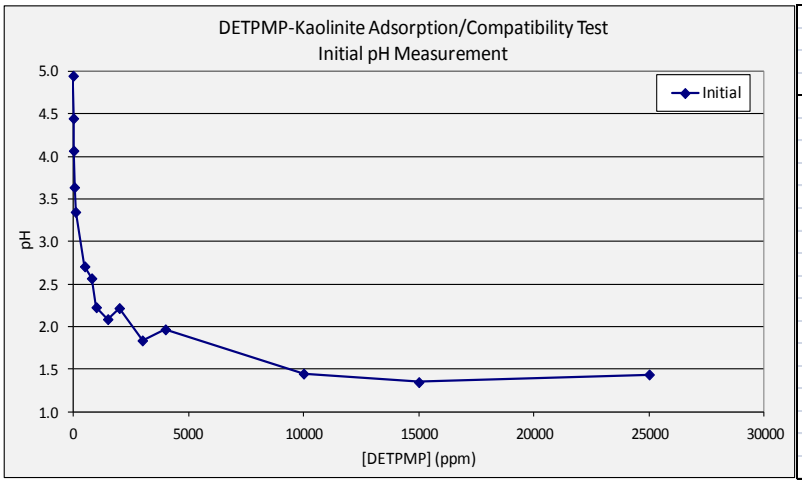

DETPMP Conc (ppm)	pH Initial	pH Adjusted
0	4.95	3.99
10	4.45	4.01
20	4.07	4
50	3.64	4
100	3.35	4
500	2.71	4
800	2.57	4
1000	2.23	4
1500	2.09	4
2000	2.22	4
3000	1.84	4
4000	1.97	4
10000	1.45	4
15000	1.35	4
25000	1.44	4

Figure 4.31: DETPMP SI initial pH measurement of each stock solutions before adjustment. The decreasing trend of the pH indicates acidic nature of OMTHP SI.

Figure 4.32 and Figure 4.33 show the adsorption ("apparent" or actual) level of scale inhibitor (DETPMP in mg SI / g rock) for different masses of kaolinite as a function of the scale inhibitor concentration (after adsorption, i.e. [SI] = c_{1f} – see above) in synthetic NFFW at pH 4 at 95°C. From these figures, we mainly wish to determine whether, and in which concentration regions, only pure adsorption or coupled adsorption/precipitation are taking place. Results in Figure 4.32 and Figure 4.33 show that only pure adsorption is seen up to ~500ppm of SI, before the Γ_{app} vs. [SI] curves for different (m/V) values start to deviate at higher concentration values due to the occurrence of coupled adsorption/precipitation behaviour. This is evident also from the actual numerical *levels* of apparent adsorption; if only pure adsorption were present,

Γ_{app} would plateau at a level of ~5.0 mg/g. In fact, at higher concentrations, we see that the Γ_{app} level is ~20.0 – 50.0 mg/g which is clearly indicative of a "coupled adsorption/precipitation" process. We note that, although normally pure adsorption only occurred to levels below 1.0 mg/g, in these experiments it is seen as high as 5.0 mg/g. This is expected as kaolinite contains clay minerals and the size distribution is such that its surface area is much larger than that of sand; in fact it is approximately 10x larger, and hence the 5 mg/g of DETPMP adsorption on kaolinite is quite reasonable.

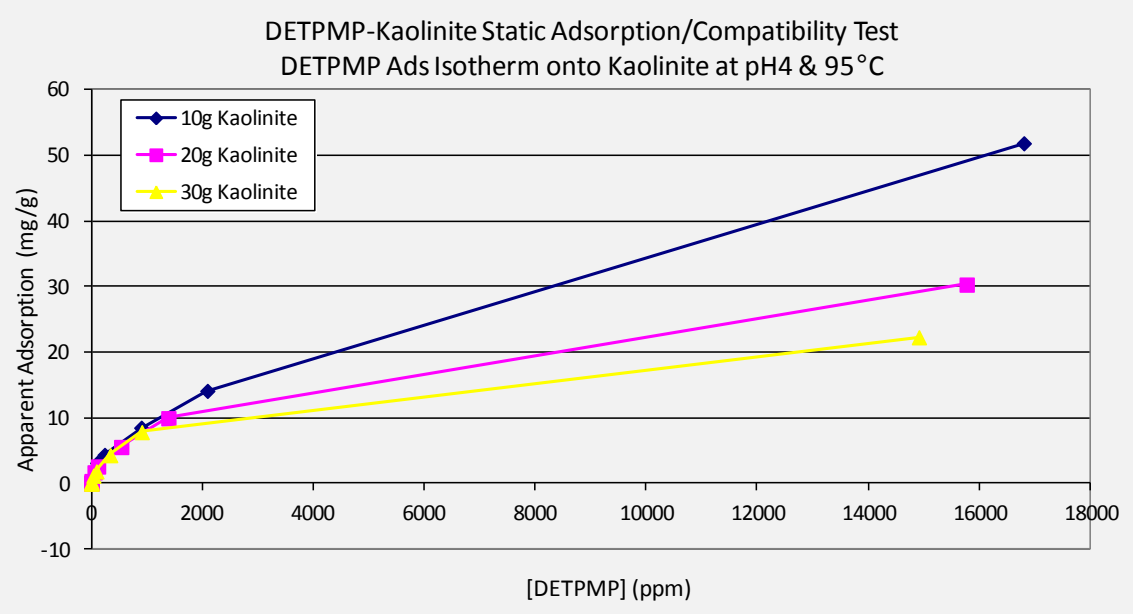

Figure 4.32: DETPMP-Kaolinite Static Adsorption/Compatibility Test. DETPMP Adsorption Isotherm onto different masses of sand at pH4 & 95°C.

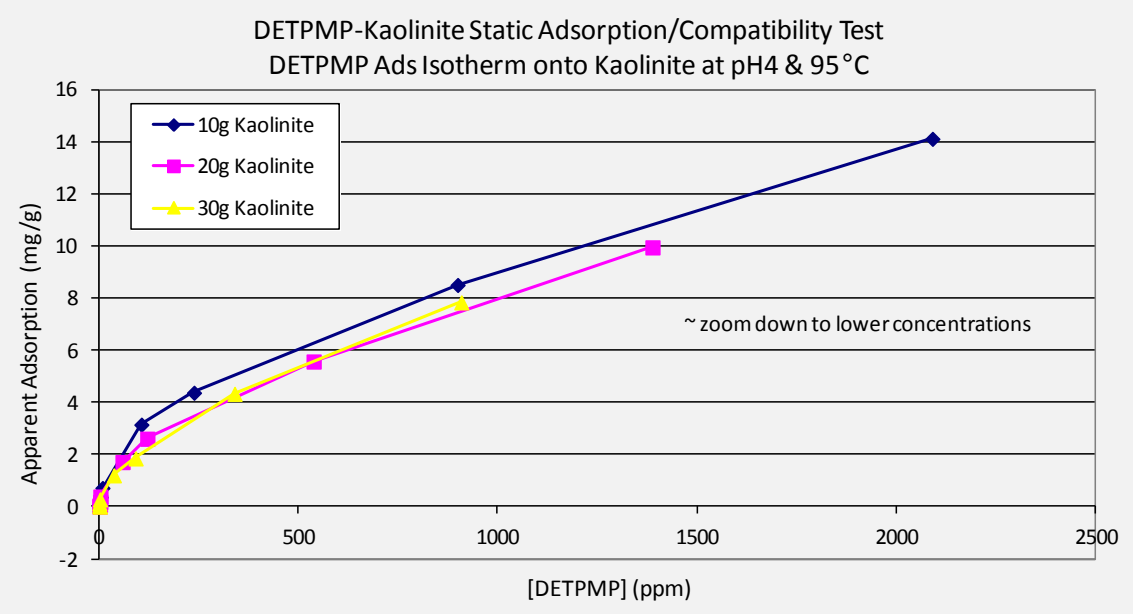

Figure 4.33: DETPMP-Kaolinite Static Adsorption/Compatibility Test. DETPMP Adsorption Isotherm onto different masses of sand at 95°C and pH4; zoomed down to lower concentration.

To further establish the pure adsorption and coupled adsorption/precipitation behaviour, changes of [phosphorous], [Ca^{2+}] and [Mg^{2+}] concentration in the mixture of SI and NFFW solution in both adsorption and compatibility tests were measured. Any divalent ion level above stock solution concentration is not expected or must be within its analytical error of less than 5%. The decrease in the solution divalent ion levels are due to either precipitation of M-DETPMP complex or because of involvement of the divalent ions in the adsorption process (e.g. by cation bridging). The change in [Li+] is also observed to check whether there was any evaporation taking place. There should not be any changes in [Li+] as it is an inert tracer ion which does not adsorb onto sand or react with DETPMP SI. The [Li+] value was used to correct for the increase in concentration for all the other elements due to evaporation.

Figure 4.34, Figure 4.35 and Figure 4.36 show the differences in the levels of [phosphorous], [Ca^{2+}] and [Mg^{2+}] for both compatibility and adsorption tests. The differences in the amounts show that there are definitely concentrations regions where pure adsorption and where coupled adsorption/precipitation are taking place. It is known that Ca^{2+} and Mg^{2+} ions do not significantly adsorb* onto kaolinite, and so any

differences are due to cation bridging of phosphorous to Ca^{2+} and Mg^{2+} ions onto the kaolinite. [*NB however, there may be some ion exchange of Ca^{2+} and Mg^{2+} ions onto the rock/mineral surface but this is not a very large effect for kaolinite and is even less for pure quartz sand]. It is also noted that in almost all cases, there is a small increase in [Ca^{2+}] and [Mg^{2+}] ions, which is not expected, but they are all within the analytical error of less than 5%. Even changes in [Li^{+}] ions are observed for all the cases, but again, they are within its analytical error of less than 5%. The increase in Li^{+} also shows slight evaporation was taking place. The % increase was used to correct the concentrations for all the other elements.

Figure 4.34 show that phosphorous starts adsorbing onto sand even at a low concentration of 10ppm for the different masses of sand used, where the difference between the stock solution and the filtrate is about 8 to 12ppm as the mass of sand increases from 10g to 30g sand. As the concentration of DETPMP SI increases from 10ppm to 25000ppm, the changes in phosphorous ion loss from solution are also increased. Whereas, in the precipitation case where there is no kaolinite present, reduction in phosphorous can only be observed at 800ppm, where 4ppm was left as precipitates, and increases to 5000ppm (left as precipitates) as the DETPMP concentration increases to 25000ppm. The figure indicates pure adsorption of phosphorous onto kaolinite until 500ppm and coupled adsorption/precipitation from 800ppm onward.

Figure 4.35 shows the change in Ca^{2+} ion concentrations for both compatibility and adsorption tests. Referring to adsorption tests at 10g to 30g kaolinite; the figure shows that Ca^{2+} ions starts to show a significant reduction from 2000ppm and are even further reduced at 25000ppm. The reduction in Ca^{2+} ions increases as the mass of sand increases from 10g to 30g. Whereas for precipitate ion test (referring to compatibility tests), reduction in Ca^{2+} is also observed at 2000ppm. The difference of Ca^{2+} ion in both experiments shows that Ca^{2+} must have precipitated at 2000ppm and above as an M-DETPMP complex. At 25000ppm DETPMP, 700 to 850ppm of Ca^{2+} was lost from the solution at different masses of sand tested.

Figure 4.36 shows the change in Mg^{2+} ion concentrations for both compatibility and adsorption tests. Referring to adsorption tests at 10g to 30g kaolinite; the figure shows significant changes in Mg^{2+} can only be seen at 4000ppm onward. The difference in Mg^{2+} ion concentration shows that Mg^{2+} must have precipitated as an M-DETPMP complex. For compatibility test with no minerals, significant reduction in Mg^{2+} is also observed at 4000ppm and above. Again, comparing phosphorous to Ca^{2+} and Mg^{2+} binding, Ca^{2+} has more affinity to DETPMP SI as shown from the amount of concentration precipitated; where 800ppm and 175ppm of Ca^{2+} and Mg^{2+} loss from solution, respectively.

Figure 4.37 shows the change in Li^{+} ions. Li^{+} is an inert tracer ion and should not adsorb or precipitate. It is analysed to determine if any evaporation occurred in the experiment. Based on the variation in Li+ concentration, its analytical error is < 2% on and only slight evaporation is indicated which was taken into account for the calculation made for all the other elements (P, Ca, Mg).

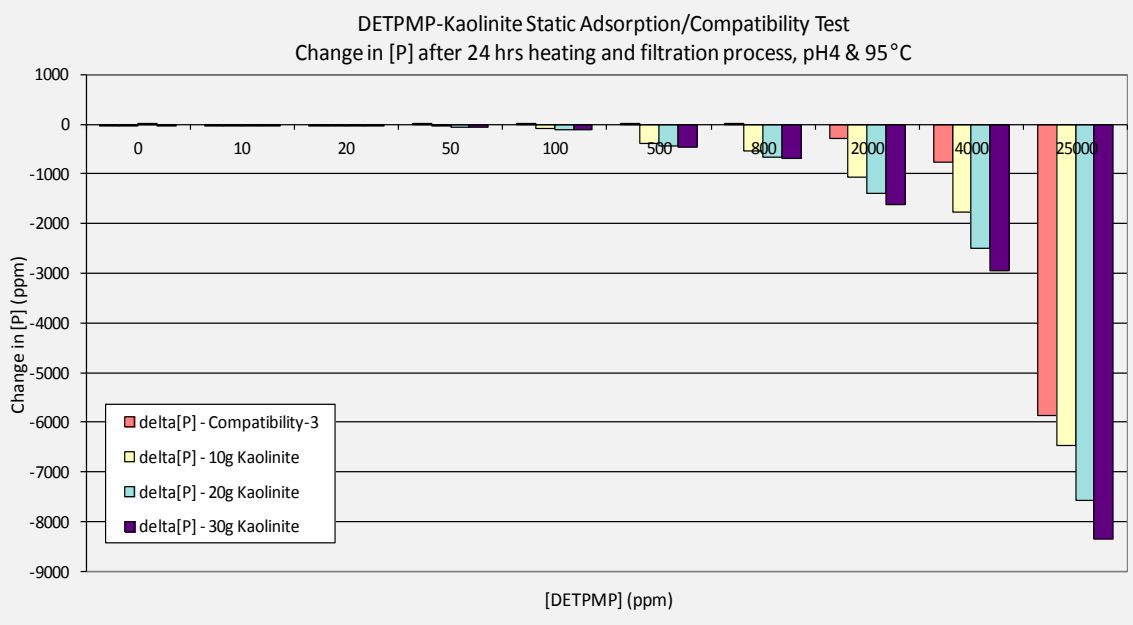

Figure 4.34: DETPMP-Kaolinite Static Adsorption/Compatibility Test (10g, 20g & 30g Sand). Change in [P] vs [DETPMP].

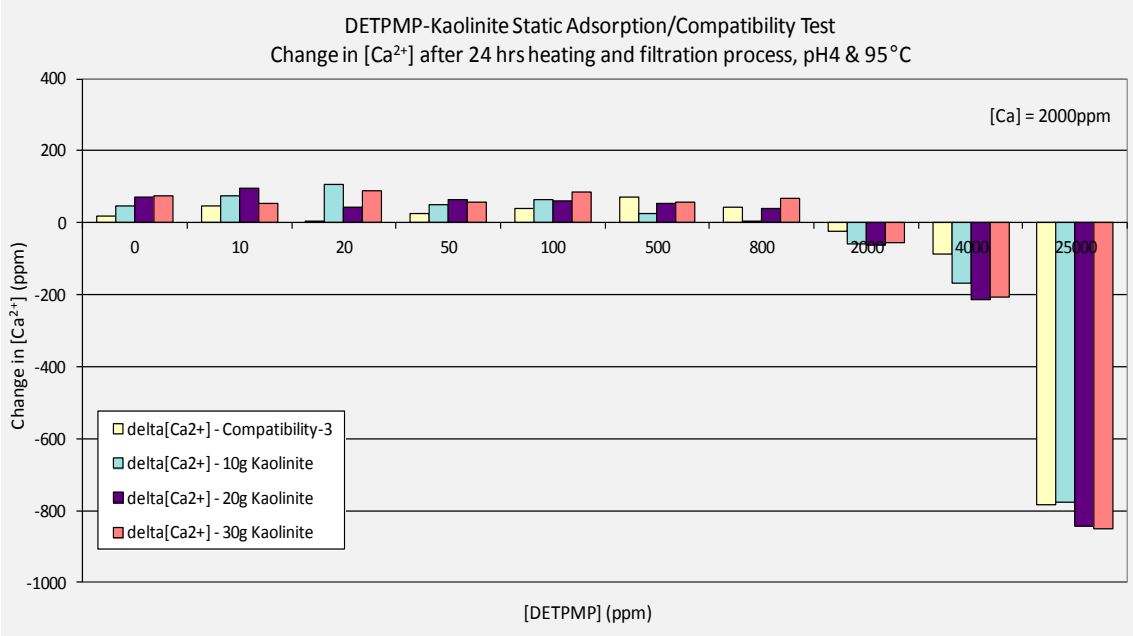

Figure 4.35: DETPMP-Kaolinite Static Adsorption/Compatibility Test (10g, 20g & 30g Sand). Change in $[Ca^{2+}]$ vs [DETPMP].

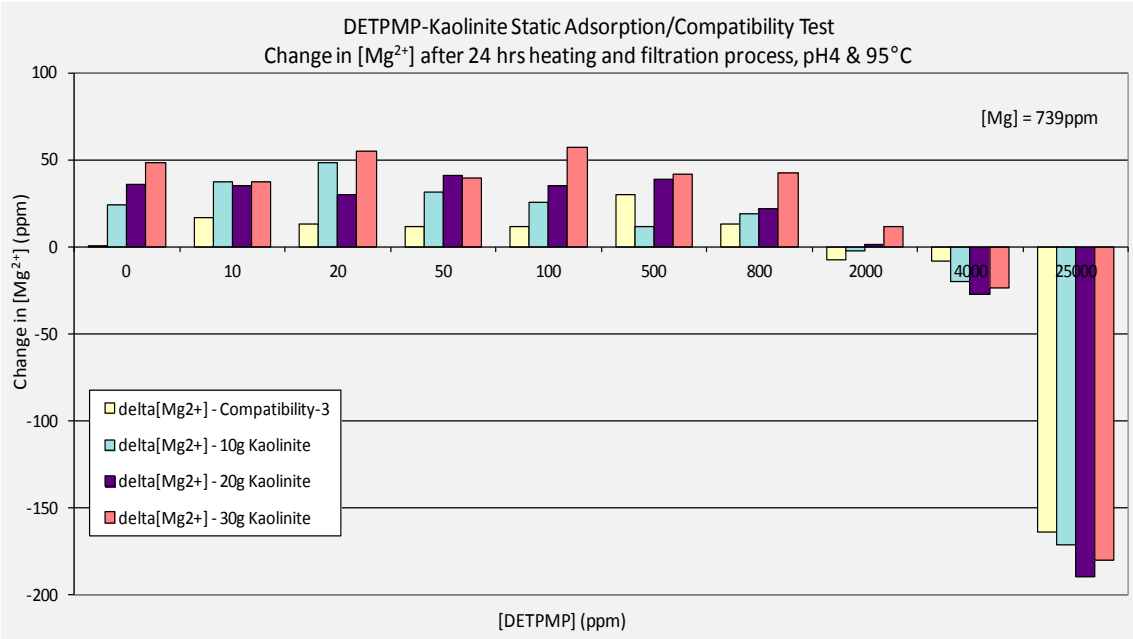

Figure 4.36: DETPMP-Kaolinite Static Adsorption/Compatibility Test (10g, 20g & 30g Sand). Change in $[Mg^{2+}]$ vs [DETPMP].

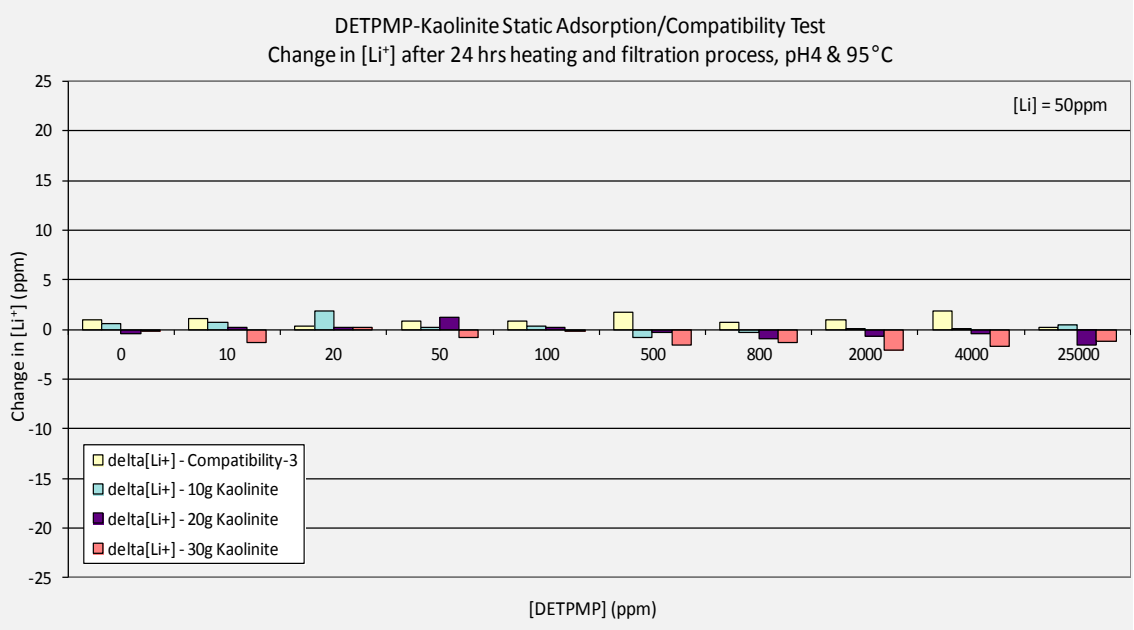

Figure 4.37: DETPMP-Kaolinite Static Adsorption/Compatibility Test (10g, 20g & 30g Sand). Change in [Li^+] vs [DETPMP].

After the filtration, all the filter papers were dried, weighed, photographed and sent for ESEM-EDAX analysis. The sample solutions were measured for pH. The weight of the samples that precipitated out of the solutions and the corresponding photographed filter papers after filtration are shown in Figure 4.38. Only at 1000ppm do we clearly see differences in both the weight and the appearance of precipitate, although there were some tracers of precipitates at 800ppm. As the concentration increases, the weight increases as expected and more significant precipitates can be seen clearly on the filter paper. These results are very consistent with observations (above) on the amount of phosphorous, Ca^{2+} ions and Mg^{2+} ions that were measured in solution, which was less than in the stock solutions.

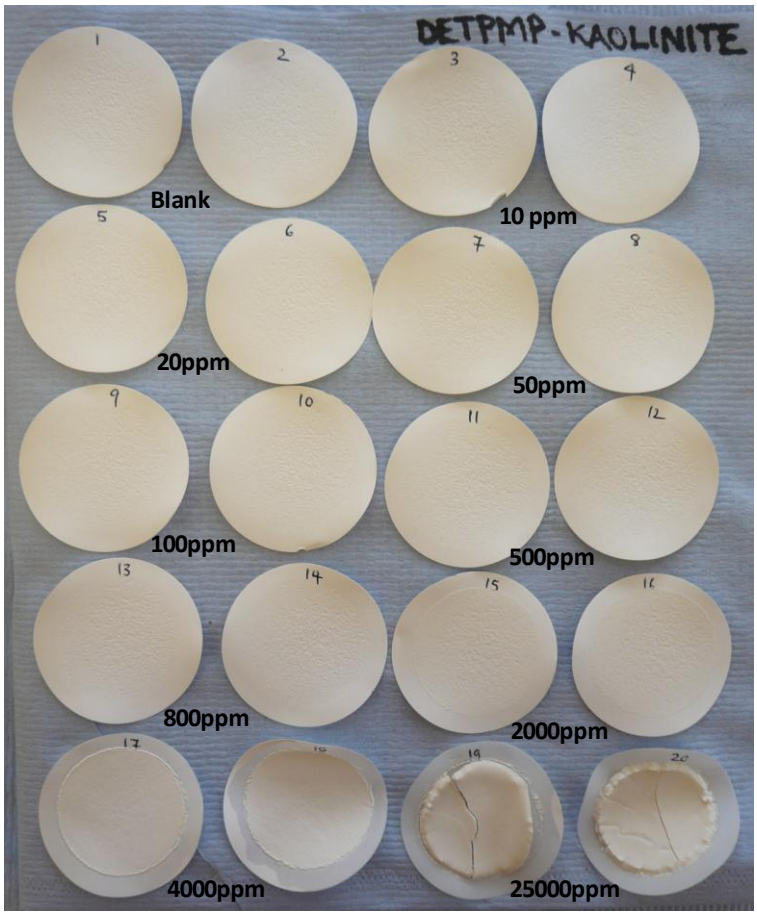

DETPMP Conc. (ppm)	Weight of Ppt (g)
0	0.02
10	0.02
20	0.02
50	0.02
100	0.02
500	0.02
800	0.02
1000	0.04
1500	0.06
2000	0.06
3000	0.12
4000	0.14
10000	0.48
15000	0.69
25000	0.86

Figure 4.38: DETPMP-Kaolinite Static Adsorption/Compatibility Test. Precipitates on filter papers and weight of precipitates at different concentrations of DETPMP.

Table 4.8 and Figure 4.39 show ESEM-EDAX atomic and weight percentage, and photographed samples of phosphorous, Ca^{2+}, Mg^{2+} and other ions presents on the filter papers. For each concentration, one or two points were taken for analysis. The hazy black background was identified to be the filter paper itself, the solid white marks are the salts and the hazy white background is the compound of phosphorous, Ca^{2+} and Mg^{2+} ions. The blank samples without any SI shows only filter paper and some salts on them. Based on the atomic % from ESEM-EDAX, there is no phosphorous compound identified below 500ppm, but variable values of Ca^{2+} and Mg^{2+} ions are identified. It must be noted that the EDAX signals are localized and variable and inaccurate values are expected depending on which point has been analyzed. Only when it reached 800ppm and above, was a clear hazy white background seen on the filter paper samples, which is identified to be phosphorous, Ca^{2+} and Mg^{2+} ions. Above 800ppm

concentration, base on the atomic%, phosphorous, Ca^{2+} and Mg^{2+} are seen consistently, although the atomic % are quite variable. Atomic% of phosphorous ranges from 2 to 11; Ca^{2+} from 2 to 5 and Mg^{2+} from 1 to 2. Though the value are quite variable, the clear presence of phosphorous, Ca^{2+} and Mg^{2+} as precipitates above 800ppm is proven.

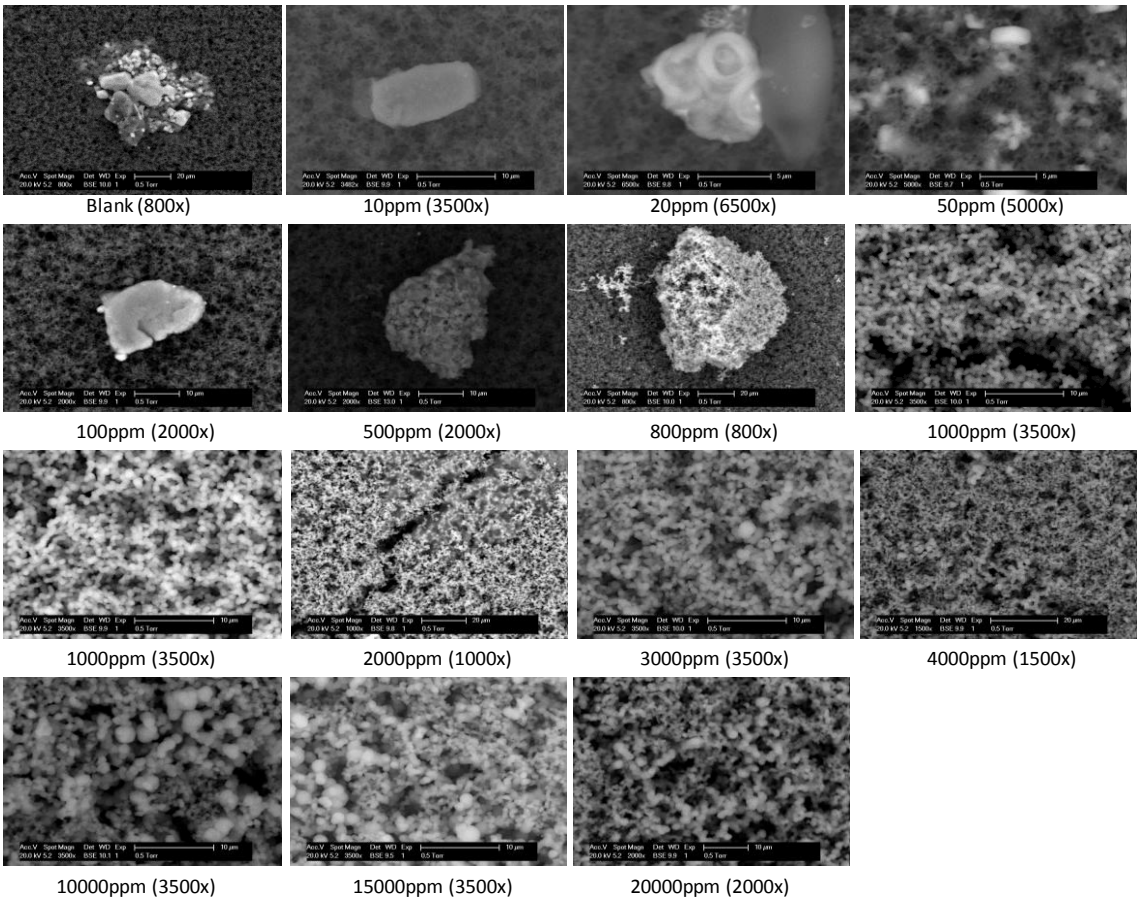

Figure 4.39: DETPMP-Kaolinite Static Adsorption/Compatibility Test. Morphology of precipitates on ESEM photographed samples.

	Blank		10ppm		20ppm		50ppm		100ppm		500ppm		800ppm		1000ppm	
Element	Wt %	At %	Wt %	At %	Wt %	At %	Wt %	At %	Wt %	At %	Wt %	At %	Wt %	At %	Wt %	At %
C K	27.51	37.73	28.91	45.73	33.65	43.96	52.84	65.22	26.25	35.81	26.89	51.85	43.6	55.01	26.97	41.26
N K																
O K	45.61	46.96	37.82	44.92	45.44	44.57	27.05	25.07	47.96	49.12	14.51	21	38.4	36.38	32.35	37.16
NaK	1.94	1.39	1.45	1.2	1.17	0.8	5.86	3.78	0.63	0.45	1.25	1.26	1.88	1.24	0.77	0.62
MgK	0.96	0.65									0.61	0.58	1.25	0.78	2.96	2.24
P K													7.43	3.64	16.72	9.92
AlK	8.18	5	0.16	0.11	7.74	4.5			1.02	0.62	0.57	0.49				
SrL	8.45	4.96	2.78	0.6											3.18	0.67
S K	5.52	2.56	6.48	3.84												
SiK	0.53	0.22			8.35	4.66			23.5	13.71	2.19	1.81				
ClK	1.31	0.54	0.63	0.34	1.3	0.58	13.75	5.75	0.63	0.29	1.18	0.77	2.92	1.25	5.32	2.76
K K					2.34	0.94					0.27	0.16				
CaK			0.53	0.25			0.49	0.18			0.45	0.26	4.52	1.71	11.71	5.37
BaL			20.93	2.9												
CrK											10.03	4.47				
FeK			0.32	0.11							37.41	15.52				
NiK											4.64	1.83				
Total	100	100	100	100	100	100	100	100	100	100	100	100	100	100	100	100

	1500ppm		2000ppm		3000ppm		4000ppm		10000ppm		15000ppm		25000ppm	
Element	Wt %	At %	Wt %	At %	Wt %	At %	Wt %	At %	Wt %	At %	Wt %	At %	Wt %	At %
C K	27.86	42.54	28.85	42.82	26.67	39.99	29.08	43.95	27.65	40.35	26.91	39.25	30.67	44.01
N K					5.37	6.91			4.86	6.09	4.76	5.96		
O K	30.83	35.34	33.85	37.71	29.05	32.69	30.47	34.57	32.27	35.36	33.56	36.75	36.01	38.8
NaK	1.25	1	1.44	1.12	1.07	0.83	1.69	1.33	1.63	1.24	1.88	1.44	2.06	1.54
MgK	2.47	1.86	1.81	1.33	2.03	1.5	1.93	1.44	1.95	1.41	1.68	1.21	1.81	1.28
P K	18.24	10.8	16.8	9.67	2.46	0.51	2.79	10.88	16.71	9.46	17.15	9.7	2.35	9.17
AlK					17.77	10.33	18.57						16.48	
SrL	2.64	0.55	2.34	0.48			4.08	0.58	2.57	0.51	2.66	0.53	2.8	0.46
S K							11.4						0.08	
SiK							100						7.74	
ClK	4.41	2.28	4.36	2.19	4.1	2.08		2.09	3.15	1.56	3.06	1.51	100	1.36
K K														0.04
CaK	12.3	5.63	10.54	4.69	11.48	5.16		5.16	9.2	4.02	8.33	3.64		3.33
BaL														
CrK														
FeK														
NiK														
Total	100	100	100	100	100	100		100	100	100	100	100		100

Table 4.8: DETPMP-Kaolinite Static Adsorption/Compatibility Test. EDAX signals on the precipitates from ESEM.

4.5.4 OMTHP-KAOLINITE Adsorption/Compatibility Test

A stock solution of 10,000ppm OMTHP in NFFW was prepared for these experiments. At this concentration, OMTHP SI is not fully dissolved and is whitish and opaque in appearance. It starts to precipitate/phase separate after a few hours and distinctly precipitates after ~24 hours. This preparation was then diluted to attain the lower concentration levels of 10, 20, 50, 100, 500, 800, 2000 and 4000ppm which were used for all the experiments. pH was measured for all the stock solutions and was later adjusted to pH 4. At pH4, all the particles (if any) dissolved in the solutions at the different concentrations at which they were prepared. Figure 4.40 shows the initial pH values of the various OMTHP stock solutions before pH adjustment. The blank sample (0 ppm OMTHP) had a pH value of 5.41 and this decreased gradually to pH 4.46 at 4000ppm. The decreasing trend of pH indicates the acidic nature of the OMTHP scale

inhibitor as the concentration increases. OMTHP is less acidic than DETPMP (DETPMP, had pH 1.97 at 4000ppm).

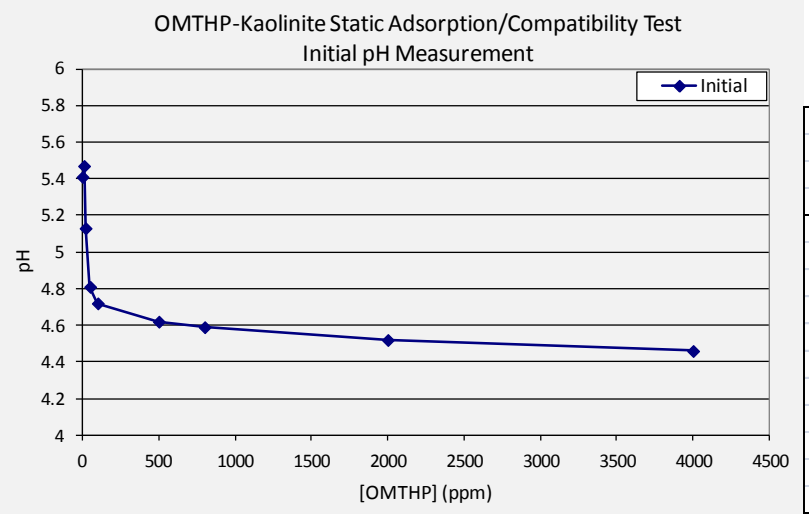

OMTHP Conc. (ppm)	pH (Initial)	pH (Adjusted)
0	5.41	4.01
10	5.47	3.99
20	5.13	3.99
50	4.81	3.99
100	4.72	4
500	4.62	4
800	4.59	4.01
2000	4.52	4
4000	4.46	4

Figure 4.40: OMTHP SI initial pH measurement of each stock solutions before adjustment. The decreasing trend of the pH indicates acidic nature of OMTHP SI.

Figure 4.41 shows the adsorption ("apparent" or actual) level of scale inhibitor (OMTHP in mg SI / g rock) on different masses of kaolinite as a function of the scale inhibitor concentration (i.e. after adsorption, [SI] = c_{1f} – see above) in synthetic NFFW at pH values of 4 and 95°C. The apparent adsorption value ranges from near zero to 16 mg/g as the SI concentration increases to 1300ppm. The Γ_{app} vs. [SI] curves for the different values of (m/V) overlap (with +/- 4% error) up to around 150ppm which indicating pure adsorption behaviour. At higher concentrations, the behaviour is observed to change to coupled adsorption/precipitation as the different (m/V) curves start to deviate from each other. At 150ppm, the Γ_{app} value is around ~4 - 5 mg/g, which is quite high for pure adsorption but this is due to the large surface area of the kaolinite as discussed above. Also, the very high adsorption levels for OMTHP onto kaolinite (due to high surface areas) lead to a less clear transition between the pure adsorption and the coupled adsorption/precipitation regions.

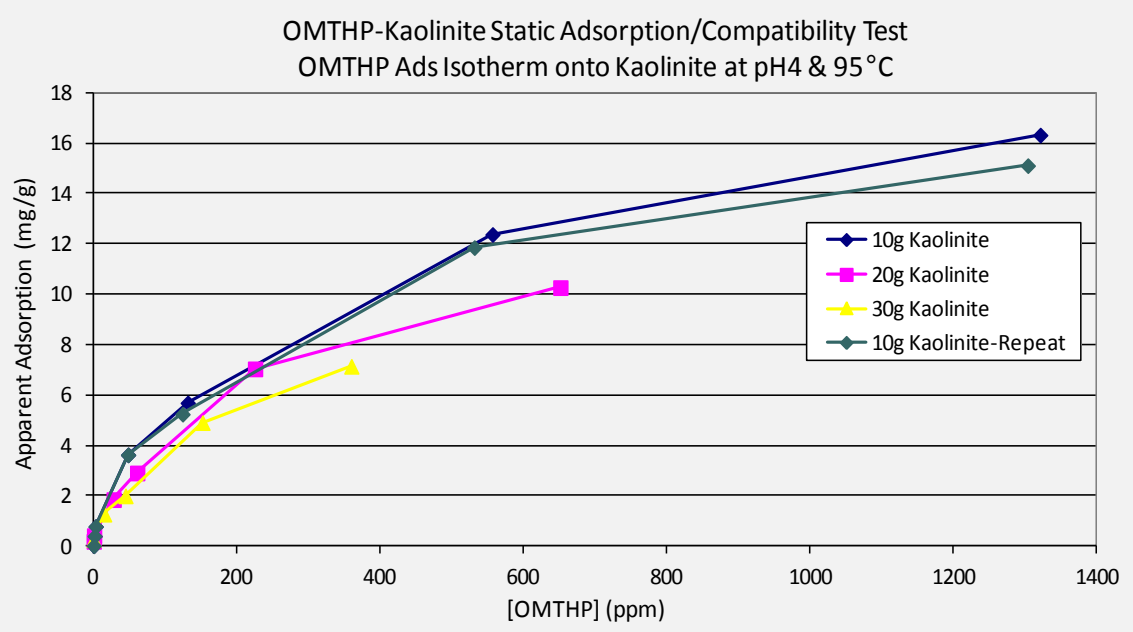

Figure 4.41: OMTHP-Kaolinite Static Adsorption/Compatibility Test. OMTHP Adsorption Isotherm onto different masses of sand at pH4 & 95°C.

To further establish the pure adsorption and coupled adsorption/precipitation behaviour,

change in [phosphorous], [Ca^{2+}] and [Mg^{2+}] concentration in the mixture of SI and NFFW solution in both adsorption and compatibility test were measured. Any divalent ion level above stock solution concentration is not expected or must be within its analytical error of less than 5%. The decrease in the solution divalent ion levels are due to either precipitation of M-OMTHP complex or involvement of the divalent ions in the pure adsorption process (e.g. by cation bridging). The change in [Li^{+}] is also observed to establish if any evaporation takes place. There should not be any changes in [Li^{+}] as it is an inert tracer ion which does not react with OMTHP SI or adsorb onto sand.

Figure 4.42, Figure 4.43 and Figure 4.44 show the differences in the solution levels of [phosphorous], [Ca^{2+}] and [Mg^{2+}] for both compatibility and adsorption tests for the OMTHP/NFFW/kaolinite system. The differences in the amounts in each test show that there are definitely regions of pure adsorption and coupled adsorption/precipitation occurring in the range of concentrations tested. It is known that Ca^{2+} and Mg^{2+} ions do not significantly adsorb* onto kaolinite, so the differences are due to cation bridging of

phosphorous to Ca^{2+} and Mg^{2+} ions onto the kaolinite. [*NB however, there may be some ion exchange of Ca^{2+} and Mg^{2+} ions onto the rock/mineral surface but this is not a large effect for kaolinite and is even less for pure quartz sand]. It is also noted that in almost all cases, there is a small increase in [Ca^{2+}] and [Mg^{2+}] ions, which is not expected, but they are all within its analytical error of less than 5%. Even changes in [Li^{+}] are observed for all the cases, but again, they are within its analytical error of less than 5% and due to small amounts of evaporation. The % increase in [Li^{+}] was used to correct the concentrations for all the other elements.

Figure 4.42 shows the change in phosphorous ions for both compatibility and adsorption tests. Referring to adsorption tests, the figure shows that phosphorous starts adsorbing onto kaolinite even at a low concentration of 10ppm for the different masses of kaolinite used, where the difference between the stock solution and the filtrate is about 9, 10 and 11 ppm as the mass of kaolinite increases for 10g, 20g and 30g of kaolinite. As the concentration of OMTHP SI increases from 10ppm to 4000ppm, the changes in phosphorous ions also increase. Essentially, pure adsorption is observed up to 500ppm and coupled adsorption/precipitation is seen from 800ppm onward for the OMTHP/NFFW/kaolinite system.

Figure 4.43 shows the change in Ca^{2+} ion concentrations in both compatibility and adsorption tests. Referring to adsorption tests, the Ca^{2+} ions start to show a significant reduction from 2000ppm and is further reduced at 4000ppm. For the compatibility tests, reduction in Ca^{2+} is only observed at 4000 ppm, but with less precipitation.

Figure 4.44 shows the change in Mg^{2+} ion concentrations in both compatibility and adsorption tests. Significant changes in Mg can only be seen at 4000ppm for all the masses of kaolinite used. For compatibility test with no minerals, significant reduction is also observed at 4000ppm, but with much smaller amounts of ion loss from solution compared to adsorption tests. Comparing phosphorous (SI) to Ca^{2+} and Mg^{2+} binding, phosphorous has more affinity to Ca^{2+}than Mg^{2+} as shown in the amount of concentration precipitated.

Figure 4.45 shows the change in Li^{+} ion concentration. It is analyzed to see if there was

any evaporation. The figure shows there was fluctuation in the region of 1 to 3%. This indicates the fluctuation was due to analytical error and small evaporation. Li^+ is an inert tracer ion does not adsorb or precipitates onto kaolinite minerals. This factor was taken into account for all the calculation made for all the elements.

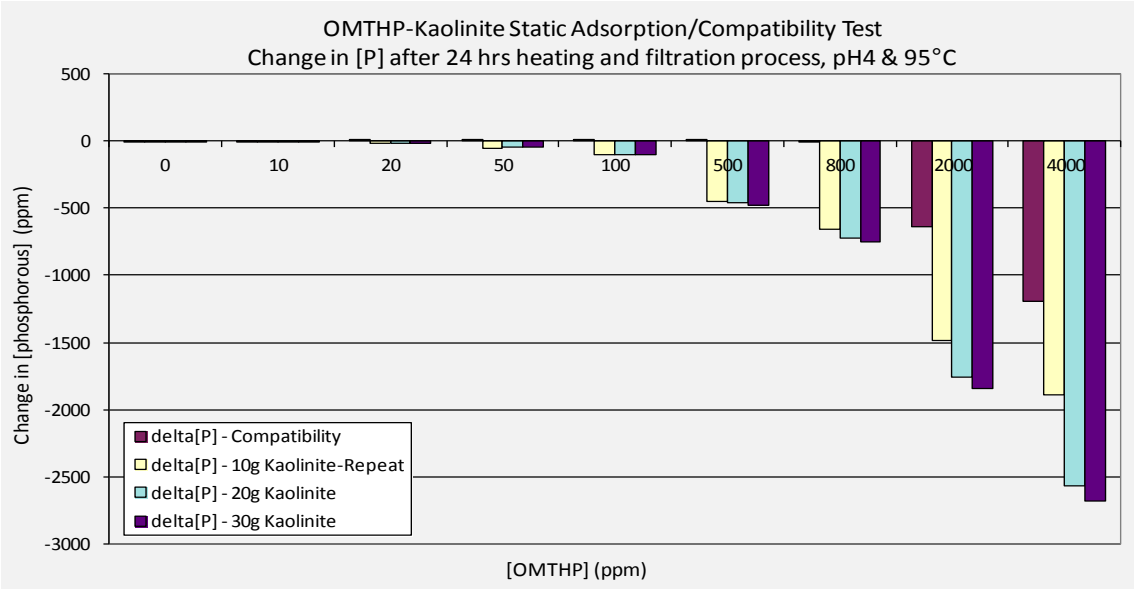

Figure 4.42: OMTHP-Kaolinite Static Adsorption/Compatibility Test (10g, 20g & 30g Sand). Change in [P] vs [OMTHP].

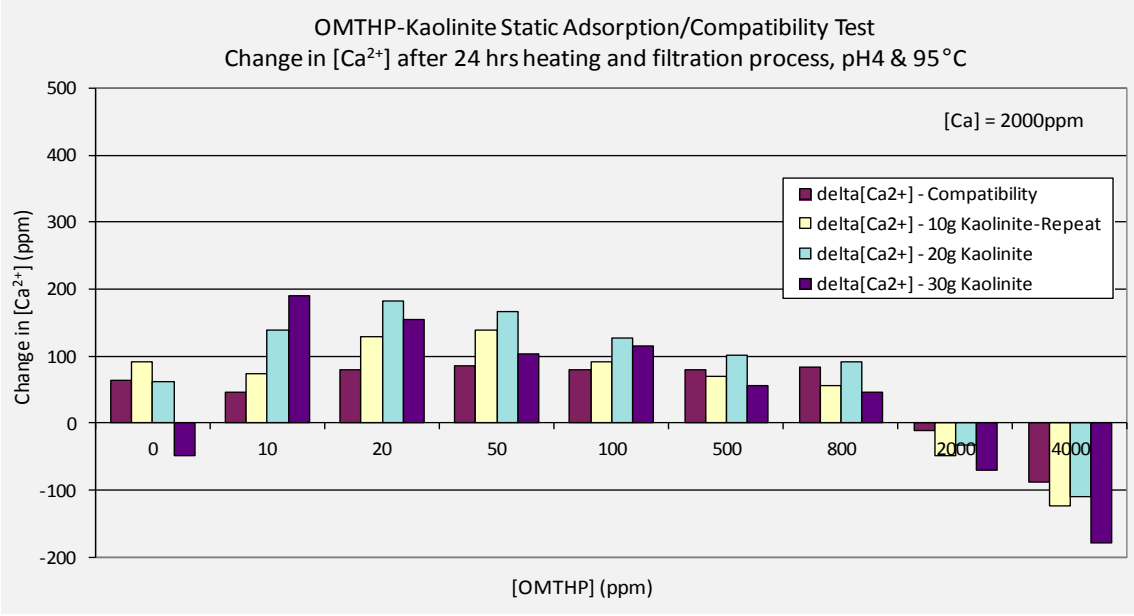

Figure 4.43: OMTHP-Kaolinite Static Adsorption/Compatibility Test (10g, 20g & 30g Sand). Change in $[Ca^{2+}]$ vs [OMTHP].

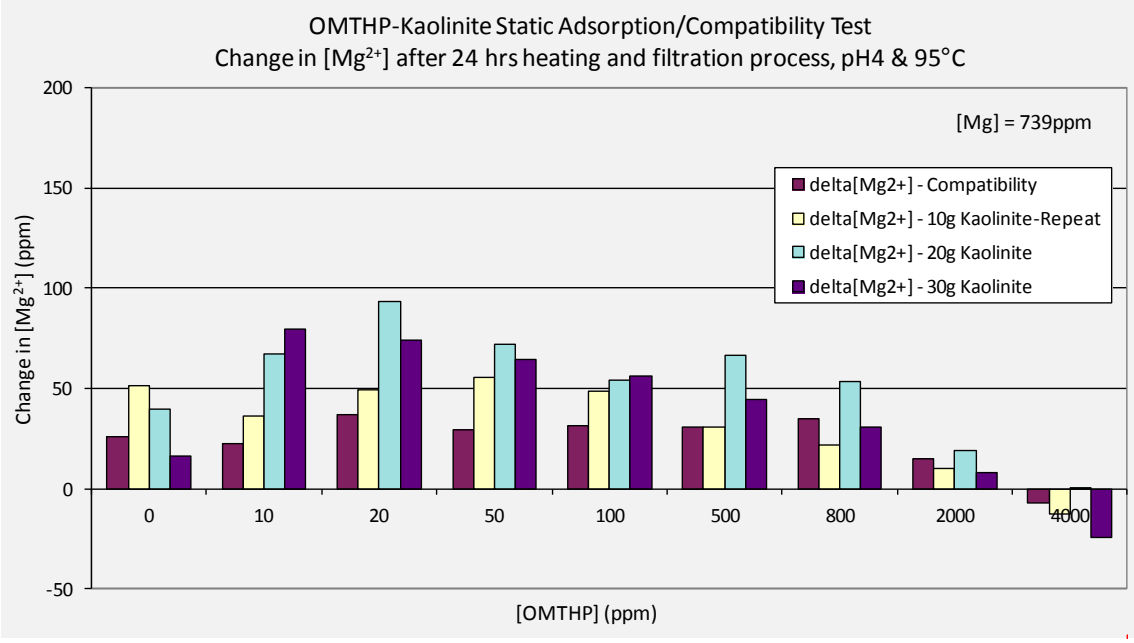

Figure 4.44: OMTHP-Kaolinite Static Adsorption/Compatibility Test (10g, 20g & 30g Sand). Change in [Mg^{2+}] vs [OMTHP].

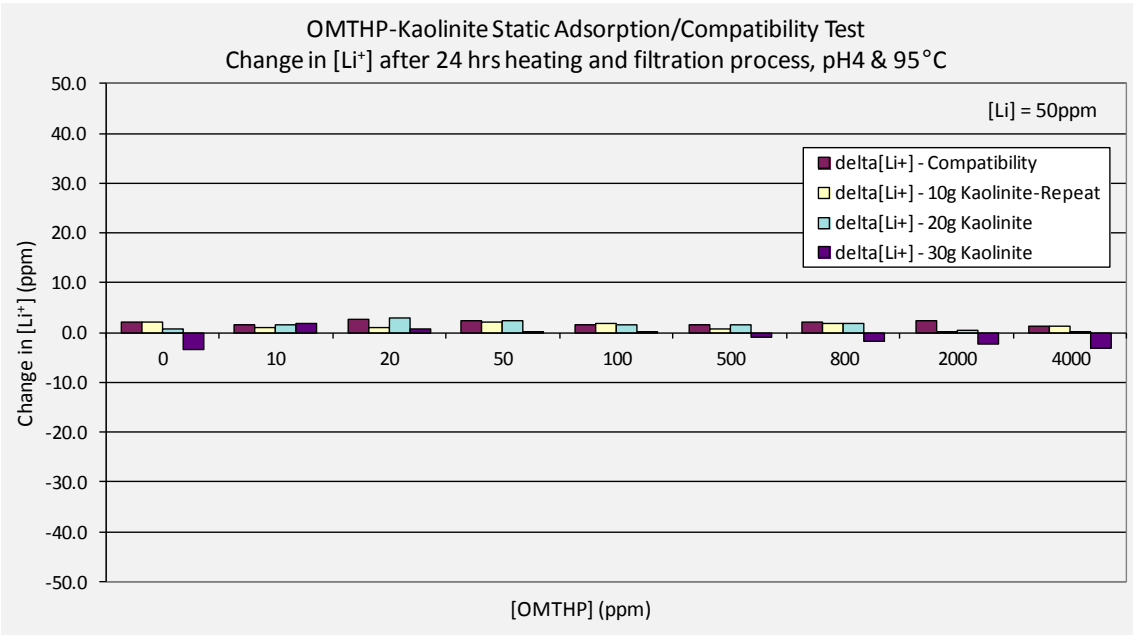

Figure 4.45: OMTHP-Kaolinite Static Adsorption/Compatibility Test (10g, 20g & 30g Sand). Change in [Li^{+}] vs [OMTHP].

After filtration, all the filter papers were dried, weighed, photographed and sent for ESEM-EDAX analysis. The sample solutions were measured for pH. The weight of the samples that precipitated out of the solutions and the corresponding photographed filter

papers after filtration are shown in Figure 4.46. Only at 2000ppm and 4000ppm do we clearly see differences in both the weight and the appearance of precipitate on filter paper, although some traces of precipitate may be seen at 800ppm. These results are very consistent with observations (above) on the amount of phosphorous, Ca^{2+} ions and Mg^{2+} ions that were measure in the filtered samples, which took place at 2000ppm and above. The result proves that precipitation starts from 800ppm onward.

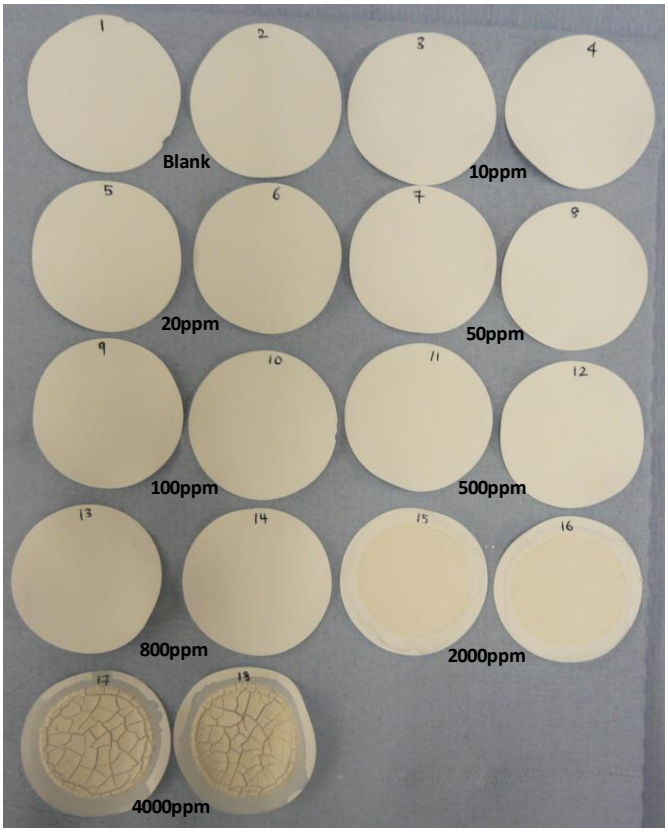

OMTHP Conc. (ppm)	Weight of Ppt (g)
0	0.02
10	0.02
20	0.02
50	0.02
100	0.02
500	0.02
800	0.02
2000	0.10
4000	0.27

Figure 4.46: OMTHP-Kaolinite Static Adsorption/Compatibility Test. Precipitates on filter papers and weight of precipitates at different concentrations of OMTHP.

Table 4.9 and Figure 4.47 show ESEM-EDAX atomic percentage and photographed samples of phosphorous, Ca^{2+}, Mg^{2+} and other ions presents on the filter papers. For each concentration, two points were taken for analysis. The hazy black background was identified as being the filter paper itself, the solid white marks are the salts and the hazy white background is the compound of phosphorous, Ca^{2+} and Mg^{2+} ions. The blank samples without any SI shows only filter paper and some salts on it. Based on the atomic% from ESEM-EDAX, there is no phosphorous compound identified below

500ppm, but variable value of Ca^{2+} and Mg^{2+} ions were identified. It must be noted that the EDAX signals are localized and inaccurate values are expected. Only when it reaches 800ppm and above, can a clear hazy white background be seen on the filter paper samples, which is identified to be phosphorous, Ca^{2+} and Mg^{2+} ions. Above 800ppm concentration, based on the atomic %; phosphorous, Ca^{2+} and Mg^{2+} are seen consistently, although the atomic % values are quite variable. Atomic % of phosphorous ranges from 3 to 8; Ca^{2+} from 1 to 3 and Mg^{2+} about 1. Although the values are rather inaccurate, the presence of phosphorous, Ca^{2+} and Mg^{2+} as precipitates above 800ppm is proven.

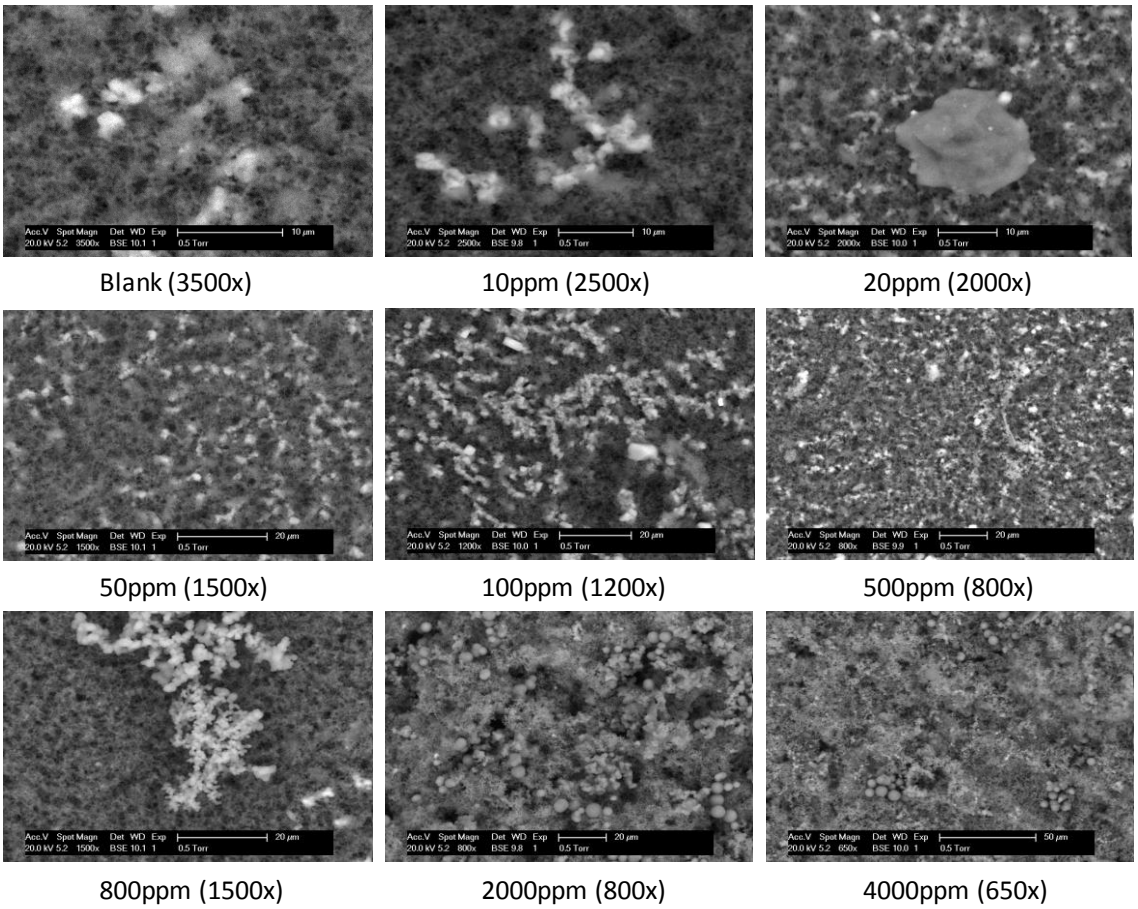

Figure 4.47: OMTHP-Kaolinite Static Adsorption/Compatibility Test. Morphology of precipitates on ESEM photographed samples.

	Blank		10ppm		20ppm		50ppm		100ppm		500ppm		800ppm		2000ppm		4000ppm	
Element	Wt %	At %	Wt %	At %	Wt %	At %	Wt %	At %	Wt %	At %	Wt %	At %	Wt %	At %	Wt %	At %	Wt %	At %
C K	54.5	64.97	31.76	43.11	54.32	65.21	33.07	45.01	53.57	64.68	51.41	61.82	45.06	56.17	38.43	53.35	35.41	50.64
O K	32.42	29.01	39.36	40.12	31.21	28.13	36.95	37.75	30.79	27.91	35.48	32.03	38.85	36.37	28.69	29.9	29.03	31.16
NaK	3.46	2.15	1.62	1.15	3.68	2.31	0.95	0.68	4.64	2.93	3.69	2.32	1.03	0.67	1.45	1.05	2.01	1.51
MgK							0	0					1.1	0.68	1.27	0.87	1.64	1.16
P K											0.38	0.18	6.59	3.18	16.38	8.82	15.56	8.63
AlK			11.6	7.01			2.45	1.48										
SiK			11.95	6.94			23.74	13.82										
SrL																	1.96	0.38
ClK	9.22	3.72	2.93	1.35	9.97	4.06	1.68	0.78	10.74	4.39	8.56	3.49	3.55	1.5	5.2	2.44	6.32	3.06
CaK	0.4	0.14			0.81	0.29			0.27	0.1	0.47	0.17	3.83	1.43	8.59	3.57	8.06	3.45
K K			0.78	0.32			1.16	0.49										
Total	100	100	100	100	100	100	100	100	100	100	100	100	100	100	100	100	100	100

Table 4.9: OMTHP-Kaolinite Static Adsorption/Compatibility Test. EDAX signals on the precipitates from ESEM.

4.5.5 DETPMP-SIDERITE Adsorption/Compatibility Test

A stock solution of 10,000ppm DETPMP in NFFW was prepared for this experiment on the static adsorption/precipitation of DETPMP onto the iron mineral, siderite ($FeCO_3$). At this concentration, DETPMP SI is fully dissolved and yellowish in colour. It was then diluted to attain lower concentrations of 20, 50, 100, 500, 1500, 4000 and 10000ppm which were used for all the experiments. In addition to that, 15000ppm of DETPMP in NFFW was prepared to complete the total set of concentrations used for this experiment. pH was measured for all the stock solutions and was later adjusted to pH 4. At pH 4, all of the particles (if any) dissolved in the solutions at the different concentrations at which they were prepared. No precipitation was observed even after the solution was left for 24 hours at room temperature. Figure 4.48 shows the initial pH values of the various stock solutions before adjustment. The blank sample has a pH value of 6.05 and this decreased gradually to pH 1.48 at 15000ppm. The decreasing trend of pH indicates the acidic nature of the DETPMP scale inhibitor as the concentration increases.

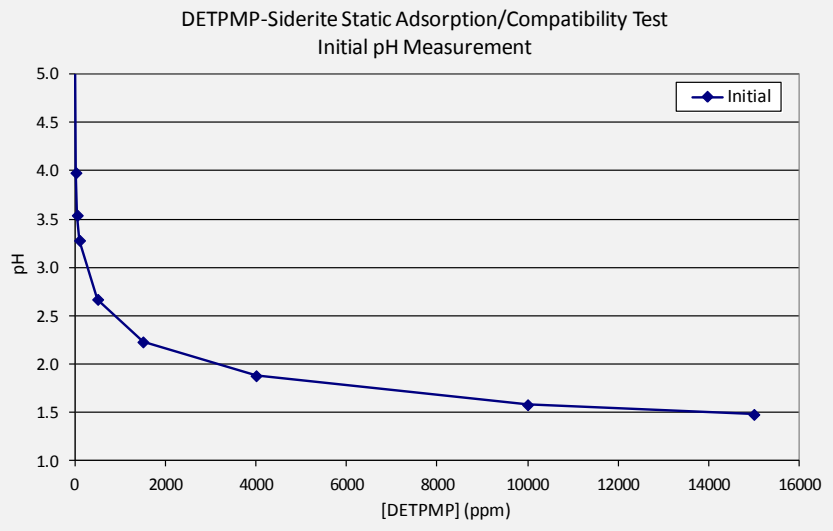

DETPMP Conc. (ppm)	pH (Initial)	pH (adjusted)
0	6.05	4.01
20	3.98	4.01
50	3.54	4
100	3.28	4
500	2.67	4
1500	2.23	4
4000	1.88	4
10000	1.58	4
15000	1.48	4

Figure 4.48: DETPMP SI initial pH measurement of each stock solutions before adjustment. The decreasing trend of the pH indicates acidic nature of DETPMP SI.

Figure 4.49 shows the adsorption ("apparent" or actual) level of scale inhibitor (DETPMP in mg SI / g rock) on different masses of siderite as a function of the scale inhibitor concentration (i.e. the concentration after adsorption, [SI] = c_{1f} – see above) in synthetic NFFW at pH 4 at 95°C. The main observations from these figures can establish whether only pure adsorption or coupled adsorption/precipitation is taking place. From the Γ_{app} vs. [SI] results in , it is less clear where the regions of pure adsorption and coupled adsorption/precipitation occur for the siderite mineral substrate under these conditions. However, at the very low concentration of around 100ppm, the Γ_{app} vs. [SI] lines do appear to overlap for each values of (m/V) before they start to deviate and diverge somewhat at higher concentration levels. Above [SI] ~ 1500, it appears that the Γ_{app} vs. [SI] curves do depend on the (m/V) ratio- hence indicating that coupled adsorption/precipitation behaviour is occurring. Also, in the pure adsorption region ([SI] $\leq$ ~100ppm), the absolute values of the adsorption are quite high, with Γ_{app} ~2 – 3 mg/g. This may be associated with the higher surface area of the siderite or indeed the surface may have a very high adsorptive affinity for scale inhibitor (as noted by earlier work, Gdanski and Funkhouser, 2001). However, at [SI] > 1500ppm, then very high levels of Γ_{app} are observed, Γ_{app} ~ 20 – 70 mg/g onto the siderite and these levels can only be due to precipitation.

In addition to the relatively high surface area, another factor that may have contributed to the high apparent adsorption results for the DETPMP/siderite system may be the amount of [Fe^{3+}] in the system. Results in Figure 4.50 show that, at 1500ppm, 25ppm [Fe^{3+}] went through the filter paper while at 15000ppm, 200ppm [Fe^{3+}] went through the filter paper. It shows that not only phosphorous, calcium and magnesium ions leached out of the system, but also iron, which is part of siderite minerals also leached out of the system. The full effects of the Fe^{3+} will need further investigation to assess its impact on the pure adsorption or couple adsorption/precipitation behaviour in the DETPMP/siderite system.

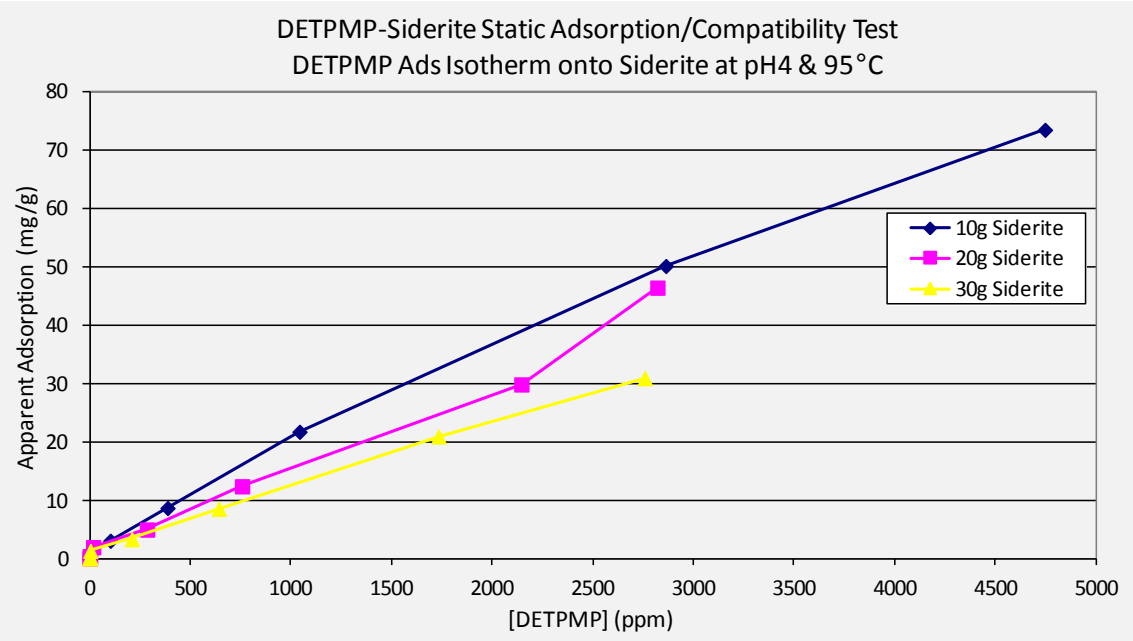

Figure 4.49: DETPMP-Siderite Static Adsorption/Compatibility Test. DETPMP Adsorption Isotherm onto different masses of siderite at pH4 & 95°C.

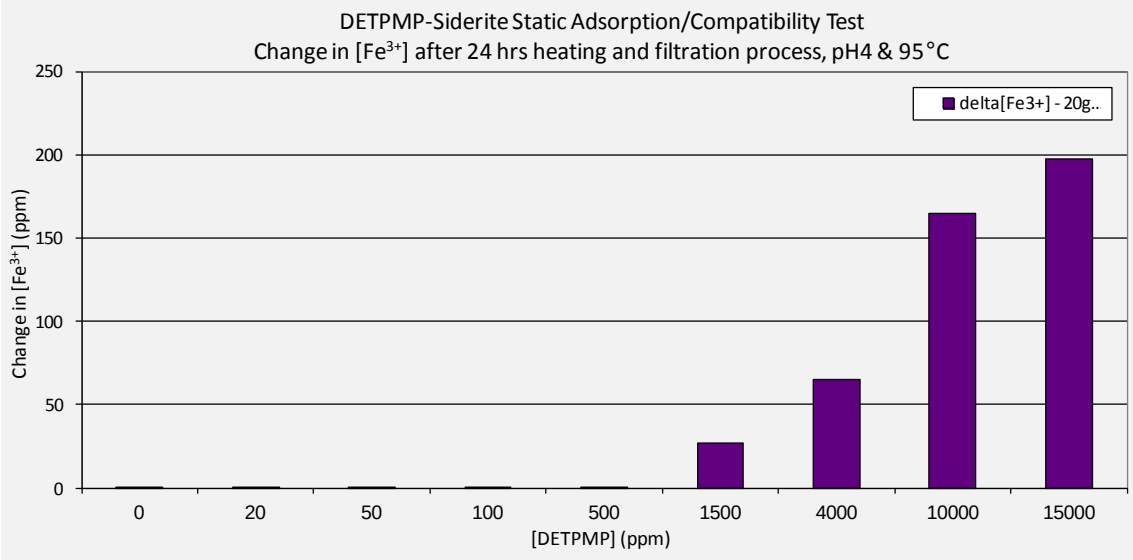

Figure 4.50: DETPMP-Siderite Static Adsorption/Compatibility Test (10g, 20g & 30g siderite). Change in [Fe^{3+}] vs [DETPMP].

To further establish the pure adsorption and coupled adsorption/precipitation behaviour, changes of [phosphorous], [Ca^{2+}] and [Mg^{2+}] concentration in the mixture of SI and NFFW solution in both adsorption and compatibility test were observed. Any divalent ion level above stock solution concentration is not expected or must be within its analytical error of less than 5%. The decrease in the solution divalent ion levels are due to either precipitation of M-DETPMP complex or involvement of the divalent ions in the pure adsorption process (e.g. by cation bridging). The change in [Li^{+}] is also observed to establish if any evaporation takes place. There should not be any changes in [Li^{+}] as it is an inert tracer ion which does not react with DETPMP SI or adsorb onto sand. The %evaporation was used to correct the increase in concentration for all the other elements involved.

Figure 4.51, Figure 4.52 and Figure 4.53 show the differences in the solution levels of [phosphorous], [Ca^{2+}] and [Mg^{2+}] for both compatibility and adsorption tests. The differences in the amounts in each test show that regions of pure adsorption and couple adsorption/precipitation occur in different SI concentration regions. It is known that Ca^{2+} and Mg^{2+} ions do not significantly adsorb* onto siderite, so the differences are probably due to cation bridging of phosphorous to Ca^{2+} and Mg^{2+} ions onto the siderite.

[*NB however, there may be some ion exchange of Ca^{2+} and Mg^{2+} ions onto the rock/mineral surface but this is not a large effect for siderite and is even less for pure quartz sand]. It is also noted that in almost all cases, there is an increase in [Ca^{2+}] and [Mg^{2+}] ions, which is not expected, but they are all within its analytical error of less than 5%. Even changes in [Li^{+}] are observed for all the cases, but again, they are within its analytical error of less than 5%. Apart from the analytical error, slight evaporation was observed in these tests which was corrected for.

Figure 4.51 shows the change in phosphorous ion concentrations for both compatibility and adsorption tests. Figure 4.51 shows that phosphorous starts adsorbing onto siderite even at a low concentration of 20ppm for the different masses of siderite used, where the difference between the stock solution and the filtrate is about 15 to 20ppm as the mass of siderite increases from 10g, 20g and 30g siderite. As the concentration of DETPMP SI increases from 20ppm to 15000ppm, the changes in phosphorous ions also increase to show more precipitation. At stock concentration of 15000ppm DETPMP; about 9000ppm to 11800ppm of DETPMP is lost from solution by precipitation (clearly due to the m/V dependence and also the very high apparent adsorption value). Thus, it appears that we are observing pure adsorption in the DETPMP/siderite system up to [SI] ~500ppm, before going into coupled adsorption/precipitation region for [SI] > 500ppm.

Figure 4.52 shows the change in Ca^{2+} ion concentrations for both compatibility and adsorption tests. Ca^{2+} ions start to show a significant reduction from 4000ppm and they are further reduced at 15000ppm. The reduction in Ca^{2+} increases as the mass of siderite increases. For the compatibility tests, reduction in Ca^{2+} is also observed starting at 4000 ppm, but with less precipitation. The difference of Ca^{2+} ion in both experiments shows that some must have precipitated and some bridged along with phosphorous onto the mineral surface.

Figure 4.53 shows the change in Mg^{2+} ion concentrations for both compatibility and adsorption tests. Referring to adsorption tests at 10g to 30g siderite; the figure shows that significant changes can only be seen at 10000ppm for all the masses of siderite

used. For compatibility test with no minerals, significant reduction is also observed at 10000ppm, but with a lower amount of precipitation. Again, the difference in these experiments only proves that some calcium precipitated and some bridged along with phosphorous(SI). The results show that only at 10000ppm onward, Mg^{2+} ion starts bridge along with phosphorous and adsorb/precipitate onto siderite minerals.

Figure 4.54 shows the change in Li^{+} ion concentration. Li^{+} is an inert tracer ion and there should not be any adsorption or precipitation. It is analysed to see if there was any evaporation. Base on the figure, there is an increase of 1% to 3% in Li+ concentration, which is due to slight evaporation apart from analytical error. The evaporation % factor was taken into account for all the calculation made for all the other elements involved.

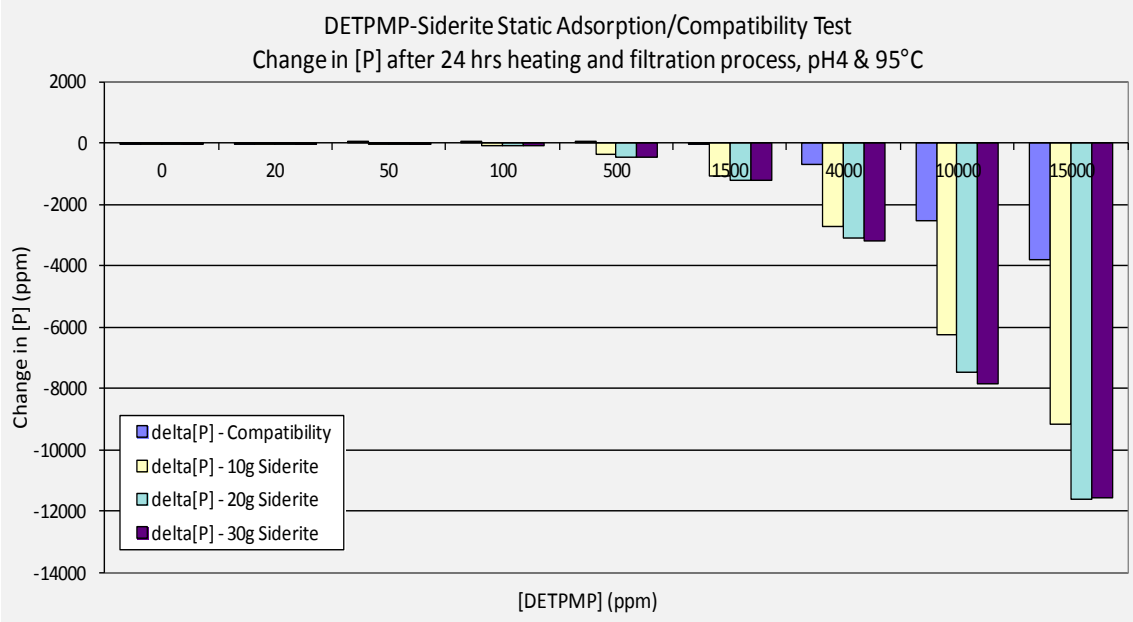

Figure 4.51: DETPMP-Siderite Static Adsorption/Compatibility Test (10g, 20g & 30g siderite). Change in [P] vs [DETPMP].

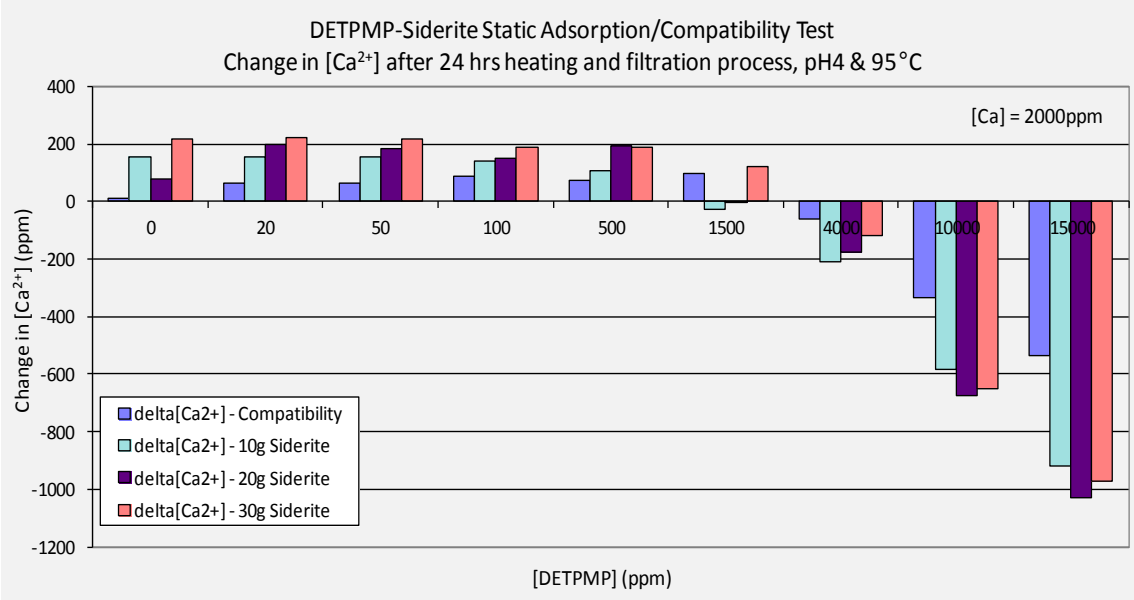

Figure 4.52: DETPMP-Siderite Static Adsorption/Compatibility Test (10g, 20g & 30g siderite). Change in $[Ca^{2+}]$ vs [DETPMP].

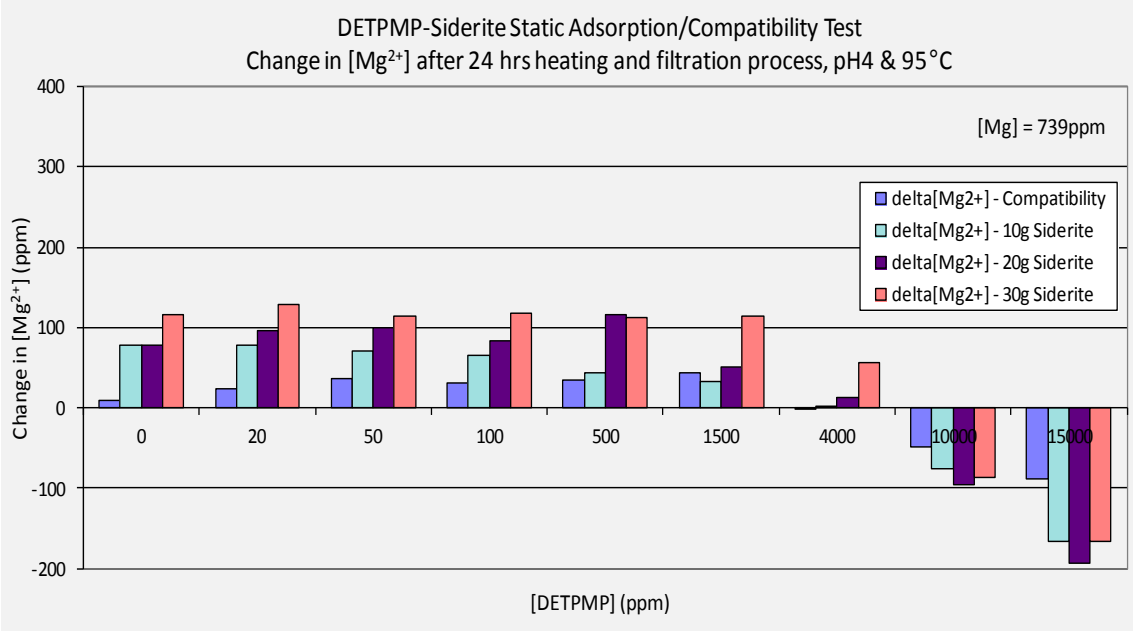

Figure 4.53: DETPMP-Siderite Static Adsorption/Compatibility Test (10g, 20g & 30g siderite). Change in $[Mg^{2+}]$ vs [DETPMP].

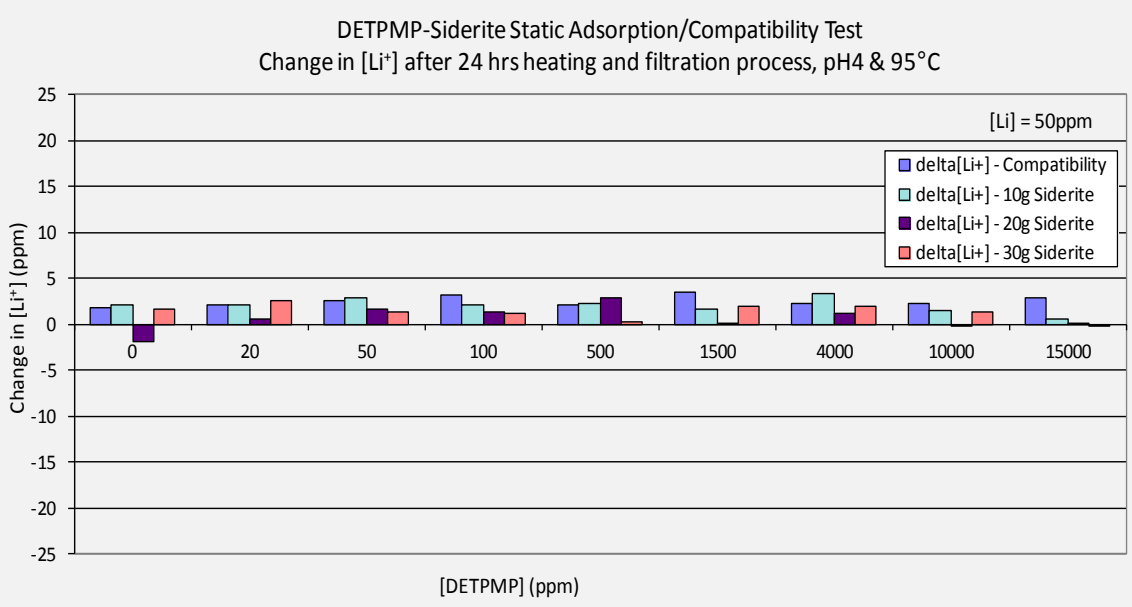

Figure 4.54: DETPMP-Siderite Static Adsorption/Compatibility Test (10g, 20g & 30g siderite). Change in [Li^+] vs [DETPMP].

After filtration, all the filter papers were dried, weighed, photographed and sent for ESEM-EDAX analysis. The sample solutions were measured for pH. The weights of the various samples that precipitated out of the solutions and the corresponding photographed filter papers after filtration are shown in Figure 4.55. Only at 1500ppm and above do we clearly see differences in both the weight and the appearance of precipitate. As the concentration increases, the weight of filter paper also increases as expected and more significant precipitates can be seen clearly on the filter papers. These results are very consistent with observations (above) on the amount of phosphorous, Ca^{2+} ions and Mg^{2+} ions that were measure in the filtered samples, which is less than in the stock solutions. The results proves that precipitation took place from 1500ppm onward.

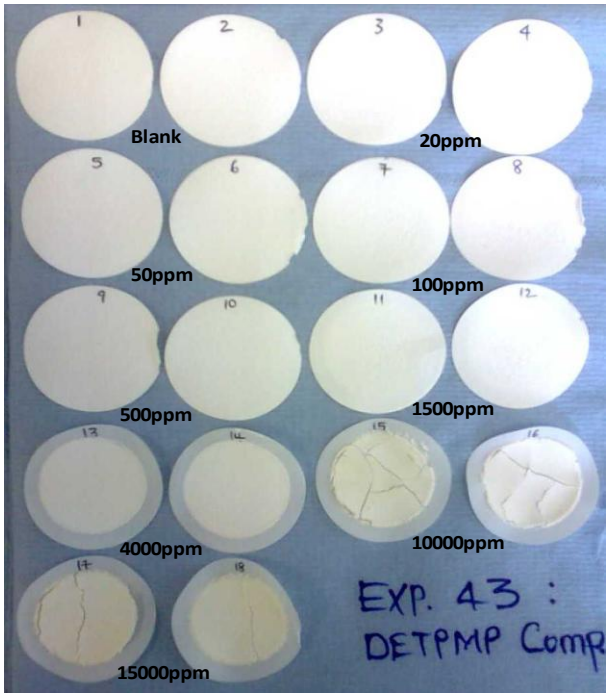

DETPMP Conc. (ppm)	Weight of Ppt (g)
0	0.02
20	0.02
50	0.02
100	0.02
500	0.02
1500	0.04
4000	0.14
10000	0.42
15000	0.60

Figure 4.55: DETPMP-Siderite Static Adsorption/Compatibility Test. Precipitates on filter papers and weight of precipitates at different concentrations of DETPMP.

Table 4.10 and Figure 4.56 show ESEM-EDAX atomic percentage and photographed samples of phosphorous, Ca^{2+}, Mg^{2+} and other ions presents on the filter papers. For each concentration, two points were taken for analysis. The hazy black background was identified as being the filter paper itself, the solid white marks are the salts and the hazy white background is due to the compound of phosphorous, Ca^{2+} and Mg^{2+} ions. The blank samples without any SI show only filter paper and some salts on them. Based on the atomic % from ESEM-EDAX, there is no phosphorous compound identified below 500ppm, but traces and variable values of Ca^{2+} and Mg^{2+} ions are identified. It must be noted that the EDAX signals are localized and inaccurate values are expected. Only when it reaches 1500ppm and above, was a clear hazy white background seen on the filter paper samples, which is identified to be phosphorous, Ca^{2+} and Mg^{2+} ions based on EDAX. Above 1500ppm SI concentration, based on the atomic %, phosphorous, Ca^{2+} and Mg^{2+} are seen consistently. Atomic% of phosphorous ranges from 10 to 11; Ca^{2+} from 4 to 5 and Mg^{2+} about 1.5. The results prove the presence of phosphorous, Ca^{2+} and Mg^{2+} as precipitates above 1500ppm.

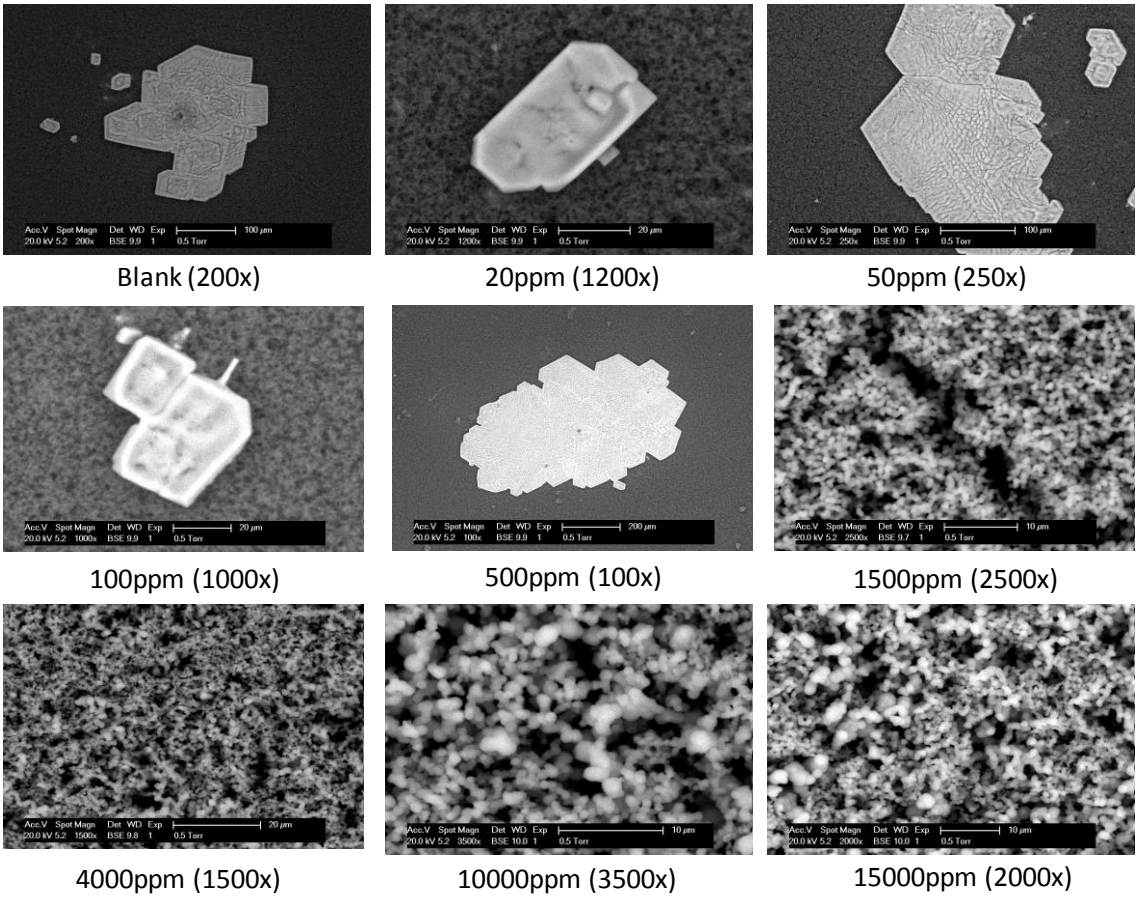

Figure 4.56: DETPMP-Siderite Static Adsorption/Compatibility Test. Morphology of precipitates on ESEM photographed samples.

	Blank		20ppm		50ppm		100ppm		500ppm		1500ppm		4000ppm		10000ppm		15000ppm	
Element	Wt %	At %	Wt %	At %	Wt %	At %	Wt %	At %	Wt %	At %	Wt %	At %	Wt %	At %	Wt %	At %	Wt %	At %
C K											29.33	44.34	28.69	42.9	29.26	43.87	27.66	41.72
O K	8.17	13.94	12.32	20.22	6.5	11.17	7.5	12.92	4.82	8.53	30.14	34.2	31.38	35.23	31.33	35.27	32.89	37.24
NaK	36.6	43.49	36.95	42.21	38.78	46.39	35.82	42.97	35.77	44.04	1.3	1.02	1.75	1.36	1.82	1.42	1.94	1.52
MgK											2.19	1.63	2.06	1.52	2.03	1.51	2.12	1.58
SrL											2.66	0.55			2.99	0.61	3.05	0.63
P K											18.02	10.56	19.19	11.13	18.94	11.01	18.72	10.95
ClK	55.24	42.57	50.73	37.57	54.71	42.44	56.69	44.1	59.4	47.43	4.63	2.37	4.48	2.27	3.29	1.67	3.56	1.82
CaK											11.75	5.32	12.45	5.58	10.34	4.65	10.06	4.55
Total	100	100	100	100	100	100	100	100	100	100	100	100	100	100	100	100	100	100

Table 4.10: DETPMP-Siderite Static Adsorption/Compatibility Test. EDAX signals on the precipitates from ESEM.

4.6 SUMMARY AND CONCLUSIONS

Scale inhibitor retention within the reservoir formation is the main feature which governs the lifetime of a scale inhibitor squeeze treatment. In this part of the work, we present the results on our coupled (static) adsorption/precipitation experiments using two phosphonate scale inhibitors, namely DETPMP and OMTHP, and three types of minerals, e.g. sand, kaolinite and siderite.

In this chapter, we studied the possible SI retention mechanisms onto rocks due to either **pure adsorption (Γ)** or by **coupled adsorption/precipitation (Γ/Π)**. The theory describing pure adsorption and coupled adsorption/precipitation processes has been summarised. We performed various series of carefully designed experiments on DETPMP and OMTHP SIs onto sand, kaolinite and siderite. This theory suggested a way of analysing static adsorption results for Γ_{app} vs. [SI] at various (m/V) ratios (i.e. [SI] is the final level after adsorption has occurred, [SI] = c_{1f} – see above). When all these Γ_{app}/c_{1f} curves for different (m/V) ratios collapse onto a single curve, then this indicates pure adsorption (Γ). However, when these curves diverge for different values of (m/V), then coupled adsorption/precipitation (Γ/Π) is being observed. Thus, experimentally, we are sure when the system exhibits either pure adsorption only or it is in the coupled adsorption/precipitation regime.

Two SIs, namely DETPMP (a penta-phosphonate) and OMTHP (a hexa-phosphonate) have been studied in a series of adsorption/precipitation experiments at a range of (m/V) ratios. A fixed volume of SI solution has been used in all experiments (V = 0.08L) with different masses of sand, kaolinite and siderite as adsorbent; m = 10g, 20g & 30g samples of each minerals were used to investigate this theory. The analysis of these is assisted by using the solution ion data – particular the effect of adsorption/precipitation on the [Ca] and [Mg] levels in solution. ESEM-EDAX analysis is also used to establish the presents of phosphorous, calcium and magnesium in the deposits (although this is not a quantitatively accurate technique). The brine used in this work was a synthetic Nelson Forties Formation Water (NFFW) with the composition given in Table 4.1; NFFW has [Ca^{2+}] = 2000ppm and [Mg^{2+}] = 739 ppm and all experiments were performed at pH 4 and T = 95°C.

4.6.1 DETPMP and OMTHP Scale Inhibitors onto SAND Mineral

At pH 4 and T = 95°C, both pure adsorption and coupled adsorption/precipitation regions were observed for DETPMP and OMTHP onto sand mineral in NFFW. Based on the "apparent adsorption" isotherm figures at various (m/V) ratios, only pure adsorption was observed below ~750ppm and coupled adsorption/precipitation behaviour was observed above ~750ppm for all the (m/V) ratios used for both SIs. For each (m/V) ratio, the isotherm curves plateau at a level of ~ 0.25mg/g and 0.30mg/g for DETPMP and OMTHP respectively at ~750ppm. Above ~750ppm, the "apparent adsorption" isotherm curves deviate for different (m/V) ratios, clearly indicative of coupled adsorption/precipitation. That is, below ~750ppm, the measured adsorption isotherms are independent of the (m/V) ratio and all collapse onto one curve. Whereas, above ~750ppm, the "apparent adsorption" isotherm depends on the (m/V) ratio, where the curves branches out independently at the different mass used. This is precisely in line with theory in terms of the qualitative observed behaviour.

The levels of pure adsorption seen in the lower SI concentration region for both phosphonates are ~0.2 – 0.3 mg/g and this is quite consistent with the lower adsorptive capacity of quartz and the low surface area of this sand (size range ~80 – 400µm). In the coupled adsorption/precipitation region, the apparent adsorption values rang

e from ~2 – 12mg/g and these much higher levels are certainly too high for pure adsorption of DETPMP or OMTHP onto low surface area quartz sand.

A significant reduction is observed in [phosphorous], [Ca^{2+}] and [Mg^{2+}] as the concentration of SI increases in both bulk solution and in the adsorption experiments for both SIs. This M^{2+} reduction in solution is mainly associated with the precipitation of a M^{2+}-DETPMP complex. This has been analysed by ESEM EDAX in all cases and this is clearly a Ca/Mg-DETPMP precipitated complex (Ca, Mg and P are *all* seen in the EDAX signal).

These results on the coupled adsorption/precipitation of DETPMP and OMTHP SIs onto sand agree very well with the theory.

4.6.2 DETPMP and OMTHP Scale Inhibitors onto KAOLINITE Mineral

The DETPMP /kaolinite system again shows clear regions of pure adsorption (Γ) and coupled adsorption/precipitation (Γ/Π) at pH4 and T=95°C. Based on the "apparent adsorption" isotherm figures (Γ_{app} vs. [SI]) at various (m/V) ratios, pure adsorption was observed below [SI] ~800ppm and coupled adsorption/precipitation behaviour was observed above ~800ppm. That is, below ~800ppm, the measured adsorption isotherms are independent of the (m/V) ratio and all collapse onto one curve. Whereas, above ~800ppm, the "apparent adsorption" isotherm depends on the (m/V) ratio, as discussed above. This conclusion is further strengthen by the observed changes in phosphorous (SI) concentration, where clear reduction in phosphorous (SI) was seen at ~800ppm and phosphorous was also found in precipitates base on the EDAX signal at 800ppm.

From the Γ_{app} vs. [SI] curves for the OMTHP/kaolinite system, it is less clear where the transition occurs between the s pure adsorption and coupled adsorption/precipitation regions at pH4 and T=95°C although both are present. However, these regions are better defined by considering the observed difference in the amounts of phosphorous concentration in solution since these results show that clear adsorption and coupled adsorption/precipitation regions occur. Up to [SI] ~ 500ppm, a region of pure adsorption is observed for this system and for [SI] > 500ppm, coupled adsorption/precipitation is observed. This finding is further strengthened by from the filtered precipitate and ESEM-EDAX data. It is thought that the reason for the less clear transition between the two regions of Γ and Γ/Π is due to the very high levels of DETPMP pure adsorption onto the kaolinite due to its very high specific surface area. Both DETPMP and OMTHP SIs show pure adsorption levels onto kaolinite minerals between Γ ~ 7 to 13 mg/g at 800ppm SI.

Significant reduction is also observed in both [Ca^{2+}] and [Mg^{2+}] as the concentration of SI increases in coupled adsorption/precipitation experiments both SIs. This M^{2+} reduction in solution is mainly associated with the precipitation of a M^{2+}-DETPMP/OMTHP complex. This has been analysed by ESEM EDAX in some cases and this is clearly a Ca/Mg-DETPMP/OMTHP precipitated complex (Ca, Mg and P are *all* seen in the EDAX signal).

4.6.3 DETPMP Scale Inhibitor onto SIDERITE Mineral

For the DETPMP/siderite system, results similar to those for the OMTHP/kaolinite system are observed where the transition between pure adsorption and coupled adsorption/precipitation is not clear, although both regions are observed. From the compatibility and adsorption tests, it appears that pure adsorption is observed up to [SI] ~500ppm, and at higher concentrations, then coupled adsorption/precipitation is observed. This finding is further strengthened by the filtered precipitate and ESEM-EDAX results. Again, the reason for the less clear transition observed for the DETPMP/siderite system maybe due to both (i) the high levels of adsorption of the DETPMP onto the siderite, and also (ii) the role of the higher levels of [Fe^{3+}] released in these lower pH (pH 4) experiments. At 1500ppm, 25ppm [Fe^{3+}] was observed in the bulk solution while at 15000ppm, 200ppm [Fe^{3+}] was found (see Figure 4.50). .

Again, significant reductions were observed in both [Ca^{2+}] and [Mg^{2+}] as the concentration of SI increases in coupled adsorption/precipitation experiments for the DETPMP/siderite system. This M^{2+} reduction in solution is mainly associated with the precipitation of a M^{2+}-DETPMP complex and this has been confirmed by ESEM EDAX.

CHAPTER 5: NON-EQUILIBRIUM SAND PACK EXPERIMENTS ON OMTHP SCALE INHIBITOR APPLIED IN BOTH ADSORPTION AND PRECIPITATION TREATMENTS

5.1 INTRODUCTION

In a scale inhibitor squeeze treatment, it is known that adsorption/desorption (Vetter, 1973; Meyers *et al*., 1985; Yuan *et al*., 1993; and Sorbie *et al*., 1993) or a precipitation/dissolution (Yuan *et al*., 1993; Carlberg, 1983, 1987; and Olson *et al*., 1992) (phase separation) mechanism governs the interaction between the scale inhibitor and the formation rock system. Previous work has demonstrated that the adsorption isotherm, $\Gamma(C)$ (Sorbie *et al*., 1992; Hong and Shuler, 1987; and Jordan *et al*., 1997) governs the inhibitor/rock interaction for adsorption/desorption inhibitor squeeze processes. This adsorption isotherm is the key parameter required for successful modelling of both core flood returns and also field treatment design using computer codes such as SQUEEZE V. On the other hand, in the precipitation squeeze mechanism two factors govern the return curve, viz. the *solubility* (C_s) of the inhibitor-calcium complex and the *rate of dissolution* (r_4) of the precipitation complex (Yuan *et al*., 1993; Jordan *et al*., 1997; and Malandrino *et al*., 1995)**.** The dissolution rate effect implies that the steady state concentration level in the returns depends on the local fluid velocity as it sweeps over the rock containing the surface precipitated complex. This local velocity depends on the depth of penetration of the precipitated slug into the radial near well formation, which therefore affects the level of inhibitor concentration in the return curves. A simple model for this process has been developed within FAST and this will be published in the near future ("Sorbie –personal communication, June 2011").

Non-equilibrium adsorption/desorption (Bourne *et al*., 1992) and non-equilibrium inhibitor return behaviour during precipitation/dissolution (phase separation) core flooding experiments of a phosphonate based scale inhibitor on limestone material (Lawless *et al*., 1994) have been published previously. The reported results demonstrate that the actual inhibitor desorption process occurring under the conditions tested is a

non-equilibrium process, whereby the concentration of scale inhibitor in the post flush effluent is affected by the post flush flow rate.

In this current study, we designed a set of variable rate adsorption and precipitation sand pack flooding experiments using OMTHP scale inhibitor under a range of carefully controlled similar conditions. Very comprehensive dynamic flood data was measured in order to extend our understanding both of inhibitor adsorption/desorption and the precipitation/dissolution processes including non-equilibrium systems. From the results obtained in this study, very clear non equilibrium effects are apparent for OMTHP scale inhibitors, when applied both as adsorption and coupled adsorption/precipitation treatments. Furthermore, the effect on post flush effluent inhibitor concentration is in the same direction for each system under tests, i.e. reduced flow rate leads to higher effluent concentrations and vice versa. The extent and quality of this dataset make it the most complete available to date for modelling studies.

5.2 EXPERIMENTAL DETAILS

As mentioned earlier, the unique feature of this series of floods is that the ***bulk*** coupled adsorption/precipitation behaviour of this system (OMTHP/sand) has been fully characterized in previous bulk work and further extended in this pack flooding work. Therefore, we know precisely when the system is in the adsorption only or in the coupled adsorption/precipitation regime.

In Chapter 4, all the bulk static compatibility and adsorption tests were conducted at 95°C; whereas, in this work, they were conducted at room temperature. It must be noted that all main treatments were carried out at room temperature.

In chronological order, the following experiments were conducted to give a systematic approach to the study of these adsorption and adsorption/precipitation phenomena:

1. Static Compatibility/Adsorption Test @ room temperature
2. Sand Pack A: Dynamic Precipitation Flood –Singe Flow rate
3. Sand Pack C: Dynamic Precipitation Flood – Multi Flow rate

4. Sand Pack D: Dynamic Precipitation Flood – Multi Flow rate with Solubility Effect
5. Static Compatibility Test @ 95°C designed for Sand Pack E
6. Sand Pack E: Low Concentration Adsorption Flood – Multi Flow rate
7. *Static Compatibility Test @ 95°C designed for Sand Pack F
8. Sand Pack F: High Concentration Adsorption Flood – Multi Flow rate
9. *Static Compatibility Test @ 95°C designed for Sand Pack G
10. Sand Pack G: Medium-High Concentration Adsorption Flood – Multi Flow rate

Notes: *This Static Compatibility Test @ 95°C uses a different brine composition, where [Ca^{2+}] is 428ppm; whereas, in other experiments [Ca^{2+}] is 2000ppm. Sand Packs F and G utilize this brine composition in their flood experiments.

5.2.1 Materials

Adsorbents: Silica sand was chosen as the mineral adsorbent since it replicates a simple model of a sandstone formation and the results are also reproducible. The sand used in these experiments is commercially available (BDH GPR, 150-300mesh). A Malvern Master Particle Size Analyzer was used to analyze the sand. The particle size is less than 300 µm with a distribution mode of 253 µm. Refer to Chapter 4 for details on size of particles and elements in the sand which were obtained from particle size analyzer (PSA) and X-Ray Diffraction (XRD). It has been reported that the surface of hydroxylated amorphous silica, which plays an important role in adsorption of inhibitor, is negatively charged at pH 4 (Lecourtier *et al*., 1981 and Iler, 1979)**.** Experimental results show that this sand has a point of zero charge (pzc), which carry the same SiOH group on the surface which is between pH ~ 1.5 (Lecourtier *et al*., 1981) and ~2 (Iler, 1979). The concentration of negative surface charge increases as the pH increases**.** Core minerals are not used because they show complex petrography effects and the results are not easily reproducible.

Adsorbate: The adsorbate or scale inhibitor (SI) used in this work is Octa-methylene-tetramine hexa (methylene-phosphonic acid) or OMTHP, which is a hexa-phosphonate. This is one of a range of commercial products used in oilfield applications (Briquest

684-30S). The typical active content is 30%. The structure is shown in Figure 5.1. Refer to Chapter 4 and Appendix for details of OMTHP SI properties and MSDS. All SI concentrations including lithium tracers were prepared in the standard Synthetic NFFW and pH adjusted to pH4. Inductive Coupled Plasma (ICP) analytical method (Water Analysis Handbook, 1989) was used in this study and we are able to assay down to 1ppm (±0.2ppm). Results from different concentration and inhibitors floods using the phosphonate inhibitor in outcrop sandstone core were presented in a previous paper (Sorbie *et al*., 1992) and other workers have reported work on this material (Meyers *et al*., 1985; Sorbie *et al*., 1993; Przybylinski, 1989; and Kan *et al*., 1991, 1992)**.**

Brine: The brine solution used in the experiment is Synthetic Nelson Forties Formation Water (NFFW), which is prepared by dissolving appropriate quantity of salts in distilled water. The composition is given in Table 5.1. The synthetic brine used in this study is sulphate free formation water, which is used to prevent any precipitation due to barium sulphate. For this study, it is important not to have other form of precipitation except SI related precipitation. The brine solution was filtered through 0.45µm filter paper and degassed overnight prior to use. 0.45µm filter paper is commonly used by the industry to filter water sample to allow for adequate filtration of suspended solid content in the water (Patton, Oilfield Water System, 1977).

This brine was used to make all SI concentration; whereas, the post-flush or back production stage was carried out with the same brine but excluding Li^+ ion. For both purposes, the brine was degassed under vacuum and pH adjusted to pH4.

Ion	Conc. (ppm)	Comp	Mass g/l	g/5L	g/10L	g/15L	g/20L
Na^{+}	31275	NaCl	79.50	397.50	795.00	1192.50	1590.01
Ca^{2+}	2000	$CaCl_2 6.H_20$	10.93	54.66	109.32	163.98	218.64
Mg^{2+}	739	$MgCl_2.6H_20$	6.18	30.90	61.80	92.69	123.59
K^{+}	654	KCl	1.25	6.23	12.47	18.70	24.94
Ba^{2+}	269	$BaCl_2.2H_2O$	0.48	2.39	4.78	7.18	9.57
Sr^{2+}	771	$SrCl_2.6H_2O$	2.35	11.73	23.46	35.19	46.92
SO_4^{-2}	0	Na_2SO_4	0.00	0.00	0.00	0.00	0.00
Li^{+}	50	LiCl	0.305	1.53	3.05	4.58	6.11
Cl^{-}	50000						
		Actual Cl ppm	55278.64				
		If CaCl2.2H2O is used	7.32	36.62	73.25	109.87	146.49
TDS =	91036.64	ppm					

Table 5.1: Synthetic Nelson Forties Formation Water (NFFW) Composition

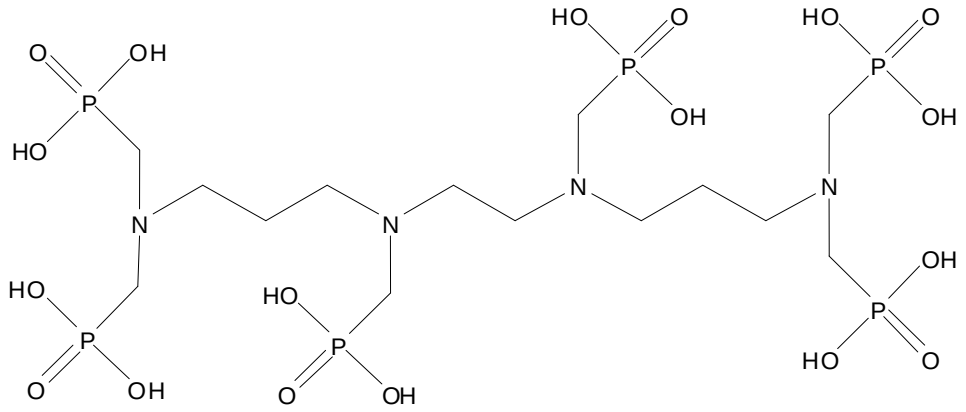

Figure 5.1: Chemical Structure of Scale Inhibitor – Octa-methylene-tetramine hexa (methylene-phosphonicn acid) - OMTHP

5.2.2 Experimental Apparatus

Schematic diagram of the sand pack flooding apparatus is shown in Figure 5.2. The apparatus was designed to carry out low pressure flood experiments, as opposed to core flood apparatus which is designed to tackle high pressure and high temperature core floods. The adsorption column, fittings and tubing were supplied by Anachem. The sand

pack column is made of glass which is 23 cm long and has an internal diameter of 1.50 cm. A wet slurry method (Figure 5.3) was adopted for packing the sand in order to prevent formation of air bubbles in the column and to minimize sagging of sand. A high precision pump, (Model P-500 – Pharmacia) and fraction collector (Model FRAC -100, Pharmacia) were employed to provide a stable flow rate and accurate sample volume collection.

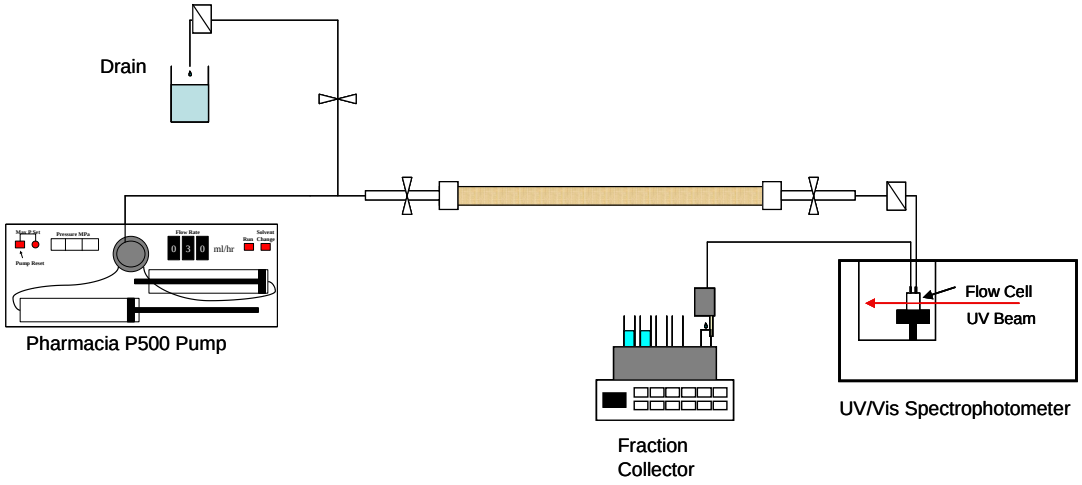

Figure 5.2: Schematic diagram of sand pack flooding apparatus

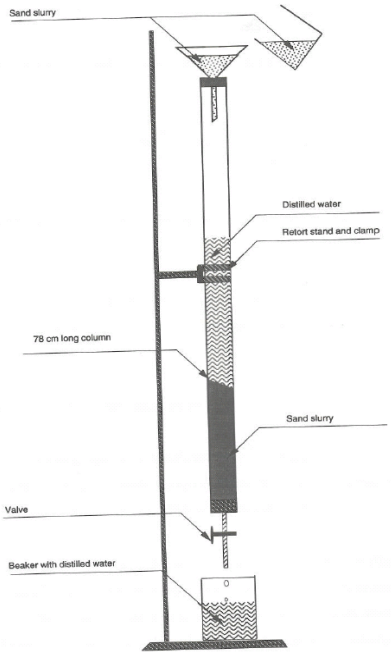

Figure 5.3: Schematic diagram of sand pack "packing" technique

5.2.3 Experimental Procedure

The whole set of experiments in this chapter was executed systematically from bulk static to dynamic sand pack tests. Many of the static experiments were conducted previously and these have been reported in Chapter 4. In this chapter, we perform some further static experiments (mainly at room temperature) in order to understand what the conditions are for certain dynamic experiments, in terms of being able to clearly define when adsorption and coupled adsorption/precipitation are occurring.

Sand Pack Characterization- Dead Volume and Pore Volume/Porosity Measurement: Before each sand pack experiment, dead and pore volume (and porosity by calculation) must be measured. A similar setup as for the sand pack experiments is required to perform these measurements. For dead volume measurements, no sand was introduced into the sand pack; whereas for pore volume/porosity measurements, sand was introduced and the same pack was used for the rest of each experiment. Although the packing method and its results are known to be reproducible (Sorbie *et al*., 1993), each flood went through dead and pore volume/porosity measurements to ascertain the reproducibility of these quantities. Table 5.2 shows the sand pack characterization for all the sand pack experiments. The diameter is exactly the same for all but the length differs slightly due to how tightly they were packed in the column. As shown from the results, the dead and pore volume/ porosity are very similar to each other, which show the reproducibility of the methodology to pack the sand. Based on these parameters and sand density (ρ= 2.65 g/cm^3), the sand weight is calculated.

Sand Pack ID	A	C	D	E	F	G
Length (cm)	20.05	20.50	20.40	20.40	20.70	20.9
Diameter (cm)	1.5	1.5	1.5	1.5	1.5	1.5
Dead Volume (ml)	1.54	1.54	1.24	1.34	1.34	1.34
Pore Volume (ml)	13.64	14.69	14.73	14.60	14.66	14.11
Porosity (%)	38.49	40.52	40.85	40.87	40.06	38.21
Sand Wt. (g)	93.58	95.68	95.21	95.21	96.61	97.87

Table 5.2: Sand Pack Characterization Results

Flood Procedures: After the measurement of dead and pore volume/porosity, the sand pack was conditioned by flushing with NFFW brine (no Li^+) overnight before any measurements were taken. This is to make sure that the sand pack is fully saturated with only NFFW brine, as such there is no unwanted materials that would cause uncontrolled adsorption or precipitation. The methodology for adsorption and precipitation floods is the same for all the experiments. The only experimental differences between the adsorption and precipitation floods are in the applied concentration of SI chosen and the calcium level in the main treatment. As for the post flush, the presence and/or amount of calcium were different and the flow rates were changed accordingly, depending of the objective for that specific flood. In each flood, the flow was stopped for at least 24 hours at 95°C between each flow rate from main treatment to end of the post flush. Table 5.3 gives the main experimental details for all sand pack experiments.

Sand Pack ID	Flood Type	Main Treatment					Shut-In		Post Flush		
		[SI] (ppm)	[Ca] (ppm)	pH	T (°C)	Q (ml/hr)	T (°C)	T (hrs)	T (°C)	Q (ml/hr)	[Ca] (ppm)
SP-A	Pptn	4000	2000	4	20	20	95	>20	95	20	2000
SP-C	Pptn	4000	2000	4	20	20	95	>20	95	20 10 5 5 2	2000 2000 2000 2000 2000
SP-D	Pptn	4000	2000	4	20	20	95	>20	95	20 20 10 5 2	2000 0 0 0 0
SP-E	Ads	500	2000	4	20	20	95	>20	95	20 10 5 2	2000 2000 2000 2000

SP-F	Ads	4000	428	4	20	20	95	>20	95	20 10 5 2	428 428 428 428
SP-G	Ads	2000	428	4	20	20	95	>20	95	20 10 5 2	428 428 428 428

Table 5.3: Sand Pack Experimental Details and Chronologies of Injection

For all the precipitation floods, namely SP-A, SP-C and SP-D; during the main treatment, the SI and calcium concentrations are set at, [OMTHP] = 4000ppm and [Ca^{2+}] = 2000ppm. Whereas, for the adsorption floods, SI and calcium concentration were set at [OMTHP] = 500ppm and [Ca^{2+}] = 2000ppm for sand pack (SP-E); [OMTHP] = 4000ppm and [Ca^{2+}] = 428ppm for sand pack (SP-F) and [OMTHP] = 2000ppm and [Ca^{2+}] = 428ppm for sand pack (SP-G).

All main treatment SI solutions were adjusted to pH 4. The solutions were injected at 20ml/hr at room temperature thus ensuring that no precipitation took place during the main treatment placement (this had already been established in the bulk jar tests). Referring to chapter 4, detailed study has been conducted in static jar tests to define at which condition (temperature, pH, and SI and calcium concentration) either adsorption only or coupled adsorption/precipitation occurred. From the experimental results, it is clear that no precipitation takes place at room temperature. After ~10 pore volumes of SI injection, the sand pack inlet and outlet valves were closed and the whole pack was put into a water bath and heated to 95°C. Once the temperature reaches 95°C, the whole set up was left at this temperature for at least 24 hours. After the 24hrs heating at 95°C, brine without lithium was injected as post flush.

Effluents from the main treatment and the subsequent post flush were collected at regular intervals for analysis. The effluents were analyzed for SI, Ca^{2+}, Mg^{2+} and Li^{+} elements using Inductive Coupled Plasma (ICP). The relative positions of Lithium tracer and SI effluents profile during the main treatment gave a direct indication of the

extent of SI retention either by adsorption or coupled adsorption/precipitation. Whereas, the SI concentration during post flush indicates the amount of SI retrieved due to desorption/dissolution that has occurred.

5.3 EXPERIMENTAL RESULTS AND DISCUSSION

Considering the rate of desorption and dissolution compared with the fluid flow rate close to a well, it is evident that process often does not have sufficient time to reach equilibrium. Whereas, when the fluid is stagnant for a long period, the fluid-rock system has enough time to reach equilibrium which replicates static adsorption or desorption test in the lab. These phenomena can be studied directly using dynamic sand pack and/or static bulk adsorption/precipitation experiments. In sand pack experiments, the process taking place, whether it is adsorption/desorption or precipitation/dissolution, is likely to be a non-equilibrium or kinetic process. The non-equilibrium behaviour can be seen as a change of inhibitor effluent concentration as the flow rate changes (Malandrino *et al*., 1995; Bourne *et al*., 1992; and Lawless *et al*., 1994)**.**

In order to study such non-equilibrium behaviour, dynamic sand pack experiments were designed using well characterized silica sand, in which the post-flush was performed at different flow rates. This chapter will summarize the results obtained from hexa-phosphonate (OMTHP) SI in both kinetic adsorption and precipitation sand pack floods.

For this purpose, these experiments have been designed directly from static experiments, which have mostly been described and reported in Chapter 4, but some further results are presented in this section to ascertain the conditions for adsorption and precipitation for certain cases. These experiments are very important before moving to dynamic experiments as we must be sure whether we are performing an adsorption flood or an adsorption/precipitation flood. The following sets of experiments were designed to study these various retention processes in detail. Details and chronologies of these experiments can be found in experimental details, which are elaborated in this section individually.

5.3.1 Static Adsorption/Compatibility Study at Room Temperature

Prior to conducting the non-equilibrium sand pack studies, some additional static compatibility/adsorption tests were conducted at room temperature. This is to make sure that there is no precipitation taking place at room temperature but only pure adsorption. Main treatments for all the sand pack study were carried out at room temperature, which is why this part of the study was carried out.

A stock solution at 10,000ppm OMTHP in NFFW was prepared. At this concentration, the OMTHP SI is not fully dissolved and is whitish in colour. When left for a few hours, it starts to precipitate. The solution was then diluted to attain the desired concentrations of 500, 750, 1000, 2000, 3000, 4000 and 6000ppm which were used for adsorption and compatibility experiments. pH was measured for all the stock solutions and adjusted to pH4. Figure 5.4 shows the solutions before and after pH adjustment. Before pH was adjusted to 4, it was seen that some tracers of precipitate at the lowest concentration of 500ppm. As the concentration increases, the amount of precipitate increases as well and can be observed clearly. After pH adjustment to 4, all precipitates dissolved in the solution except at 6000ppm. They are yellowish in colour from 1000ppm. Even after 24hrs, there were no changes taking place after the pH adjustment. The initial and adjusted pH values are shown in Figure 5.5. The blank solution without any SI is at pH6, whereas the other concentrations are between pH 4.7 to 4.9. The initial pH decreases as the concentration increases to 6000ppm, which shows the acidic nature of the OMTHP SI.

Immediately after the pH adjustment, samples at all concentrations were used in both compatibility and adsorption tests. The adsorption tests were conducted with 10g and 20g silica sand. Figure 5.6 shows the adsorption isotherm onto sand at room temperature after 24hrs. It is clearly observed that only adsorption is taking place up to 4000ppm stock solution of OMTHP. The adsorption of SI onto sand shows a plateau at 0.25mg/g. For both masses of sand used, only pure adsorption behaviour observed since both results collapse onto a single line. If there was any precipitation, the lines would deviate and branch out independently, as discussed and shown in the result in Chapter 4. For pure adsorption, the behaviour is independent of (m/V) ration, whereas for coupled

adsorption/precipitation, the behaviour depends on the (m/V) ratio (i.e. V=0.08L and m= 10g & 20g). Slight pH reduction (below pH4) also indicates that some SI was absorbed onto sand (refer to Figure 5.5).

Figure 5.7, Figure 5.8, Figure 5.9 and Figure 5.10 show the change in concentration of phosphorous, calcium, magnesium and lithium respectively after 24 hrs at room temperature for these static compatibility and adsorption tests. Negative value indicates adsorption or precipitation. In the compatibility tests, SI precipitation is only observed at 6000ppm. Some slight calcium precipitation is seen but no loss of magnesium is measured. If left at 95°C, calcium and magnesium would both show significant drops in concentration based on the compatibility results in Chapter 4. The binding between calcium and magnesium to SI to form a SI_M complex is not observed at room temperature (or at least the complex is not insoluble). Lithium exhibits no change for all concentrations, which indicates almost no evaporation or loss in fluids during the experiments. For static adsorption test at 10g and 20g sand, phosphorous can been seen to adsorb from the lowest stock concentrations from 500ppm onward. As in the compatibility tests, calcium and magnesium were not seen adsorbing (or bridging along with SI). Detail analysis of the absolute value of the differences in these elements show slight adsorption.

After the static compatibility test, the filter papers were weighted and sent for ESEM-EDAX analysis to find out if any precipitate present on the filter papers. Figure 5.11 shows the observation and weight of filter papers. Only at 6000ppm, clear precipitates observed and change in weight measured. The remaining filtrate is yellowish in colour from 500ppm and above, changing from light to dark yellow. Figure 5.12 shows ESEM-EDAX analysis. ESEM pictures show phosphorous precipitate at 6000ppm and EDAX table show clear presents of phosphorus on the filter paper. Very low amount of calcium and magnesium are found at 6000ppm. At 4000ppm and below, only traces or zero concentrations of phosphorous, calcium and magnesium were found on the filter paper.

These data prove that only pure adsorption is taking place at 4000ppm and below.

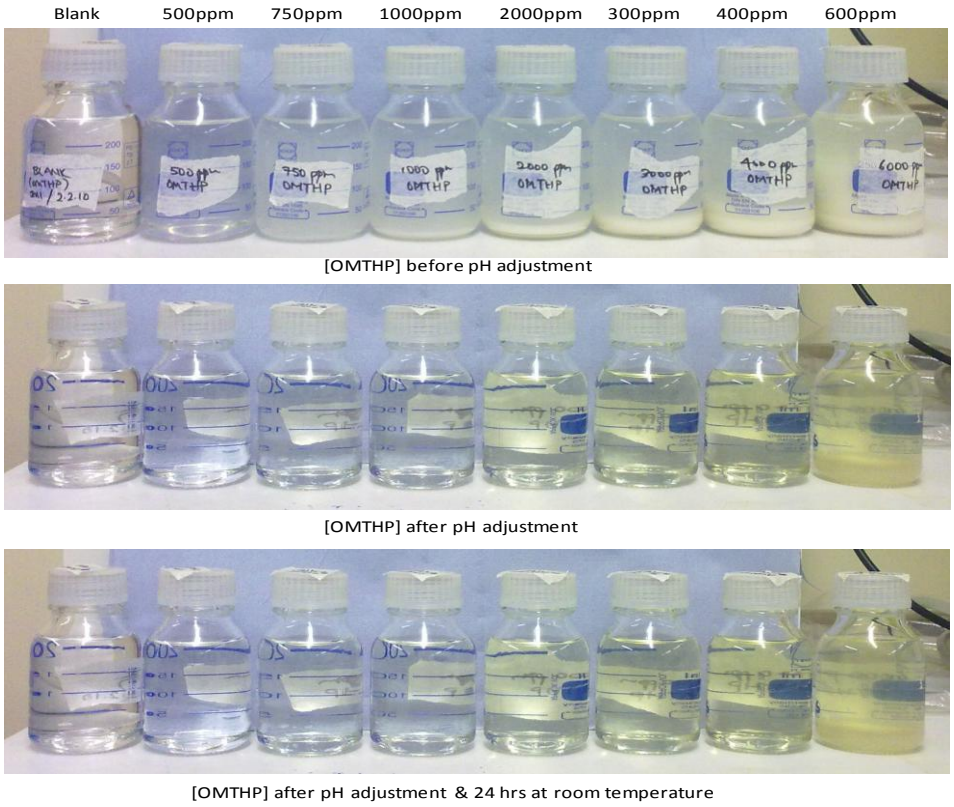

Figure 5.4: OMTHP SI from Blank to 6000ppm before and after pH adjustment, and after 24 hrs at room temperature

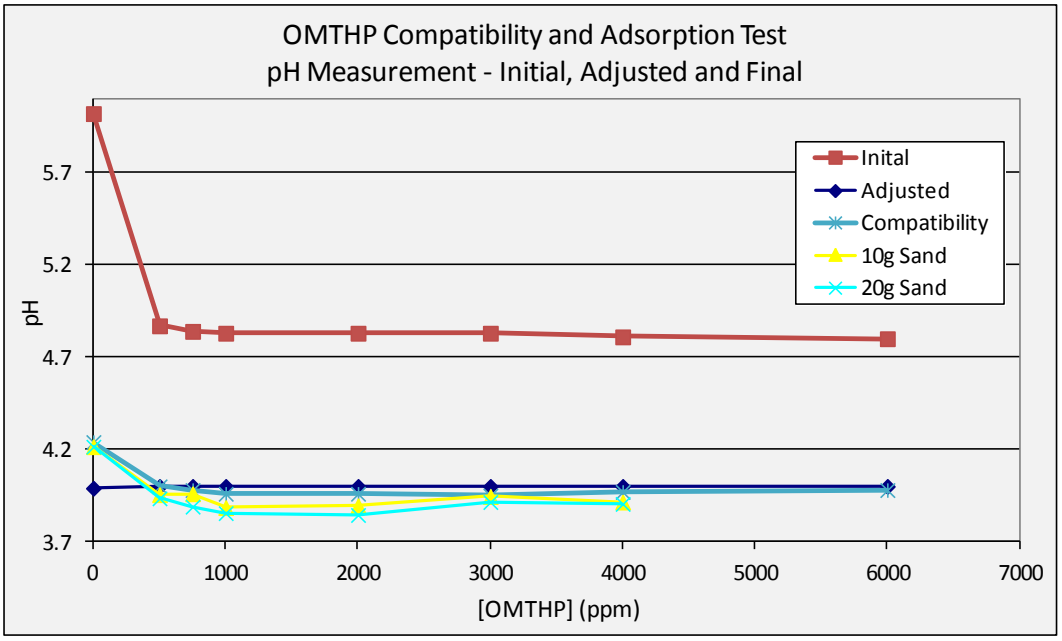

Figure 5.5: OMTHP from Blank to 6000ppm. Initial, Adjusted and Final pH measurement

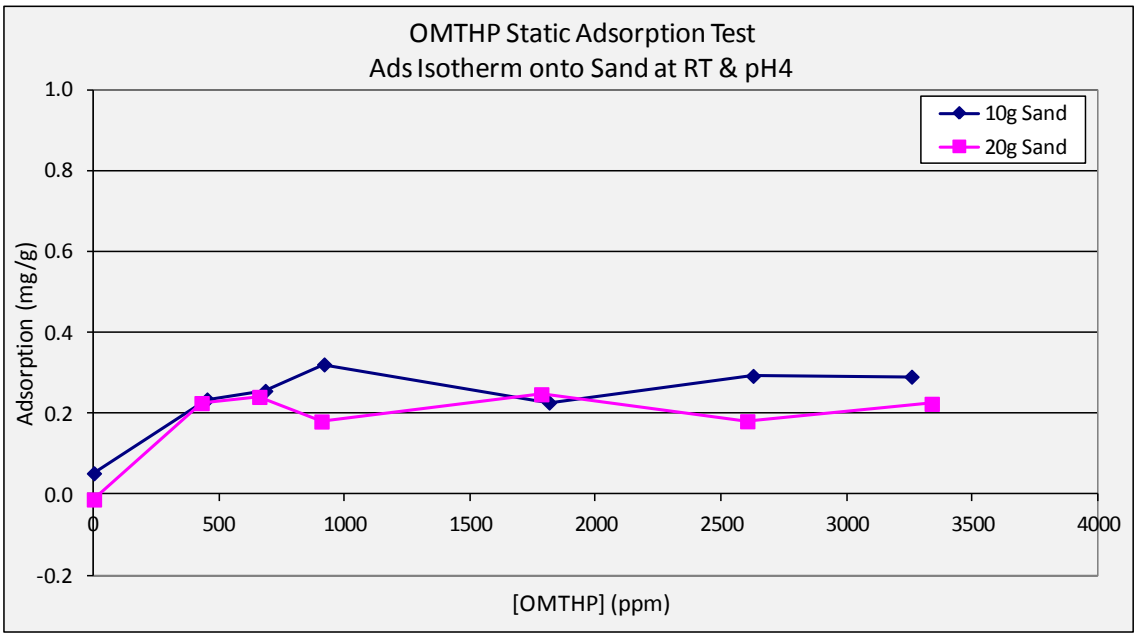

Figure 5.6: OMTHP Adsorption Isotherm onto Sand after 24 hrs at room temperature and pH4

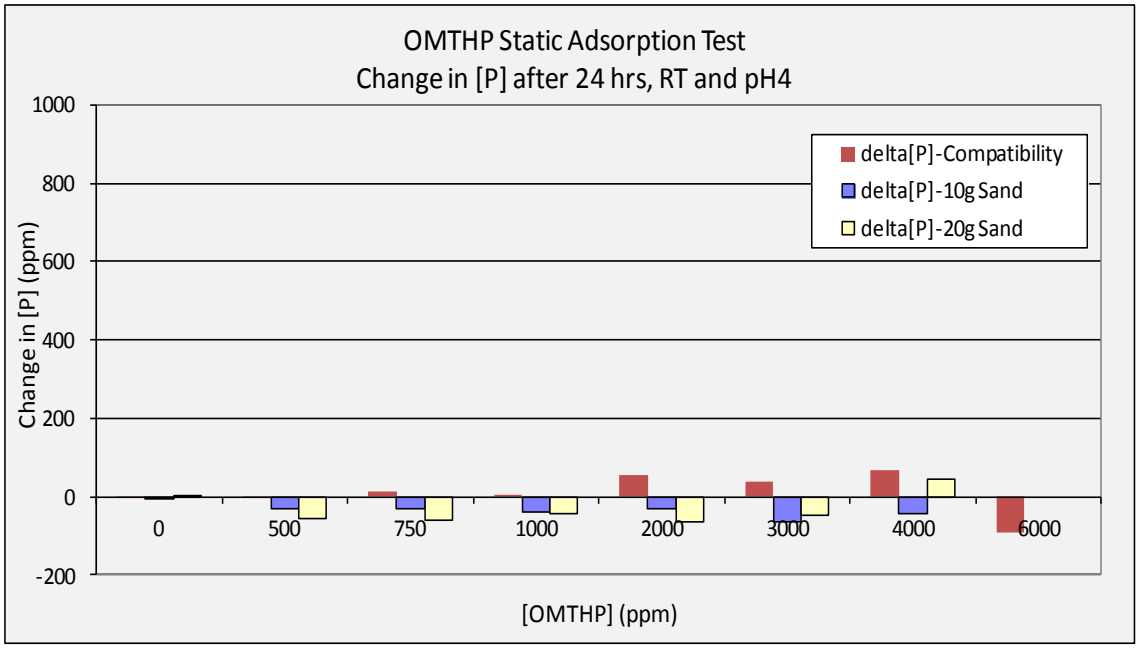

Figure 5.7: OMTHP Static Compatibility and Adsorption Test. Change in [P] ion after 24 hrs at room temperature and pH4

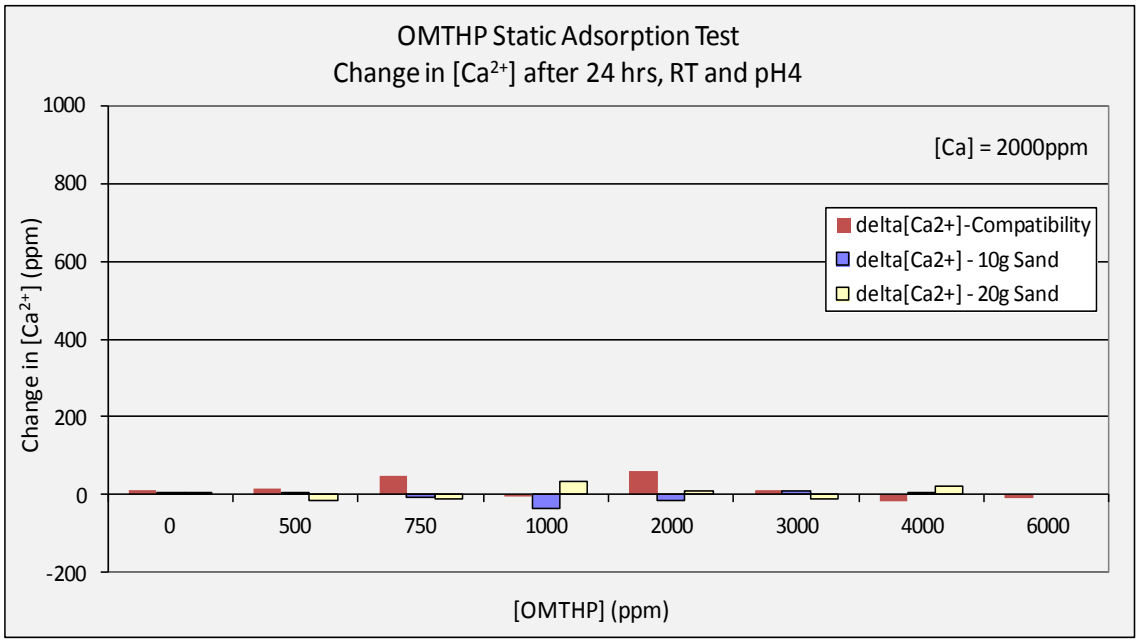

Figure 5.8: OMTHP Static Compatibility and Adsorption Test. Change in [Ca^{2+}] ion after 24 hrs at room temperature and pH4

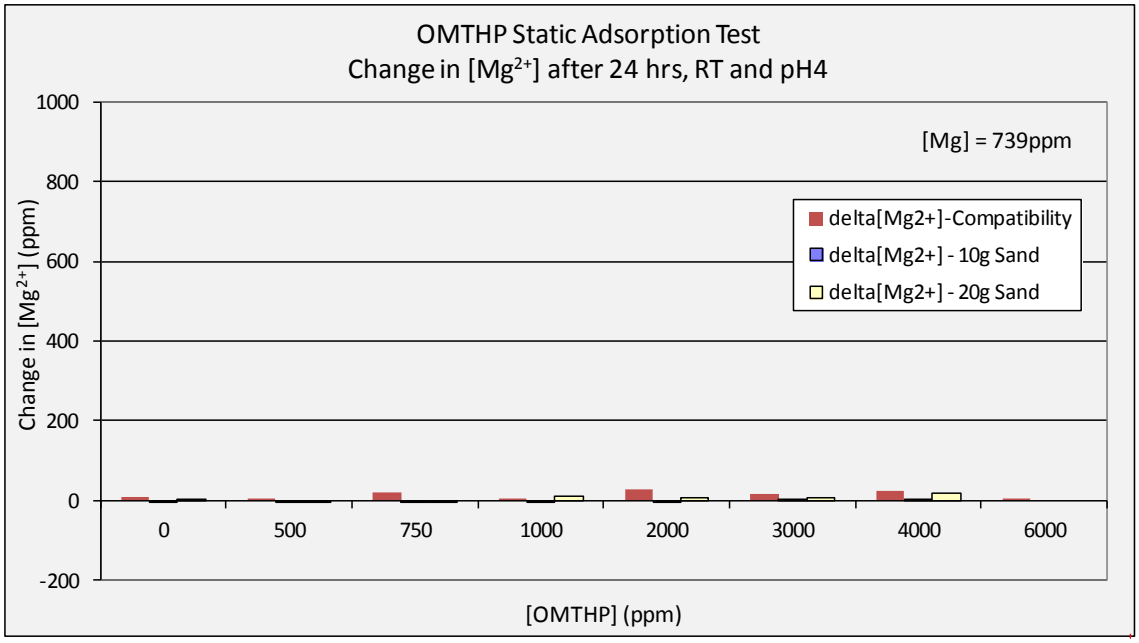

Figure 5.9: OMTHP Static Compatibility and Adsorption Test. Change in $[Mg^{2+}]$ ion after 24 hrs at room temperature and pH4

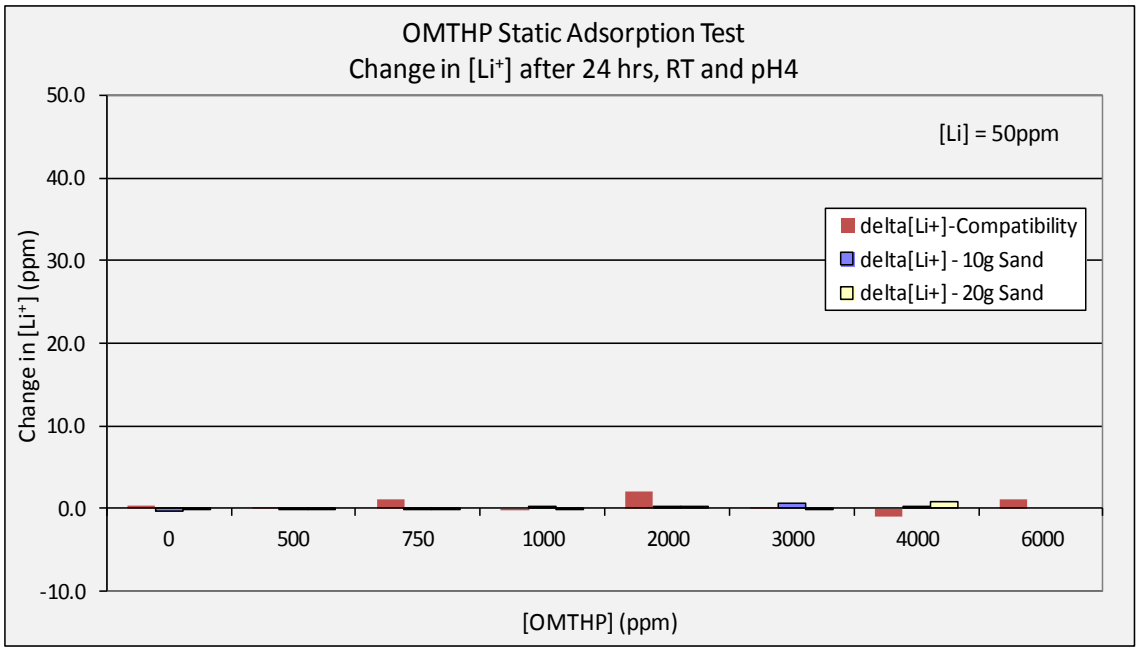

Figure 5.10: OMTHP Static Compatibility and Adsorption Test. Change in $[Li^{+}]$ ion after 24 hrs at room temperature and pH4

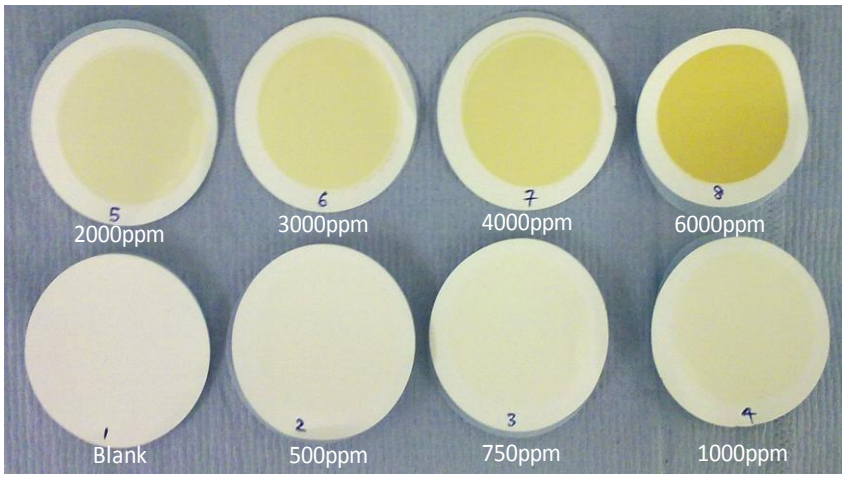

[OMTHP] (ppm)	Weight of Ppt (g)
0	0.01
500	0.01
750	0.01
1000	0.01
2000	0.01
3000	0.01
4000	0.01
6000	0.04

Figure 5.11: OMTHP Static Compatibility Test. Filtrate picture and weight of precipitate after filtration.

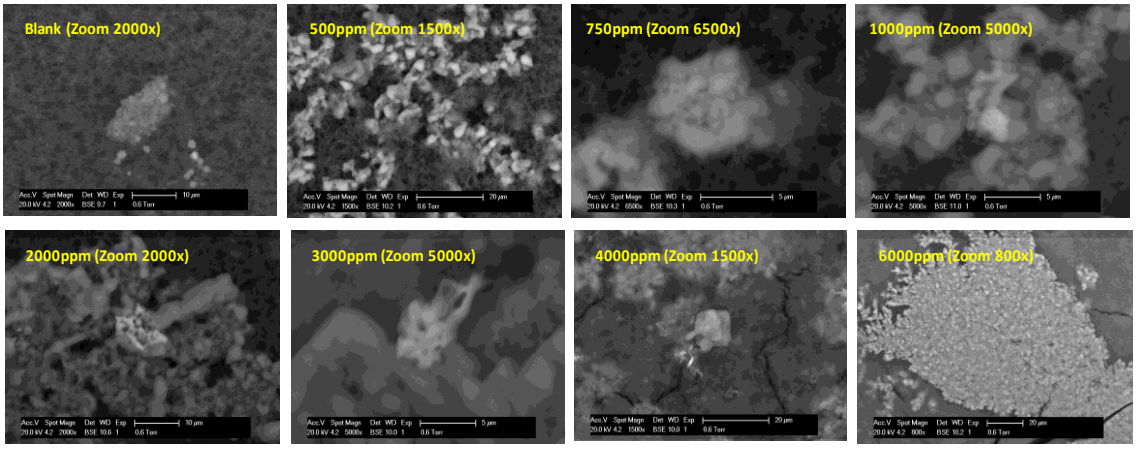

	Blank		500 ppm		750 ppm		1000 ppm		2000 ppm		4000 ppm		6000 ppm	
Element	Weight%	Atomic%	Weight%	Atomic%	Weight%	Atomic%	Weight%	Atomic%	Weight%	Atomic%	Weight%	Atomic%	Weight%	Atomic%
-	-	-	-	-	-	-	-	-	-	-	-	-	-	-
C	40.57	50.53	30.51	45.37	35.75	51.73	31.77	47.95			21.69	37	25.5	37.71
O	45.08	42.15	26.36	29.43	19.4	21.07	21.44	24.29	22.3	40.45	17.82	22.83	35.99	39.96
Na	1.08	0.7	12.77	9.92	19.58	14.8	17.36	13.69	16.7	21.08	20.06	17.87	9.6	7.42
Al	0.96	0.53												
Si	8.27	4.4												
Mg													1.45	1.06
P											1.13	0.75	3.02	1.73
Cl	3.54	1.49	29.81	15.02	25.28	12.39	25.99	13.29	40.67	33.29	35.5	20.52	22.27	11.16
K	0.51	0.19							0	0				
Ca			0.56	0.25			0.6	0.27	1.22	0.88	1.31	0.67	2.17	0.96
Sr							1.7	0.35	2.1	0.7				
Ba							1.15	0.15	17.02	3.6	2.49	0.37		
Totals	100		100		100		100		100		100		100	

Figure 5.12: OMTHP Static Compatibility Test. Filtrate ESEM-EDAX results.

5.3.2 Sand Pack A: Dynamic Precipitation Flood –Singe Flow rate

Sand Pack A represents a Dynamic Precipitation Flood at a single flow rate. The main treatment uses 4000ppm OMTHP in NFFW ($+Li^+$) brine at 20 ml/hr flow rate; whereas all post flush uses NFFW (no Li^+) brine at 20 ml/hr. The main treatment was conducted at room temperature (~20°C) and the post flushes were conducted at 95°C. The pH values of all fluids injected, which includes main treatment and post flush, were adjusted to pH4. OMTHP at 4000ppm does not precipitate at pH4 at room temperature as reported above in the static compatibility/adsorption tests. At each interval from main treatment to post flush, the flow was stopped and maintained for at least 24 hrs at 95°C. This is the first sand pack experiment with the new set-up of the sand pack apparatus. The purpose of this particular sand pack experiment is to understand the behaviour of the phosphorous (SI), calcium, magnesium and lithium throughout the experiment.

Before the dynamic experiment was conducted, the sand pack was characterized. The characterization of sand pack measures dead volume and pore volume and based on this information, porosity was calculated. The dead volume and pore volume were measured as being 4.54ml and 13.64ml respectively. The dead volume and pore volume were used for the entire experiment to track the amount of volume passed through the sand pack**.** Details of Sand Pack characterization are presented in Table 5.4.

Sand Pack A : Characterization Results			
Length of Sandpacking	=	20.05	cm
Diameter	=	1.5	cm
Dead Volume	=	4.54	ml
Pore Volume @ RT	=	13.64	ml
Porosity @ RT	=	38.49	%

Table 5.4: Sand Pack A – Characterization Results

Once the sand pack characterization is completed, NFFW (no Li^+) brine was injected through the sand pack overnight to saturate the column. The purpose is to remove unwanted materials and any impurities present in the sand pack. Immediately, the

dynamic sand pack experiment was initiated starting with main treatment. Refer to Table 5.5 for experimental details and chronologies of injection.

The main treatment was carried out with 4000ppm OMTHP in NFFW ($+Li^+$) at room temperature, at 20 ml/hr. The flow continued for about 8 PV before shutting in the pack. At this point, the system must be saturated with 4000ppm OMTHP. Normally, it took only 3 to 4 PV to have the sand pack saturated as shown in Figure 5.13, where the concentration of phosphorous and lithium level was up at its stock concentration. The temperature was increased to 95°C and left for at least 24 hrs. Based on OMTHP static compatibility/adsorption tests, precipitation will have taken place at 95°C. After the 24 hrs shut in, the first post flush with NFFW (no Li^+) brine was initiated at 20 ml/hr. This was continued for about 400PV, stopping from time to time for a few hours to add to the water bath and/or to change the carousel. The post flush was continued for a long time to make sure the effluent concentration reaches a very low values of [SI] (which we expect to be below any likely MIC level); in this case it was set at 1ppm. Effluents were taken at a set interval and sent for inductive coupled plasma (ICP) analysis.

Based on the concentration analyzed using ICP, the mass of recovered from the pack SI is calculated and compared with the known injected mass to decide whether further flow is required. If the mass-out does not match the mass-in of the SI, further flow is required to establish the where about of the SI mass. The mass balance shows that there is still significant SI mass in the sand pack when these low levels of [SI] are first reached. In this case, additional flow was required, where acidized Na^+(pH=1) ion was used to extract the SI left in the sand pack since it is expected that the solubility of the SI_M complex will be higher in this low calcium brine. Details of the flow rate of this acidized NaCl brine and injected pore volumes are presented in Table 5.5.

No.	Description	Conditions	Flow rate (ml/hr)	PV (Total PV)	Volume (ml) (Total Vol)
1	Main Treatment – 4000ppm OMTHP in NFFW (+50ppm Li+)	T = 20°C pH = 4	20	1–7.99 (7.99)	1-109 (109)
Shut-in at reservoir temperature (95°C) for 24 hrs.					
2	Post Flush # 1 : NFFW (no Li+)	T = 95°C pH = 4	20	7.99–21.19 (13.2)	109-289 (180)
3	Post Flush # 2 : NFFW (no Li+)	T = 95°C pH = 4	20	21.19–41.64 (20.45)	289-568 (279)

4	Post Flush # 3 : NFFW (no Li+)	T = 95°C pH = 4	20	41.64–48.09 (6.45)	568-656 (88)
5	Post Flush # 4 : NFFW (no Li+)	T = 95°C pH = 4	20	48.09–73.31 (25.22)	656-1000 (344)
6	Post Flush # 5 : NFFW (no Li+)	T = 95°C pH = 4	20	73.31–87.39 (14.08)	1000-1192 (192)
7	Post Flush # 6 : NFFW (no Li+)	T = 95°C pH = 4	20	87.39–114.66 (27.27)	1192-1564 (372)
8	Post Flush # 7 : NFFW (no Li+)	T = 95°C pH = 4	20	114.66-183.36 (68.7)	1564-2501 (937)
9	Post Flush # 8 : NFFW (no Li+)	T = 95°C pH = 4	20	183.36-253.01 (69.65)	2501-3451 (950)
10	Post Flush # 9 : NFFW (no Li+)	T = 95°C pH = 4	20	253.01-322.65 (69.64)	3451-4401 (950)
11	Post Flush # 10 : NFFW (no Li+)	T = 95°C pH = 4	20	322.65-391.57 (68.92)	4401-5341 (940)
12	Post Flush # 11 : NFFW (no Li+)	T = 95°C pH = 4	20	391.57–417.23 (25.66)	5341-5691 (350)
Shut-in at room temperature (20°C) for 4 days. COMPLETED POST FLUSH.					
13	Acid Wash # 1 : NFFW (no Li+)	T = 20°C pH = 1	20	417.23–427.49 (10.26)	5691-5831 (140)
14	Acid Wash # 2 : 1% Na+	T = 20°C pH = 1	20	427.49–533.43 (105.94)	5831-7276 (1445)
15	Acid Wash # 3 : 1% Na+	T = 20°C pH = 1	20	533.43–705.90 (172.47)	7276-9628 (2352)
16	Acid Wash # 4 : 1% Na+	T = 20°C pH = 1	20	705.90–780.68 (74.78)	9628-10648 (1020)
Shut-In at room temperature (20°C). COMPLETED.					

Table 5.5: Sand Pack A – Experimental Details and Chronologies of Injection

The outcomes of the main treatment and initial post-flush stages are shown in Figure 5.13 and Figure 5.14. These figures show the actual and normalized concentrations against pore volumes (PV) respectively for each element. The profiles of each element under study, viz. OMTHP SI and lithium (Li^+) concentrations vs. PV can be observed from these figures. Li^+ is an inert element which is being used as a tracer in this study.

The first eight (8) PV is the main treatment using 4000ppm OMTHP in NFFW (+ Li^+) where the acidity/alkalinity has been adjusted to pH4 and it is known that no precipitation will occur at room temperature. The main treatment is carried out at 20 ml/hr and room temperature, 20°C. As the flow goes through the first 3 to 4 PV, the OMTHP SI starts deviating from the Lithium (inert tracer) curve. Thus, the deviation between the SI and Lithium tracer is a measure of the amount of SI adsorption and/or precipitation. In this case, it is due to pure adsorption, as this has been established in the

corresponding static adsorption/compatibility tests at room temperature (reported above)where it is known that no precipitation is taking place. From 4PV to 9PV, all the elements stabilized at their stocks concentrations; which indicates the sand pack is fully saturated.

After 8 PV of injection, flow is stopped and the sand pack is placed in a water bath. The water bath temperature is increased from room temperature to 95°C. The set-up is left shut in under these conditions for 65 hrs. After the shut-in, the flow is returned at 20 ml/hr and 95°C. This is the initial post flush using NFFW brine with no Li^+, where the pH is adjusted to 4. The post flush was carried out until 400PV.

When the flow is initiated after the shut-in after 8 PV, a considerable drop in SI concentration from 4000ppm to 1000ppm (normalized at 0.25) was observed, which indicates a very high SI retention due to coupled adsorption/precipitation. The observed behaviour is clear evidence of SI coupled adsorption/precipitation onto sand minerals. Similar behaviour has been observed in our bulk studies of this exact system.

As the post flush flow continues, initially the SI concentration dropped drastically and stabilizes at ~0.2ppm, see Figure 5.15. It is not expected to drop much further below this baseline trend which is stabilizing. An important observation can be seen; when the flow was stopped and restart after several hours, the effluent concentration went back almost to the same level, i.e. in this case ~0.2ppm. No change in effluent concentration is observed when the flow rate remains the same.

At the end of post flush, the flow is shut-in and the temperature was reduced from 95°C to room temperature, 20°C. In this flood, the sand pack was then shut-in for 4 days. The mass balance of SI left in the sand pack and returned during post flush is also calculated to determine if all the retained SI mass in the sand pack is returned after the final post flush. Details of the mass balance are presented in Table 5.7. After the main treatment, 76% of the SI mass has been returned. But after the main treatment, the returned SI mass during the post flush was only an additional of 8%, which add up to 84%; leaving 16% SI mass in the sand pack. This shows that there is still SI in the sand pack after the final post flush.

The mass balance results led us to carry out an acid wash on the sand pack. Table 5.7 shows the results of the acid wash mass balance. Figure 5.16 shows the results of the whole injection chronologies including the acid wash. Initially, NFFW brine at pH=1 was used to extract the SI in the sand pack, where only an additional of 0.2% SI mass was out after 10PV. Then 1% Na^+ at pH=1 was used to acid wash the sand pack. The flush with 1% Na+ produce another 6.6% SI mass after 350PV, still leaving almost 9% SI mass in the sand pack.

Finally, the sand was removed from the sand pack and was stirred in a 1% Na^+ at pH 1 for 24 hours. Fluid samples were extracted and sent for ICP analysis and the sand was sent for ESEM-EDAX analysis to determine if SI was still present on the sand. Referring to Table 5.7, an additional of 1% SI mass was found in the sand solution. No SI mass is found in the ESEM-EDAX analysis, referring to Table 5.6 and Figure 5.17. It must be noted that ESEM-EDAX does not detect these elements at micro level and the detection refers only to a very localized area. In contrast, the mass balance shows that there is still 8% SI mass present in the sand pack undetected, which indicates irreversible retention has occurred (Kerver and Heilhecker, 1969).

Mass balance based on the mass left in sand pack after the main treatment + 2PV of post flush: All the above mass balance calculation were made base on total mass-in (throughput) during main treatment. Here, mass balance is calculated base on mass left in sand pack after main treatment + 2PV of initial post flush. The additional SI mass of 2PV is removed from the post flush to take into account the mobile phase in the sand pack. As such, mass left in sand pack is the actual amount of mass that is being absorbed and/or precipitated. By this definition, the mass left in sand pack is 72.47mg, which is being used as the "total mass". Base on this calculation, only 54% of the SI came out of sand pack, leaving 46% SI mass left in sand pack. Again, these findings demonstrate irreversible retention of SI. Detailed mass balance comparison are presented in Table 5.8 and Figure 5.18.

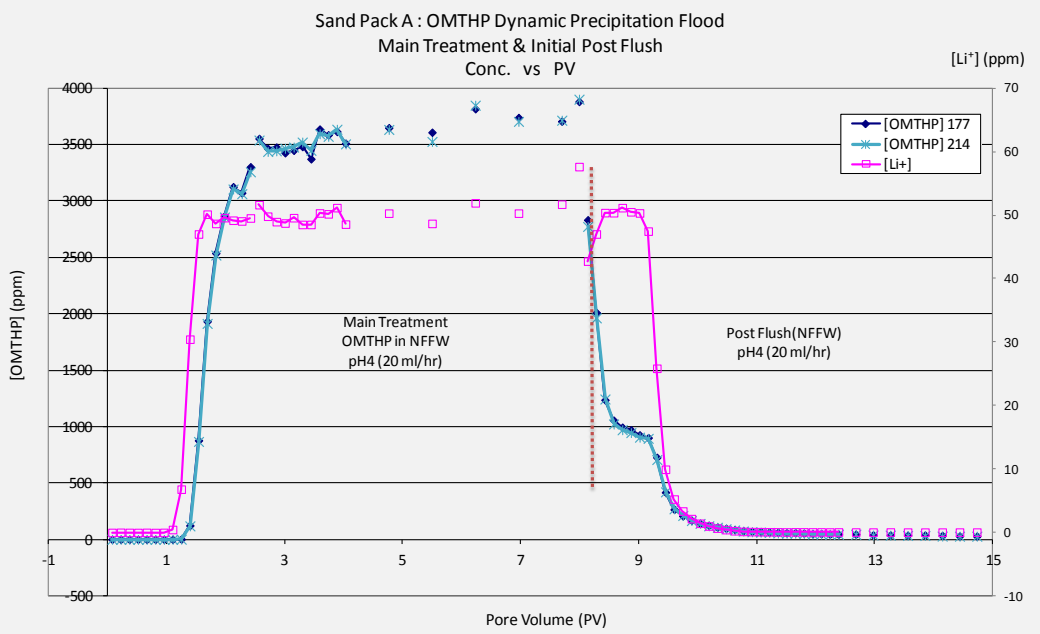

Figure 5.13: Sand Pack A- Main Treatment and Initial First Post Flush Stages.

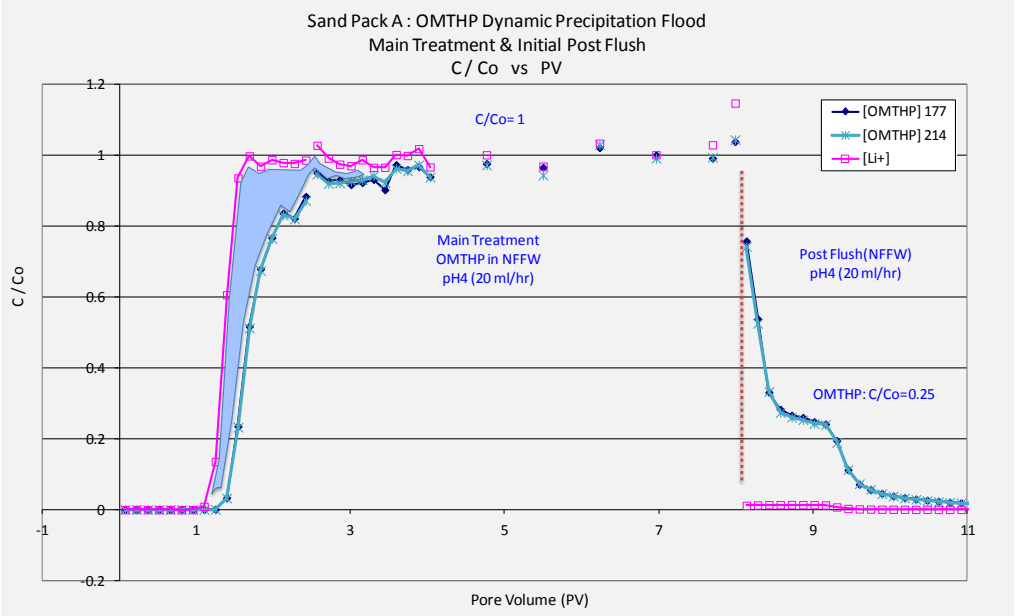

Figure 5.14: Sand Pack A- Main Treatment and Initial First Post Flush Stages. Normalized Concentration vs. PV

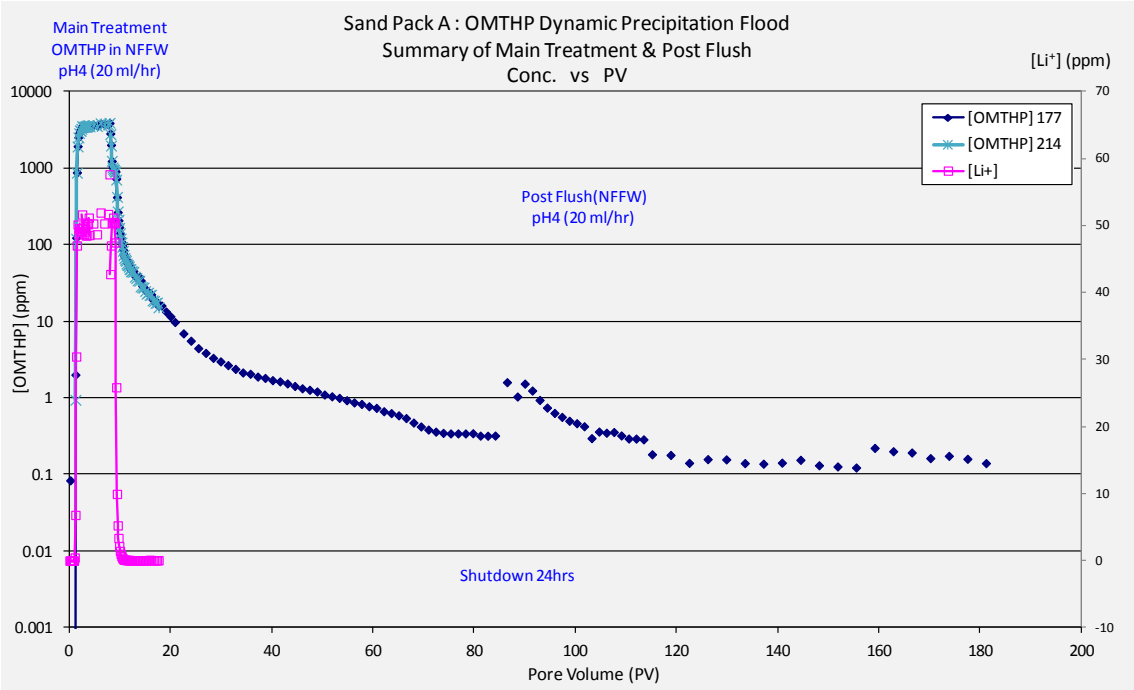

Figure 5.15: Sand Pack A- Main Treatment and Post Flush Stages.

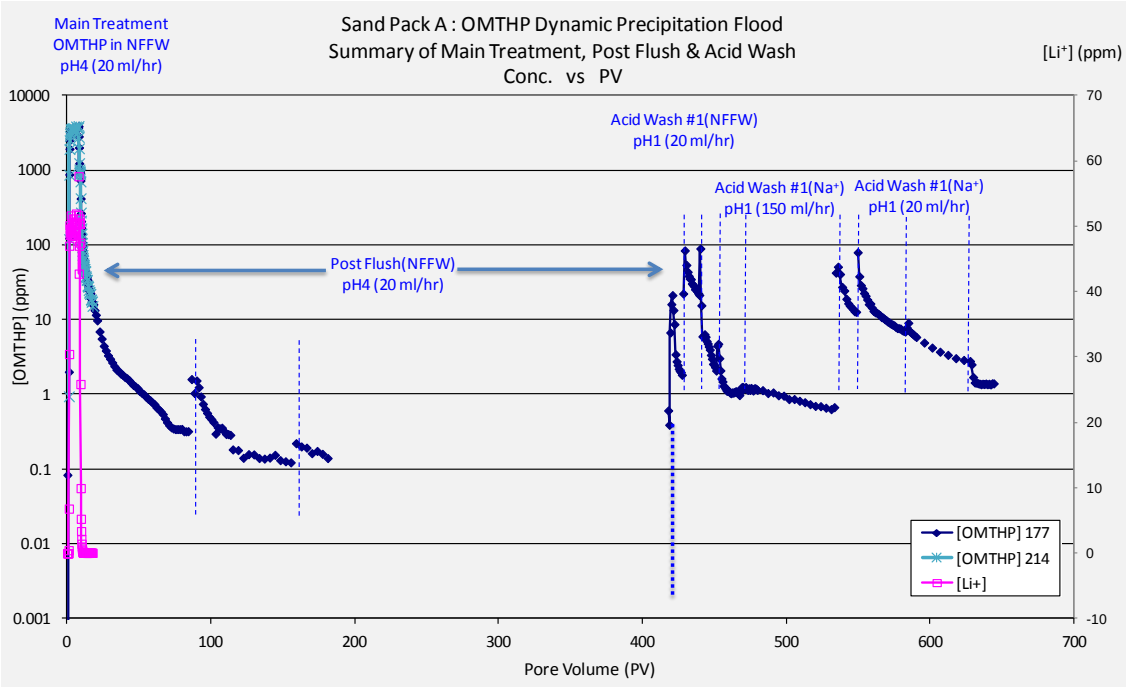

Figure 5.16: Sand Pack A- Main Treatment, Post Flush and Acid Wash Stages.

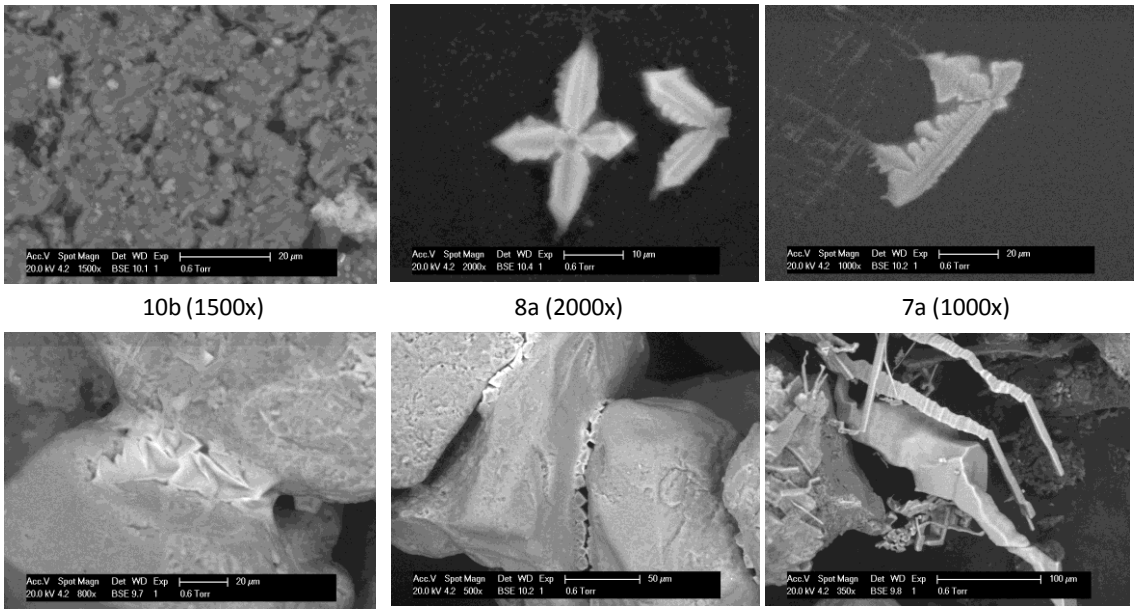

Figure 5.17: Sand Pack A- ESEM picture of sand washed with Na^+ (pH=1) after the experiment. The higher no. indicates at the inlet and lower no. at outlet. 10b is taken from behind the inlet filter at the sand pack.

	10a		10b		9a		8a		7a		6a		4a		2		1	
Element	Weight%	Atomic%	Weight%	Atomic%	Weight%	Atomic%	Weight%	Atomic%	Weight%	Atomic%	Weight%	Atomic%	Weight%	Atomic%	Weight%	Atomic%	Weight%	Atomic%
C			23.27	32.57			46.97	64.49	47.85	64.55								
F	9.81	14.42	75.19	66.53														
O					49.38	73.06	11.2	11.55	13.26	13.43	55.2	68.51	22.82	35.17	25.03	38.2	8.86	15
Na	34.52	41.95	0.65	0.47	0.66	0.68	17.13	12.29	16.68	11.76	6.66	5.76	25.57	27.42	24.69	26.23	35.98	42.4
Al							0.27	0.17										
Mg																		
P	0.51	0.46																
Si					4.23	3.56	1.19	0.7	1	0.57	29.74	21.03	8.28	7.27	5.24	4.56	2.26	2.18
Cl	54.05	42.6	0.72	0.34	0.75	0.5	23.23	10.81	21.21	9.69	8.4	4.7	43.33	30.14	45.03	31.01	52.91	40.43
S			0.17	0.09														
Ca																		
Cr	0.48	0.26																
Ti					44.57	22.03												
Fe	0.64	0.32			0.42	0.18												
Totals	100		100		100		100		100		100		100		100		100	

Table 5.6: Sand Pack A- EDAX results of sand washed with Na^+ (pH=1) after the experiment. The higher no. indicates at the inlet and lower no. at outlet. 10b is taken from behind the inlet filter at the sand pack.

Sand Pack A : Mass Balance of SI OMTHP

Mass In during Main Treatment =	410.85	mg
Mass Left In Sand Pack (after MT + PF) =	65.45	mg
Mass Left In Sand Pack (after MT+PF+AcW) =	37.63	mg

Description	PV (ml)	Mass Out (mg)	Cum Mass (mg)	Cum Mass (%)	Mass In (mg)	Mass In (%)
MT~20/ml/hr (OMTHP)	7.99	312.67	312.67	76.10	98.18	23.90
PF~20ml/hr (NFFW)	21.19	30.57	343.24	83.54	67.61	16.46
PF~20ml/hr (NFFW)	41.64	0.89	344.13	83.76	66.72	16.24
PF~20ml/hr (NFFW)	48.09	0.12	344.25	83.79	66.60	16.21
PF~20ml/hr (NFFW)	73.31	0.25	344.51	83.85	66.34	16.15
PF~20ml/hr (NFFW)	87.39	0.09	344.59	83.87	66.26	16.13
PF~20ml/hr (NFFW)	114.6628	0.21	344.81	83.93	66.04	16.07
PF~20ml/hr (NFFW)	183.3578	0.15	344.96	83.96	65.89	16.04
PF~20ml/hr (NFFW)	253.0059	0.13	345.09	83.99	65.76	16.01
PF~20ml/hr (NFFW)	322.654	0.13	345.22	84.03	65.63	15.97
PF~20ml/hr (NFFW)	391.5689	0.13	345.35	84.06	65.50	15.94
PF~20ml/hr (NFFW)	417.2287	0.05	345.40	84.07	65.45	15.93
AcW~(NFFW) pH=1	427.4927	0.84	346.24	84.27	64.61	15.73
AcW~(Na+) pH=1	533.4311	8.80	355.04	86.42	55.81	13.58
AcW~(Na+) pH=1	705.9018	16.75	371.79	90.49	39.06	9.51
AcW~(Na+) pH=1	780.6818	1.43	373.22	90.84	37.63	9.16
Sand from the column + 250 ml DW		4.55	377.77	91.95	33.08	8.05

Table 5.7: Sand Pack A- Mass balance base on total mass throughput

Sand Pack A : Mass Balance of SI OMTHP

Mass In during Main Treatment =	410.85	mg
Mass Left In Sand Pack (after MT + PF) =	65.45	mg
Mass Left In Sand Pack (after MT+PF+AcW) =	37.63	mg

Description	PV (ml)	Mass Out (mg)	(X) Cum Mass Return (mg)	(X) Cum Mass Return (%)	Mass Left In Sand Pack (mg)	Mass Left In Sand Pack (%)	(Y) Cum Mass Return (mg)	(Y) Cum Mass Return (%)
MT~20/ml/hr (OMTHP)	10.04	338.38	338.38	82.36	72.47	17.64		
PF~20ml/hr (NFFW)	19.14	4.86	343.24	83.54	67.61	16.46	4.86	6.70
PF~20ml/hr (NFFW)	41.64	0.89	344.13	83.76	66.72	16.24	5.75	7.93
PF~20ml/hr (NFFW)	48.09	0.12	344.25	83.79	66.60	16.21	5.87	8.10
PF~20ml/hr (NFFW)	73.31	0.25	344.51	83.85	66.34	16.15	6.13	8.45
PF~20ml/hr (NFFW)	87.39	0.09	344.59	83.87	66.26	16.13	6.21	8.57
PF~20ml/hr (NFFW)	114.6628	0.21	344.81	83.93	66.04	16.07	6.43	8.87
PF~20ml/hr (NFFW)	183.3578	0.15	344.96	83.96	65.89	16.04	6.58	9.07
PF~20ml/hr (NFFW)	253.0059	0.13	345.09	83.99	65.76	16.01	6.71	9.26
PF~20ml/hr (NFFW)	322.654	0.13	345.22	84.03	65.63	15.97	6.84	9.44
PF~20ml/hr (NFFW)	391.5689	0.13	345.35	84.06	65.50	15.94	6.97	9.62
PF~20ml/hr (NFFW)	417.2287	0.05	345.40	84.07	65.45	15.93	7.02	9.69
AcW~(NFFW) pH=1	427.4927	0.84	346.24	84.27	64.61	15.73	7.86	10.85
AcW~(Na+) pH=1	533.4311	8.80	355.04	86.42	55.81	13.58	16.66	22.99
AcW~(Na+) pH=1	705.9018	16.75	371.79	90.49	39.06	9.51	33.41	46.10
AcW~(Na+) pH=1	780.6818	1.43	373.22	90.84	37.63	9.16	34.84	48.07
Sand from the column + 250 ml DW		4.55	377.77	91.95	33.08	8.05	39.39	54.35

Table 5.8: Sand Pack A- Summary of mass balance base on total mass throughput and mass after main treatment + 2PV

Note:

X: %Mass out base on total mass throughput; m= 410.85mg

Y: %Mass out base on mass after main treatment + 2PV, which is the mass left in the sand pack as being absorbed or/and precipitated; m= 72.47mg

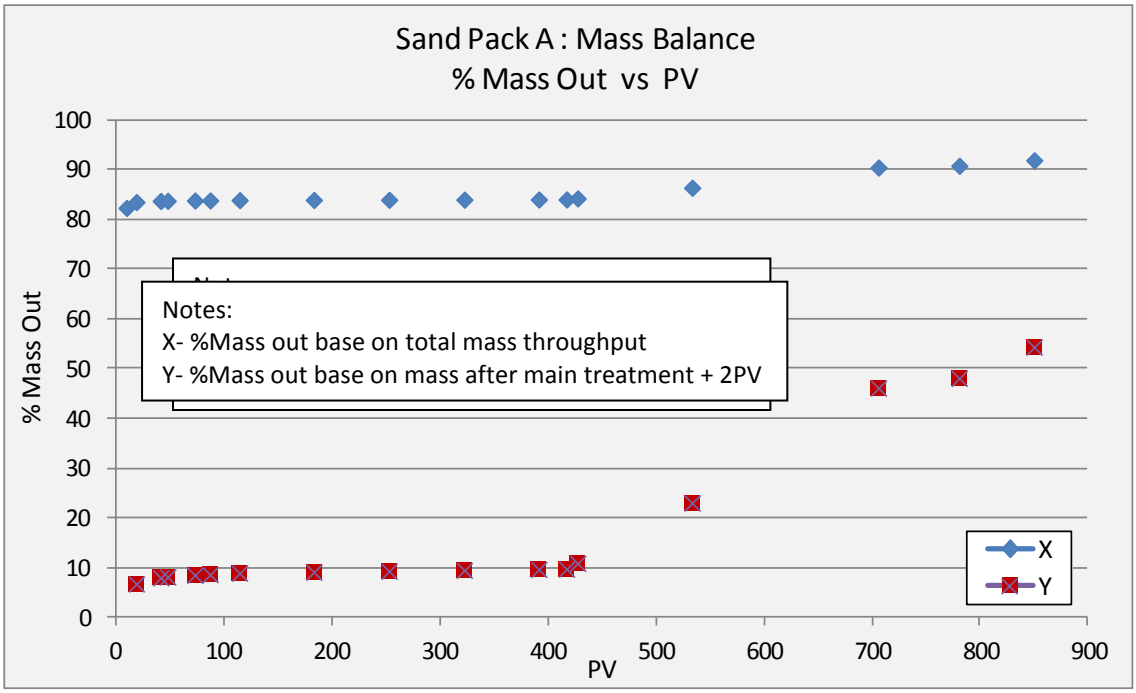

Figure 5.18: Sand Pack A- Summary of mass balance base on total mass throughput and mass after main treatment + 2PV

5.3.3 Sand Pack C: Dynamic Precipitation Flood – Multi Flow rate

Sand Pack C was used in a dynamic precipitation flood with at a range of flow rates. The main treatment contains 4000ppm OMTHP in NFFW ($+Li^+$) brine at 20 ml/hr flow rate; whereas the post flush is carried out with NFFW(no Li^+) brine at 20, 10, 5 and 2 ml/hr. The main treatment was conducted at room temperature and all post flushes were carried out at reservoir condition at 95°C. The pH of all fluids injected, which includes main treatment and post flush were adjusted to pH4, where it is known that SI solution at 4000ppm will not precipitate. At each interval from main treatment to post flush, the flow was stopped and maintained for at least 24 hrs at 95°C. The details and chronologies of the experiment can be found in Table 5.10.

Before the dynamic experiment was conducted, the sand pack was fully characterized. The characterization of the sand pack measures dead volume and pore volume. Based on this information, porosity was calculated. The dead volume and pore volume were measured to be 1.54ml and 14.69ml respectively. These volumes were used for the

entire experimental cycle to track the amount of volume passing through the sand pack. Details of sand pack characterization are presented in Table 5.9.

Sand Pack C : Characterization Results			
Length of Sandpacking =	=	20.5	cm
Diameter =	=	1.5	cm
Dead Volume =	=	1.54	ml
Pore Volume @ RT =	=	14.69	ml
Porosity @ RT =	=	40.52	%

Table 5.9: Sand Pack C – Characterization Results

Once the characterization was completed, NFFW (no Li+) brine was injected into the sand pack overnight to saturate the system. The dynamic sand pack experiment was then immediately initiated starting with main treatment. Refer toTable 5.10 for experimental details and chronologies of injection.

The main treatment was performed using 4000ppm OMTHP in NFFW ($+Li^+$) at room temperature, at 20 ml/hr. The flow was continued for ~9 PV before a shut in. At this point, the system must be saturated with 4000ppm OMTHP. Normally, it took only ~3 to 4 PV to have the sand pack saturated with full concentration SI. This can be seen from where Figure 5.19 all the elements are level at their stock concentrations by this time. After the shut-in, the temperature was increased to 95°C and left for at least 24 hrs. Based on the OMTHP static tests, coupled adsorption/precipitation is expected to take place under these conditions. After the 24 hrs shut in, the first post flush with NFFW (no Li^+) brine was initiated at 20 ml/hr. This was continued for ~72PV. The initial post flush was continued for this long duration to ensure the effluent concentration reached a very low concentration level or no large changes in effluent concentration were observed; in this case it was set at 1ppm. The flow was stopped and left for at least 24 hrs at 95°C. Then the flow was continued at 10, 5, 5 and 2 ml/hr. After each flow rate, the flow is stopped for at least 24 hrs at 95°C. Effluents were collected at set intervals at all flow rates, which were sent for ICP analysis.

Based on the concentration analyzed using ICP, the mass of SI produced was calculated to decide whether further flow was required. If the mass-out does not match the mass-in of the SI, further flow was carried out. In this case, acidized Na^+(pH=1) ion was used to extract the SI. Details of acidized flood can be found in Table 5.10.

No.	Description	Conditions	Flow rate (ml/hr)	PV (Total PV)	Volume (ml) (Total Vol)
1	Main Treatment – 4000ppm OMTHP in NFFW (+50ppm Li^+)	T = 20°C pH = 4	20	1–9.46 (9.4)	1-138 (138)
Shut-in at reservoir temperature (95°C) for 65 hrs.					
2	Post Flush # 1 : NFFW (no Li^+)	T = 95°C pH = 4	20	9.4–81.8 (72.4)	138-1202 (1064)
Shut-in at reservoir temperature (95°C) for 17 hrs.					
3	Post Flush # 2 : NFFW (no Li^+)	T = 95°C pH = 4	10	81.8–103.2 (21.4)	1202-1516 (314)
Shut-in at reservoir temperature (95°C) for 24 hrs.					
4	Post Flush # 3 : NFFW (no Li^+)	T = 95°C pH = 4	5	103.2–126.3 (23.1)	1516-1856 (340)
Shut-in at reservoir temperature (95°C) for 24 days.					
5	Post Flush # 4 : NFFW (no Li^+)	T = 95°C pH = 4	5	126.3–151.3 (25)	1856-2223 (367)
Shut-in at reservoir temperature (95°C) for 21 hrs.					
6	Post Flush # 5 : NFFW (no Li^+)	T = 95°C pH = 4	2	151.3–164.3 (13)	2223-2413 (190)
Shut-in at room temperature (20°C) for 4 days 1 hrs. COMPLETED POST FLUSH.					
7	Acid Wash # 1 : 1% Na+	T = 20°C pH = 1	20	164.3–233.7 (69.4)	2413-3433 (1020)
Shut-in at room temperature (20°C) for 18 hrs.					
8	Acid Wash # 2 : 1% Na+	T = 20°C pH = 1	20	233.7–243.6 (9.9)	3433-3578 (145)
Shut-in at room temperature (20°C) for 16 hrs.					
9	Acid Wash # 3 : 1% Na+	T = 20°C pH = 1	20	243.6–254.1 (10.5)	3578-3733 (155)
Shut-in at room temperature (20°C) for 16 hrs.					
10	Acid Wash # 4 : 1% Na+	T = 20°C pH = 1	20	254.1–265.7 (11.6)	3733-3903.5 (170.5)
Shut-in at room temperature (20°C) for 5 ½ days.					
11	Acid Wash # 5 : 1% Na+	T = 20°C pH = 1	60	265.7-297 (31.3)	3903.5-4363.5 (460)
Shut-In at room temperature (20°C). COMPLETED.					

Table 5.10: Sand Pack C – Experimental Details and Chronologies of Injection

The outcomes of the main treatment and first post-flush stages are shown in Figure 5.19 and Figure 5.20. These figures show the actual and normalized concentrations vs. pore volumes (PV) respectively for each element. The profiles of each element under study,

namely, OMTHP SI, calcium (Ca^{2+}), magnesium (Mg^{2+}) and lithium (Li^{+}) concentrations vs. PV can be observed from these figures. Ca^{2+} and Mg^{2+} are divalent cations known to bind together with phosphonates. Li^{+} is an inert element which is being used as a tracer in the study.

The first 9 PV of injection contained the main treatment with 4000ppm OMTHP in NFFW (+50ppm Li^{+}) where the acidity/alkalinity was adjusted to pH4. The main treatment is carried out at 20 ml/hr and room temperature, 20°C. As the flow goes through the first 2 to 3 PV, the OMTHP SI starts deviating from Lithium tracer curve. Thus, the deviation between the SI and Lithium tracer is a measure of the amount of SI adsorption and/or precipitation. In this case, it is due to pure adsorption, as already established by our static adsorption/compatibility tests described above. These tests showed that at room temperature no precipitation took place. The instant drop in calcium and magnesium concentrations is also evident in these figures which indicates that binding between SI and calcium and SI and magnesium occurs during adsorption. The affinity of calcium for SI is more distinct in these results compared to magnesium. From ~2 to 9 PV, all the elements stabilized at their stock concentrations; which indicates the sand pack is fully saturated with the injected brine.

After 9 PV of injection, flow is stopped and the sand pack is placed in a water bath. The water bath temperature is increased from room temperature to 95°C. The set-up was left for 65 hrs shut-in. After the shut-in, the flow was restarted at 20 ml/hr and 95°C. This is the first post flush using NFFW brine with no Li^{+}, where the pH is also 4. The first post flush was carried out from 10 to 80 PV.

When the flow recommenced after the shut-in at 9 PV, a considerable drop in SI concentration from 4000ppm to 750ppm (normalized at 0.2) was observed, which indicates a very high SI retention due to coupled adsorption/precipitation. Similar trends are also observed for calcium and magnesium; where Ca^{2+} is reduced from 1925ppm to 1550ppm (normalized at 0.85) and Mg^{2+} is reduced from 720ppm to 610ppm (normalized at 0.89). The observed behaviour is clear evidence of SI coupled adsorption/precipitation onto sand minerals; and the affinity of Ca^{2+} and Mg^{2+} with

OMTHP SI in the process of precipitation. The binding of SI to calcium/magnesium to form a SI_M complex which was retained in the pack is a clear diagnostic that precipitation has occurred. Similar behaviour has been observed in our bulk studies of this exact system.

At the end of first post flush (~80PV) based on Figure 5.21, the SI concentration was still reducing and if the flow continues the concentration is expected to drop further base on the trend. This behaviour indicates that it has yet to reach its lower concentration level. Base on the trend, the concentration is expected to go down to 0.4ppm (extrapolated). Whereas Ca^{2+} and Mg^{2+} stabilize around 1800 and 1850ppm and 670 and 690ppm (normalized at around 0.98 to 1.00 for both elements) respectively. Ca^{2+} and Mg^{2+} elements are injected with NFFW brine, as such changes is not expected during this post flush.

Figure 5.21 shows the later stage return profiles of the OMTHP precipitation floods at different flow rates using same post flush fluid. The details of the various stages are described in Table 5.10. The following observation can be summarized from the figure.

The flow was shut-in between the first (Q=20ml/hr) and second (Q=10ml/hr) post flushes during which time it was shut-in for 20 hours at 95°C. Immediately after the second post flush was initiated, the SI concentration went as high as 2.4ppm before went to 0.5ppm. The trend shows that it is stabilizing. The other observation is the increase in concentration at the start of the second post flush which indicates it reaches equilibrium at about 2.4ppm after 24 hrs. The increase shows desorption and dissolution took place during shut-in.

From 2^{nd} to 5^{th} post flush, NFFW was used, but at various flow rates. This is done in order to study if there is any impact due to non-equilibrium or kinetic processes. While the 1^{st} post flush flow period is carried out at 20 ml/hr; the 2^{nd}, 3^{rd}, 4^{th} and 5^{th} use 10, 5, 5 and 2 ml/hr respectively. At each interval between changing the flow rates, the flow was shut in more than 20 hours at 95°C. It can be observed that the concentration spikes up for all the flow rates depending upon shut-in time, before gradually decreasing to threshold concentration levels in the period of flow after this shut-in. The high

concentration at each shut-in is indicative of the dissolution of the precipitated SI where it reaches (near) equilibrium and the lowest point is when it stabilizes at its steady-state flowing level. An important point to note about the profile of SI concentration at the various flow rates is that, at the lower flow rates, a *higher* SI return concentration is observed (and vice versa). This behaviour is due to non-equilibrium effects and is as expected. At one point between the 3rd and 4th post flush, where the shut-in took place for 24 days; the flow rates for both post flush stages were at 5 ml/hr each. They show very similar stabilized flowing concentrations and this further confirms the non-equilibrium effect; i.e. at the same flow rate there was no changes in flowing concentration. After the final post flush at 2 ml/hr, the flow is shut-in and the temperature was reduced from 95°C to room temperature, 20°C. In this flood, the sand pack was shut-in for 4 days 1 hour.

The mass balance of SI left in the sand pack and returned during the post flush period was calculated. This analysis is conducted to study if all the SI mass is returned after the final post flush. Details of the mass balance at each stage are presented in Table 5.12. After the main treatment, 89.5% of the SI mass has been returned. But after the main treatment, the returned SI mass from 1st to 5th post flush only recovers an additional of 2%. Total mass returned after the 5th post flush period is 91.5%, leaving 8.5% in the sand pack. This shows that there is still SI in the sand pack after the final post flush.

The above mass balance results led us to carry out an acid wash on the sand pack using 1% Na^+ at pH=1. The purpose of this stage is to extract any SI left in the sand pack. Figure 5.22 shows the results of the whole injection chronology including the acid wash stage. Table 5.12 shows the results of the acid wash mass balance. Five (5) acid wash cycles were executed at two (2) different flow rates, which are at 20, 20, 20, 20 and 60 ml/hr. Even the acid wash at different rates show non-equilibrium behaviour. Again, in this acid wash period, the higher the flow rate, the lower the flowing threshold concentration (and vice versa).

Only an additional of 1.5% SI mass is collected after the final 5th acid wash, which account to a total of 93%, leaving 7% of the original injected SI in the sand pack.

However, one important observation can be made on the influence of flow rate throughout the 5 acid washes. As for the variable rate post flushes following the main SI treatment, the acid wash variable rate floods also show non-equilibrium behaviour. Again, the lower the flow rate, the higher the SI return concentrations (and vice versa). Figure 5.24 and Figure 5.25 show the mass balance of the sequence of cumulative mass-in and mass-out, respectively.

Finally, the sand in the sand pack was extracted from the column and dissolved while stirring in 1% Na^+ for 24 hours. Fluid samples were taken and sent for ICP analysis and the sand was sent for ESEM-EDAX analysis to determine whether SI was detectable in the sand pack (referring to Figure 5.23 and Table 5.11). There was no SI found from ESEM-EDAX analysis. It must be noted that ESEM-EDAX does not detect these elements at very low concentration levels. SI mass balance results shows an additional ~ 1% SI in the solution. The mass balance shows that there is still 7% of the SI mass present in the sand pack undetected, indicating irreversible retention behaviour (Kerver and Heilhecker, 1969).

Mass Balance based on mass left in the sand pack after main treatment + 2PV of post flush: All the above mass balance calculations were made base on the total mass-in (throughput) during the main treatment. Here, mass balance is calculated based on mass left in sand pack after the main treatment + 2PV of initial post flush. The additional 2PV of injected is to remove mobile SI (at input concentration) from the sand pack. After this 2PV postflush, all of the mass left in the sand pack is the actual amount of mass which has been absorbed or precipitated. After this 2PV brine postflush, we determine that the mass left in sand pack is 53.91mg, which is then used as the "total mass" for subsequent 5 retention calculations. Based on this calculation, only 33% of SI came out of the sand pack, leaving 67% SI mass left in the pack. These calculations indicate that there is irreversible retention of SI in the pack [28]. Detailed mass balances are presented inTable 5.13 and Figure 5.26.

A mass balance comparison at various stages of the flood is shown in Figure 5.27.

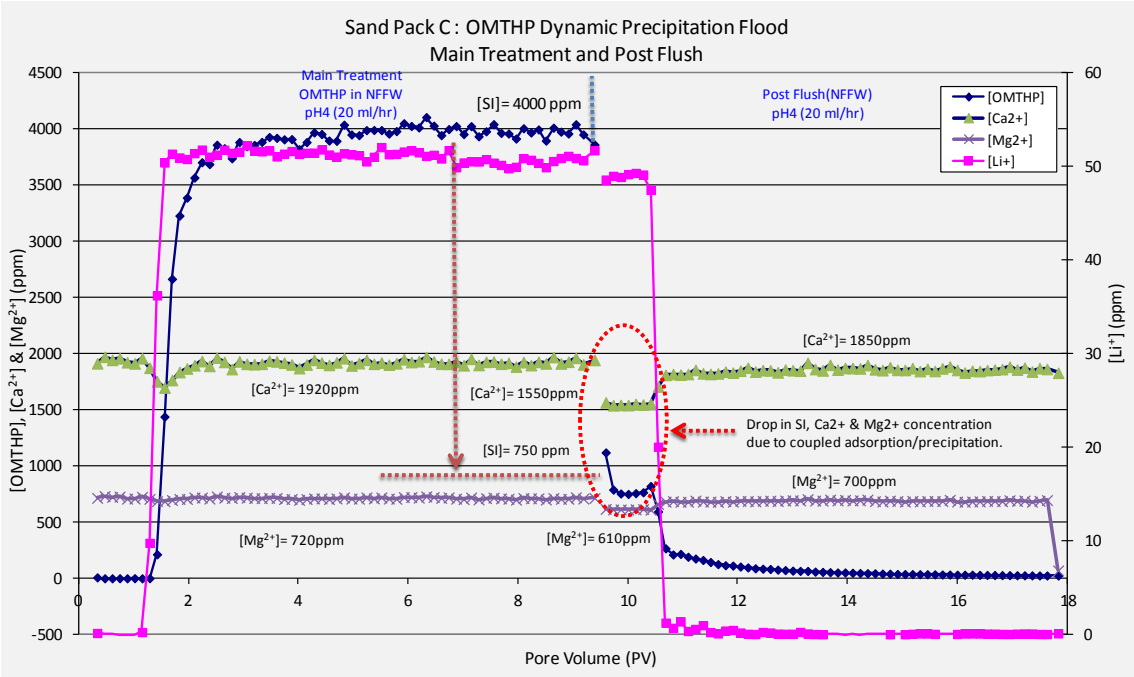

Figure 5.19: Sand Pack C - Main treatment and initial post flush stages.

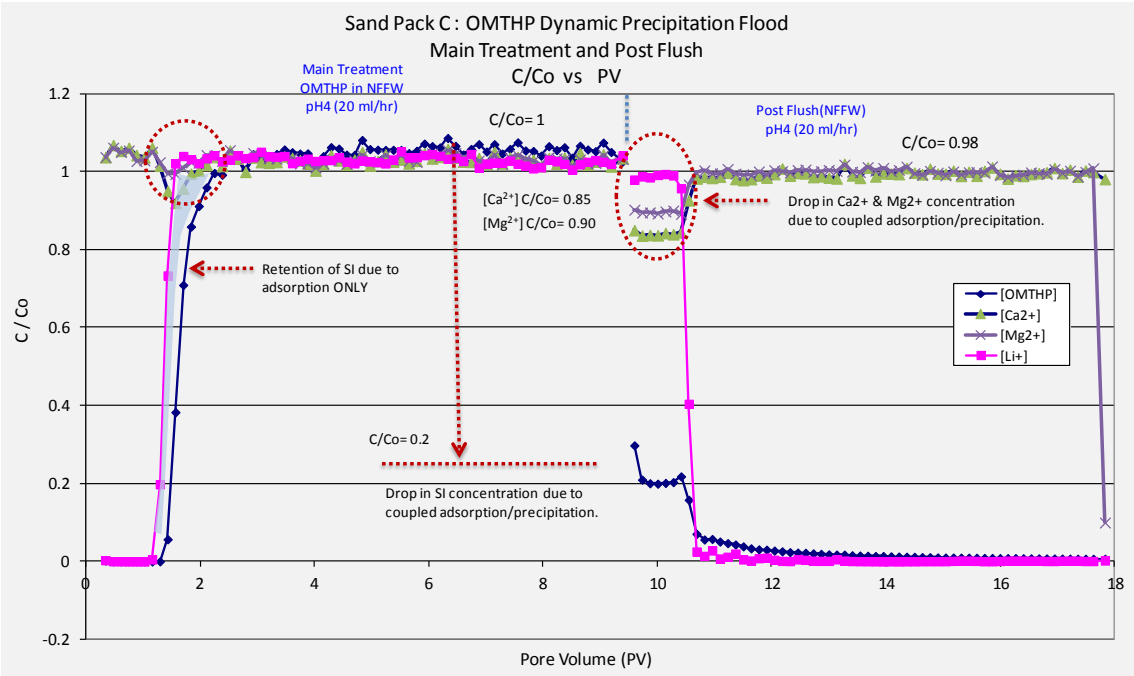

Figure 5.20: Sand Pack C- Main treatment and initial post flush stages. Normalized concentration vs. PV

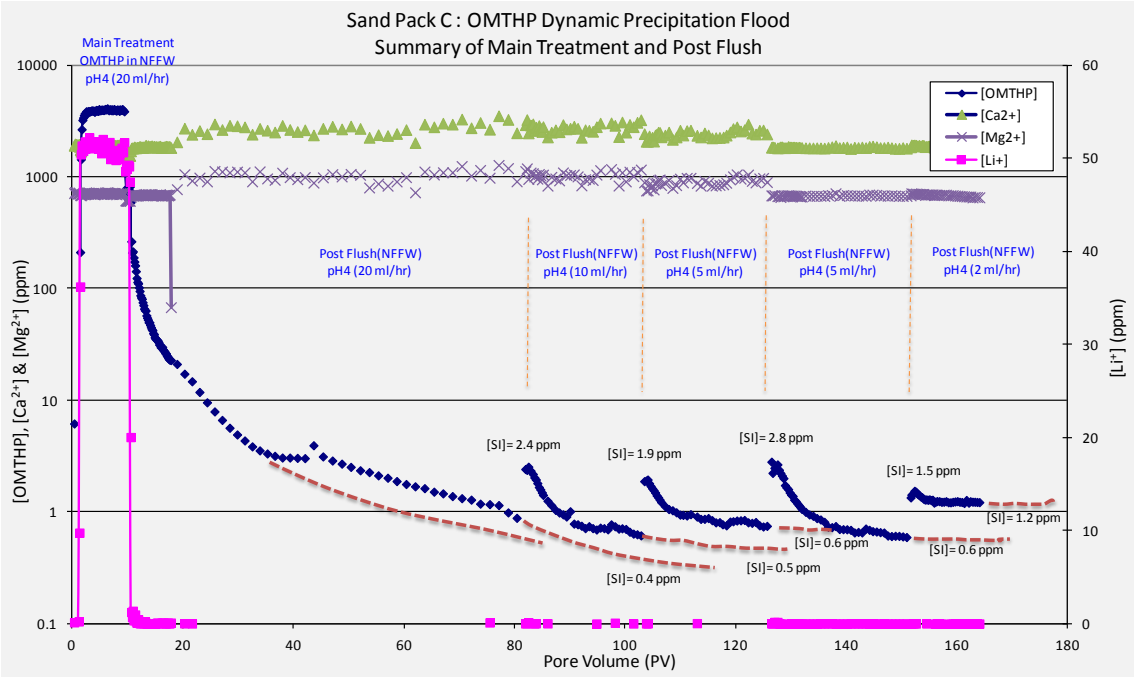

Figure 5.21: Sand Pack C- Main treatment and all post flush stages.

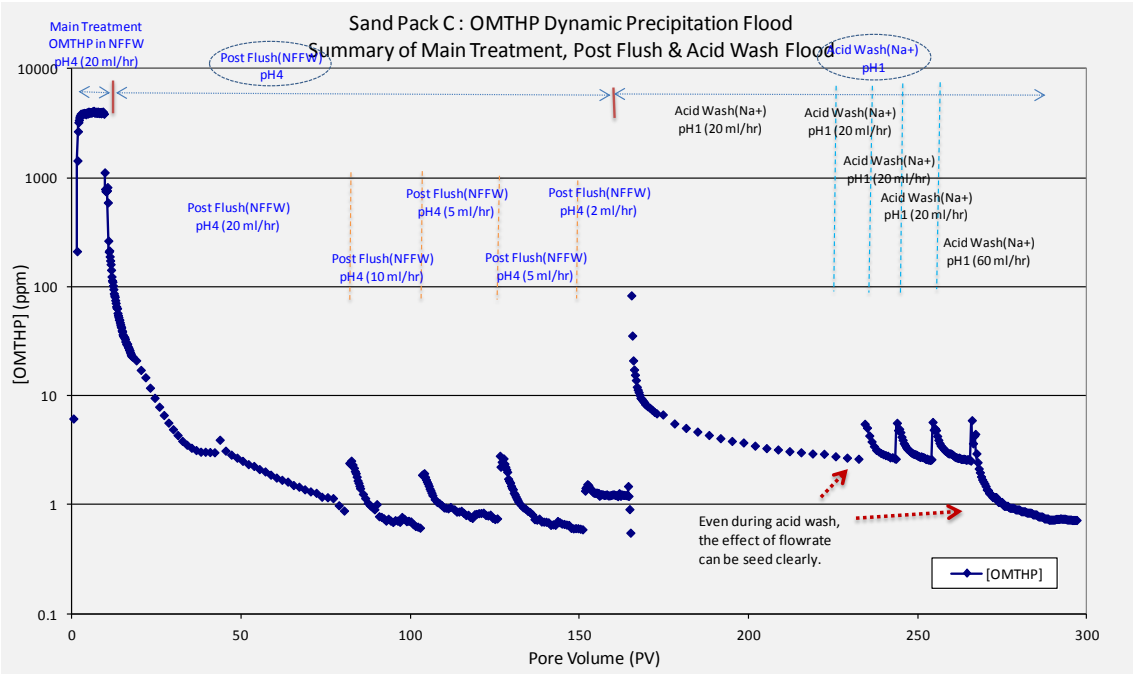

Figure 5.22: Sand Pack C- Main treatment, post flush and acid wash stages.

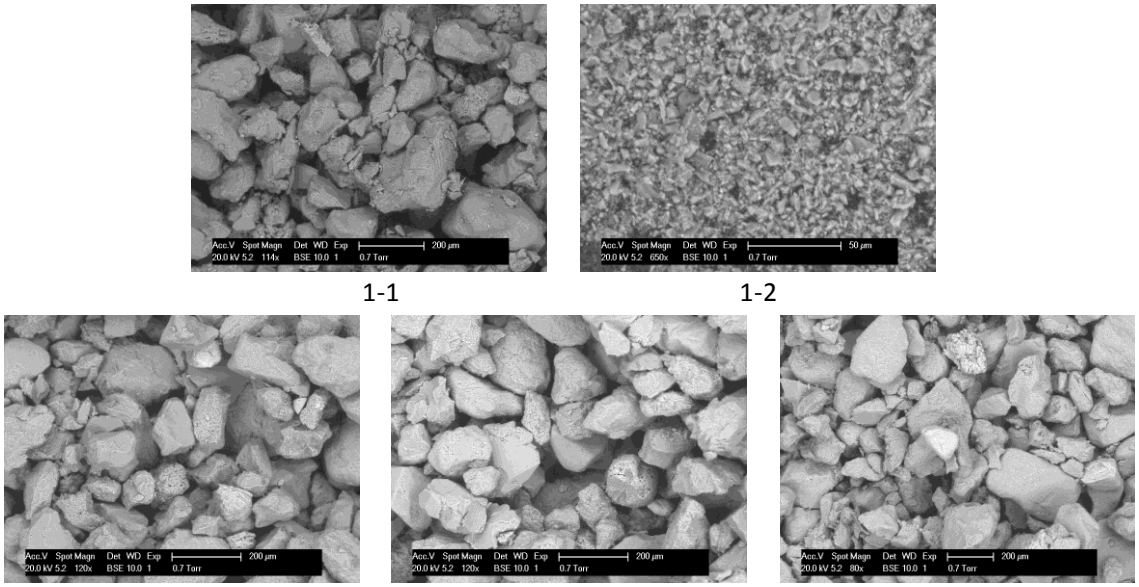

Figure 5.23: Sand Pack C- ESEM picture of sand washed with Na^+ (pH=1) after the experiment. The picture indicates no precipitation of SI

	1-1		1-2		2-1		3-1		4-1	
Element	Weight%	Atomic%	Weight%	Atomic%	Weight%	Atomic%	Weight%	Atomic%	Weight%	Atomic%
C			20	27.85						
O	59.98	72.5	54.58	57.08	60.55	73.01	58.38	71.1	59.71	72.28
Na			0.35	0.26					0.53	0.45
Al	1.03	0.74	1.9	1.18	0.63	0.45	0.9	0.65	0.93	0.67
Si	38.59	26.57	22.19	13.22	38.04	26.13	40.72	28.25	37.84	26.09
Mg										
P										
Cl					0.43	0.24			0.35	0.19
K	0.41	0.2	0.98	0.42	0.36	0.18			0.64	0.32
Ca										
Totals	100		100		100		100		100	

Table 5.11: Sand Pack C - EDAX results of sand washed with Na^+ (pH=1) after the experiment. No P, Ca^{2+} or Mg^{2+} was seen.

Sand Pack C : Mass Balance of SI OMTHP

Mass Throughput @ MT =	520.97	mg	
Mass Left In Sand Pack (after MT + PF) =	44.28	mg	
Mass Left In Sand Pack (after MT+PF+AcW) =	37.3	mg	

Description	PV (ml)	Mass Return (mg)	Cum Mass Return (mg)	Cum Mass Return (%)	Mass Left In Sand Pack (mg)	Mass Left In Sand Pack (%)
MT~20/ml/hr (OMTHP)	9.39	467.06	467.06	89.65	53.91	10.35
PF~20ml/hr (NFFW)	81.82	8.39	475.45	91.26	45.52	8.74
PF~10ml/hr (NFFW)	103.20	0.31	475.76	91.32	45.20	8.68
PF~5ml/hr (NFFW)	126.34	0.33	476.10	91.39	44.87	8.61
PF~5ml/hr (NFFW)	151.33	0.35	476.45	91.45	44.52	8.55
PF~2ml/hr (NFFW)	164.26	0.24	476.69	91.50	44.28	8.50
AcW #1~20ml/hr (Na^+)	233.70	4.91	481.60	92.44	39.37	7.56
AcW #2~20ml/hr (Na^+)	243.57	0.49	482.09	92.54	38.88	7.46
AcW #3~20ml/hr (Na^+)	254.12	0.50	482.60	92.63	38.37	7.37
AcW #4~20ml/hr (Na^+)	265.72	0.55	483.15	92.74	37.82	7.26
AcW #5~60ml/hr (Na^+)	297.04	0.53	483.67	92.84	37.30	7.16
Sand from the column + 250ml of DW		1	484.67	93.03	36.30	6.97

Table 5.12: Sand Pack C- Mass balance base on total mass throughput

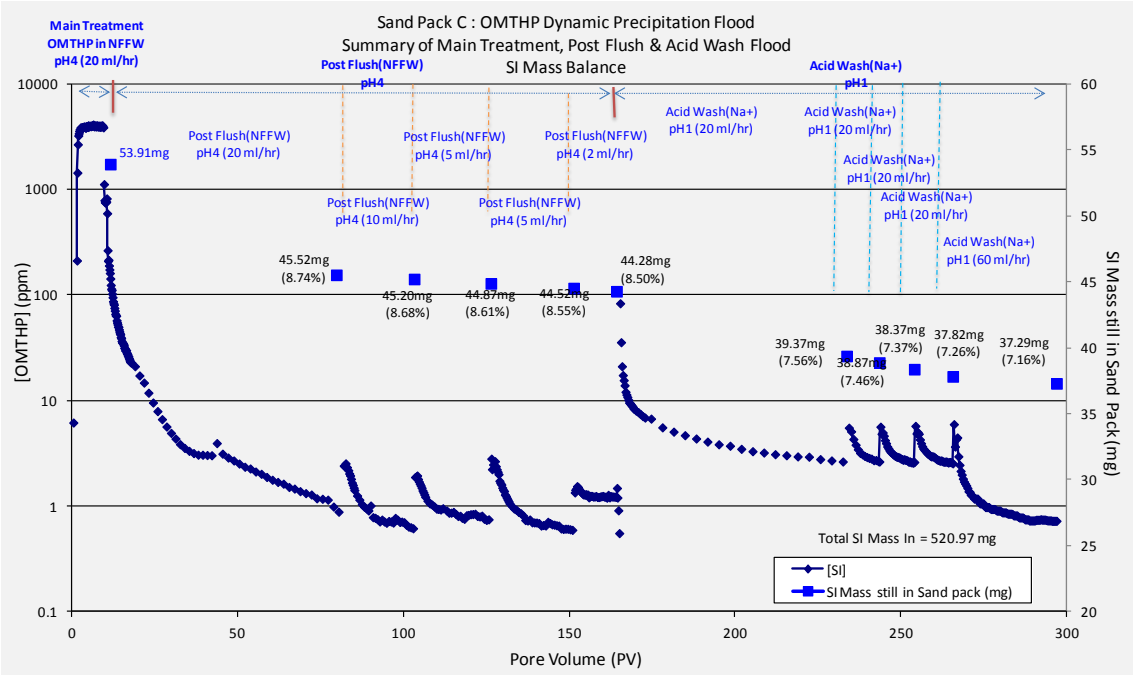

Figure 5.24: Sand Pack C- Mass still in sand pack base on total mass throughput

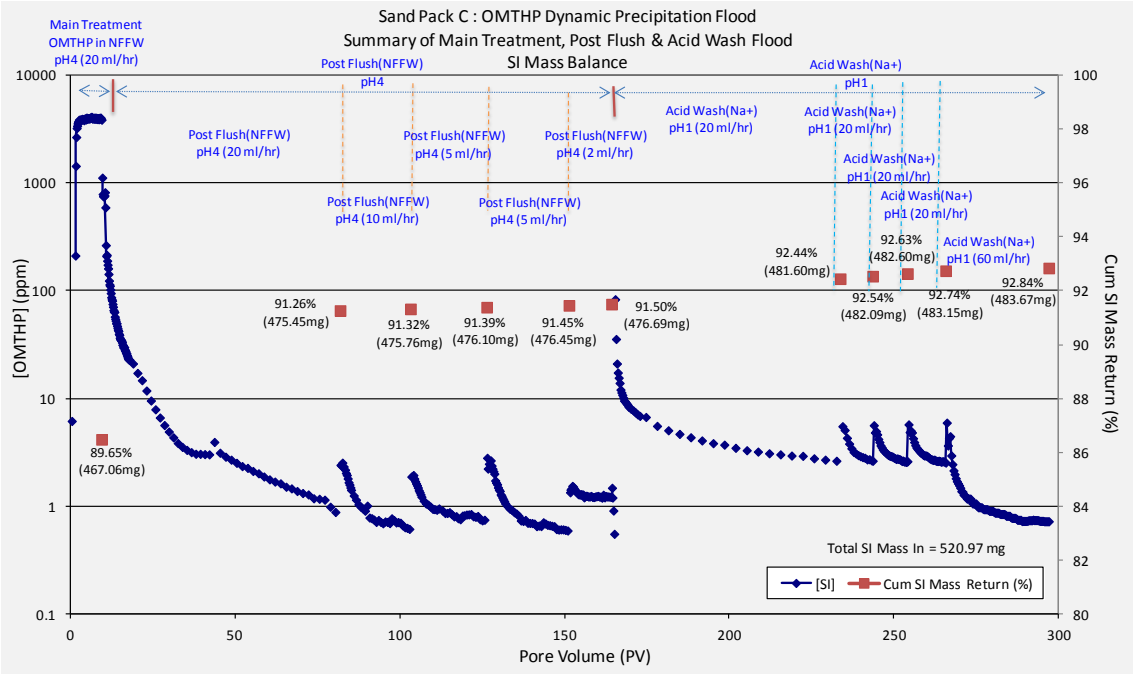

Figure 5.25: Sand Pack C- Cumulative mass out base on total mass throughput

Sand Pack C: Mass Balance of SI ~ OMTHP

Mass In during Main Treatment =	520.97	mg
Mass Left In Sand Pack (after MT + PF) =	44.28	mg
Mass Left In Sand Pack (after MT+PF+AcW) =	37.3	mg

			(X)				(Y)	
Description	PV (ml)	Mass Out (mg)	Cum Mass Return (mg)	Cum Mass Return (%)	Mass Left In Sand Pack (mg)	Mass Left In Sand Pack (%)	Cum Mass Return (mg)	Cum Mass Return (%)
MT~20/ml/hr (OMTHP)	11.50	467.06	467.06	89.65	**53.91**	10.35		
PF~20ml/hr (NFFW)	79.71	8.39	475.45	91.26	45.52	8.74	8.39	15.56
PF~10ml/hr (NFFW)	103.20	0.31	475.76	91.32	45.20	8.68	8.70	16.15
PF~5ml/hr (NFFW)	126.34	0.33	476.10	91.39	44.87	8.61	9.04	16.76
PF~5ml/hr (NFFW)	151.33	0.35	476.45	91.45	44.52	8.55	9.39	17.42
PF~2ml/hr (NFFW)	164.26	0.24	476.69	91.50	44.28	8.50	9.63	17.87
AcW #1~20ml/hr (Na+)	233.70	4.91	481.60	92.44	39.37	7.56	14.54	26.97
AcW #2~20ml/hr (Na+)	243.57	0.49	482.09	92.54	38.88	7.46	15.03	27.89
AcW #3~20ml/hr (Na+)	254.12	0.50	482.60	92.63	38.37	7.37	15.54	28.82
AcW #4~20ml/hr (Na+)	265.72	0.55	483.15	92.74	37.82	7.26	16.09	29.84
AcW #5~60ml/hr (Na+)	297.04	0.53	483.67	92.84	37.30	7.16	16.61	30.82
Sand from the column + 250ml of DW		1.03	484.70	93.04	36.27	6.96	17.64	32.73

Table 5.13: Sand Pack C – Summary of mass balance base on total mass throughput and mass after main treatment + 2PV

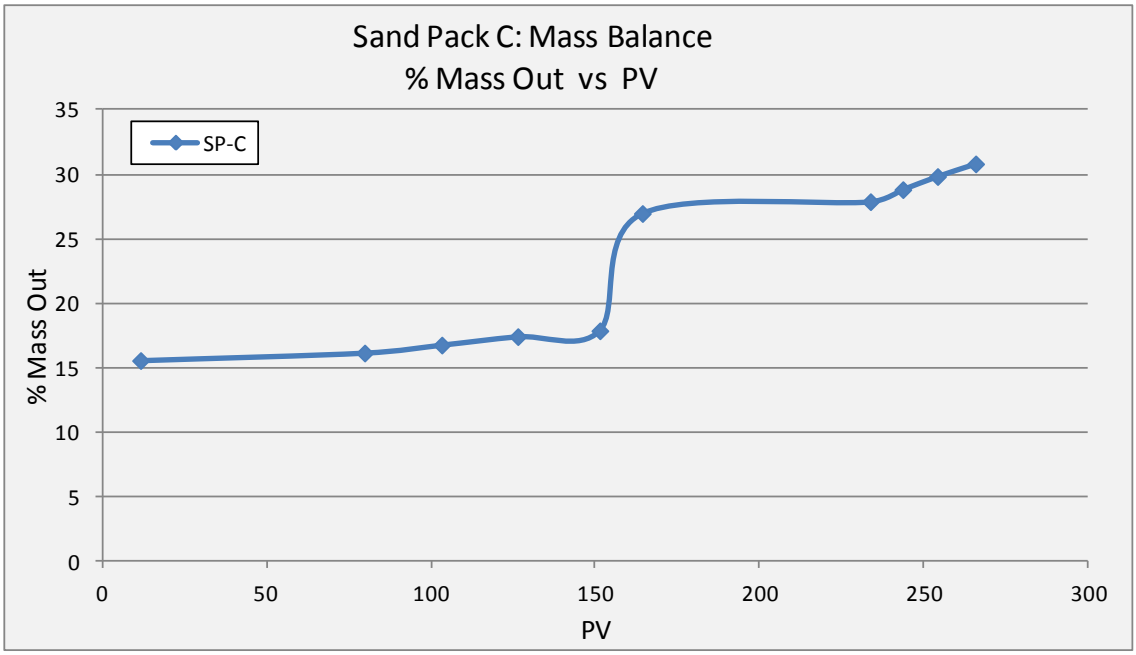

PV	Total Mass Out (mg)	Total Mass Out (%)
9.39	8.39	15.56
81.82	8.70	16.15
103.20	9.04	16.76
126.34	9.39	17.42
151.33	9.63	17.87
164.26	14.54	26.97
233.70	15.03	27.89
243.57	15.54	28.82
254.12	16.09	29.84
265.72	16.61	30.82
297.04		

Figure 5.26: Sand Pack C- Mass balance base on after main treatment + 2PV

Notes: The % mass out is calculated based on mass left in sand pack after the main treatment + the first 2 PV of post flush. The additional 2PV postflush is to remove the "mobile phase" SI concentration (*not* SI adsorbed and precipitated).

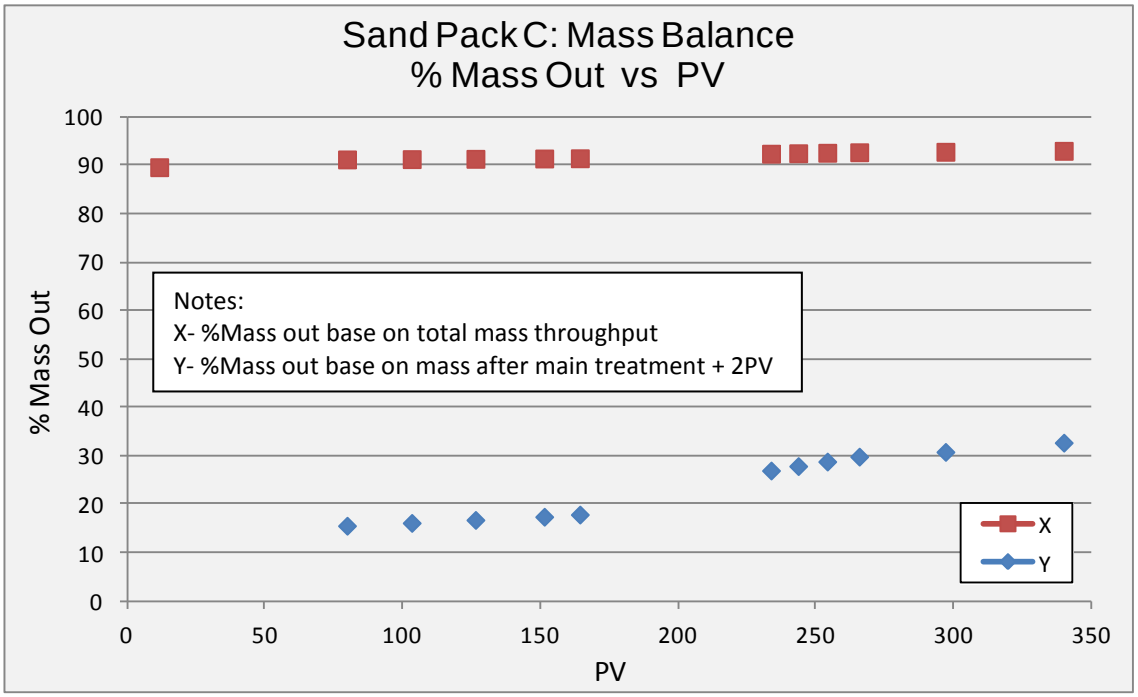

Figure 5.27: Sand Pack C- %Mass out base on total mass throughput and after main treatment + 2PV

5.3.4 Sand Pack D: Dynamic Precipitation Flood – Multi Flow rate and Solubility Effect

Sand Pack D represents a Dynamic Precipitation Flood at various flow rates and it also shows dynamic solubility effects. The main treatment uses 4000ppm OMTHP in NFFW ($+Li^+$) brine at 20 ml/hr flow rate; whereas the post flush uses NFFW brine (no Li^+) and 1% Na^+. The initial post flush is injected at 20ml/hr with NFFW brine (no Li^+). The rest of the post flush uses 1% Na^+ at variable flow rates of 20, 10, 5 and 2 ml/hr. The two different post flush solutions used (i.e. NFFW and 1% Na^+ brine) will define the solubility/desorption in the postflush period. The NFFW has more total dissolved solids (TDS =91,000ppm) compared to 1% Na^+ which has 10,000ppm. It is expected that Na^+ post flush will dissolve more precipitated SI since it contains no calcium ions. The main treatment was conducted at room temperature and the pack temperature was increased to 95°C after shut in, and all post flushes were conducted at 95°C. The pH of all fluids injected, which includes main treatment and post flush was adjusted to pH 4. At each

interval from the main treatment to post flush, the flow was stopped and maintained for at least 24 hrs at 95°C. The details and chronologies of the experiment can be found in Table 5.15.

Once the sand pack is prepared, the dead volume and pore volume were measured. The pore volume was measured at 14.73ml at room temperature, which was used for all calculations for this sand pack. Details of the sand pack characterization are presented in Table 5.14.

Sand Pack Characterization Results			
Length of Sandpacking	=	20.4	cm
Diameter	=	1.5	cm
Dead Volume	=	1.24	ml
Pore Volume @ RT	=	14.73	ml
Porosity @ RT	=	40.85	%
Pore Volume @ 95°C	=	11.44	ml
Porosity @95°C	=	31.72	%
Notes :			
1. Pore volume at room temperature is used for all calculations.			

Table 5.14: Sand Pack D – Characterization Results

Upon completing the characterization, NFFW (no Li^+) brine was injected into the sand pack overnight to saturate the system. The purpose of this stage is to remove any impurities present in the sand pack so that adsorption or precipitation are the only reasons for the observed SI behaviour. Following this conditioning stage, the dynamic sand pack experiment was initiated starting with main treatment. Refer to Table 5.15 for experimental details and chronologies of the injection stages.

No.	Description	Conditions	Flow rate (ml/hr)	PV (Total PV)	Volume (ml) (Total Vol)
1	Main Treatment – 4000ppm OMTHP in NFFW (+50ppm Li^+)	T = 20°C pH = 4	20	1–10.6 (10.6)	1-157.5 (157.5)
Shut-in at reservoir temperature (95°C) for 40 hrs.					
2	Post Flush # 1 : NFFW (no Li^+)	T = 95°C pH = 4	20	10.6–84.5 (73.9)	157.5-1249 (1091.5)
Shut-in at reservoir temperature (95°C) for 49 hrs.					
3	Post Flush # 2 : Na^+ (no Li^+)	T = 95°C pH = 4	20	84.5–108.4 (23.9)	1249-1599 (350)
Shut-in at reservoir temperature (95°C) for 22 hrs.					
4	Post Flush # 3 : Na^+ (no Li^+)	T = 95°C pH = 4	10	108.4–129.6 (21.2)	1599-1914 (315)
Shut-in at reservoir temperature (95°C) for 21 hrs.					
5	Post Flush # 4 : Na^+ (no Li^+)	T = 95°C pH = 4	5	129.6–154.9 (25.3)	1914-2284 (370)
Shut-in at reservoir temperature (95°C) for 21 hrs.					
6	Post Flush # 5 : Na^+ (no Li^+)	T = 95°C pH = 4	2	154.9–168.2 (13.3)	2284-2479 (195)
Shut-in at room temperature (20°C) for 4 days 22 hrs. COMPLETED POST FLUSH.					
7	Acid Wash # 1 : 1% Na+	T = 20°C pH = 1	60	168.2–190.4 (22.2)	2479-2809 (330)
Shut-in at room temperature (20°C) for 20 hrs.					
8	Acid Wash # 2 : 1% Na+	T = 20°C pH = 1	45	190.4–207.6 (17.2)	2809-3061 (207)
Shut-in at room temperature (20°C) for 19 hrs.					
9	Acid Wash # 3 : 1% Na+	T = 20°C pH = 1	30	207.6–250.0 (42.4)	3061-3684 (668)
Shut-in at room temperature (20°C) for 25 hrs.					
10	Acid Wash # 4 : 1% Na+	T = 20°C pH = 1	15	250.0–271.3 (21.3)	3684-3999 (315)
Shut-In at room temperature (20°C). COMPLETED.					

Table 5.15: Sand Pack D – Experimental Details and Chronologies of Injection

The effluent profile results for of the main treatment and initial post-flush stages of the flood are shown in Figure 5.28 and Figure 5.29 for Sand Pack D. These figures show the actual and normalized concentrations vs. pore volumes (PV) injected, respectively for each element. The profiles of each component under study, namely, OMTHP SI, calcium (Ca^{2+}), magnesium (Mg^{2+}) and lithium (Li^+) concentrations vs. PV are presented in these figures.

The first 10 PV injected into the pack is the scale inhibitor main treatment using 4000ppm OMTHP in NFFW(+50ppm Li^+) where pH has been adjusted to pH4. The main treatment was carried out at 20 ml/hr at room temperature. As the flow goes

through the first 2 to 4 PV, the OMTHP SI effluent deviates from the lithium curve. Lithium as an inert tracer does not react with the sand mineral. Thus, the deviation between the SI and lithium tracer is a measure of the degree of SI adsorption in the pack. The small drop in calcium and magnesium concentrations in the frontal breakthrough region (Figure 5.28) can also be seen in these figures which indicates that complex formation between SI and calcium and magnesium also occurs during adsorption. From the 4^{th} to 10^{th} PV, all the elements stabilized at their stock concentrations; which indicates all species were fully saturated in the sand pack system.

After the 10 PV of SI injection, the flow is stopped and the sand pack is placed in a water bath. The water bath temperature is increased from room temperature to 95°C. The set-up was left for 40 hours of shut-in in the water bath. Then, the flow is again set at 20 ml/hr (with the system still at 95°C). In this first post flush period, NFFW (no Li^+) at pH 4 was injected and this post flush period was carried out from the 10 PV to 85 PV of injection.

When the flow recommences after the shut-in at 10 PV, a large drop in SI concentration was observed from 4000ppm to 950ppm (C/Co ~ 0.2), which indicates a very high SI retention due to coupled adsorption/precipitation. Similar trends are also observed for calcium and magnesium; where Ca^{2+} is reduced from 1850ppm to 1580ppm (C/Co ~ 0.84) and Mg^{2+} is reduced from 680ppm to 615ppm (C/Co ~ 0.89). The observed behaviour is clear evidence of SI precipitation (and adsorption) onto sand minerals and the corresponding affinity of Ca^{2+} and Mg^{2+} to OMTHP SI in the process. Because of the corresponding bulk static studies reported in Chapter 4, this is known to be precipitation of SI as a calcium/magnesium complex onto sand minerals. Similar behaviour has been seen for this exact system in different studies (Chen and Graham, 2000).

The first postflush was carried out with NFFW (high TDS and high Ca and Mg) and, at the end of this first post flush period (85 PV) as shown in Figure 5.30 the SI concentration dropped to ~0.3ppm and, if the flow continues the concentration will gradually drop from this value. The calcium and magnesium levels are also stabilizing

around 1800 and 1850ppm and 660 and 680ppm (normalized at around C/Co ~ 0.95 for both elements), respectively**.** Figure 5.30 also shows the later stage return profiles of OMTHP precipitation floods at different flow rates and compositions of post flush fluid. The details of the various flooding stages are described in Table 5.15. The following observation can be summarized from the figure.

The flow was shut-in between the first and second post flush periods. It was shut-in for 49 hours at 95°C. Immediately after this shut in, the 2nd post flush was initiated with 1% NaCl brine (no Ca^{2+} and no Mg^{2+}). During this period, the SI concentration went as high as 18.1ppm before decreasing to 8.6ppm and stabilizing. The 2nd post flush period went from 85 PV to 110 PV at a flow rate of 20 ml/hr, similar to the first post flush. The main observation from this behaviour is that the solubility of the precipitated SI is much higher in the fresher 1%NaCl brine than in the NFFW brine. Without any calcium in the post flush the precipitated SI-complex solubility is much higher at which point the level in the return curve is 8.6ppm compared to in the presence Ca^{2+}, where the level was ~0.3ppm. This implies the higher solubility of precipitated SI in the absence of Ca^{2+} ion.

From the second to the fifth post flush periods (see Figure 5.30), 1% Na^{+} is used as the post flush fluid, but at various flow rates. This is done in order to determine if there is any effect of non-equilibrium or kinetic processes by varying the flow rates. While the 1st and 2nd post flush flow was carried out at 20 ml/hr, the 3rd, 4th and 5th used 10, 5 and 2 ml/hr, respectively. At each interval between changing the flow rates, the flow was shut in more than 24 hours at 95°C. It can be observed that the concentration spikes up for all the flow rates depending upon the length of the shut-in, before gradually decreasing to a lower level. The high concentration at each shut-in shows the dissolution of the SI concentration where it reaches (or at least approaches) equilibrium. One very important point to note is that, the lower the flow rate, the higher the SI return concentration (and vice versa). During the shut-in after the various flow rates, dissolution of Ca^{2+} and Mg^{2+} can also be seen increases before going down as the flow rate proceeds, similar to SI behaviour. After the final post flush at 2 ml/hr, the flow is

shut-in and the temperature was reduced from 95°C to room temperature, 20°C. In this flood, it was shut-in for 4 days 22 hours.

Mass balance of SI left in the sand pack and returned during post flush is also calculated. The analysis is conducted to study how much of the original SI mass is returned after the final post flush. Details of the mass balance are presented in Table 5.17. After the main treatment, 87% of the SI mass has been returned. But after the main treatment, the returned SI mass from 1st to 5th post flush is only an additional 3.6%. Total mass returned after the 5th post flush is 90.7%, leaving 9.3% in the sand pack. This shows that there is still SI in the sand pack after the final post flush.

The mass balance results suggested that an acid wash treatment should be carried out in the sand pack using 1% Na^+ at pH=1 in order to try to recover this missing 9.3% of the SI. Figure 5.31 shows the results of the whole injection chronology including the acid wash stages. Table 5.17 shows the mass balance results for the acid wash stages. Four (4) acid wash cycles were carried out at four (4) flow rates, viz. 60, 45, 30 and 15 ml/hr. Only an additional of 1% SI mass is collected after the final 4th acid wash, which accounts for a total of 91.7% of the SI, leaving 8.3% of the original SI still in the sand pack. The influence of flow rate throughout the four (4) acid wash stages was evident and clear non-equilibrium behaviour was observed. As in all floods, the lower the flow rate, the higher the SI returned concentration (and vice versa). Thus, significant quantities of SI remains in the sand pack even after the acid wash.

Finally, the sand in the sand pack was extracted and treated with stirring in 1% Na^+ for 24 hours. Fluid samples were taken and sent for ICP analysis and the sand was sent for ESEM-EDAX analysis to find out if any SI was remaining on the sand surface. Mass balance results show that an additional 1% SI was found in the solution. However, no SI could be detected on the sand. Refer to ESEM-EDAX results, Table 5.16 and Figure 5.32. The mass balance shows that there is still 8% SI mass presence in the sand pack undetected.

<u>Mass Balance base on mass left in sand pack after main treatment + 2PV of post flush:</u>
All of the above mass balance calculation were made base on total mass-in (throughput)

during the main treatment. Here, mass balance is calculated bases on the mass left in sand pack after the main treatment + 2PV of initial post flush to remove any of the mobile phase SI (as discussed above). Thus any mass left in the sand pack is the actual amount of mass that is being absorbed or precipitated. It was found that, the mass left in sand pack at this stage is 82.56mg, which is being used as the total mass. Based on this calculation, only 36% of SI came out of the sand pack, leaving 64% SI mass left in sand pack. These phenomena show irreversible retention of SI (Kerver and Heilhecker, 1969). Detailed mass balances can be found in Table 5.18 and Figure 5.35, and a mass balance comparison can be found in Figure 5.36.

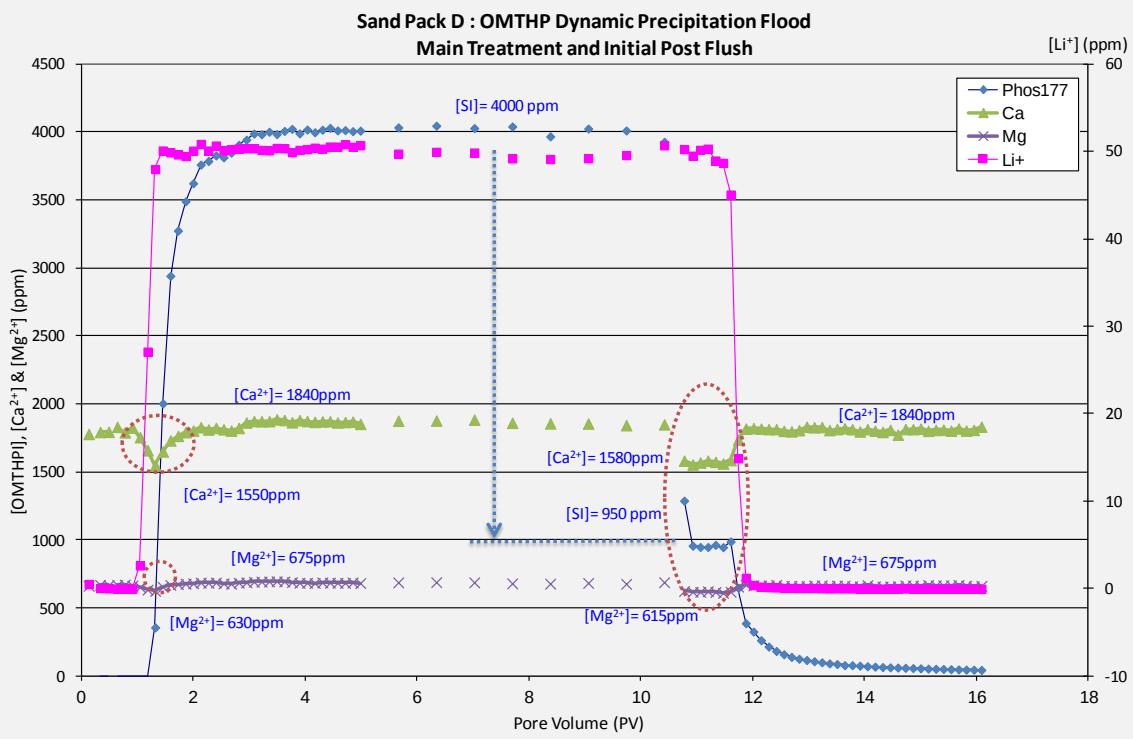

Figure 5.28: Sand Pack D- Main treatment and initial post flush stages.

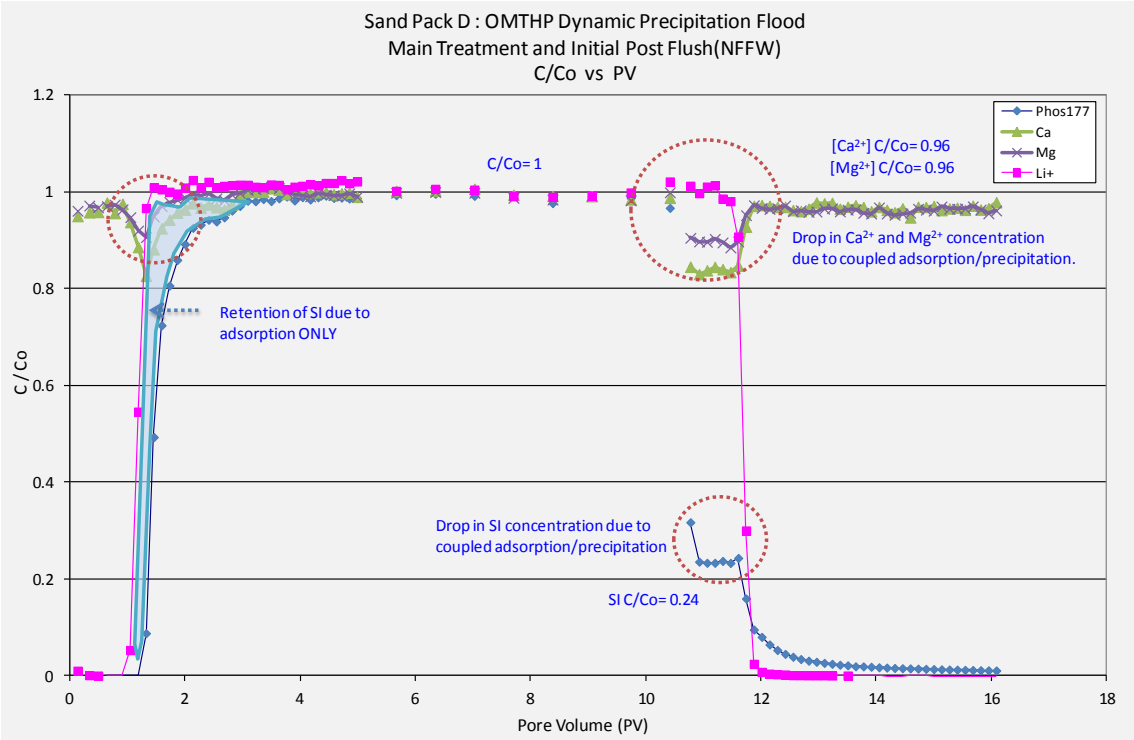

Figure 5.29: Sand Pack D- Main treatment and initial post flush stages. Normalized Concentration vs. PV

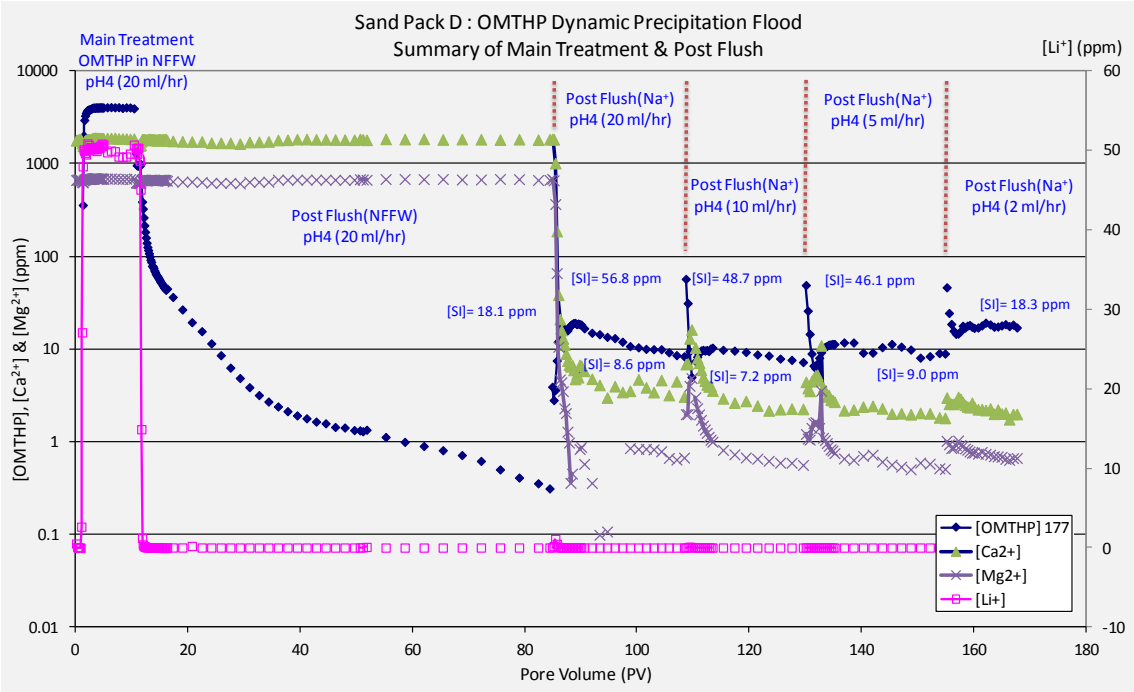

Figure 5.30: Sand Pack D- Main treatment and post flush stages.

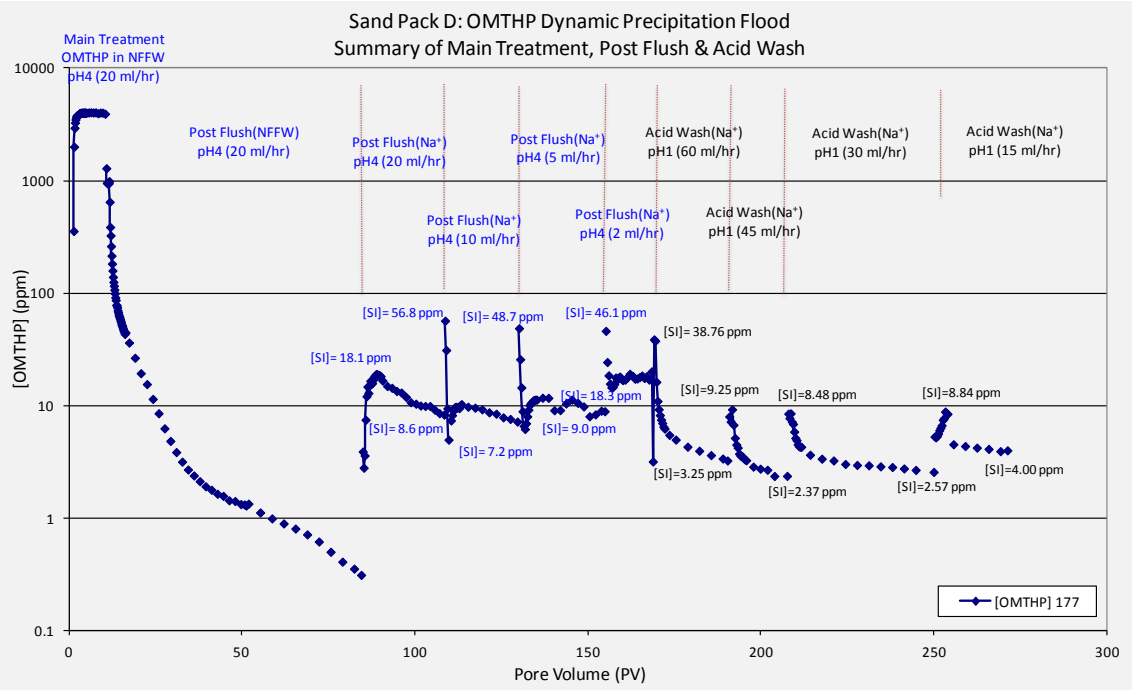

Figure 5.31: Sand Pack D- Main treatment, post flush and acid wash stages.

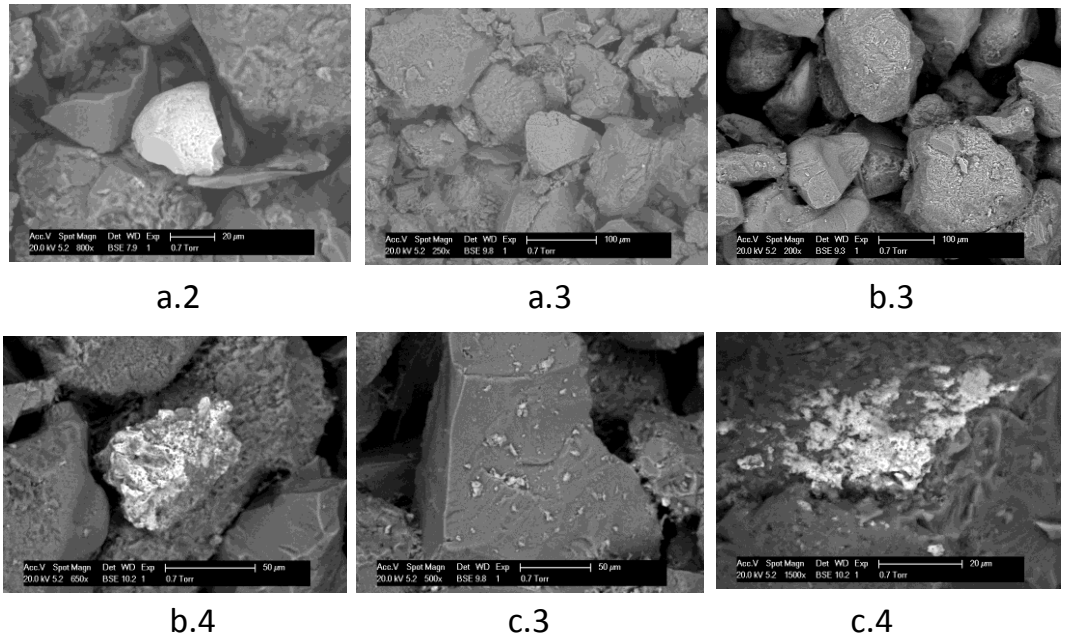

Figure 5.32: Sand Pack D- ESEM picture of sand washed with Na^+ (pH=1) after the experiment.

	a-2		a-3		a-4		b-3		b-4		b-5		c-3		c-4		c-5	
Element	Weight%	Atomic%	Weight%	Atomic%	Weight%	Atomic%	Weight%	Atomic%	Weight%	Atomic%	Weight%	Atomic%	Weight%	Atomic%	Weight%	Atomic%	Weight%	Atomic%
-	-	-	-	-	-	-	-	-	-	-	-	-	-	-	-	-	-	-
O	46.25	73.86	58.29	71.25	58.4	71.27	58.24	70.95	49.74	69.53	47.5	73.37	58.35	71.14	35.76	58.3	49.8	63.65
Na			0.43	0.37	0.59	0.5	1.81	1.54	2.5	2.43	1.24	1.33	2.47	2.1	5.09	5.77	9.28	8.25
Al			1.74	1.26	1.46	1.05	0.67	0.48	0.75	0.63	0.35	0.32	-	-	0.47	0.46	0.53	0.4
Mg	-	-	-	-	-	-	-	-	-	-	-	-	-	-	-	-	-	-
P	-	-	-	-	-	-	-	-	-	-	-	-	-	-	-	-	-	-
Si	17.61	16.02	37.37	26.02	37.78	26.26	37.7	26.16	18.83	14.99	17.17	15.1	36.11	25.08	15.16	14.08	29.37	21.38
Cl	-	-	0.42	0.23	0.61	0.34	1.57	0.86	1.84	1.16	1.52	1.06	3.06	1.68	3.69	2.72	10.76	6.21
K	-	-	1.74	0.87	1.16	0.58			0.21	0.12	-	-	-	-	-	-	-	-
Ca	-	-	-	-	-	-	-	-	-	-	-	-	-	-	-	-	-	-
Sr	-	-	-	-	-	-	-	-	-	-	-	-	-	-	-	-	-	-
Zr	36.14	10.12	-	-	-	-	-	-	-	-	31.7	8.59	-	-	-	-	-	-
Ti	-	-	-	-	-	-	-	-	10.23	4.78	-	-	-	-	-	-	0.26	0.11
Fe	-	-	-	-	-	-	-	-	15.89	6.36	0.53	0.23	-	-	33.89	15.83	-	-
Cr	-	-	-	-	-	-	-	-	-	-	-	-	-	-	3.38	1.7	-	-
Mn	-	-	-	-	-	-	-	-	-	-	-	-	-	-	0.58	0.28	-	-
Ni	-	-	-	-	-	-	-	-	-	-	-	-	-	-	1.97	0.88	-	-
Totals	100		100		100		100		100		100		100		100		100	

Table 5.16: : Sand Pack D: EDAX results of sand washed with Na^{+} (pH=1) after the experiment. No P, Ca^{2+} or Mg^{2+} was seen.

Notes: Sand pack samples after the main treatment, post flush and acid wash. Three samples were sent for analysis.

Sand Pack D: Mass Balance of SI OMTHP

Mass Throughput @ MT =	640.05	mg
Mass Left In Sand Pack (after MT + PF) =	59.62	mg
Mass Left In Sand Pack (after MT+PF+AcW) =	53.19	mg

Description	PV (ml)	Mass Return (mg)	Cum Mass Return (mg)	Cum Mass Return (%)	Mass Left In Sand Pack (mg)	Mass Left In Sand Pack (%)
MT~20/ml/hr (OMTHP)	10.59	538.14	538.14	84.08	101.91	15.92
PF~20ml/hr (NFFW)	84.45	27.35	565.49	88.35	74.56	11.65
PF~20ml/hr (Na^+)	108.42	4.26	569.75	89.02	70.30	10.98
PF~10ml/hr (Na^+)	129.60	3.09	572.84	89.50	67.20	10.50
PF~5ml/hr (Na^+)	154.89	3.94	576.79	90.12	63.26	9.88
PF~2ml/hr (Na^+)	168.23	3.64	580.43	90.68	59.62	9.32
AcW~60ml/hr(Na^+)	190.36	1.99	582.42	91.00	57.63	9.00
AcW~45ml/hr(Na^+)	207.6	0.85	583.27	91.13	56.78	8.87
AcW~30ml/hr(Na^+)	250	2.06	585.33	91.45	54.72	8.55
AcW~15ml/hr(Na^+)	271.32	1.53	586.86	91.69	53.19	8.31
Sand from the column + 250ml of Na^+ (pH=1)		1	587.86	91.85	52.19	8.15

Table 5.17: Sand Pack D- Mass balance base on total mass throughput

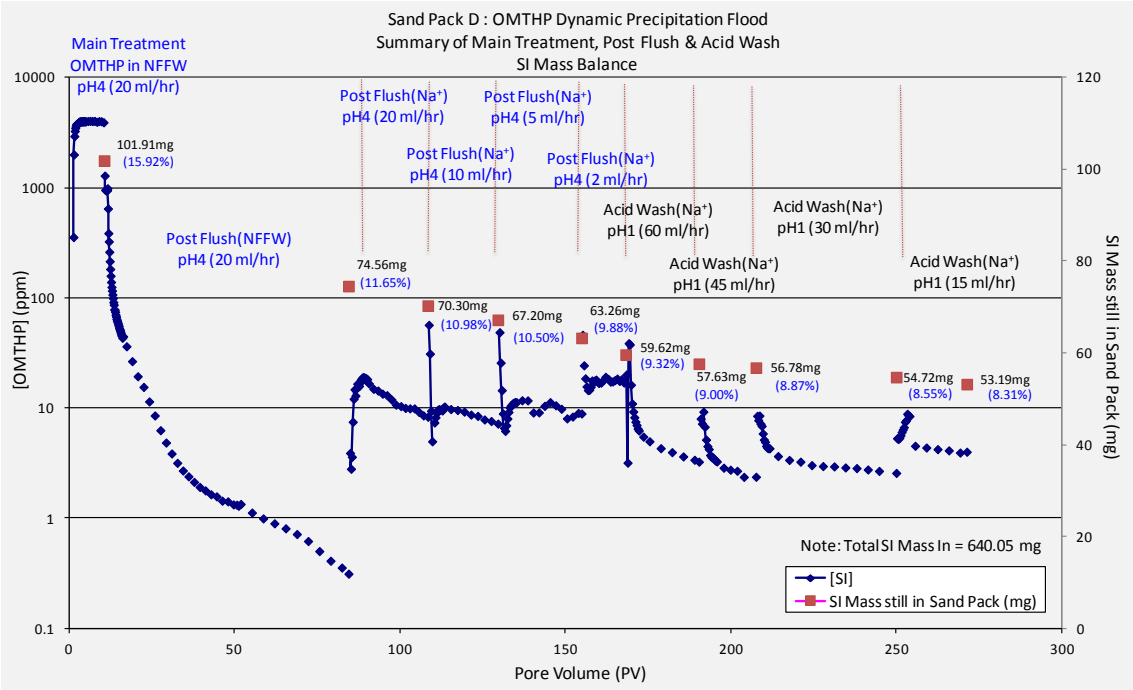

Figure 5.33: Sand Pack D- Mass still in sand pack base on total mass throughput

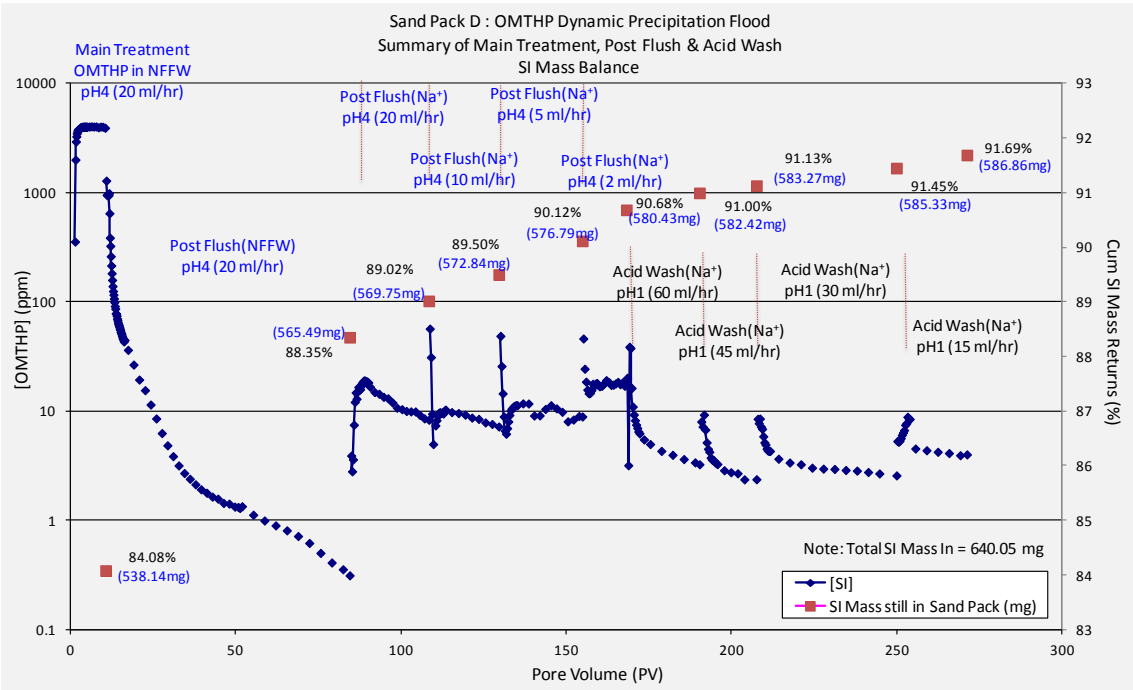

Figure 5.34: Sand Pack D- Cumulative mass out base on total mass throughput

Sand Pack D : Mass Balance of SI OMTHP

Mass In during Main Treatment =	**640.05**	mg
Mass Left In Sand Pack (after MT + PF) =	59.62	mg
Mass Left In Sand Pack (after MT+PF+AcW) =	52.19	mg

Description	PV (ml)	Mass Out (mg)	(X) Cum Mass Return (mg)	(X) Cum Mass Return (%)	Mass Left In Sand Pack (mg)	Mass Left In Sand Pack (%)	(Y) Cum Mass Return (mg)	(Y) Cum Mass Return (%)
MT~20/ml/hr (OMTHP)	12.70	557.49	557.49	87.10	**82.56**	12.90		
PF~20ml/hr (NFFW)	82.35	8.00	565.49	88.35	74.56	11.65	8.00	9.69
PF~20ml/hr (Na+)	108.42	4.26	569.75	89.02	70.29	10.98	12.26	14.86
PF~10ml/hr (Na+)	129.60	3.09	572.85	89.50	67.20	10.50	15.36	18.60
PF~5ml/hr (Na+)	154.89	3.94	576.79	90.12	63.26	9.88	19.30	23.37
PF~2ml/hr (Na+)	168.23	3.64	580.43	90.68	59.62	9.32	22.94	27.78
AcW~60ml/hr(Na+)	190.36	1.99	582.42	91.00	57.63	9.00	24.93	30.19
AcW~45ml/hr(Na+)	207.6	0.85	583.27	91.13	56.78	8.87	25.78	31.22
AcW~30ml/hr(Na+)	250	2.06	585.33	91.45	54.72	8.55	27.84	33.72
AcW~15ml/hr(Na+)	271.32	1.53	586.86	91.69	53.19	8.31	29.37	35.57
Sand from the column + 250ml of Na^+ (pH=1)	290	1	587.86	91.85	52.19	8.15	30.37	36.57

Table 5.18: Sand Pack D- Mass balance base on total mass throughput and mass after main treatment + 2PV

Notes: The % mass out is calculated based on the total mass after the main treatment + first 2 PV of post flush. The additional 2PV is to account for the "mobile phase" SI concentration (*not* SI adsorbed and precipitated).

Mass-In Sand Pack after the main treatment + 2PV of post flush is 82.56 mg.

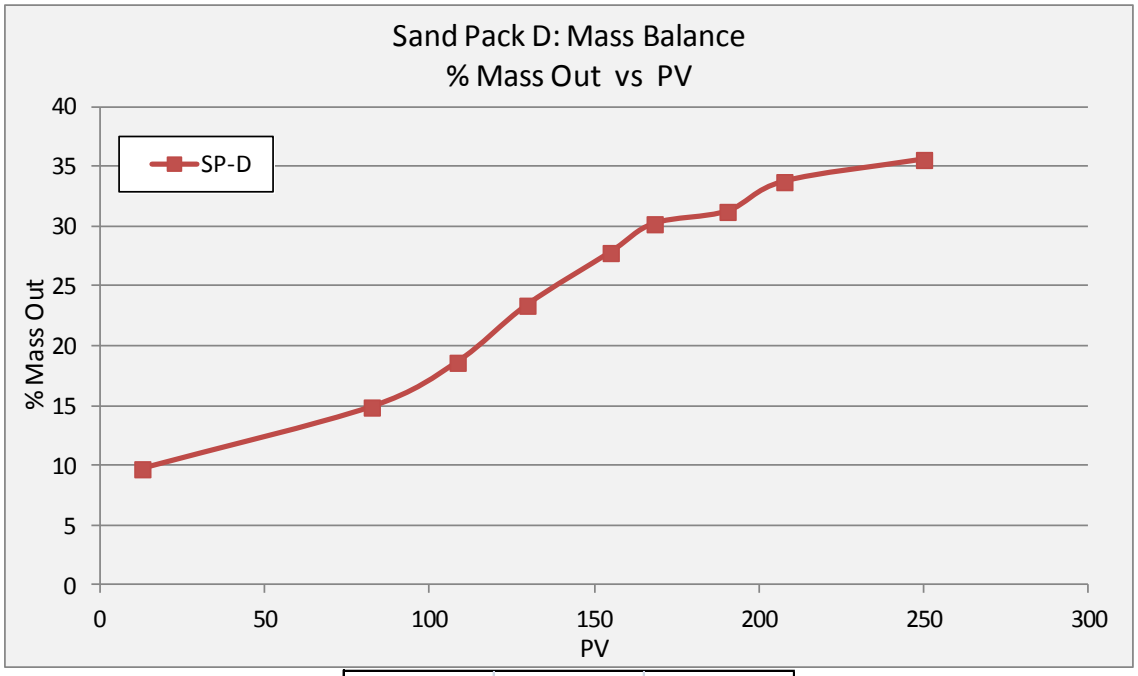

PV	Total Mass Out (mg)	Total Mass Out (%)
10.59	8.00	9.69
84.45	12.26	14.86
108.42	15.36	18.60
129.60	19.30	23.37
154.89	22.94	27.78
168.23	24.93	30.19
190.36	25.78	31.22
207.60	27.84	33.72
250.00	29.37	35.57
271.32		

Figure 5.35: Sand Pack D- Mass balance base on mass after Main Treatment + 2PV

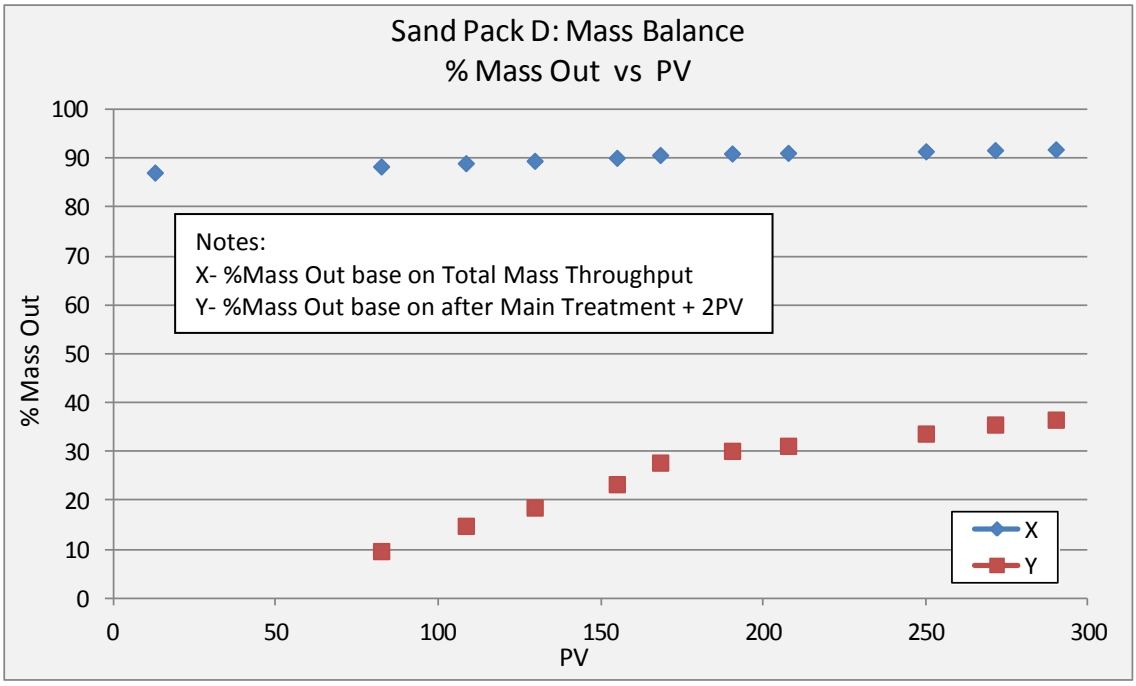

Figure 5.36: Sand Pack D- %Mass out base on total mass throughput and mass after main treatment + 2PV

5.3.5 Sand Pack E: Low Concentration Dynamic Adsorption Flood–Multi Flow Rate

OMTHP Static Compatibility Test designed for Sand Pack E

This static compatibility test was carried out prior to Sand Pack Dynamic Flood E to ensure the flood is actually a purely adsorption flood. The OMTHP static compatibility test conducted previously (see Chapter 4), clearly showed that there was no precipitation at 500ppm OMTHP in NFFW at 95°C after 24hrs. This specific static compatibility test was executed using the SI and NFFW brine prepared for this particular sand pack study. The result assures that we use the same system in both static and dynamic studies.

Figure 5.37 shows the results of phosphorous and Li^+ changes as the OMTHP concentration increases in the static compatibility test. Precipitation is only observed from 800ppm OMTHP and above. From OMTHP static adsorption tests using different

masses of sand (refer to Chapter 4), the result clearly shows that only adsorption is taking place below 800ppm OMTHP; above this concentration then coupled adsorption/precipitation is occurring.

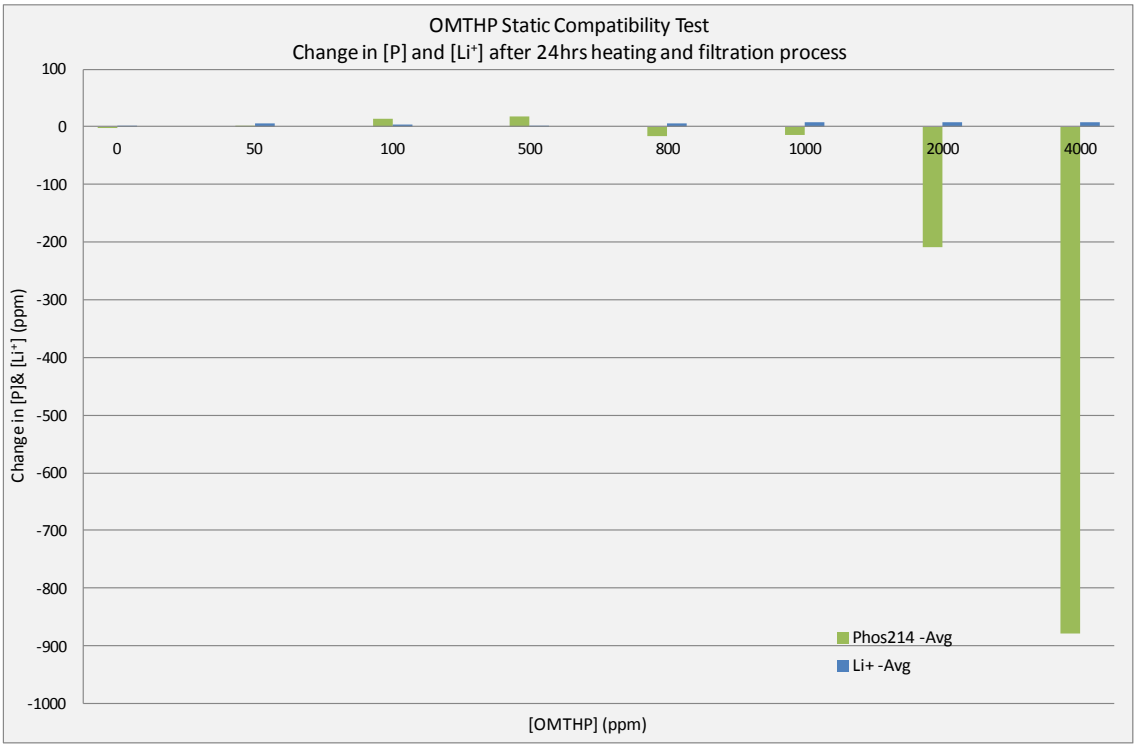

Figure 5.37: OMTHP Static Compatibility Test at 95°C. Change in P and Li^+ ion after 24 hrs at 95°C and pH4

The filtrate was weighted and sent for ESEM-EDAX analysis to see if there was any phosphorus in the precipitate. Figure 5.38 shows that traces of filtrate can be seen from 1000ppm and clear precipitate was observed from 2000ppm. The increase in weight of filtrate can also be seen from 2000ppm onward. Table 5.19 and Figure 5.39 show ESEM-EDAX results. SI can be clearly seen on the filter paper based on ESEM pictures from 800ppm and above, which is shown by the hazy white patches to indicate the presence of phosphorous. Quantitatively, EDAX shows that phosphorous, calcium and magnesium elements can be found consistently above 1000ppm. This evidence with ICP analysis above proves that only adsorption is taking place below 800ppm. This is very important evidence before proceeding to dynamic sand pack study, which shows the main treatment at 500ppm OMTHP at 95°C is a pure ***adsorption*** flood.

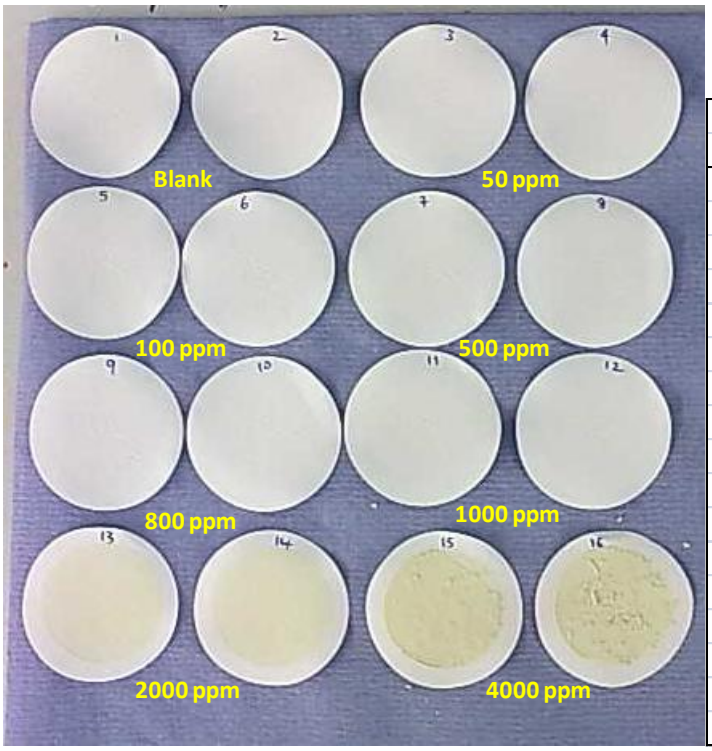

Sample Conc.(ppm)	Filtrate Weight(g)
Blank	0.02
50	0.02
100	0.02
500	0.02
800	0.02
1000	0.02
2000	0.06
4000	0.20

Figure 5.38: OMTHP Static Compatibility Test at 95°C. Filtrate picture and weight of precipitate after filtration.

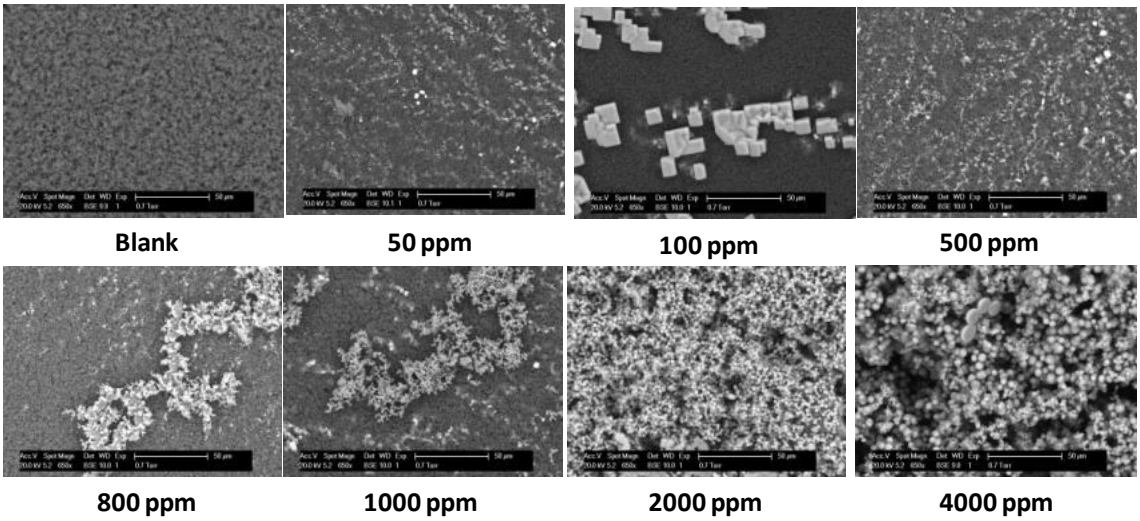

Figure 5.39: OMTHP Static Compatibility Test. ESEM picture of filtrate.

	Blank		50 ppm		100 ppm		500 ppm		800 ppm		1000 ppm		2000 ppm		4000 ppm	
Element	Weight%	Atomic%	Weight%	Atomic%	Weight%	Atomic%	Weight%	Atomic%	Weight%	Atomic%	Weight%	Atomic%	Weight%	Atomic%	Weight%	Atomic%
C	36.62	44.28	33.88	42.52	0	0	33.62	42.74	32.82	41.52	0	0	15.85	24.51	18.8	28.21
O	59.16	53.7	55.08	51.89	51.6	66.33	52.98	50.55	55.57	52.77	67.56	80.11	46.87	54.41	47.53	53.54
Na	1.27	0.8	3.97	2.61	17.97	16.08	4.05	2.69	2.5	1.66	7.58	6.25	1.06	0.86		
Mg									0.45	0.28	0.94	0.73	1.39	1.06	1.15	0.86
P							0.19	0.09	1.99	0.98	3.49	2.14	20.33	12.19	19.92	11.59
Cl	2.95	1.21	6.81	2.89	29.35	17.03	8.79	3.78	5.45	2.34	17.62	9.43	4.1	2.15	2.48	1.26
K					0.34	0.18					0.49	0.24				
Ca			0.26	0.1	0.75	0.39	0.37	0.14	1.21	0.46	2.32	1.1	10.4	4.82	10.11	4.55
Sr					0	0										
Totals	100		100		100		100		100		100		100		100	

Table 5.19: OMTHP Static Compatibility Test. EDAX results of filtrate.

Sand Pack E: Dynamic Adsorption Flood

The sand pack E flood represents a low concentration dynamic adsorption flood at variable flow rates. The main treatment uses 500ppm OMTHP in NFFW ($+Li^+$) brine at 20 ml/hr flow rate; whereas the post flush is carried out using NFFW (no Li^+) brine at flow rates of 20, 10, 5 and 2 ml/hr. The main treatment was conducted at room temperature and all post flushes were conducted at 95°C. All injected fluids were adjusted to pH 4. Between each interval from the main treatment through to the various post flush stages, the flow was stopped and shut in for at least 24 hrs at 95°C.

Once the sand pack is prepared, the dead volume and pore volume were measured. The dead volume and pore volume were measured to be 1.34ml and 14.60ml, respectively. The pore volume was used for all calculations for this sand pack, which is used to track the amount of volume which went through the sand pack. Details of sand pack characterization can be found in Table 5.20.

Sand Pack Characterization Results			
Length of Sandpacking	=	20.4	cm
Diameter	=	1.5	cm
Dead Volume	=	1.34	ml
Pore Volume @ RT	=	14.6	ml
Porosity @ RT	=	40.87	%
Pore Volume @ 95°C	=	12.18	ml
Porosity @95°C	=	33.78	%
Notes :			
1. Pore volume at room temperature is used for all calculations.			

Table 5.20: Sand Pack E – Characterization Results

Once the characterization was completed, NFFW (no Li^+) brine was injected into the sand pack overnight to saturate the system. The purpose of this was to remove any impurities present in the sand pack. After this, the dynamic sand pack experiment was initiated starting with main treatment. Refer to Table 5.21 for experimental details and chronology of the injection stages.

No.	Description	Conditions	Flow rate (ml/hr)	PV (Total PV)	Volume (ml) (Total Vol)
1	Main Treatment – 500ppm OMTHP in NFFW (+50ppm Li^+)	T = 20°C pH = 4	20	1–9.8 (9.8)	0-146 (146)
Shut-in at reservoir temperature (95°C) for 42 hrs.					
2	Post Flush # 1 : NFFW (no Li^+)	T = 95°C pH = 4	20	9.8–109.2 (99.4)	146-1600 (1454)
Shut-in at reservoir temperature (95°C) for 24 hrs.					
3	Post Flush # 2 : NFFW (no Li^+)	T = 95°C pH = 4	10	109.2–141.4 (32.2)	1600-2070 (470)
Shut-in at reservoir temperature (95°C) for 44 hrs.					
4	Post Flush # 3 : NFFW (no Li^+)	T = 95°C pH = 4	5	141.4–167.8 (26.4)	2070-2455 (385)
Shut-in at reservoir temperature (95°C) for 26 hrs.					
5	Post Flush # 4 : NFFW (no Li^+)	T = 95°C pH = 4	2	167.8–184.3 (16.5)	2455-2692 (237)
Shut-in at room temperature (20°C) for 3 days 1 hr. COMPLETED POST FLUSH.					

6	Acid Wash # 1 : 1% Na+	T = 20°C pH = 1	60	184.3–210.1 (25.8)	2692-3070 (378)
Shut-in at room temperature (20°C) for 24 hrs.					
7	Acid Wash # 2 : 1% Na+	T = 20°C pH = 1	45	210.1–257.6 (47.5)	3070-3763 (693)
Shut-in at room temperature (20°C) for 55 hrs.					
8	Acid Wash # 3 : 1% Na+	T = 20°C pH = 1	30	257.6–290.3 (32.7)	3763-4243 (480)
Shut-in at room temperature (20°C) for 24 hrs.					
9	Acid Wash # 4 : 1% Na+	T = 20°C pH = 1	15	290.3–317.7 (27.4)	4243-4643 (400)
Shut-In at room temperature (20°C). COMPLETED.					

Table 5.21: Sand Pack E – Experimental Details and Chronologies of Injection

The main treatment was carried out using 500ppm OMTHP in NFFW ($+Li^+$) at room temperature, at 20 ml/hr. The flow continued for about 10 PV before shutting in the system. At this point, the system was saturated with 500ppm OMTHP. In fact, it normally took only 3 to 4 PV to have the sand pack fully saturated with SI. This behaviour is shown in Figure 5.41 where the normalized SI concentration rises to its stock concentration after ~4PV. The temperature was then increased to 95°C and left for at least 24 hrs. Based on the OMTHP static compatibility/adsorption tests reported above, only adsorption is expected for this system at both room temperature and 95°C. After the 24 hrs shut in, the first post flush with NFFW (no Li^+) brine was initiated at 20 ml/hr and this stage was continued for 110PV to ensure that the effluent concentration reached a suitable low value (<1ppm). The flow was then stopped and left for at least 24 hrs at 95°C after which flow recommenced at 10, 5, 5 and 2 ml/hr. After each flow rate, the flow was stopped for at least 24 hrs at 95°C. Effluents were taken at a set interval at all flow rates, which were analysed by ICP for the various species of interest.

From the concentrations analyzed by ICP, the mass of returned SI was calculated to decide whether further flow is required. If the mass-out does not match the mass-in of the SI, further flow is required. In this case, the results showed there was still mass in the sand pack. This led to carrying out an acidization treatment of the sand pack with Na^+(pH=1) to extract the SI. Details of acidized flow rate and pore volumes are presented in Table 5.21.

The effluent results for the main treatment and first post-flush stages of the OMTHP SI adsorption flood are shown in Figure 5.40 and Figure 5.41 for Sand Pack E. These figures show the actual and normalized concentrations vs. pore volumes (PV) for each component, respectively; viz. OMTHP SI, calcium (Ca^{2+}), magnesium (Mg^{2+}) and lithium (Li^{+}) concentrations vs. PV.

The first 10 PV of injection is the main treatment using 500ppm OMTHP in NFFW (+50ppm Li^{+}) at pH 4 at room temperature, 20°C. At pH4 and 20°C, bulk static compatibility tests shows there is only adsorption under these conditions, and hence this flood in Pack E is purely an ***adsorption*** flood. The main treatment is carried out at 20 ml/hr, at room temperature. After ~4PV of main SI injection, the OMTHP SI effluent profile deviates from the Lithium tracer effluent curve due to SI adsorption (as established in static adsorption/ compatibility tests. A very slight drop in calcium and magnesium concentrations is observed during the first 4 PV in this adsorption flood (Figure 5.40 and Figure 5.41); this is much less than was observed in the corresponding precipitation floods (e.g. see Figure 5.19, Figure 5.20, Figure 5.29 etc). However, all species reach their input concentrations after a few PV of injection indicating that the sand pack is fully saturated with SI at full input concentration.

After 10PV of injection of 500ppm SI, the flow is stopped and the sand pack is placed in a water bath. The water bath temperature is increased from room temperature to 95°C and the system was then left for 42 hours shut-in. After the shut-in, the flow was resumed at 20 ml/hr at 95°C. This is the first post flush period and NFFW with no Li^{+} was injected at pH 4 for 110PV.

When the flow was resumed after the shut-in at 10 PV, a large drop in SI concentration was observed from 500ppm to 50ppm (normalized to C/C0 ~ 0.1), which indicates a very high SI retentions due to increased adsorption at the higher temperature. There is a slight drop in Ca^{2+} and Mg^{2+} observed after the main treatment.

At the end of first post flush period (110 PV) , the SI concentration dropped to around ~0.3ppm and seemed to be stabilizing (see Figure 5.42). This figure also shows the later stage return profiles of OMTHP adsorption flood at various flow rates with the same

post flush fluid. The details of the various stages are described in Table 5.21. The following observation can be summarized from the figure.

The flow was shut-in for 24 hours at 95°C between the first and second post flush periods. Immediately after the start of the second post flush, the SI concentration spiked up before reducing to 0.4ppm and stabilizing. The spike is expected after the shut in of more than 24hrs, during which time it equilibrates in the adsorption/desorption process.

From second to the fourth post flush periods, the same NFFW was used as the post flush brine, but at various flow rates. This was done in order to study if there is any impact due to non-equilibrium or kinetic processes. While the first post flush flow was at 20 ml/hr; the 2^{nd}, 3^{rd} and 4^{th} were carried out at 10, 5 and 2 ml/hr, respectively. At each point between changing the flow rates, the flow was shut in for more than 20 hours at 95°C. It can be observed that the concentration spikes up in all of these shut in periods and, when flow is resumed, the [SI] before gradually decreasing to a lower steady level. Again, it is observed that, the lower the flow rate, the higher the SI flowing concentration (and vice versa) indicating clear non-equilibrium behaviour. After the final post flush at 2 ml/hr, the flow is shut-in and the temperature was reduced from 95°C to room temperature, 20°C. The pack was then shut-in for 3 days 1 hour.

The mass balance of SI left in the sand pack and returned during post flush is also calculated to determine if all the SI mass is returned after the final post flush. Details of the mass balance are presented in Table 5.23. After the main treatment, 74.5% of the SI mass has been returned. But after the main treatment, the returned SI mass from 1^{st} to 4^{th} post flush is only an additional ~1.5%. The total mass returned after the 4^{th} post flush is only 76%, thus leaving 24% of the injected SI still in the sand pack after the final post flush. This SI appears to be irreversibly adsorbed in the sand pack.

The mass balance results led us to carry out an acid wash on the sand pack Using 1% NaCl brine at pH1 to acidize the sand pack. in order to extract any SI left in the system. Figure 5.43 shows the results of the whole injection chronology including the acid wash period.Table 5.23 shows the results of the acid wash mass balance. Four acid washes were executed at four flow rates, i.e. 60, 45, 30 and 15 ml/hr. An additional of 18% SI

mass was collected after the final 4th acid wash, which account to a total of 94%, leaving 6% SI in the sand pack. Figure 5.45 and Figure 5.46 show the %mass still in sand pack and %mass out respectively over all of the flooding cycles.

Finally, the sand in the sand pack was removed and treated with stirring in 1% Na^+ for 24 hours. Fluid samples were taken and sent for ICP analysis and the sand was sent for ESEM-EDAX analysis to determine if SI was present in the sand pack. Referring to Figure 5.44 and Table 5.22, the results show that there is no SI mass on the sand based on ESEM-EDAX analysis. In contrast, base on mass balance analysis there is an additional of ~ 2% SI in the solution. It must be noted that ESEM-EDAX does not detect these elements at very low levels. The mass balance shows that there is still 4% of the SI mass presence in the sand pack undetected, which indicates irreversible adsorption behaviour (Kerver and Heilhecker, 1969).

Mass Balance base on mass left in sand pack after main treatment + 2PV of post flush:
All the above mass balance calculation were made based on the total mass-in (throughput) during main treatment. Here, mass balance is calculated base on mass left in sand pack after main treatment + 2PV of initial post flush to remove the mobile phase in the sand pack (as discussed above) Thus, the mass left in the sand pack is 17.36mg, which is being used as the total mass. Based on this calculation, 85% of SI came out of the sand pack, leaving 15% SI mass left in the system. These results indicate that irreversible adsorption of SI is occurring. A detailed mass balance can be found in Table 5.24 and Figure 5.47. Comparison between the two methods for calculating %mass out is shown in Figure 5.48.

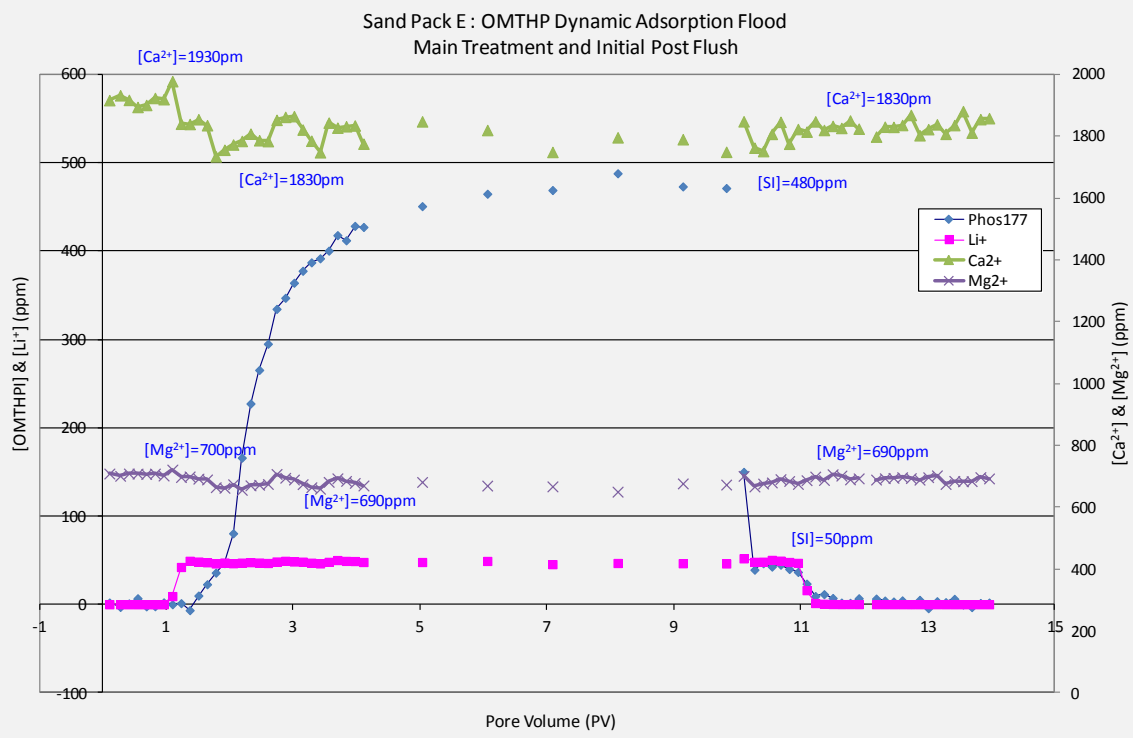

Figure 5.40: Sand Pack E- Main treatment and initial post flush stage.

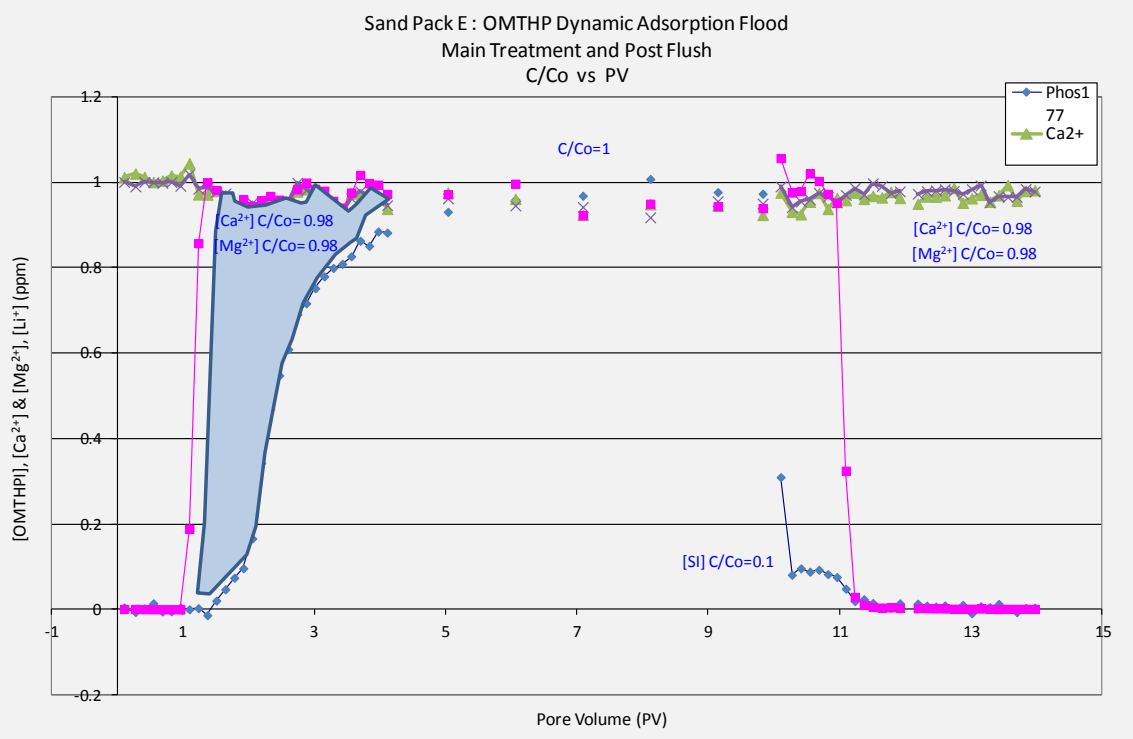

Figure 5.41: Sand Pack E- Main treatment and initial post flush stage. Normalized concentration vs. PV

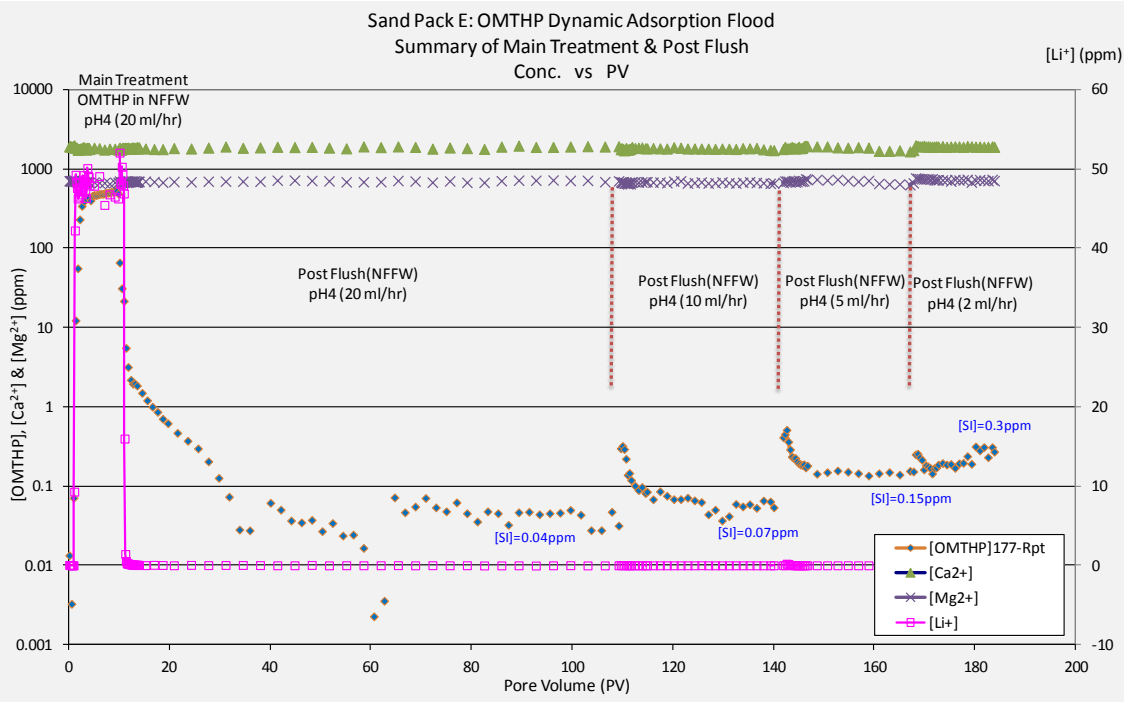

Figure 5.42: Sand Pack E- Main treatment and post flush stages.

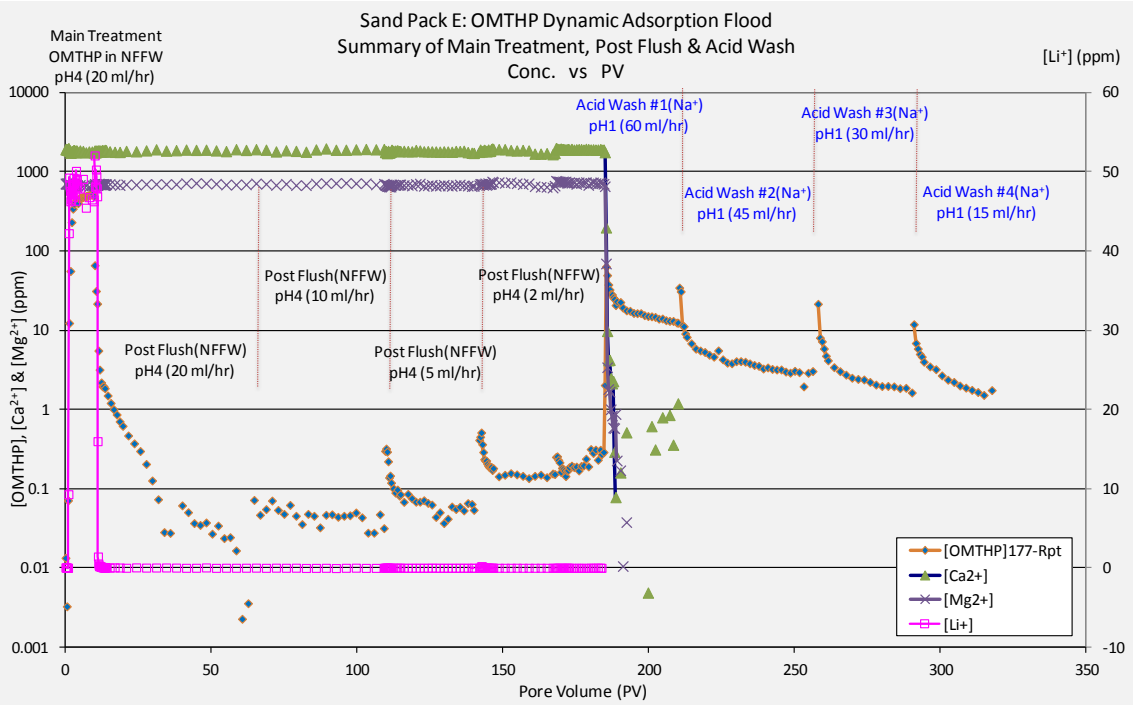

Figure 5.43: Sand Pack E- Main treatment, post flush and acid wash stages.

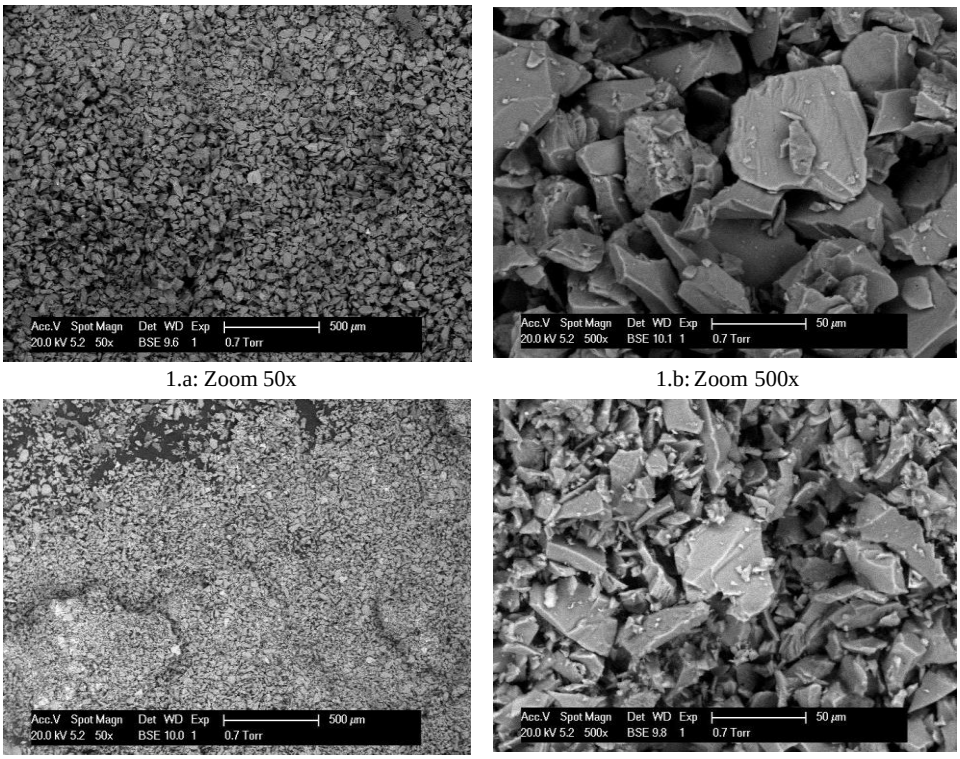

1.a: Zoom 50x 1.b: Zoom 500x

2.a: Zoom 50x 2.b: Zoom 500x

Figure 5.44: Sand Pack E- ESEM picture of sand washed with Na^+ (pH=1) after the experiment. The picture indicates no precipitation of SI

Element	Weight%	Atomic%
O	58.43	71.36
Na	0.56	0.47
Al	1.18	0.86
Si	37.69	26.22
S	0	0
Cl	0.37	0.2
K	1.77	0.88
Totals	100	99.99

Sample 1.b

Element	Weight%	Atomic%
O	57.56	70.59
Al	1.5	1.09
Si	39.49	27.59
K	1.46	0.73
Totals	100	100

Sample 2.b

Table 5.22: Sand Pack E: EDAX results of sand washed with Na^+ (pH=1) after the experiment. No presence of P, Ca^{2+} or Mg^{2+} was seen.

Notes: Sand pack samples after the main treatment, post flush and acid wash. The sand samples are repeated twice. No phosphorous, calcium and magnesium in the sand sample was found after acidized with Na^+ (pH=1).

Sand Pack E: Mass Balance of SI OMTHP

Mass Througput @ MT =	70.73	mg
Mass Left In Sand Pack (after MT+PF) =	16.97	mg
Mass Left In Sand Pack (after MT+PF+AcW) =	4.18	mg

Description	PV (ml)	Mass Return (mg)	Cum Mass Return (mg)	Cum Mass Return (%)	Mass Left In Sand Pack (mg)	Mass Left In Sand Pack (%)
MT~20/ml/hr (OMTHP)	9.83	52.67	52.67	74.47	18.06	25.53
PF~20ml/hr (NFFW)	109.25	0.94	53.61	75.79	17.12	24.21
PF~10ml/hr (NFFW)	141.44	0.04	53.64	75.84	17.08	24.16
PF~5ml/hr (NFFW)	167.81	0.07	53.71	75.94	17.02	24.06
PF~2ml/hr (NFFW)	184.28	0.05	53.76	76.01	16.97	23.99
AcW~60ml/hr(Na+)	210.07	6.82	60.58	85.65	10.15	14.35
AcW~45ml/hr(Na+)	257.64	3.31	63.89	90.34	6.83	9.66
AcW~30ml/hr(Na+)	290.27	1.50	65.39	92.46	5.34	7.54
AcW~15ml/hr(Na+)	317.67	1.16	66.54	94.09	4.18	5.91
Sand from the column + 250ml of Na^+ (pH=1).		1.5	68.04	96.21	2.68	3.79

Table 5.23: Sand Pack E- Mass balance base on total mass throughput

Notes: Finally the sand is extracted from the sand packing column, and washed with 250ml of Na+ (pH=1). The solution is stirred for 24 hrs and representative liquid samples were taken for ICP analysis. The ICP measurement indicates ~6 ppm of SI in the extracted brine, which is equivalent to ~1.5 mg of SI.

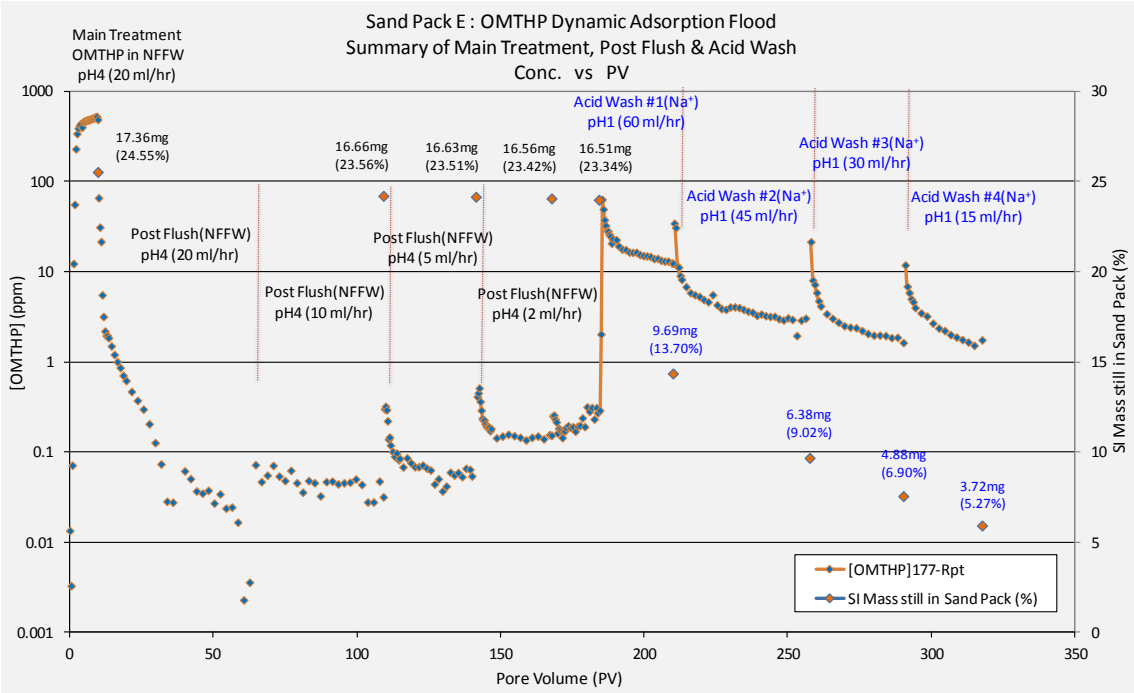

Figure 5.45: Sand Pack E- Mass still in sand pack base on total mass throughput

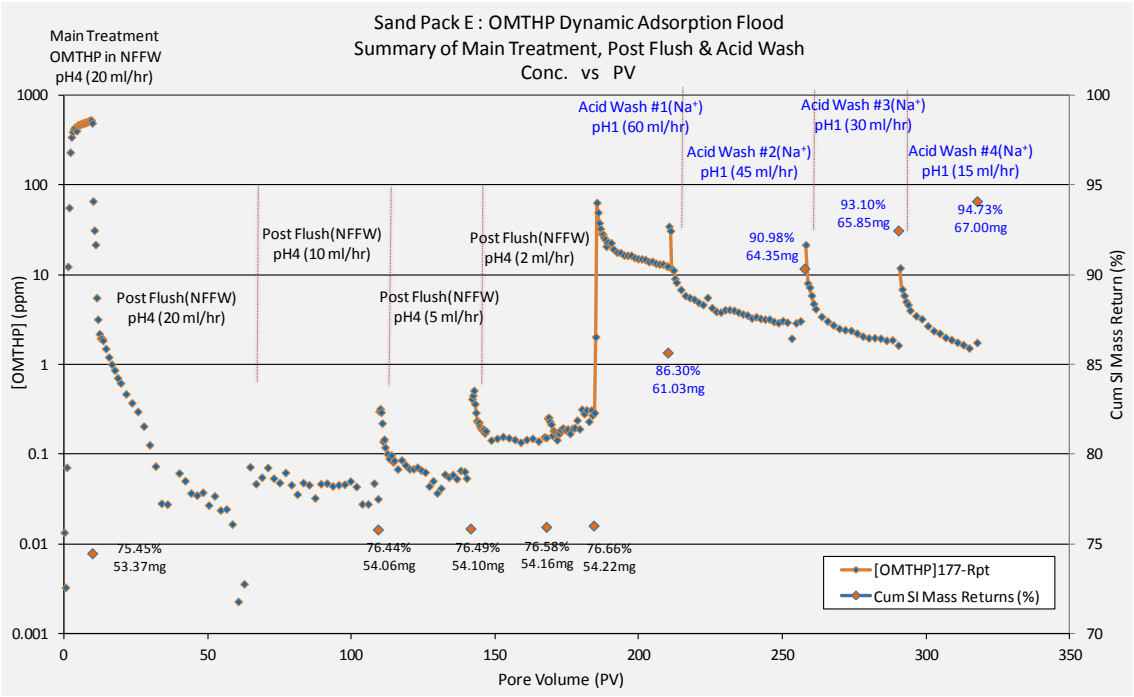

Figure 5.46: Sand Pack E- Cumulative mass out base on total mass throughput

Sand Pack E : Mass Balance of SI OMTHP

Mass In during Main Treatment =	**70.73**	mg
Mass Left In Sand Pack (after MT + PF) =	16.97	mg
Mass Left In Sand Pack (after MT+PF+AcW) =	3.79	mg

Description	PV (ml)	Mass Return (mg)	(X) Cum Mass Return (mg)	(X) Cum Mass Return (%)	Mass Left In Sand Pack (mg)	Mass Left In Sand Pack (%)	(Y) Cum Mass Return (mg)	(Y) Cum Mass Return (%)
MT~20/ml/hr (OMTHP)	11.92	53.37	53.37	75.45	**17.36**	24.55		
PF~20ml/hr (NFFW)	107.16	0.24	53.61	75.79	17.12	24.21	0.24	1.38
PF~10ml/hr (NFFW)	141.44	0.04	53.64	75.84	17.08	24.16	0.28	1.59
PF~5ml/hr (NFFW)	167.81	0.07	53.71	75.94	17.02	24.06	0.34	1.97
PF~2ml/hr (NFFW)	184.28	0.05	53.76	76.01	16.97	23.99	0.39	2.26
AcW~60ml/hr(Na+)	210.07	6.82	60.58	85.65	10.15	14.35	7.21	41.54
AcW~45ml/hr(Na+)	257.64	3.31	63.89	90.34	6.83	9.66	10.52	60.63
AcW~30ml/hr(Na+)	290.27	1.50	65.39	92.46	5.34	7.54	12.02	69.26
AcW~15ml/hr(Na+)	317.67	1.16	66.54	94.09	4.18	5.91	13.18	75.92
Sand from the column + 250ml of Na+ (pH=1).	345	1.5	68.04	96.21	2.68	3.79	14.68	84.56

Table 5.24: Sand Pack E: Summary of Mass Balance base on total mass throughput and mass after Main Treatment + 2PV

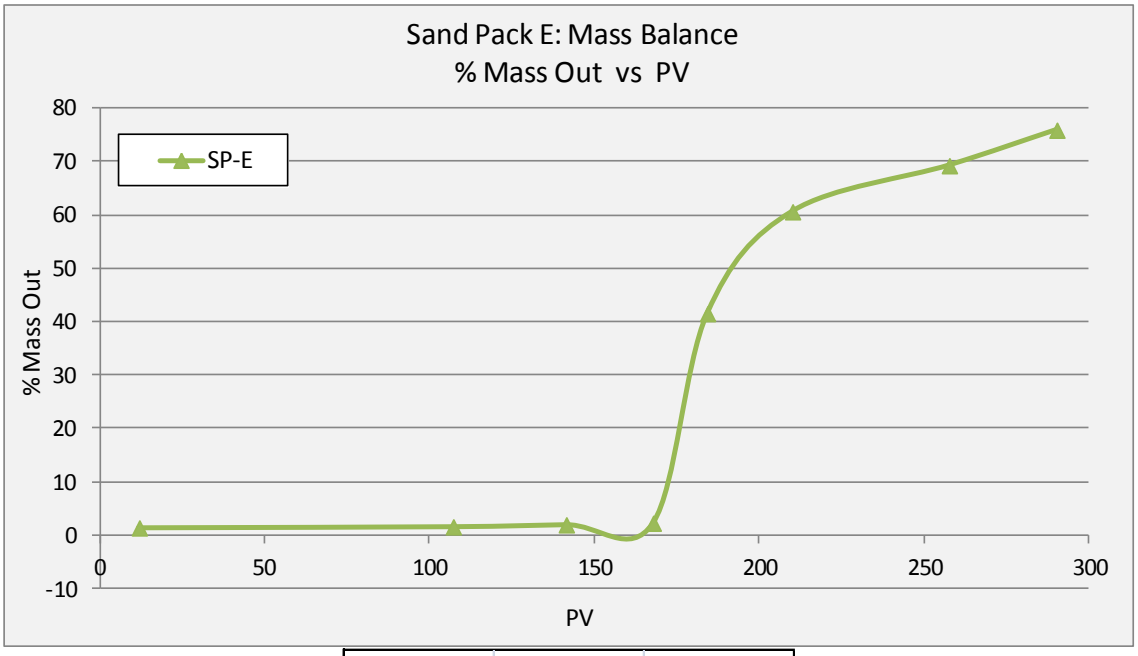

PV	Total Mass Out (mg)	Total Mass Out (%)
9.83	0.70	4.01
109.25	0.73	4.22
141.44	0.80	4.60
167.81	0.85	4.89
184.28	7.67	44.17
210.07	10.98	63.26
257.64	12.48	71.89
290.27	13.64	78.55
317.67		

Figure 5.47: Sand Pack E: Mass balance base on after main treatment + 2PV

Notes: The % mass out is calculated base on total mass after the main treatment + first 2 PV of post flush. The additional 2PV is to account for the "mobile phase" SI concentration (*not* SI adsorbed and precipitated).

Mass-In Sand Pack after the main treatment + 2PV of post flush is 17.36 mg.

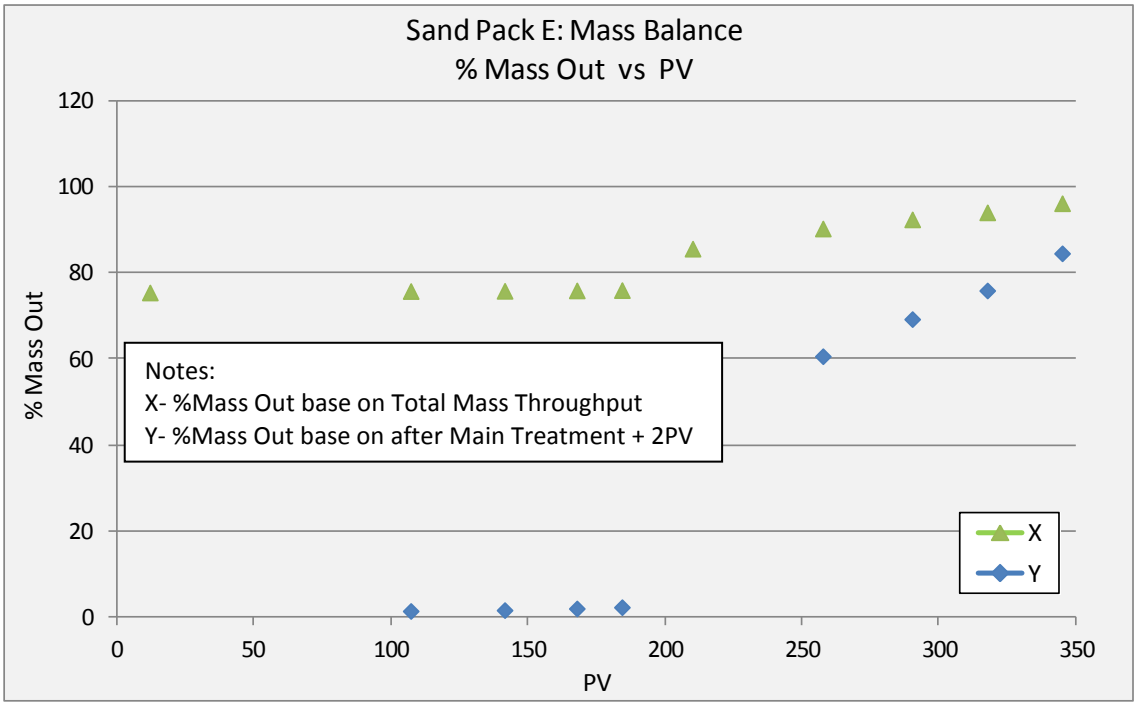

Figure 5.48: Sand Pack E- %Mass out base on total mass throughput and after main treatment + 2PV

5.3.6 Sand Pack F: High Concentration Adsorption Flood – Multi Flow rate

OMTHP Static Compatibility Test designed for Sand Pack F

For this static compatibility test, the NFFW brine has 428ppm Ca^{2+}, compared to the previously used NFFW brine, where the calcium concentration is 2000ppm. The calcium concentration is reduced to ensure that only adsorption is taking place at 4000ppm SI (Kharwad *et al*., 2008). Refer to Table 5.25 for the NFFW composition. To make sure the brine/SI solution used will lead to an adsorption only flood during the dynamic sand pack study, the corresponding static compatibility tests were carried out. This lower calcium (428ppm Ca^{2+}) brine will be used for dynamic study, sand pack F.

Ion	Conc. (ppm)	Comp	Mass g/l	g/5L	g/10L	g/15L	g/20L
Na^+	31275	NaCl	79.50	397.50	795.00	1192.50	1590.01
Ca^{2+}	428	$CaCl_26.H_20$	2.34	11.70	23.39	35.09	46.79
Mg^{2+}	739	$MgCl_2.6H_20$	6.18	30.90	61.80	92.69	123.59
K^+	654	KCl	1.25	6.23	12.47	18.70	24.94
Ba^{2+}	269	$BaCl_2.2H_2O$	0.48	2.39	4.78	7.18	9.57
Sr^{2+}	771	$SrCl_2.6H_2O$	2.35	11.73	23.46	35.19	46.92
SO_4^{-2}	0	Na_2SO_4	0.00	0.00	0.00	0.00	0.00
Li^+	50	LiCl	0.305	1.53	3.05	4.58	6.11
Cl	50000						
		Actual Cl ppm	52497.59				
		If CaCl2.2H2O is used	**1.57**	**7.84**	**15.67**	**23.51**	**31.35**
TDS =	86683.59	ppm					

Table 5.25: Synthetic Nelson Forties Formation Water (NFFW) Composition used for Sand Pack F. Note the changes in Calcium concentration.

Figure 5.49 shows the results for phosphorous, calcium, magnesium and lithium changes at 4000ppm OMTHP after 24hrs at 95°C in static compatibility tests. It is observed that there was no precipitation of any components The slight positive *increase* in the P figure in Figure 5.49 arises from the analytical error which is less than 1%.

Thus, if there were to be any concentration loss during the sand pack study, it must definitely be due to ***adsorption***. Figure 5.50 also shows the filtrate picture and its weight after 24hrs at 95°C. This also shows no precipitate or increase in weight on the filter paper. All this evidence proves that the conditions for dynamic flood F are such that only adsorption will take place.

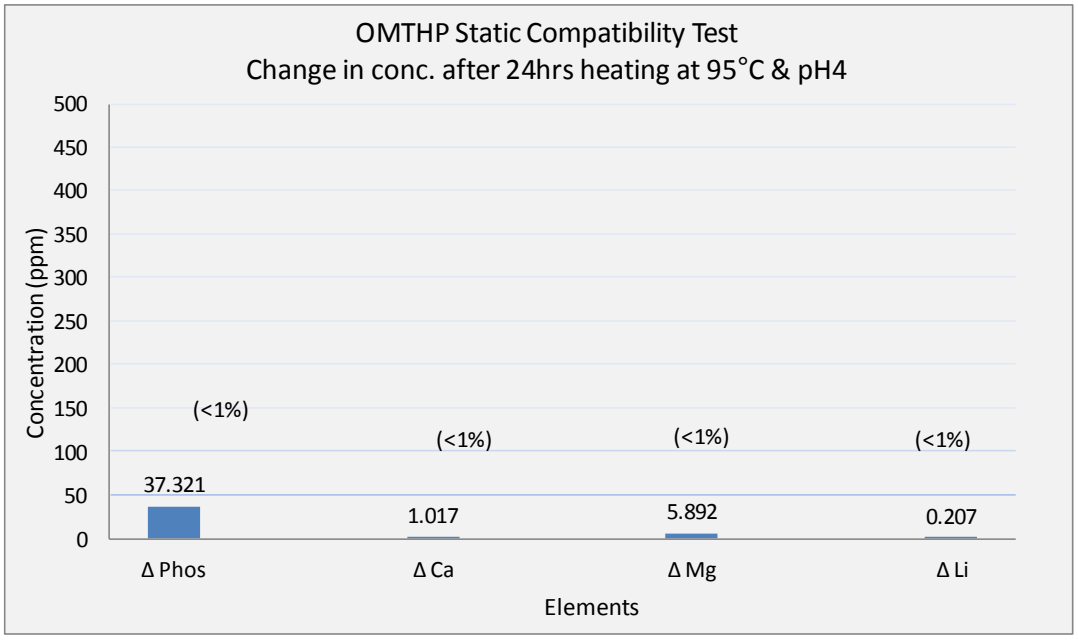

Figure 5.49: OMTHP Static Compatibility Test at 95°C. Change in P, Ca^{2+}, Mg^{2+} and Li^{+} ion after 24 hrs at 95°C and pH4

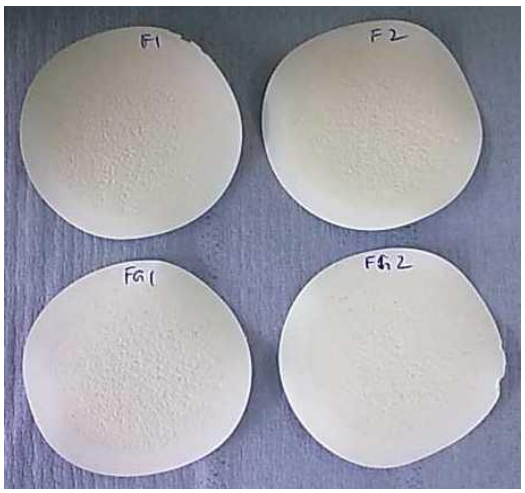

Sample Identification	(Weight (g) Filter Paper (Before)	Filter Paper (After)	Filtrate
F1	0.0908	0.1065	0.02
F2	0.091	0.1067	0.02
FG1	0.0913	0.1097	0.02
FG2	0.0918	0.1154	0.02

Figure 5.50: OMTHP Static Compatibility Test at 95°C. Filtrate picture and weight of precipitate after filtration.

Sand Pack F: Dynamic Flood

Sand Pack F represents a high concentration SI dynamic adsorption flood at variable flow rates. The main treatment uses 4000ppm OMTHP in NFFW ($+Li^+$) brine at 20 ml/hr flow rate; whereas post flush uses NFFW (no Li^+) brine at 20, 10, 5 and 2 ml/hr. The main treatment was conducted at room temperature and all post flushes were conducted at 95°C at pH 4. Between each of the flow periods, from the main treatment to the various post flush stages, the flow was stopped and maintained for at least 24 hrs at 95°C.

Once the sand pack was prepared, the dead volume and pore volume were measured. The dead and pore volume were measured at 1.34ml and 14.66ml, respectively. This pore volume was used for all calculations for this sand pack, presented below. Details of Sand Pack characterization are presented in Table 5.26.

Sand Pack F : Characterization Results		
Length of Sandpacking =	20.7	cm
Diameter =	1.5	cm
Dead Volume =	1.34	ml
Pore Volume @ RT =	14.66	ml
Porosity @ RT =	40.06	%

Table 5.26: Sand Pack F – Characterization Results

Upon completing the characterization, NFFW (no Li+) brine was injected into the sand pack overnight to saturate the system. The purpose of this stage was to remove any impurities present in the sand pack. Immediately, the dynamic sand pack experiment was initiated starting with main treatment. Refer to Table 5.27 for experimental details and the chronology of injection.

No.	Description	Conditions	Flow rate (ml/hr)	PV (Total PV)	Volume (ml) (Total Vol)
1	Main Treatment – 4000ppm OMTHP in NFFW (+50ppm Li^+)	T = 20°C pH = 4	20	1–9.75 (9.75)	0-143 (143)
Shut-in at reservoir temperature (95°C) for 40 hrs.					
2	Post Flush # 1 : NFFW (no Li^+)	T = 95°C pH = 4	20	9.75–108.2 (98.4)	143-1586 (1443)
Shut-in at reservoir temperature (95°C) for 24 hrs.					
3	Post Flush # 2 : NFFW (no Li^+)	T = 95°C pH = 4	10	108.2–141.2 (33.0)	1586-2070 (484)
Shut-in at reservoir temperature (95°C) for 24 hrs.					
4	Post Flush # 3 : NFFW (no Li^+)	T = 95°C pH = 4	5	141.2–173.4 (32.23)	2070-2542 (472)
Shut-in at reservoir temperature (95°C) for 24 hrs.					
5	Post Flush # 4 : NFFW (no Li^+)	T = 95°C pH = 4	2	173.4–219.5 (46.1)	2542-3218 (676)
Shut-in at room temperature (20°C) for 4 days. COMPLETED POST FLUSH.					
6	Sand Wash using 1% Na+	T = 70°C pH = 1	-	-	-
COMPLETED.					

Table 5.27: Sand Pack F – Experimental Details and Chronologies of Injection

The effluent profiles of the main treatment and initial post-flush stages of the OMTHP SI adsorption flood are shown in Figure 5.51 and Figure 5.52 for Sand Pack F. These figures show the actual and normalized (C/Co) concentrations against pore volumes (PV) for each component respectively. The profiles of each component under study, namely, OMTHP SI, Calcium (Ca^{2+}), Magnesium (Mg^{2+}) and Lithium (Li^+) concentrations vs. PV are presented in Figure 5.51 and Figure 5.52.

The first 10 PV of injection in sandpack F is the main treatment using 4000ppm OMTHP in NFFW(+50ppm Li^+; with 428ppm Ca^{2+}) at pH 4 at room temperature, 20°C. As demonstrated above, at pH4 and 20°C, bulk static compatibility tests show that there is only ***adsorption*** of SI onto the sand under these conditions. The main treatment is carried out at 20 ml/hr, at room temperature. As the flow goes through the first 4 PV, the OMTHP SI effluent profile starts deviating from the Lithium effluent curve and this

is a measure of the degree of SI adsorption in the pack. Slight drop in calcium and magnesium concentrations observed during the 1st two PV in this adsorption flood. From the 3th to 10th PV, all the components stabilized at their injected concentrations which indicates no further adsorption or precipitation taking place.

After 10 PV of injection, the flow is stopped and the sand pack is placed in a water bath. The water bath temperature is increased from room temperature to 95°Cand the system was then left for 40 hrs. After this shut-in period, the flow was resumed at 20 ml/hr and 95°C. This is the first post flush using NFFW with no Li^+, at pH 4 which was injected for ~110PV.

When the flow was resumed after the shut-in at 10PV, a large drop in SI concentration was observed from 4000ppm to 1000ppm (normalized, C/Co ~0.25), which indicates a very high SI retentions due to adsorption. There is a slight drop in Ca^{2+} and Mg^{2+} observed after the main treatment (refer to Figure 5.53). The observed behaviour is clear evidence of SI adsorption onto the sand minerals. It also indicates the associated binding between SI and Ca/Mg to form a complex. The affinity of calcium to SI is more apparent compared to magnesium to SI.

At the end of first post flush period (110PV), the SI concentration dropped to around ~0.09ppm (see Figure 5.54). It also shows the later stage return profiles of OMTHP adsorption floods at different flow rates with the same post flush fluid. The details of the various stages are described in Table 5.27. The flow was shut-in for 24 hours at 95°C between the first and second post flush periods. Immediately after the 2nd post flush was initiated, the SI concentration spiked up to ~0.9ppm before reducing to ~0.2ppm and then stabilizing. The spike is expected after shutting in for more than 24hrs, during which time the adsorption/ desorption process equilibrates (or at least approaches equilibrium).

Over the second to the fourth post flush periods, the same NFFW is used as the post flush brine, but at various flow rates. This is to study if there is any impact due to non-equilibrium or kinetic processes. While the 1st post flush flow was at 20 ml/hr; the 2nd, 3rd and 4th were carried out at 10, 5 and 2 ml/hr, respectively. At each interval between

changing the flow rates, the flow was shut in for more than 20 hours at 95°C. In all of these shut in periods, the SI concentration spikes up depending upon the length of the shut-in. The most important observation is the effect of the flow rate on the steady level of [SI] in the pack effluent. The lower the flow rate, the higher the SI flowing concentration (and vice versa) indicating clear non-equilibrium conditions. After the final post flush at 2 ml/hr, the flow is shut-in and the temperature was reduced from 95°C to room temperature, 20°C. The pack was then shut-in for 4 days.

The mass balance of SI left in the sand pack and returned during post flush was also calculated. Details of the mass balance are presented in Table 5.28. After the main treatment, 89% of the SI mass was returned. But after the main treatment, the returned SI mass from 1st to 4th post flush is only an additional ~4%. Total mass returned after the 4th post flush is 93%, leaving 7% of the injected SI mass still in the sand pack after the final post flush.

Finally, the sand was extracted and mixed up in 1% Na^+ (at pH 1) for 24 hrs; this was done rather than acid washing through the sand pack. The purpose is to see if significant SI mass still exists in the sand pack, similar to the observations for previous sand packs. Fluid samples were taken and sent for ICP analysis and sand sent for ESEM-EDAX analysis to determine how much SI was in the original sand pack. Referring to Figure 5.55, the results show that no SI was found on the sand. In contrast, there was an additional of 6mg (1%) of SI in the solution. It must be noted that ESEM-EDAX does not detect these elements at very low concentration levels. The mass balance shows that there is still 6% SI mass presence in the sand pack undetected, which indicates irreversible behaviour (Kerver and Heilhecker, 1969). Refer to Figure 5.56 and Figure 5.57 for the %mass still in sand pack and %mass out throughout the increasing PV.

<u>Mass Balance base on mass left in sand pack after main treatment + 2PV of post flush:</u>
All the above mass balance calculation were made based on total mass-in (throughput) during main treatment. Here, mass balance is calculated based on mass left in sand pack after main treatment + 2PV of initial post flush to allow for the mobile phase in the sand pack. Thus, the mass left in sand pack is the actual amount of mass that is being

absorbed or precipitated. It was found that the mass left in the sand pack was 44.08mg, which was being used as the total mass. Based on this calculation, only 24% of SI came out of the sand pack, leaving 76% SI mass left in the pack. These results show irreversible adsorption of SI. Detailed mass balance can be found in Table 5.28 and Figure 5.58.

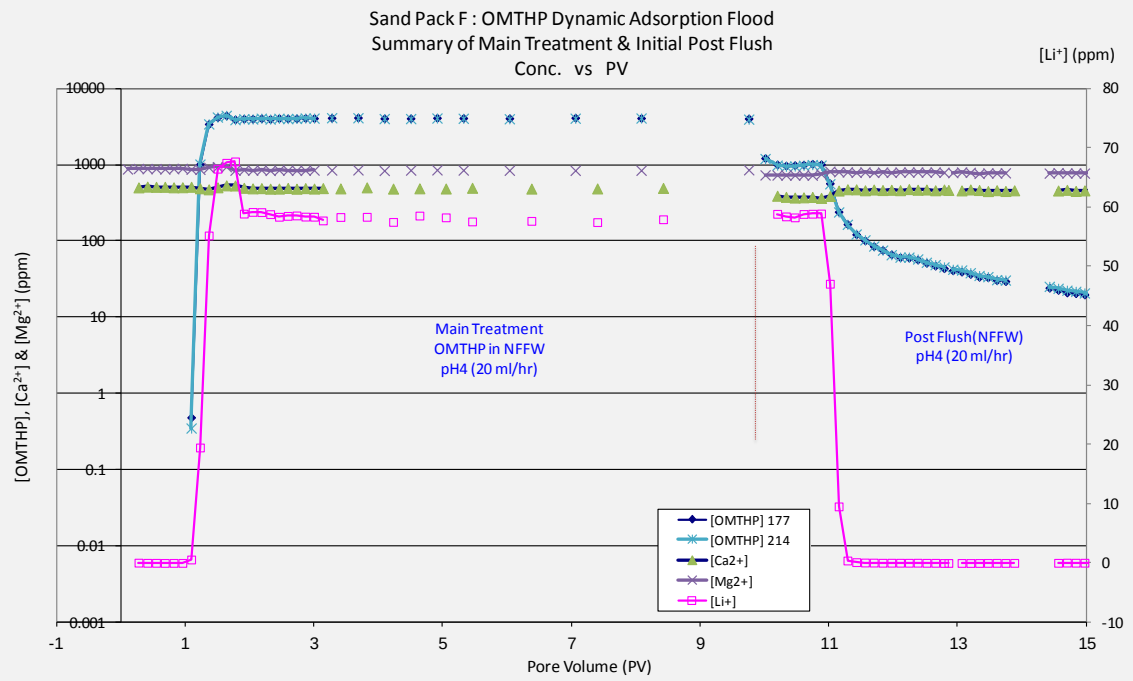

Figure 5.51: Sand Pack F- Main treatment and initial post flush stage.

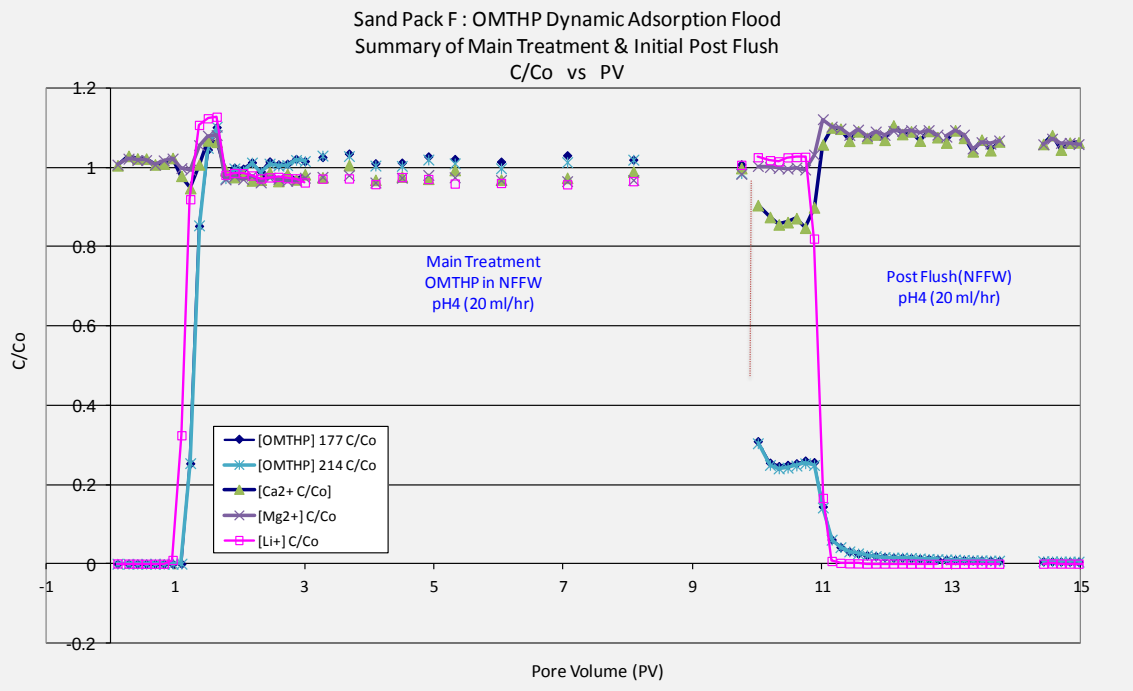

Figure 5.52: Sand Pack F- Main treatment and initial post flush stage. Normalized concentration vs. PV

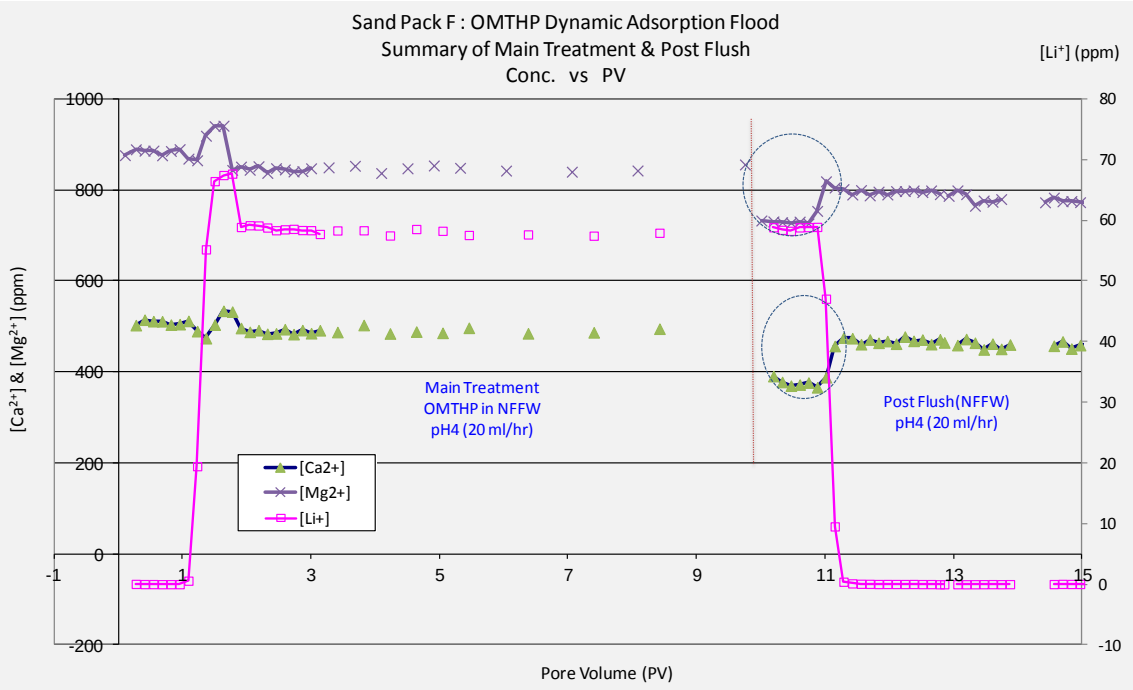

Figure 5.53: Sand Pack F- Main treatment and initial post flush stage. Change in Ca^{2+} and Mg^{2+} ions.

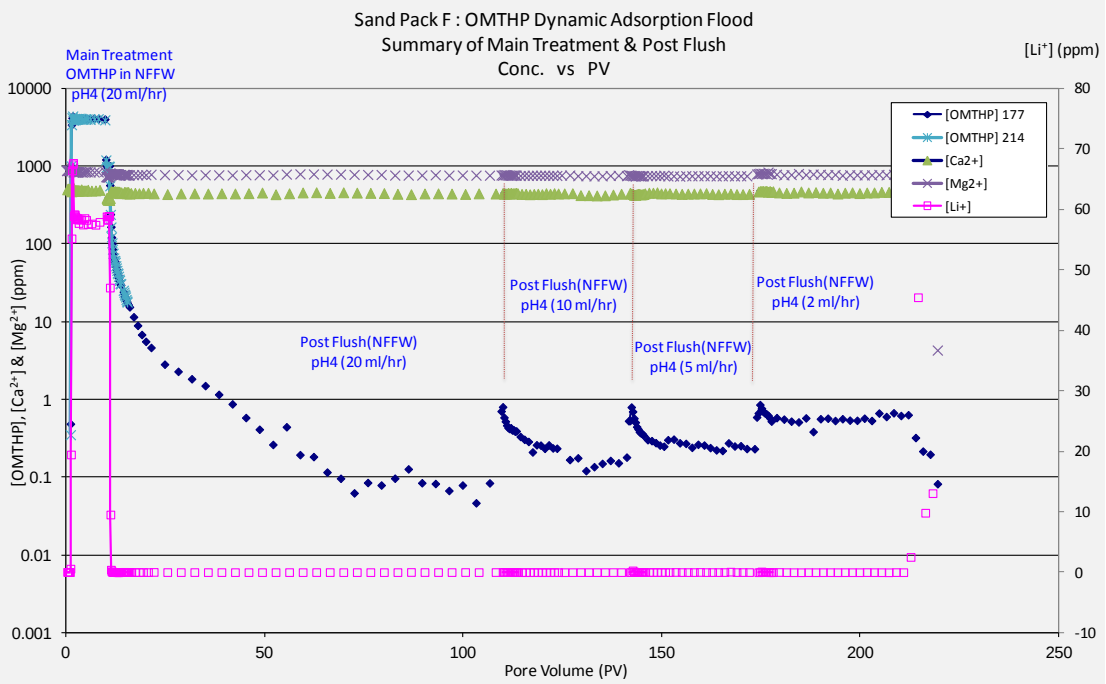

Figure 5.54: Sand Pack F- Main treatment and post flush stages.

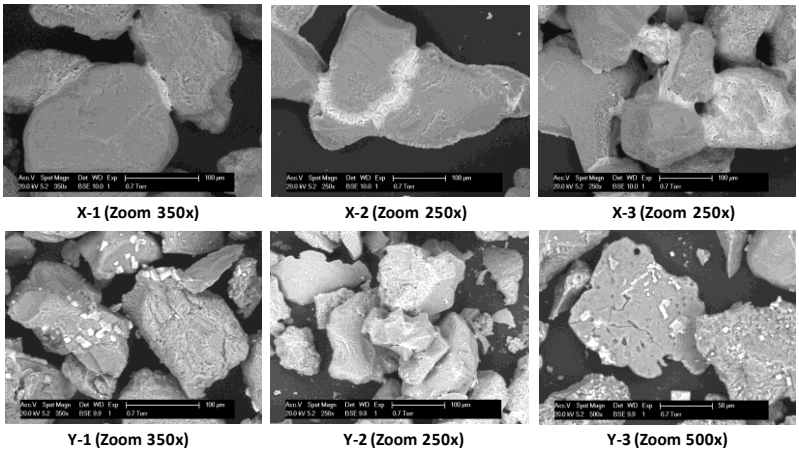

	X-1		X-2		X-3		Y-1		Y-2		Y-3	
Element	Weight%	Atomic%	Weight%	Atomic%	Weight%	Atomic%	Weight%	Atomic%	Weight%	Atomic%	Weight%	Atomic%
C	-	-	23.88	34.54	27.45	38.27	-	-	24.07	33.21	21.38	30.37
O	54.02	67.47	39.51	42.9	41.24	43.16	50.38	64.43	49.21	50.98	47.66	50.83
Na	4.66	4.05	9.44	7.13	5.94	4.33	8.85	7.88	2.05	1.48	2.49	1.85
Al	2.04	1.51	-	-	0.91	0.57	-	-	-	-	3.59	2.27
Si	33.23	23.64	16.55	10.24	17.43	10.39	27.46	20.01	22.75	13.43	21.48	13.05
Cl	4.54	2.56	10.61	5.2	6.17	2.91	13.32	7.69	1.92	0.9	3.39	1.63
K	1.5	0.77	-	-	0.85	0.36	-	-	-	-	-	-
Totals	100		100		100		100		100		100	

Figure 5.55: Sand Pack F- ESEM-EDAX results of sand washed with Na^+ (pH=1) after the experiment. The results indicates no precipitation of SI

Sand Pack F : Mass Balance of SI OMTHP

Mass In during Main Treatment =	572.75	mg
Mass Left In Sand Pack (after MT + PF) =	39.66	mg
Mass Left In Sand Pack (after MT+PF+AcW) =	33.66	mg

Description	PV (ml)	Mass Out (mg)	(X) Cum Mass Return (mg)	(X) Cum Mass Return (%)	Mass Left In Sand Pack (mg)	Mass Left In Sand Pack (%)	(Y) Cum Mass Return (mg)	(Y) Cum Mass Return (%)
MT~20/ml/hr (OMTHP)	11.83	528.67	528.67	92.30	44.08	7.70		
PF~20ml/hr (NFFW)	106.11	3.82	532.49	92.97	40.26	7.03	3.82	8.67
PF~10ml/hr (NFFW)	141.17	0.11	532.60	92.99	40.15	7.01	3.93	8.91
PF~5ml/hr (NFFW)	173.40	0.14	532.73	93.01	40.02	6.99	4.06	9.22
PF~2ml/hr (NFFW)	219.47	0.35	533.09	93.07	39.66	6.93	4.42	10.02
Sand Wash using 250m of Na+ (pH=1)	290	6.00	539.09	94.12	33.66	5.88	10.42	23.63

Table 5.28: Sand Pack F- Mass balance base on total mass throughput

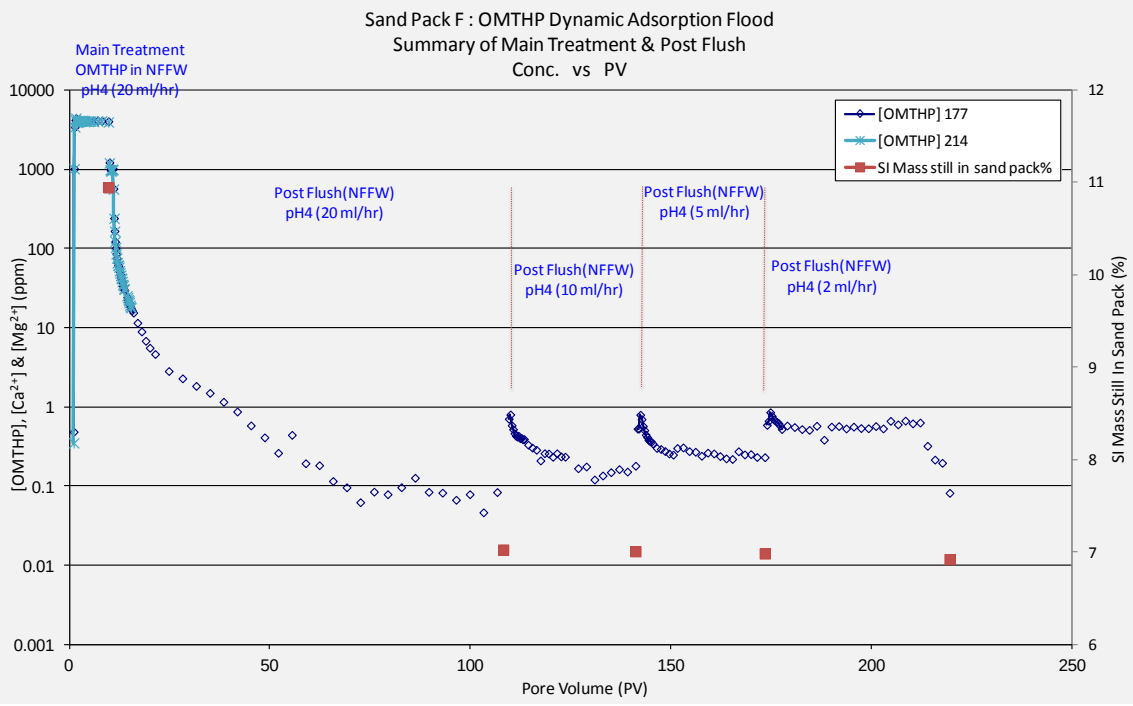

Figure 5.56: Sand Pack F- Mass still in sand pack base on total mass throughput

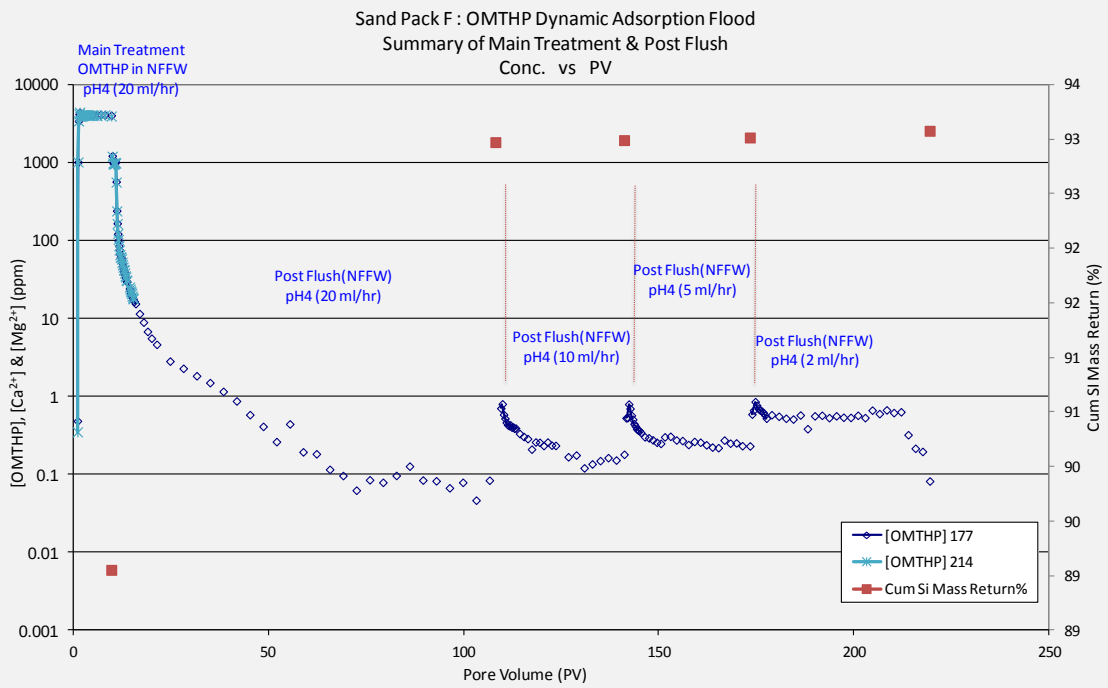

Figure 5.57: Sand Pack F- Cumulative mass out base on total mass throughput

Sand Pack F : Mass Balance of SI OMTHP

Mass In during Main Treatment =	**572.75**	mg
Mass Left In Sand Pack (after MT + PF) =	39.66	mg
Mass Left In Sand Pack (after MT+PF+AcW) =	39.66	mg

			(X)				(Y)	
Description	PV (ml)	Mass Out (mg)	Cum Mass Return (mg)	Cum Mass Return (%)	Mass Left In Sand Pack (mg)	Mass Left In Sand Pack (%)	Cum Mass Return (mg)	Cum Mass Return (%)
MT~20/ml/hr (OMTHP)	11.83	528.67	528.67	92.30	**44.08**	7.70		
PF~20ml/hr (NFFW)	106.11	3.82	532.49	92.97	40.26	7.03	3.82	8.67
PF~10ml/hr (NFFW)	141.17	0.11	532.60	92.99	40.15	7.01	3.93	8.91
PF~5ml/hr (NFFW)	173.40	0.14	532.73	93.01	40.02	6.99	4.06	9.22
PF~2ml/hr (NFFW)	219.47	0.35	533.09	93.07	39.66	6.93	4.42	10.02
Sand Wash using 250m of Na+ (pH=1)	290	6.00	539.09	94.12	33.66	5.88	10.42	23.63

Table 5.29: Sand Pack F- Summary of mass balance base on total mass throughput and mass after main treatment + 2PV

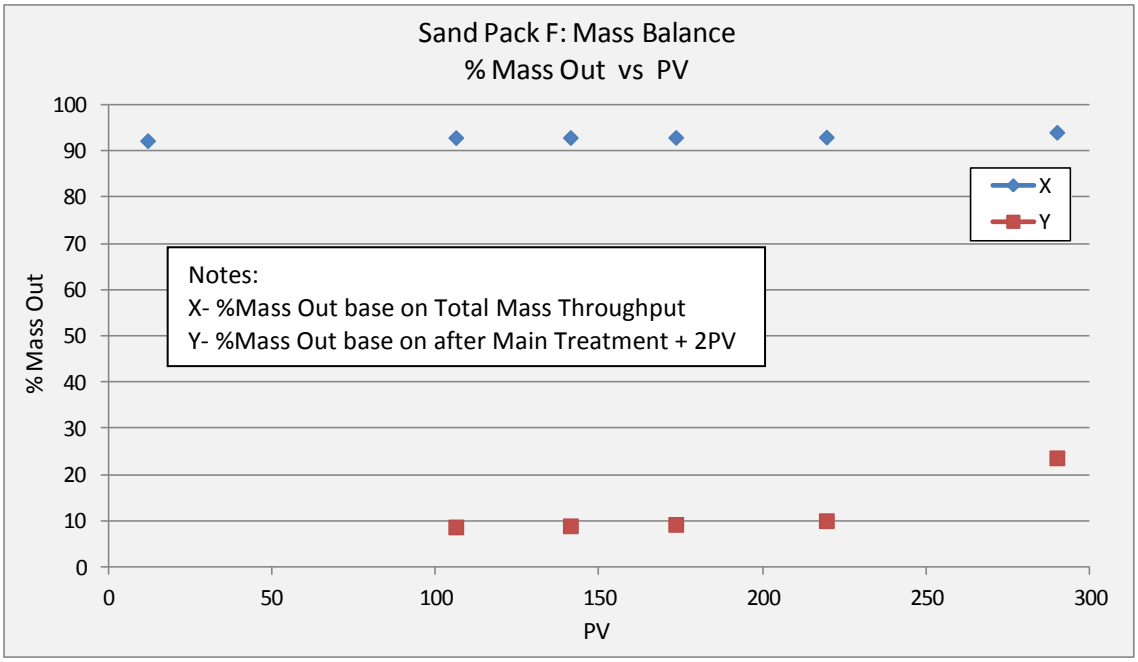

Figure 5.58: Sand Pack F- %Mass out base on total mass throughput and after main treatment + 2PV

5.3.7 Sand Pack G: 2000ppm Concentration Adsorption Flood – Multi Flow rate

OMTHP Static Compatibility Test designed for Sand Pack G

For this static compatibility test, the NFFW brine has 428ppm Ca^{2+}, similar to the brine used for sand pack F, compared to all the previous NFFW brine, where the calcium concentration was 2000ppm. The calcium concentration is reduced to make sure that only adsorption is taking place at 2000ppm SI (Kharwad et al., 2008). Refer to Table 5.25 for the NFFW composition. To make sure the brine used will yield an adsorption flood during the dynamic study, static compatibility test were carried out. This particular brine will be used for dynamic study, sand pack G.

Figure 5.59 shows the observation before and after 24 hrs at 95°C and filtration. The appearance in the bottles shows that there was no precipitate before and after the experiment. Samples from these bottles were taken and sent for ICP analysis to determine if any SI concentration loss had occurred. Figure 5.60 shows the ICP results for phosphorous, calcium, magnesium and lithium change ion concentrations at 2000ppm OMTHP after 24hrs at 95°C in static compatibility tests. No loss in

concentration was observed indicating that no precipitation of any of the elements occurs. The slight increase in the concentration figure in the experiments is due to the analytical tolerance which is less than 1.5%. Thus, if any concentration loss in the sand pack study is observed then it is definitely due to ***adsorption***. Figure 5.61 also shows the observations on the filter paper and its weight after 24hrs at 95°C. These result again show no precipitate or increase in weight on the filter paper. All this evidence proves that no precipitation is taking place at this concentration and conditions which will be used in the sand pack G ***adsorption*** flood presented below.

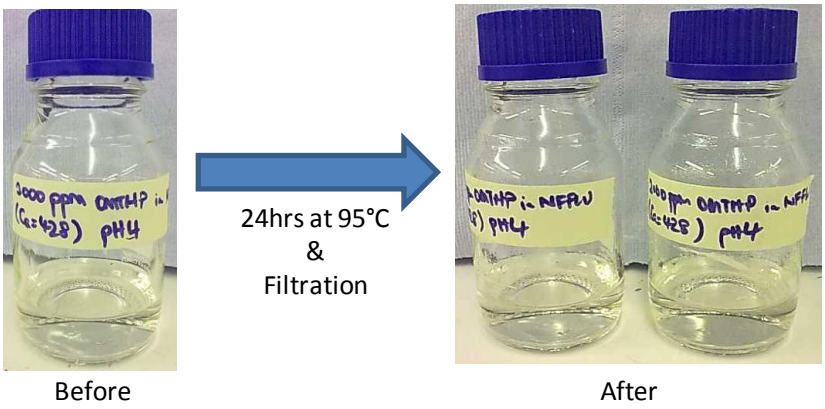

Figure 5.59: 2000ppm OMTHP in NFFW. It shows the observation before and after 24 hrs at 95°C and filtration.

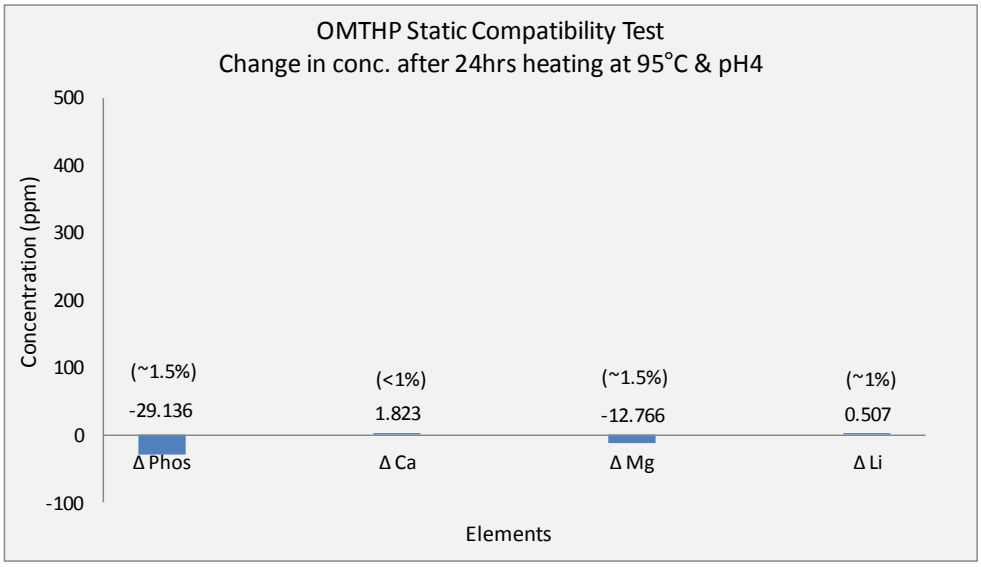

Figure 5.60: OMTHP Static Compatibility Test. Change in P, Ca2+, Mg2+ and Li+ ion after 24 hrs at 95°C and pH4.

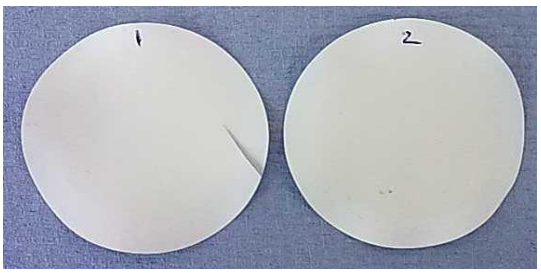

Sample Identification	(Weight (g)		
	Filter Paper (Before) (g)	Filter Paper (After)	Filtrate
1	0.0923	0.1097	0.02
2	0.091	0.1073	0.02

Figure 5.61: OMTHP Static Compatibility Test. Filtrate picture and weight of precipitate after 24 hrs at 95°C and filtration.

The filtrate was sent for ESEM-EDAX analysis to see if there was any phosphorous, calcium and magnesium ions on the precipitate. Figure 5.62 shows that there are no elements observed from the EDAX signal and the ESEM pictures also do not show the presence of phosphorous. All this evidence along with the ICP analysis above, proves that only adsorption is taking place at 2000ppm. This is very important evidence before proceeding to dynamic sand pack study, which shows the main treatment at 2000ppm OMTHP at 95°C is an ***adsorption*** flood.

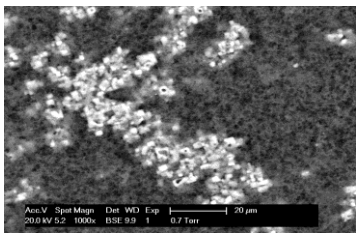

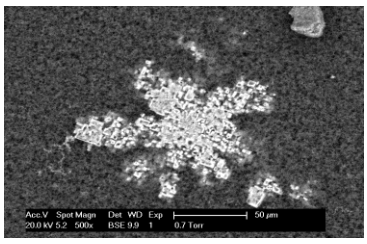

1 (Zoom 1000x) 2 (Zoom 500x)

Element	1		2	
	Weight%	Atomic%	Weight%	Atomic%
C	37.87	48.98	35.34	45.22
O	41.95	40.73	48.09	46.19
Na	6.09	4.12	6.08	4.06
Al				
Si				
Cl	14.08	6.17	10.12	4.39
Ca			0.37	0.14
Totals	100		100	

Figure 5.62: OMTHP Static Compatibility Test. ESEM-EDAX results of filtrate after 24 hrs at 95°C.

Sand Pack G: Dynamic Flood

Sand Pack G represents a medium-high concentration dynamic adsorption flood at multiple flow rates. The main treatment uses 2000ppm OMTHP in NFFW ($+Li^+$) brine at 20 ml/hr flow rate; whereas the post flush uses NFFW (no Li^+; 428ppm Ca^{2+}) brine at 20, 10, 5 and 2 ml/hr. The main treatment was conducted at room temperature and all post flushes were conducted at 95°C at pH 4. Between each flowing period in the postflush, the flow was shut in for at least 24 hrs at 95°C.

Once the sand pack was prepared, the dead volume and pore volume were measured. The dead volume and pore volume were measured at 1.34ml and 14.11ml, respectively. The pore volume was used for all calculations for this sand pack. Details of Sand Pack characterization can be found in Table 5.30.

Sand Pack G : Characterization Results		
Length of Sandpacking =	20.9	cm
Diameter =	1.5	cm
Dead Volume =	1.34	ml
Pore Volume @ RT =	14.11	ml
Porosity @ RT =	38.21	%

Table 5.30: Sand Pack G – Characterization Results

Upon completing the characterization, NFFW (no Li^+; 428ppm Ca^{2+}) was injected into the sand pack overnight to saturate the system. The purpose of this stage was to remove any impurities present in the sand pack. Then, the dynamic sand pack experiment was initiated starting with main treatment, followed by periods of post flushing and acid washes. Refer to Table 5.31 for experimental details and the chronology of injection.

No.	Description	Conditions	Flow rate (ml/hr)	PV (Total PV)	Volume (ml) (Total Vol)
1	Main Treatment – 2000ppm OMTHP in NFFW (+50ppm Li^+)	T = 20°C pH = 4	20	1–10.56 (10.56)	0-153 (153)
Shut-in at reservoir temperature (95°C) for 40 hrs.					
2	Post Flush # 1 : NFFW (no Li^+)	T = 95°C pH = 4	20	10.56–112.5 (101.91)	153-1592 (1439)
Shut-in at reservoir temperature (95°C) for 24 hrs.					
3	Post Flush # 2 : NFFW (no Li^+)	T = 95°C pH = 4	10	112.5–146.3 (33.84)	1592-2067 (475)
Shut-in at reservoir temperature (95°C) for 24 hrs.					
4	Post Flush # 3 : NFFW (no Li^+)	T = 95°C pH = 4	5	146.3–175.6 (29.31)	2067-2483 (416)
Shut-in at reservoir temperature (95°C) for 22 hrs.					
5	Post Flush # 4 : NFFW (no Li^+)	T = 95°C pH = 4	2	175.6–208.7 (33.1)	2483-2947 (464)
Shut-in at room temperature (20°C) for 7 days. COMPLETED POST FLUSH.					
6	Acid Wash # 1 : 1% Na+	T = 20°C pH = 1	40	208.7–211.3 (2.62)	2947-2987 (40)
Shut-in at room temperature (20°C) for 17 hrs.					
7	Acid Wash # 2 : 1% Na+	T = 20°C pH = 1	60	211.3–247.8 (36.43)	2987-3501 (514)
Shut-in at room temperature (20°C) for 17hrs.					
8	Acid Wash # 3 : 1% Na+	T = 20°C pH = 1	20	247.8–276.8 (29.05)	3501-3911 (410)
Shut-in at room temperature (20°C) for 24 hrs.					
9	Acid Wash # 4 : 1% Na+	T = 20°C pH = 1	40	276.8–305.9 (29.06)	3911-4321 (410)
Shut-In at room temperature (20°C). COMPLETED.					

Table 5.31: Sand Pack G – Experimental Details and Chronologies of Injection

The effluent profiles of the main treatment and initial post-flush stages of the OMTHP SI adsorption flood are shown in Figure 5.63 and Figure 5.64 for Sand Pack G. These figures show the actual and normalized (C/Co) concentrations vs. pore volumes (PV) for each element respectively. The profiles of each element under study, namely, OMTHP SI, Calcium (Ca^{2+}), Magnesium (Mg^{2+}) and Lithium (Li^+) concentrations against PV are shown in these figures.

The first ten (10) PV is the main treatment using 2000ppm OMTHP in NFFW (no Li^+; 428ppm Ca^{2+}) at pH 4 at room temperature, 20°C. At pH4 and 20°C, the bulk static compatibility tests presented above show that only SI ***adsorption*** occurs under these conditions; hence this Pack G flood is a pure adsorption flood. The main treatment is carried out at 20 ml/hr, at room temperature. Over the first 4 PV, the OMTHP SI effluent profile deviates from the Lithium effluent curve which is a measure of the degree of (pure) SI adsorption in the pack. The very slight drop in calcium and magnesium concentrations observed during the first four PV in this adsorption flood shows that these elements do complex to some extent with the SI. All elements reach full input concentration well before 5 PV in the main treatment stage of this flood.

After 10 PV, the flow is stopped and the sand pack is placed in a water bath. The water bath temperature is increased from room temperature to 95°C and the set-up was then left for 7 days. After this shut-in period, the flow was resumed at 20 ml/hr and 95°C. This is the first post flush period using NFFW (with no Li^+; 428ppm Ca^{2+}) at pH 4 for ~112PV.

When the flow was resumed after the shut-in at 10PV, a large drop in SI concentration was observed from 2000ppm to 400ppm (normalized C/Co ~0.2), which indicates high SI retentions due to adsorption. There is a slight drop in Ca^{2+} and Mg^{2+} observed after the main treatment (refer to Figure 5.64). At the end of the first post flush period (~112PV) based on Figure 5.65, the SI concentration dropped to around ~0.08ppm and was stabilizing. Figure 5.65 also shows the later stage return profiles of the Pack G OMTHP adsorption floods at various flow rates with the same post flush fluid. The details of the various stages are described in Table 5.31. The flow was shut-in for 24 hours at 95°C between the first and second post flush periods. Immediately after the 2^{nd}, 3^{rd} and 4^{th} post flush was initiated, the SI concentration spiked up before reducing and stabilizing. These spikes are expected after shutting in for more than 24hrs, during which adsorption/ desorption processes reached (or approached) equilibrium .

From the second to fourth post flush periods, the same NFFW was used as the post flush brine, but at various flow rates in order to study non-equilibrium or kinetic processes.

While the 1st post flush flow period was at 20 ml/hr; the 2nd, 3rd and 4th were carried out at 10, 5 and 2 ml/hr, respectively. At each interval between changing the flow rates, the flow was shut in for more than 20 hours at 95°C and the concentration spikes up in all cases depending upon the length of the shut-in. The high concentration at each shut-in shows the adsorption process approaching equilibrium. Due to some discrepancy in the experiment, the data for second and third post flush cycles were not used to analyse to study the kinetic behaviour. But the fourth post flush at 2 ml/hr was analysed to investigate the non-equilibrium behaviour, which stabilise at 0.6ppm. Comparing the effluent concentration at 20 and 2 ml/hr also clearly shows the impact of non-equilibrium behaviour. The lower the flow rate, the higher the SI flowing concentration (and vice versa) as a result of non-equilibrium effects. After the final post flush at 2 ml/hr, the flow is shut-in and the temperature was reduced from 95°C to room temperature, 20°C and the pack was then shut-in for 7 days.

The mass balance of SI left in the sand pack and returned during post flush was also calculated to study if all the SI mass is returned after the final post flush. Details of the mass balance are presented in Table 5.32. After the main treatment, 86% of the SI mass has been returned. But after the main treatment, the returned SI mass from 1st to 4th post flush is only an additional of 2.5% which includes the mobile phase left in the sand pack. Total mass returned after the 4th post flush is 88.8%, leaving 11.2% of the injected SI still in the sand pack after the final post flush.

The mass balance results led us to carry out an acid wash on the sand pack using 1% Na^+ at pH 1. The purpose of the acidization was to extract any SI left in the sand pack. Figure 5.66 shows the results of the whole injection chronology including acid washes. Table 5.32 shows the results of the acid wash mass balances. Four acid washes were carried out at four flow rates, i.e. 40, 60, 20 and 40 ml/hr. An additional of 2.1% SI mass is collected after the final 4th acid wash, which accounts for a total of 91% of the SI being produced from the pack, leaving 9% SI in the sand pack.

Finally, the sand in the sand pack was extracted and stirred in 1% Na^+ for 24 hours. Fluid samples were taken and sent for ICP analysis and the sand was sent for ESEM-

EDAX analysis to determine if SI was present in the sand pack. Referring to Figure 5.67, the results shows that there is no SI mass on the sand based on ESEM-EDAX analysis. In contrast, based on mass balance analysis there is an additional of ~ 1.5% (4.8mg) SI in the solution. It must be noted that ESEM-EDAX does not detect these elements at very low concentration levels. The mass balance shows that there is still 7% SI mass presence in the sand pack undetected, which indicates irreversible adsorption/retention behaviour (Kerver and Heilhecker, 1969).

Mass Balance based on mass left in sand pack after main treatment + 2PV of post flush:
All the above mass balance calculations were made based on total mass-in (throughput) during main treatment. Here, mass balance is calculated based on mass left in sand pack after main treatment + 2PV of initial post flush to take into account of the mobile SI phase in the sand pack. Thus, using this approach the mass left in sand pack is the actual amount of mass that is being absorbed or precipitated. It is found that the mass left in the sand pack is 35mg, which is then used as the total mass. Base on this calculation, only 37% of SI came out of the sand pack, leaving 63% SI mass left in sand pack thus indicating irreversible retention behaviour of SI. Detailed mass balances are presented in Table 5.33. A comparison between the two methods for calculating %mass out is shown in Figure 5.48.

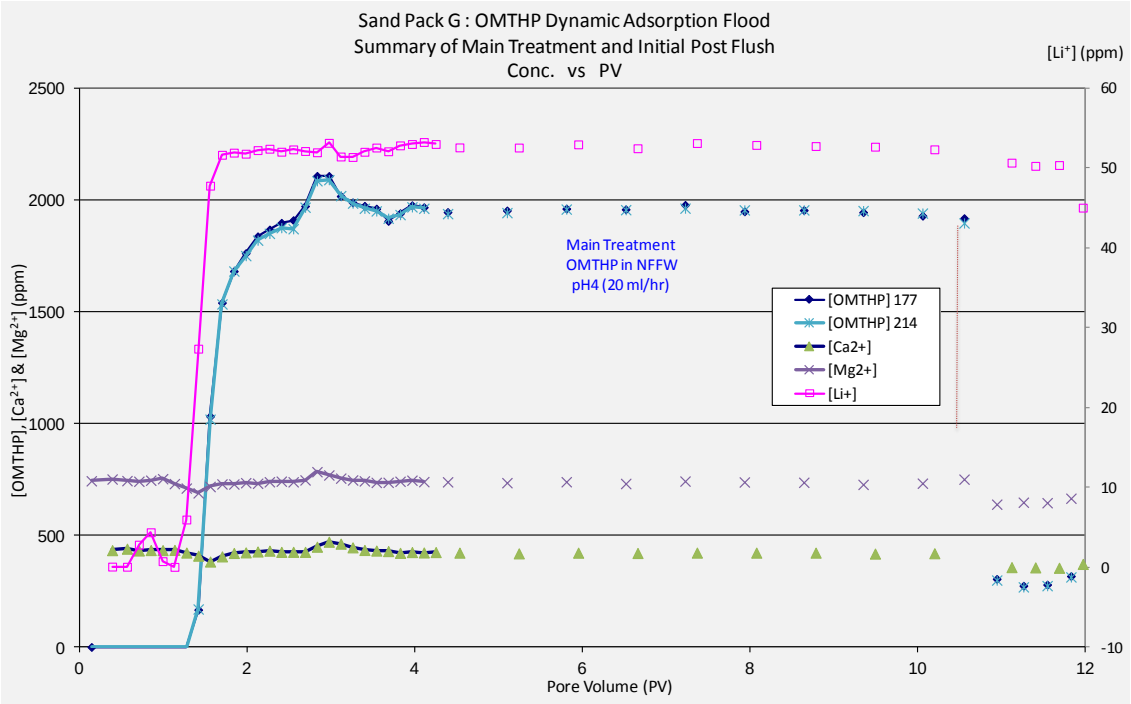

Figure 5.63: Sand Pack G – Main treatment and initial post flush stage.

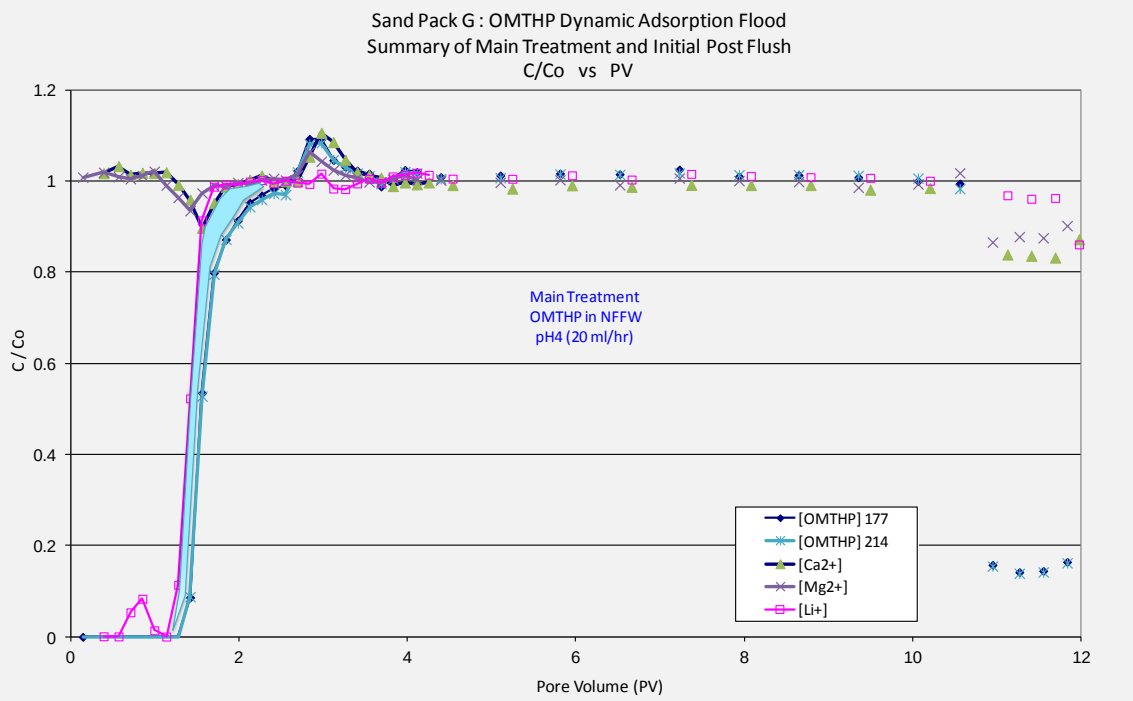

Figure 5.64: Sand Pack G – Main treatment and initial post flush stage. Normalized concentration vs. Pore Volume.

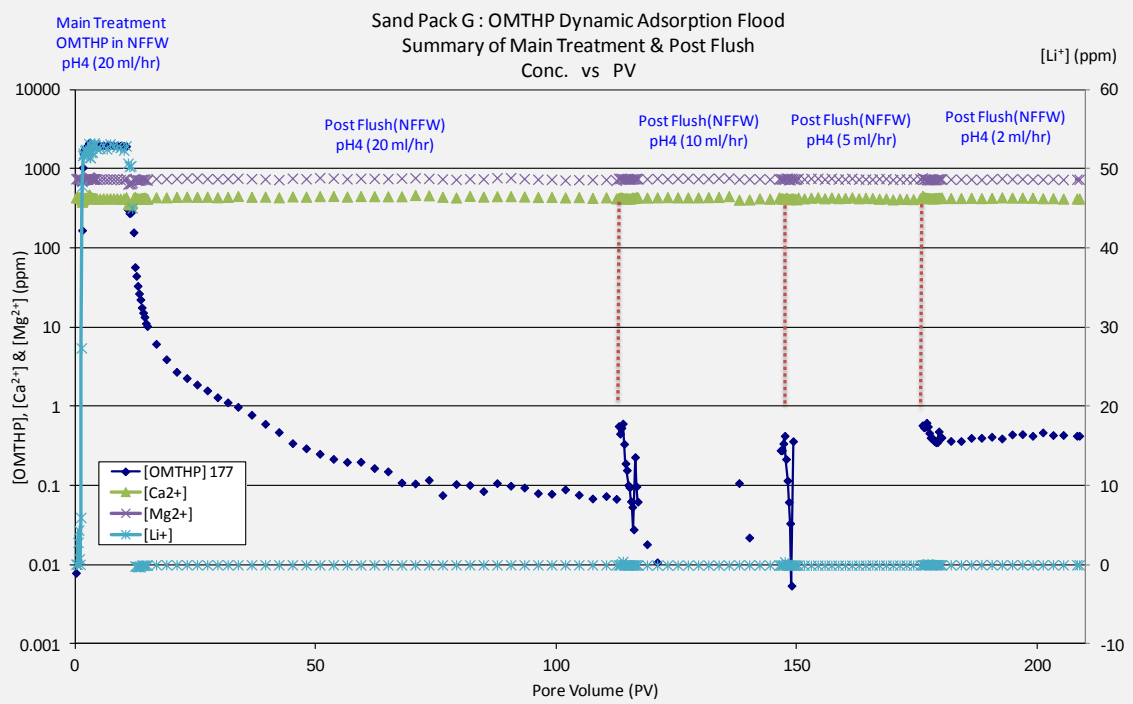

Figure 5.65: Sand Pack G – Main treatment and all post flush stages.

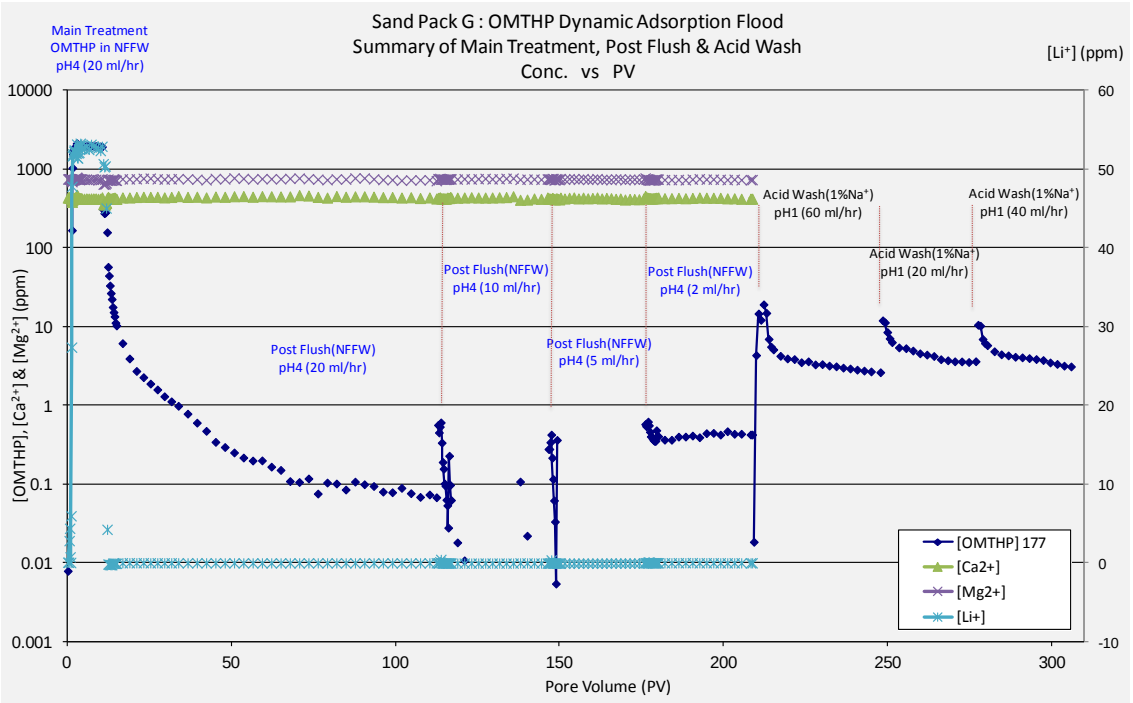

Figure 5.66: Sand Pack G – Main treatment, post flush and acid wash stages.

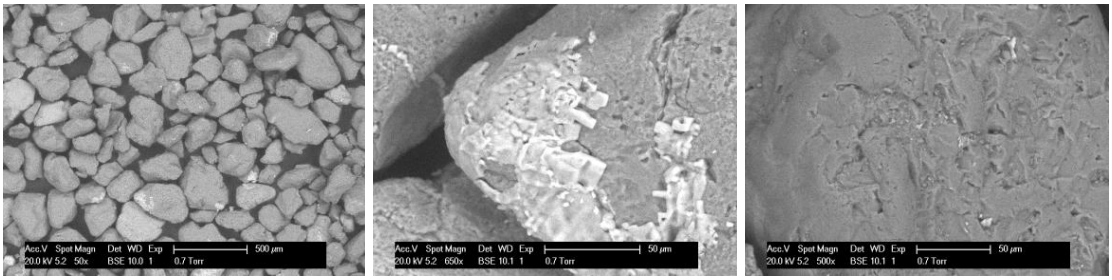

a-1 (Zoom 50x) a-2 (Zoom 650x) a-3 (Zoom 500x)

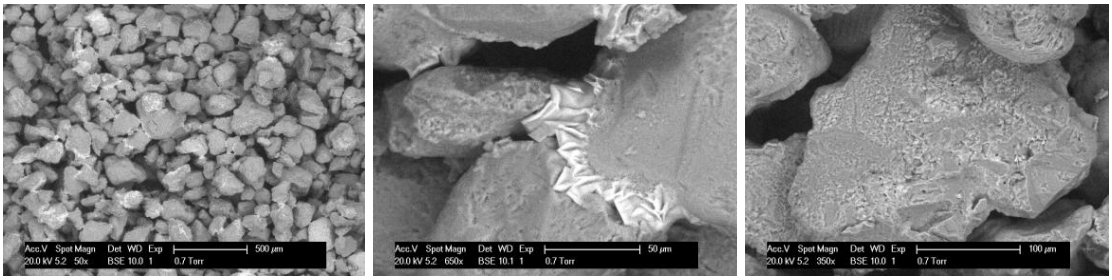

b-1 (Zoom 50x) b-2 (Zoom 650x) B-3 (Zoom 350x)

	a-2		a-3		b-2		b-3	
Element	Weight%	Atomic%	Weight%	Atomic%	Weight%	Atomic%	Weight%	Atomic%
C								
O	47.88	62.16	59.32	71.91	47.22	61.31	54.4	67.66
Na	7.57	6.84			7.33	6.63	4.1	3.55
Al					0.79	0.61		
Si	32.05	23.7	40.68	28.09	34.38	25.43	37.33	26.45
Cl	11.99	7.02			10.27	6.02	4.18	2.34
K	0.52	0.28						
Totals	100		100		100		100	

Figure 5.67: Sand Pack G – ESEM-EDAX results of sand extracted from sand pack column after acid wash treatment.

Notes:

All the sand samples were extracted from the sand pack column after the acid wash treatment at different flow rates. The only differences are; b is after soaking and stirring in 1% Na+ (pH1), whereas a sample is purely from the sand pack.

Sand Pack G : Mass Balance of SI OMTHP						
Mass In during Main Treatment =			**295.17**	mg		
Mass Left In Sand Pack (after MT + PF) =			33.14	mg		
Mass Left In Sand Pack (after MT+PF+AcW) =			22.10	mg		
Description	PV (ml)	Mass Out (mg)	Cum Mass Return (mg)	Cum Mass Return (%)	Mass In Sand Pack (mg)	Mass In Sand Pack (%)
MT~20/ml/hr (OMTHP)	10.56	254.56	254.56	86.24	40.61	13.76
PF~20ml/hr (NFFW)	112.47	7.29	261.85	88.71	33.32	11.29
PF~10ml/hr (NFFW)	146.31	0.01	261.86	88.71	33.31	11.29
PF~5ml/hr (NFFW)	175.62	0.00	261.86	88.71	33.31	11.29
PF~2ml/hr (NFFW)	208.72	0.20	262.05	88.78	33.12	11.22
AcW~40ml/hr(Na+)	211.34	0.3108	262.36	88.89	32.81	11.11
AcW~60ml/hr(Na+)	247.77	2.11	264.47	89.60	30.70	10.40
AcW~20ml/hr(Na+)	276.82	1.9999	266.47	90.28	28.70	9.72
AcW~40ml/hr(Na+)	305.88	1.8148	268.29	90.89	26.88	9.11
Sand Wash using 200ml of Na+ (pH=1)		4.80	273.09	92.52	22.08	7.48

Table 5.32: Sand Pack G – Mass balance base on total mass throughput.

Sand Pack G : Mass Balance of SI OMTHP								
Mass In during Main Treatment =		**295.17**	mg					
Mass Left In Sand Pack (after MT + PF) =		33.14	mg					
Mass Left In Sand Pack (after MT+PF+AcW) =		22.10	mg					
				(X)			(Y)	
Description	PV (ml)	Mass Out (mg)	Cum Mass Return (mg)	Cum Mass Return (%)	Mass In Sand Pack (mg)	Mass In Sand Pack (%)	Cum Mass Return (mg)	Cum Mass Return (%)
MT~20/ml/hr (OMTHP)	10.56	260.16	260.16	88.14	**35.01**	11.86		
PF~20ml/hr (NFFW)	112.47	1.69	261.85	88.71	33.32	11.29	1.69	4.82
PF~10ml/hr (NFFW)	146.31	0.01	261.86	88.71	33.31	11.29	1.70	4.85
PF~5ml/hr (NFFW)	175.62	**0.00**	261.86	88.71	33.31	11.29	1.70	4.85
PF~2ml/hr (NFFW)	208.72	0.20	262.05	88.78	33.12	11.22	1.89	5.41
AcW~40ml/hr(Na+)	211.34	0.3108	262.36	88.89	32.81	11.11	2.20	6.29
AcW~60ml/hr(Na+)	247.77	2.11	264.47	89.60	30.70	10.40	4.31	12.32
AcW~20ml/hr(Na+)	276.82	1.9999	266.47	90.28	28.70	9.72	6.31	18.03
AcW~40ml/hr(Na+)	305.88	1.8148	268.29	90.89	26.88	9.11	8.13	23.21
Sand Wash using 200m of Na+ (pH=1)	340	4.80	273.09	92.52	22.08	7.48	12.93	36.92

Table 5.33: Sand Pack G – Summary of mass balance base on total mass throughput and mass after main treatment + 2PV.

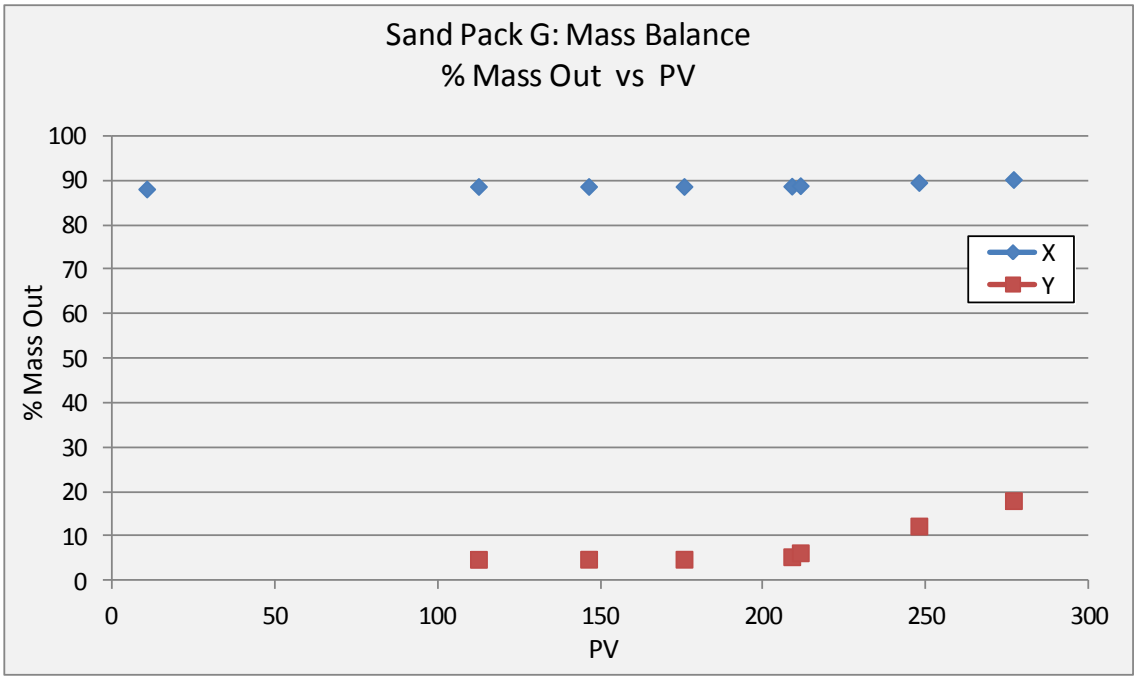

Figure 5.68: Sand Pack G – %Mass out base on total mass throughput and mass after main treatment + 2PV.

5.4 SUMMARY, DISCUSSION AND CONCLUSIONS

This chapter presents the experimental results from a novel series of variable rate adsorption and precipitation sand packs for a hexa-phosphonate SI, OMTHP. The sand pack floods were carried out using well characterized silica sand which has previously been used extensively in bulk coupled adsorption/precipitation tests under almost identical (but not flowing) conditions. All sand pack SI floods were conducted using almost identical procedures, with minor variants depending on the objective of that flood. The objective of performing these core flood experiments was to (i) carry out very well characterised "adsorption only" or "coupled adsorption/precipitation" SI return experiments in sand packs; (ii) the level of characterisation is intended to give quantitative results which can be used to test adsorption (Γ) and coupled adsorption precipitation (Γ/Π) models of these processes; and (iii) to quantify the extent of non-equilibrium (kinetic) effects on the return profile of the inhibitor when applied under both adsorption and precipitation conditions. This data will help in the development of a more suitable coupled adsorption/precipitation model describing the non-equilibrium

squeeze processes. Using experiments of this type will enable us to develop more realistic isotherms and rate kinetic functions for use subsequently in field applications. To our knowledge, this is the most complete dataset of such floods which has been carried out to date in this field of study.

The variable rate adsorption and precipitation floods for the hexa-phosphonate (OMTHP) includes the effects of flow rate and solubility on the effluents of SI concentration, [Ca^{2+}] and [Mg^{2+}], and provides data for testing non-equilibrium flow models for describing coupled adsorption/precipitation squeeze treatments.

5.4.1 Methodology

The methodology which was developed earlier has been improved to carry out these dynamic pack flood experiments successfully. Referring to Table 5.2, the results show consistency in all the sand pack experiments. The pore volume (and porosity) for all the sand pack are around 14.60 to 14.70ml with porosity of 40.50%. The small difference in PV is due to how well the sand was packed into the column. Overall results from all the sand pack also indicate that the assembled sand pack flooding apparatus is reliable. Refer to Figure 5.3 and Figure 5.4 for schematic diagram of the flooding apparatus and packing technique.

5.4.2 Non-Equilibrium Returns

The sand pack effluent results demonstrate clear non-equilibrium behaviour as the flow rate for the different floods is varied and indicates the importance of flow rate on the derivation of dynamic isotherms prior to field application modelling. That is, as the brine velocity decreases, the inhibitor concentration level increases (and vice versa). Figure 5.69 and Figure 5.70 show the variation in effluent concentration as the flow rates changes and this is observed in *both* adsorption and coupled adsorption/ precipitation processes. This has important implications for field treatments whereby the penetration depth may considerably influence the return concentration since deeper penetration, results in a slower localized fluid velocity.

5.4.3Adsorption vs. Precipitation

For all the sand pack flood experiments main treatments, for both adsorption and precipitation floods, the deviation between SI to lithium behaviour shows retention of SI is taking place. Based on static compatibility tests results, the retention in the sand pack during main treatment is clearly due to pure adsorption at low temperature conditions since we observe no precipitation at room temperature, 20°C. Calcium and magnesium also plays some role but this is much clearer in the precipitation floods, and cannot be easily observed (if indeed it occurs) in the adsorption flood. Table 5.34 clearly indicates that during the first 3 to 4 PV, the retention is due to pure adsorption.

During shut-in after the main treatment, we observed significant drops in the normalized calcium and magnesium profiles for all the precipitation floods in the early post flush period. It is a clear diagnostic that it is precipitation which is occurring in the core during shut-in at elevated temperature. In one of the adsorption flood, sand pack E; there is no (or very little) calcium loss observed in adsorption flood, which is probably due to the low SI concentration, [OMTHP] = 500ppm and/or low calcium concentration, [Ca^{2+}] = 428ppm.

Comparing the precipitation and adsorption treatments for the SI, it is found that the effluent SI concentrations were always much higher for the precipitation treatments. Figure 5.72 shows effluent concentration at 20ml/hr for all the floods. All adsorption floods (E, F & G) show lower return effluent concentrations over the main flow back period compared to precipitation floods (A, C & D). This behaviour is summarised in Figure 5.72. This gives a good justification as to why the industry should at least consider the application of precipitation squeeze treatments, although care must be taken to prevent excessive precipitation, or formation damage in the squeeze process.

5.4.4 Desorption and Dissolution

In sand pack C (precipitation flood), the post flush brine was normal FW contained both calcium and magnesium ([Ca] = 2000ppm; [Mg] = 700ppm) whereas in sand pack D (precipitation flood), only 1% Na^{+} brine was used. Hence, in both precipitation floods where the calcium concentration is 2000ppm (Pack C), the solubility of SI is lower than

that in the no calcium at all (sand pack D) case. This is shown in the return curve where the steady state SI return concentration for the Pack C flood ([Ca]=2000ppm) is lower than that in the Pack D flood ([Ca]=0) for the same flow rate, Q. The direction of the non-equilibrium effect on the inhibitor concentration level is the same for both adsorption and precipitation floods i.e. at slower rate the effluent inhibitor concentration is higher, and vice versa. This is consistent with the theory as presented by Sorbie (2010) and Vazquez e.tal (2010).

5.4.5 Inhibitor Retention

During shut-in, for all the precipitation and adsorption floods, the mobile inhibitor concentration declines significantly. As shown in Table 5.34, the normalized inhibitor concentration for adsorption flood range from 0.15 to 0.20 which is slightly lower than the precipitation flood from 0.2 to 0.25. It is clear evidence that enhanced adsorption/precipitation occurs during the shut-in at elevated temperature. At room temperature, we already know from static compatibility tests that no precipitation (only adsorption) is taking place.

Calcium is also reduced during the shut-in in the precipitation floods and only a very slight drop is observed in the adsorption flood. For both precipitation floods (C and D), the normalized figures for calcium are C/Co ~0.85 and 0.84, respectively. Whereas for adsorption floods (E, F and G), the normalized figures are C/Co ~0.96, 0.87 and 0.85 respectively. We note the drop in calcium (and magnesium) concentration in adsorption floods but it may not be observed in sand pack E due to the levels were too low to detect when using a fairly low level of SI (we used, [SI] = 500ppm).

5.4.6 Irreversible Behaviour

Mass balance base on all the floods screened show that there is still a significant amount of SI mass left in the sand pack even after sand is washed with acidized Na^+ (pH=1). Table 5.35 shows that the levels of SI mass remaining in the sand pack are in the range of 5 to 8% of total mass throughput. In contrast, ESEM-EDAX results show that there is no SI in the sand after the final sand wash. All results show ESEM-EDAX does not detect these elements at a very low concentrations. Refer to Figure 5.73.

Sand Pack ID	Stage(s)	Temp. (°C)	SI (C/Co)	Ca (C/Co)	Mg (C/Co)
A	• 1^{st} – 3^{rd} PV • Shut-In	RT 95°C	Adsorption 0.25	- -	- -
C	• 1^{st} – 3^{rd} PV • Shut-In	RT 95°C	Adsorption 0.20	observed 0.85	observed 0.90
D	• 1^{st} – 3^{rd} PV • Shut-In	RT 95°C	Adsorption 0.24	observed 0.82	observed 0.90
E	• 1^{st} – 3^{rd} PV • Shut-In	RT 95°C	Adsorption 0.15	observed (slight) 0.96	observed (slight) 0.98
F	• 1^{st} – 3^{rd} PV • Shut-In	RT 95°C	Adsorption 0.20	observed (slight) 0.87	observed (slight) hardly seen
G	• 1^{st} – 3^{rd} PV • Shut-In	RT 95°C	Adsorption 0.18	observed (slight) 0.85	observed (slight) 0.90

Table 5.34: Normalized [SI], [Ca^{2+}] and [Mg^{2+}]

No	Description	A	C	D	E	F	G
1	Pore Volume (ml)	13.64	14.69	14.73	14.60	14.66	14.11
2	Porosity (%)	38.49	40.52	40.85	40.87	40.06	38.21
3	Sand Mass (g)	93.58	95.68	95.21	95.21	96.61	97.87
4	MT - [SI] (ppm)	4000	4000	4000	500	4000	2000
5	MT - [Ca^{2+}] (ppm)	2000	2000	2000	2000	428	428
6	PF - [Ca^{2+}] (ppm)	2000	2000	0	2000	428	428
7	PF Pore Volume	417 (5691ml)	164 (2413ml)	168 (2479ml)	184 (2692ml)	220 (3218ml)	209 (2947ml)
8	AcW Pore Volume	363 (4957ml)	133 (1951ml)	103 (1520ml)	133 (1951ml)	-	97 (1374ml)
9	Total of PF & AcW	780 (10648ml)	297 (4364ml)	271 (3999ml)	317 (4643ml)	220 (3128ml)	306 (4321ml)
10	Total Mass Throughput (mg)	410.85	520.97	640.05	70.73	572.75	295.17
11	Mass In Sandpack after MT + 2PV (mg)	72.47	53.91	82.56	17.36	44.08	35.01
12	Mass in Sand Wash (mg)	4.55 (1.1%)	1.03 (0.2%)	1.00 (0.16%)	1.50 (2.12%)	6.00 (1.03%)	408 (1.63%)

13	*Mass Out @ end of MT (%)	82.36	89.65	87.10	75.45	92.30	88.14
14	*Mass Out @ end of PF (%)	84.07	91.50	90.68	76.01	93.07	88.78
15	*Mass Out @ end of AcW (%)	91.95	93.04	91.85	96.21	94.12	92.52
16	**Mass Out @ end of PF (%)	9.69	17.87	27.78	2.26	10.02	5.41
17	**Mass Out @ end of AcW (%)	54.35	32.73	36.57	84.56	23.63	36.92

Table 5.35: Summary of floods characteristics and mass balance

Notes:

1. *The mass is calculated base on total mass throughput
2. **The mass is calculated base on mass in sand pack after MT + 2PV
3. AcW= Acid Wash

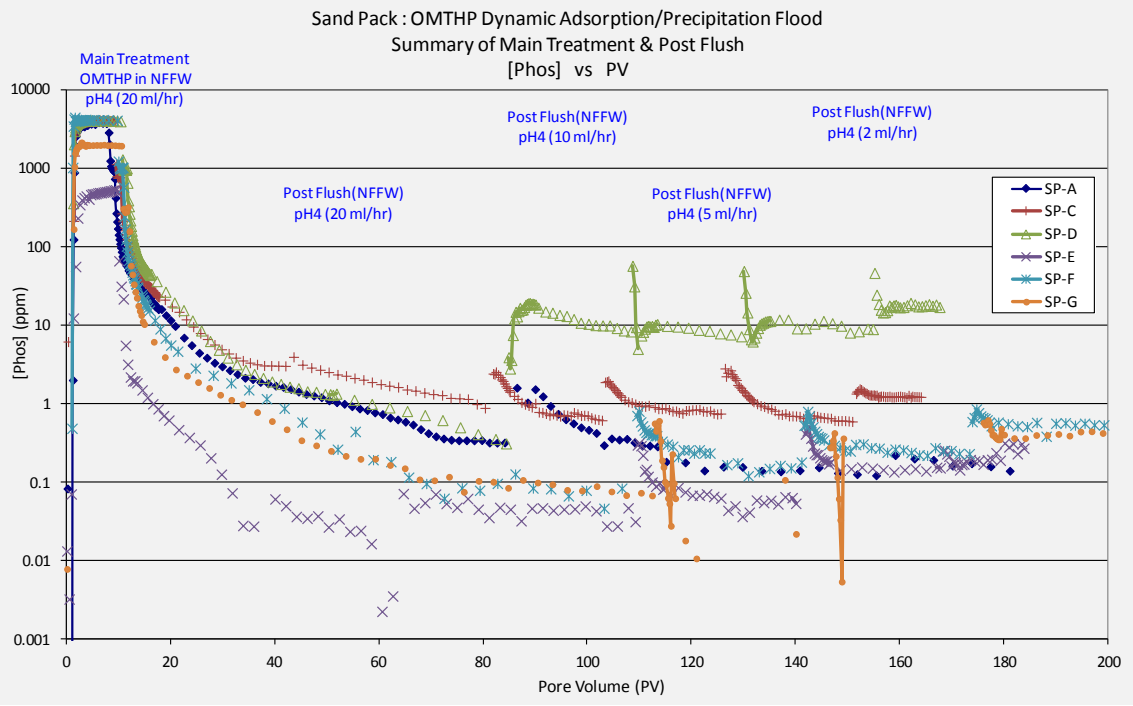

Figure 5.69: Summary of main treatment and post flush behaviour. Sand pack A, C, D, E, F & G

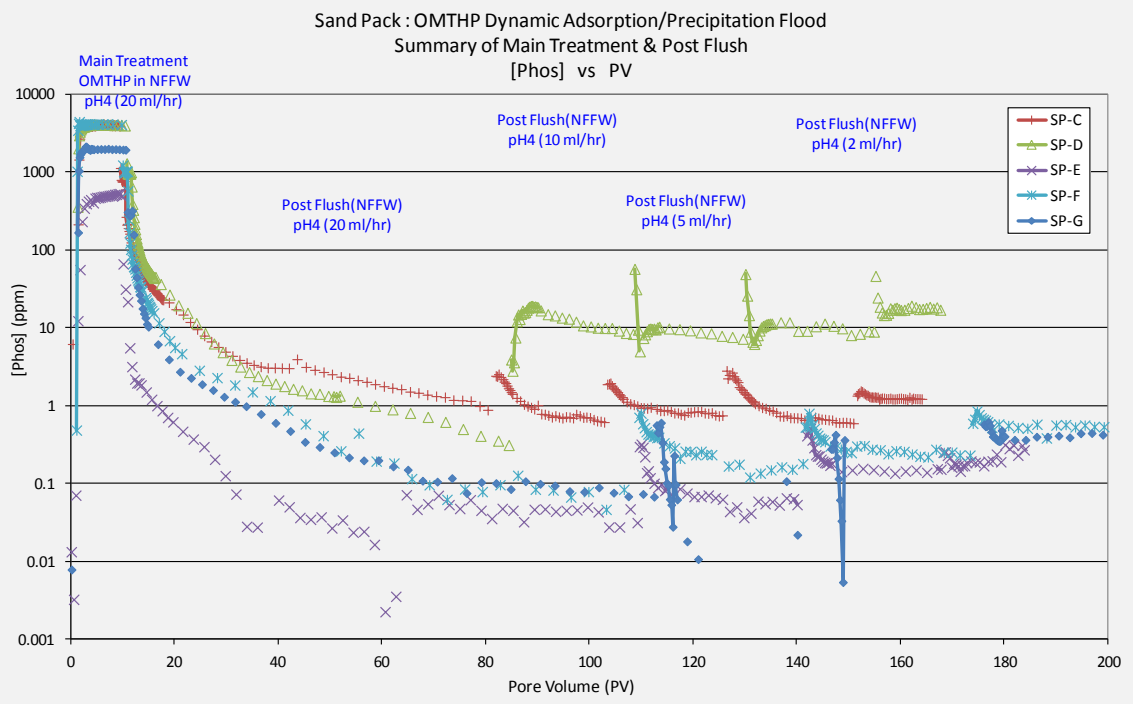

Figure 5.70: Summary of main treatment and post flush behaviour. Sand pack C, D, E, F & G

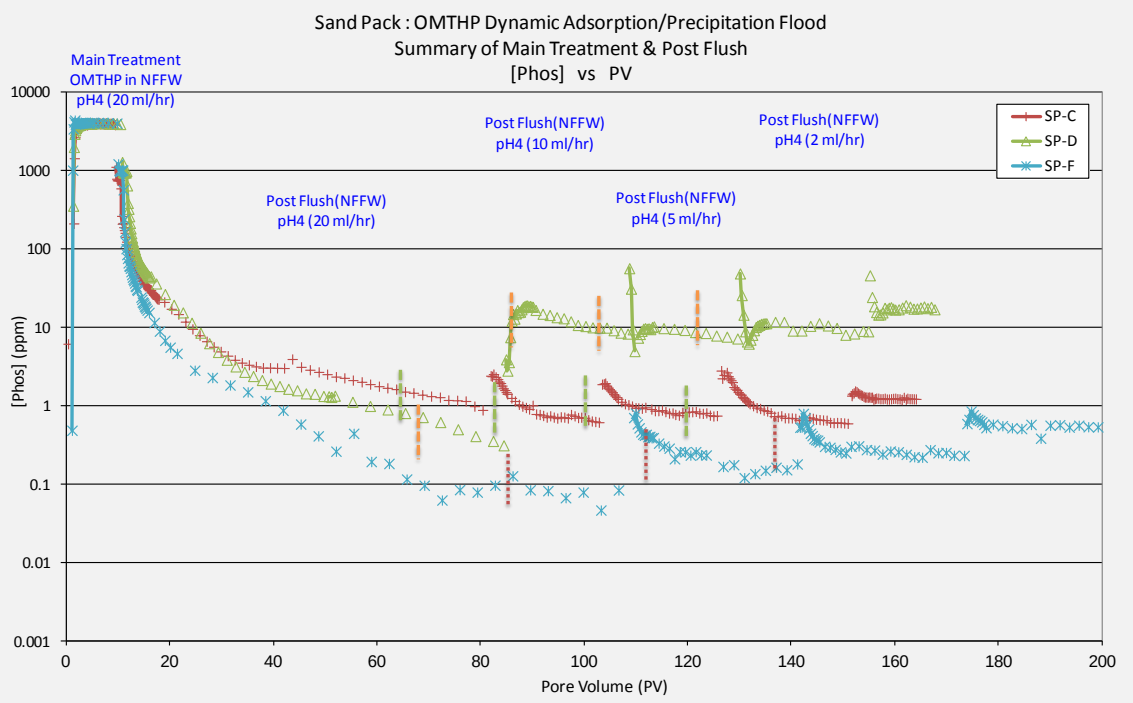

Figure 5.71: Summary of main treatment and post flush behaviour. Sand pack C, D, & F

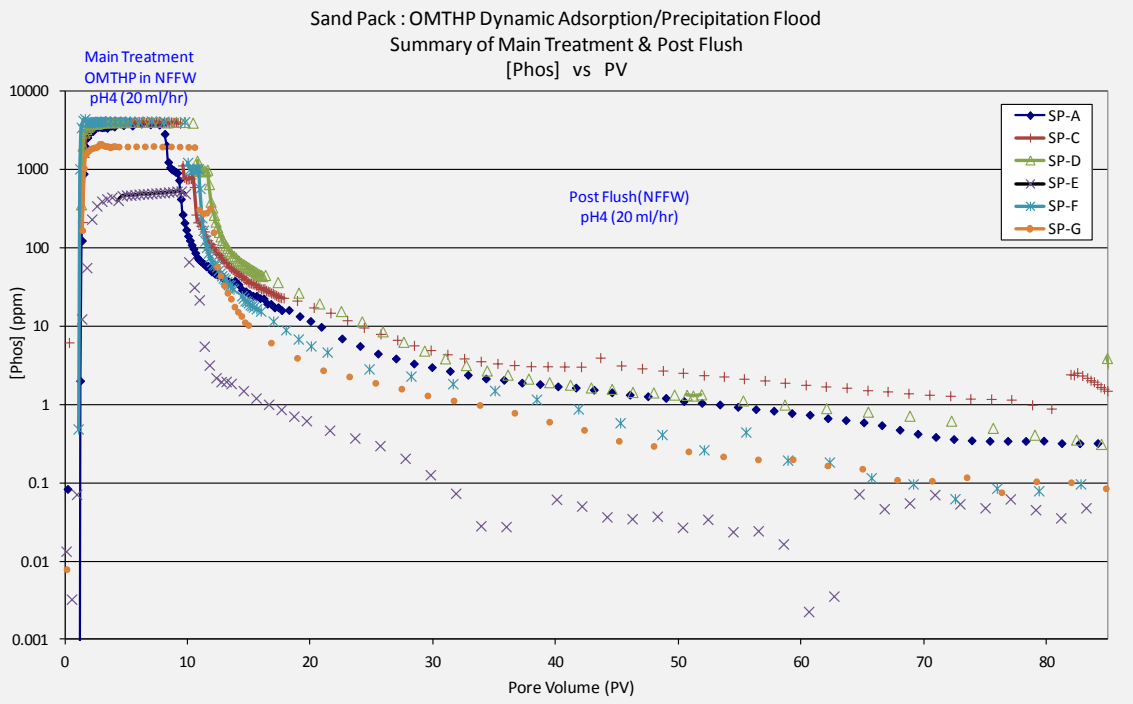

Figure 5.72: Summary of main treatment and initial post flush behaviour.

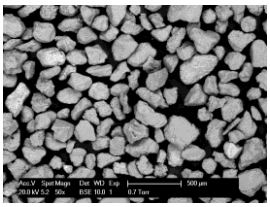
S1 (Zoom 50x)

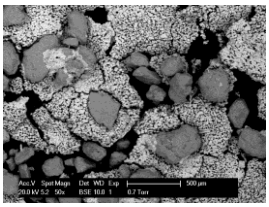
S2 (Zoom 50x)

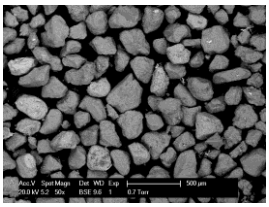
C1 (Zoom 50x)


C2 (Zoom 1200x)

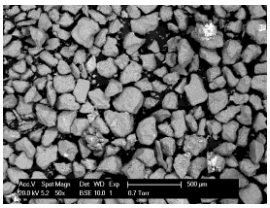
D1 (Zoom 50x)

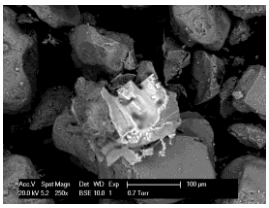
D2 (Zoom 250x)

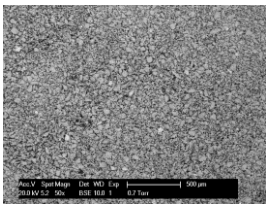
E1 (Zoom 50x)

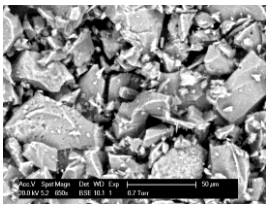
E2 (Zoom 650x)

	s1		s2		c1		c2		d1		d2		e1		e2	
Element	Weight%	Atomic%	Weight%	Atomic%	Weight%	Atomic%	Weight%	Atomic%	Weight%	Atomic%	Weight%	Atomic%	Weight%	Atomic%	Weight%	Atomic%
C	32.43	42.24							28.75	38.33						
O	47.88	46.81	27.85	41.24	59.86	72.58	63.8	75.93	48.96	49	12.8	20.91	58.58	71.38	58.27	71.03
Na			24.7	25.44					0.65	0.45	34.92	39.69			0.45	0.38
Al	0.63	0.36			1.19	0.85	2.64	1.86	0.45	0.27						
Mg																
P																
Si	18.84	10.49	9.22	7.77	37.02	25.57	30.47	20.65	20.14	11.49	4.46	4.15	40.76	28.29	40.93	28.42
Cl			38.24	25.55	0.7	0.39	1.04	0.56	0.8	0.36	47.82	35.25				
K	0.23	0.09			1.22	0.61	2.06	1	0.26	0.1			0.66	0.33	0.35	0.18
Ca																
Totals	100		100		100		100		100		100		100		100	

Figure 5.73: ESEM-EDAX analysis of sand after final acid wash. These are repeat analysis done independently

Notes:

S1 – Pure Sand

S2 – Pure Sand + 6% NaCl

C1&C2 – Sand pack C after experiment

D1&D2 – Sand pack D after experiment

E1&E2 – Sand pack E after experiment

CHAPTER 6: CONCLUSIONS AND RECOMMENDATIONS

6.1 CONCLUSIONS

The key objectives of the study undertaken in this PhD thesis were as follows:

(i) To improve and establish an experimental methodology to study static adsorption and compatibility tests and non-equilibrium sand pack tests for both adsorption and precipitation processes.

(ii) To study static compatibility and coupled adsorption/precipitation experiments to understand the mechanism that is taking place and what parameters are involved during the process. Specifically, we wished to establish pure adsorption and coupled adsorption/precipitation regions for DETPMP and OMTHP scale inhibitors and NFFW brine at pH4 and 95°C.

(iii) To study the influence of flow rates on inhibitor return concentrations in non-equilibrium sand pack floods using OMTHP scale inhibitor applied in both adsorption and precipitation treatments. The mechanisms and parameters (pH, temperature, $[Ca^{2+}]$, [SI], etc.) involved were studied under dynamic condition. The full effluent scale inhibitor concentration and mass balances of SI throughout the experiment were collected and analyzed for use in future modelling.

6.2 STATIC COMPATIBILITY AND COUPLED ADSORPTION / PRECIPITATION EXPERIMENTS

The aim of these experiments is to study the possible SI retention mechanisms onto rocks due to either **pure adsorption (Γ)** or by **coupled adsorption/precipitation (Γ/Π)**. This theory predicts that, when all the measured apparent adsorption vs. final [SI] (Γ_{app}/c_{1f}) curves for different (m/V) ratios collapse onto a single curve, then this indicates pure adsorption (Γ). However, when these curves diverge for different values of (m/V), then coupled adsorption/precipitation (Γ/Π) is being observed. The theory behind this is explained in this thesis.

In Chapter 4, results on static compatibility and coupled adsorption/precipitation experiments were presented using two phosphonate scale inhibitors, namely DETPMP and OMTHP, and three types of minerals, e.g. sand, kaolinite and siderite with synthetic Nelson Forties Formation Water (NFFW). The composition is given in Table 4.1; NFFW has [Ca^{2+}] = 2000ppm and [Mg^{2+}] = 739ppm and all experiments were performed at pH 4 and T = 95°C.

(i) ***DETPMP and OMTHP SIs onto SAND Mineral***

At pH 4 and T = 95°C, both ***pure adsorption (Γ)*** *and* ***coupled adsorption/precipitation (Γ/Π)*** regions were observed for DETPMP and OMTHP onto sand in NFFW. Figure 4.11 and Figure 4.22 show these static "apparent adsorption" isotherms for DETPMP and OMTHP onto sand, respectively. Pure adsorption was observed only at SI concentrations below ~750ppm. Coupled adsorption/precipitation behaviour was observed for SI concentrations above ~750ppm. For each (m/V) ratio, the isotherm curves plateau at a level of ~ 0.25mg/g and 0.30mg/g for DETPMP and OMTHP respectively at ~750ppm. In the coupled adsorption/precipitation region, the apparent adsorption values range from ~2 - 12mg/g.

A considerable reduction is observed in [phosphorous], [Ca^{2+}] and [Mg^{2+}] as the concentration of SI increases in both bulk solution and in the adsorption experiments for both SIs. This M^{2+} reduction in solution is mainly associated with the precipitation of a M^{2+}-DETPMP complex. The M^{2+}, particularly calcium ions, plays a major role in adsorption and coupled adsorption/precipitation process by bridging between the SI molecule and the rock surface.

(ii) ***DETPMP and OMTHP SIs onto KAOLINITE Mineral***

The DETPMP/kaolinite system in NFFW brine also shows clear regions of ***pure adsorption (Γ)*** *and* ***coupled adsorption/precipitation (Γ/Π)*** at pH4 and T=95°C. Refer to Figure 4.32 and Figure 4.41 for "apparent adsorption" isotherms for DETPMP and OMTHP onto kaolinite, respectively. Pure adsorption was observed below [SI] ~800ppm and coupled adsorption/precipitation behaviour was found above [SI] ~800ppm. This conclusion is further strengthen by the observed changes in phosphorous

(SI) concentration, where clear reduction in phosphorous (SI) was seen at ~800ppm and phosphorous was also found in precipitates base on the EDAX signal at 800ppm.

From the Γ_{app} vs. [SI] curves for the OMTHP/kaolinite system in NFFW brine; both **pure adsorption (Γ)** and **coupled adsorption/precipitation (Γ/Π)** regions were also observed at pH 4 and T=95°C. However, in this mineral/SI system, it is less clear where the transition occurs between the two mechanisms. However, the observed difference in the amounts of phosphorous concentration in solution ion data shows that clear adsorption and coupled adsorption/precipitation regions do occur. Pure adsorption is observed up to [SI] ~ 500ppm, and coupled adsorption/precipitation is observed for [SI] > ~500ppm. This finding is further strengthened by observations on the filtered precipitate and the associated ESEM-EDAX data. Another reason that might have caused the less clear transition between the two regions of Γ and Γ/Π is due to the very high levels of DETPMP pure adsorption onto the kaolinite due to its very high specific surface area. Both DETPMP and OMTHP SIs show pure adsorption levels onto kaolinite minerals between Γ ~ 7 to 13 mg/g at 800ppm SI.

Significant reduction is also observed in both [Ca^{2+}] and [Mg^{2+}] as the concentration of SI increases in coupled adsorption/precipitation experiments for both SIs. This M^{2+} reduction in solution is mainly associated with the precipitation of a M^{2+}-DETPMP/OMTHP complex.

(iii) ***DETPMP Scale Inhibitor onto SIDERITE Mineral***

For the DETPMP/siderite system in NFFW brine, results similar to those for the OMTHP/kaolinite system are observed where again the transition between pure adsorption and coupled adsorption/precipitation is not clear, although both regions are observed. From the solution ion data for the compatibility and adsorption tests, it appears that pure adsorption is observed up to [SI] ~500ppm, and at higher concentrations, then coupled adsorption/precipitation is observed. This finding is further strengthened by ESEM-EDAX observations on the filtered precipitate. Again, the reason for the less clear transition observed for the DETPMP/siderite system maybe due to both (i) the high levels of adsorption of the DETPMP onto the siderite, and also (ii)

the role of the higher levels of [Fe^{3+}] released in these lower pH (pH 4) experiments. At 1500ppm, 25ppm [Fe^{3+}] was observed in the bulk solution while at 15000ppm, 200ppm [Fe^{3+}] was found (see Figure 4.50).

Again, significant reductions were observed in both [Ca^{2+}] and [Mg^{2+}] as the concentration of SI increases in coupled adsorption/precipitation experiments for the DETPMP/siderite system. This M^{2+} reduction in solution is mainly associated with the precipitation of a M^{2+}-DETPMP complex and this has been confirmed by ESEM EDAX observations.

6.3 NON-EQUILIBRIUM SAND PACK EXPERIMENTS ON BOTH ADSORPTION AND PRECIPITATION FLOOD

Chapter 5 presents the experimental results from a novel series of variable rate sand pack experiments for both adsorption and precipitation floods using a hexa-phosphonate SI, OMTHP. The objective of performing these sand pack experiments was as follows;

(i) to carry out very well characterised "adsorption only" or "coupled adsorption/precipitation" SI return experiments in sand packs (using systems that have been fully characterised in static tests);

(ii) gather data where the level of characterisation is intended to give quantitative results which can be used to test adsorption (Γ) and coupled adsorption precipitation (Γ/Π) models of these processes; and

(iii) to quantify the extent of non-equilibrium (kinetic) effects on the return profile of the inhibitor when applied under both adsorption and precipitation conditions.

(i) *Methodology*

The improved technique shows consistency in all the experiments performed. The pore volume (and porosity) for all the sand pack were around 14.60 to 14.70ml with porosity of 40 to 40.5%. Overall results from all the sand pack indicate that the assembled sand pack flooding apparatus and packing technique are reliable.

(ii) ***Non-Equilibrium Returns***

The sand pack effluent results demonstrate clear non-equilibrium behaviour. That is, as the brine velocity decreases, the inhibitor concentration level increases (and vice versa). Figure 5.69 and Figure 5.70 show the variation in effluent concentration as the flow rates changes. The direction of the non-equilibrium effect on the inhibitor concentration level is the same for both adsorption and precipitation floods i.e. at slower rate the effluent inhibitor concentration is higher, and vice versa.

(iii) ***Adsorption vs. Precipitation***

For all the sand pack flood experiments, the main treatments (at room temperature, 20°C), for both adsorption and precipitation floods, show a deviation between SI and lithium effluent behaviour indicating retention due to pure adsorption of SI. Calcium and magnesium also plays some role but this is much clearer in the precipitation floods. Table 5.34 clearly indicates that during the first 3 to 4 PV, the retention is due to pure adsorption, as had been proven earlier in the static adsorption/compatibility tests.

During shut-in at 95°C after the main treatment, sharp decreases were observed in the normalized SI, calcium and magnesium profiles for all the adsorption and precipitation floods in the early post flush period. These drops are much more significant for precipitation floods. It is a clear diagnostic that it is precipitation which is occurring in the core during shut-in at elevated temperature. Note: For one of the adsorption flood, sand pack E, there is no (or very little) calcium loss, which is probably due to low SI concentration, [OMTHP] = 500ppm and/or low calcium concentration, [Ca^{2+}] = 428ppm.

Comparing the precipitation and adsorption treatments for the SI, it is found that the effluent SI concentrations were always significantly higher in the precipitation treatments. All adsorption floods (E, F & G) showed lower return effluent concentrations over the main flow back period compared to the precipitation floods (A, C & D). Figure 5.72 shows the effluent concentration profiles (at Q =20ml/hr) for all these floods.

(iv) ***Desorption and Dissolution***

In sand pack C (precipitation flood), the post flush brine was normal FW contained both calcium and magnesium ([Ca]=2000ppm; [Mg]=739ppm), whereas in sand pack D (precipitation flood), the posflush was performed using 1% Na^+ brine. Hence, in both precipitation floods where the calcium concentration is 2000ppm (Pack C), the solubility of SI is lower than that in the no calcium case (sand pack D). This is shown in the return curves where the steady state SI return concentration for the Pack C flood ([Ca]=2000ppm) is lower than that in the Pack D flood ([Ca]=0) for the same flow rate, Q.

(v) ***Inhibitor Retention***

During shut-in at elevated temperature (95°C), for all the precipitation and adsorption floods, the mobile inhibitor concentration declines significantly. As shown in Table 5.34, the normalized inhibitor concentration for adsorption flood range from 0.15 to 0.20 which is slightly lower than the precipitation flood from 0.2 to 0.25. It is clear evidence that enhanced adsorption/precipitation occurs during the shut-in at elevated temperature compared to room temperature.

Calcium is also reduced during the shut-in in the precipitation floods and only a very slight drop is observed in the adsorption flood. For both precipitation floods (C and D), the normalized figures for calcium are C/Co ~0.85 and 0.84, respectively. Whereas for adsorption floods (E, F and G), the normalized values are C/Co ~0.96, 0.87 and 0.85, respectively. We note the drop in calcium (and magnesium) concentrations in adsorption floods but it is not observed in sand pack E, due to the low SI levels used in this flood([SI]=500ppm).

(vi) ***Irreversible Behaviour***

Mass balance results for all the floods in this study showed that there is still a significant amount of SI mass left in the sand pack even after sand is washed with acidized Na^+ (pH=1). Table 5.35 shows that the levels of SI mass remaining in the sand pack are in the range of 5 to 8% of total mass throughput. The results indicate that there was still SI left in the sand pack, which appears to be due to irreversible SI retention.

6.4 SUMMARY

We believe that the experiments reported in this thesis represent one of the most comprehensive data set of experimental SI work executed to date. The work ranges from static adsorption and coupled adsorption precipitation SI/mineral tests to *dynamic* pack flooding tests under almost identical conditions. Exactly the same system (i.e. OMTHP SI, sand mineral, NFFW brine and conditions, pH 4 and T=95°C) was used in bulk coupled adsorption/precipitation tests, as in the dynamic sand pack floods. The outcome from static tests provided unambiguous information on whether the system was in a pure adsorption (Γ) or a coupled adsorption/precipitation (Γ/Π) process, which was of relevance to the dynamic sand pack tests.

The dynamic sand pack tests investigated both adsorption and precipitation of the hexa-phosphonate (OMTHP) including the effects of flow rate and solubility on the effluents of SI concentration, $[Ca^{2+}]$ and $[Mg^{2+}]$. This data provides enough information for testing non-equilibrium flow models for describing coupled adsorption/precipitation squeeze treatments. Therefore, in future this data will help in the development of more suitable coupled adsorption/precipitation models describing non-equilibrium squeeze processes. Using experiments of this type will enable us to develop more realistic isotherms and rate kinetic functions for use subsequently in field applications. To our knowledge, this is the most complete dataset of such floods which has been produced to date in this field of study. Indeed, work is already in progress within the FAST group at Heriot-Watt University to develop such kinetic coupled adsorption/precipitation (Γ/Π) models (Sorbie, SPE130702, 2010).

6.5 RECOMMENDATIONS FOR FUTURE WORK

This thesis reports experimental work in the following areas:

(i) Experimental technique used to study static adsorption/compatibility tests and non-equilibrium sand pack tests.

(ii) Static compatibility and coupled adsorption/precipitation experiments.

(iii) Non-equilibrium sand pack floods for both adsorption and precipitation treatments.

Although, much has been discovered, there are still many aspects of adsorption and precipitation processes that must be studied in detail in the future and some of the areas for further study are listed below:

(i) ***Other Minerals:*** This work should be extended to include static adsorption and compatibility tests for phosphonate SIs with kaolinite and siderite minerals. This thesis already gives detail understanding of pure adsorption and coupled adsorption/precipitation regions for these minerals based on adsorption isotherm and solution ion data. But, it will be an improvement if this region can be decided solely base on adsorption isotherms. Based on our understanding from this work, this can be achieved by; (a) carefully characterizing the minerals to understand their detailed surface chemistry and their particle size distributions. Homogenous and narrower distributions are understood to provide consistent results compared to wider size distribution, (b) understanding the impact of Fe^{3+} and Al^{3+} ions on adsorption and precipitation.

This work can give reliable data to improve and test non-equilibrium coupled adsorption/precipitation model. So far, the model is being tested base on phosphonate SIs and sand minerals.

(ii) ***XRD/XPS Mechanistic Studies:*** To further understand the mechanism and parameters that influence adsorption and coupled adsorption/precipitation, we believe that much can be learned by using x-ray diffraction (XRD) and/or x-ray photoelectron spectroscopy (XPS). In this work, ESEM-EDX was used extensively, which provides sufficient information to identify the presence of the various elements involved (e.g. P, Ca etc.). However, when the amount of these elements is very small, ESEM-EDX had some difficulty to detect them accurately and was only able to give some qualitative indications of when certain elements were present. The use of XRD and/or XPS would provide more quantitative information on the elements presence on the mineral which can be used to determine the atomic ratio even at microscopic level.

(iii) ***Adsorption/Precipitation of Polymeric SIs:*** It is recommended that similar static adsorption/compatibility tests are carried out in future for polymer scale inhibitors

before proceeding to non-equilibrium pack flood experiments. This work with polymeric SIs should start with sand minerals and later extend to kaolinite, siderite, etc.

(iv) ***Effluent Characterisation of Inhibition Efficiency:*** The dynamic sand pack flood at different rates should be extended to incorporate "inhibition efficiency" tests on the effluent concentrations. These tests can be compared to static tests, and the objective is to determine if the MIC measured for both static and dynamic tests are the same i.e. has the species altered in any way from the “stock” solution which is usually used in bulk inhibition efficiency tests.

(v) ***Dynamic Γ/Π Modelling:*** This data should be used by modellers for assessing non-equilibrium flow models for application in laboratory core flood and field scale systems. This data set is the most complete in existence for testing and developing non-equilibrium coupled adsorption/precipitation (Γ/Π) squeeze models. It has data for exactly the same bulk and dynamic systems and phase diagrams of adsorption/precipitation (Γ/Π) regimes are known. The effluent concentrations for SI and all ancillary ions (Ca^{2+}, Mg^{2+} and Li^{+}), and mass balance for SI are known. Using experiments of this type will enable us to develop more realistic isotherms and rate kinetic functions for use subsequently in field applications.

APPENDIX A: FULL DERIVATION OF COUPLED ADSORPTION/ PRECIPITATION MODEL

Static Adsorption: Figure A.1 shows a schematic of a static adsorption experiment. A SI of initial concentration, c_0 (ppm or mg/L), in a volume, V (L), is allowed to come to equilibrium with a mass, m (g), of mineral. At equilibrium concentration of the SI, c_{eq}, then by material balance the adsorption level is as follows:

$$\Gamma = \frac{V(c_0 - c_{eq})}{m} \tag{A.1}$$

where in the units used, then Γ is in mg of SI/g of rock. Fig. A.2 shows measured experimental static adsorption isotherms, Γ(C), for DETPMP on crushed core material at various pH values, 2, 4 and 6 at T = 25^{o}C (Yuan et al, 1994). It is quite clear from these results that the level of SI adsorption is also strongly dependent in pH as well as on [SI], thus, Γ=Γ(C, pH) or Γ=Γ(C, [H^+]). However, for simplicity purposes, the assumption that Γ is a function of C = [SI] only, and we will denote the equilibrium adsorption isotherm as, $\Gamma_{eq}(c_{eq})$, as shown in Fig. A.3. Following the idea in Fig. A.3, we note that the initial mass of SI in the system is by definition given by Vc_0 since all the SI is in the aqueous phase. However, at equilibrium the mass of SI is partly in solution ($V.c_{eq}$) and partly adsorbed on the rock mineral ($m\Gamma_{eq}(c_{eq})$) but since the original mass is conserved, then:

$$Vc_0 = m\Gamma_{eq}(c_{eq}) + V.c_{eq} \tag{A.2}$$

If the analytical form of the isotherm is known (e.g. it is a Freundlich or a Langmuir isotherm with known parameters), then Eq. (A.2) gives a simple non-linear equation for finding c_{eq} which is the only unknown quantity. Another way to write Eq. (A.2) which highlights how our later experiments are carried out is by dividing through by V to obtain:

$$c_0 = \left(\frac{m}{V}\right)\Gamma_{eq}(c_{eq}) + c_{eq} \tag{A.3}$$

which indicates that the mass/volume ratio, (m/V), is an important parameter in these adsorption experiments, as we will show later. We can also define a function $F(c_{eq})$ as follows:

$$F(c_{eq}) = \left(\frac{m}{V}\right)\Gamma_{eq}(c_{eq}) + c_{eq} - c_0 \tag{A.4}$$

where the correct equilibrium concentration, c_{eq}, is given by the root of $F(c_{eq})$ i.e. where:

$$F(c_{eq}) = 0 \tag{A.5}$$

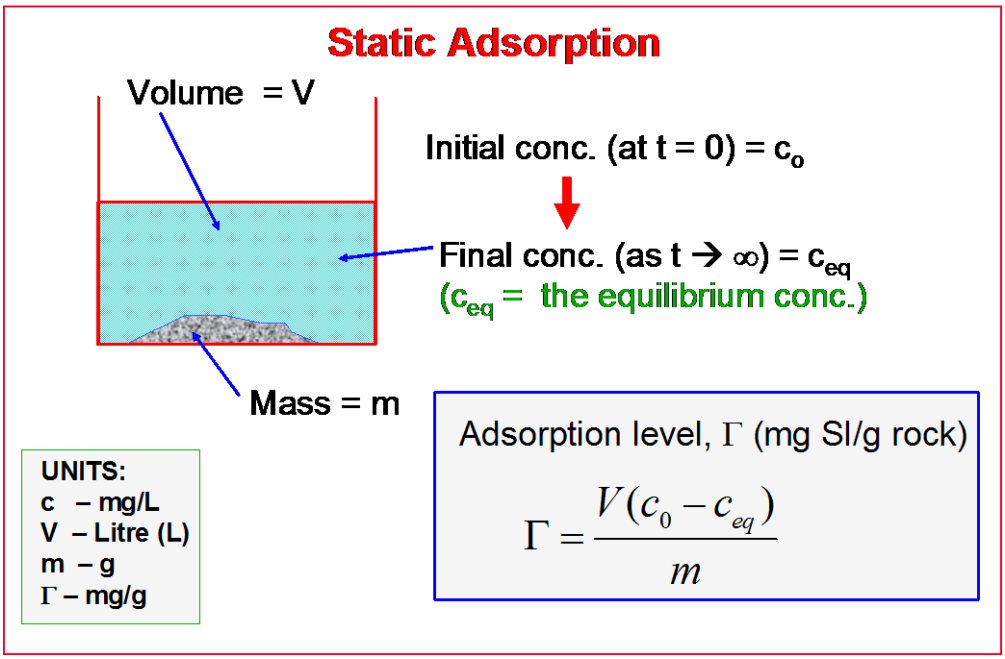

Figure A.1: Shows the process of simple static adsorption on a porous medium comprising a mineral separate, of mass(m) e.g. sand, kaolinite, siderite etc. See units.

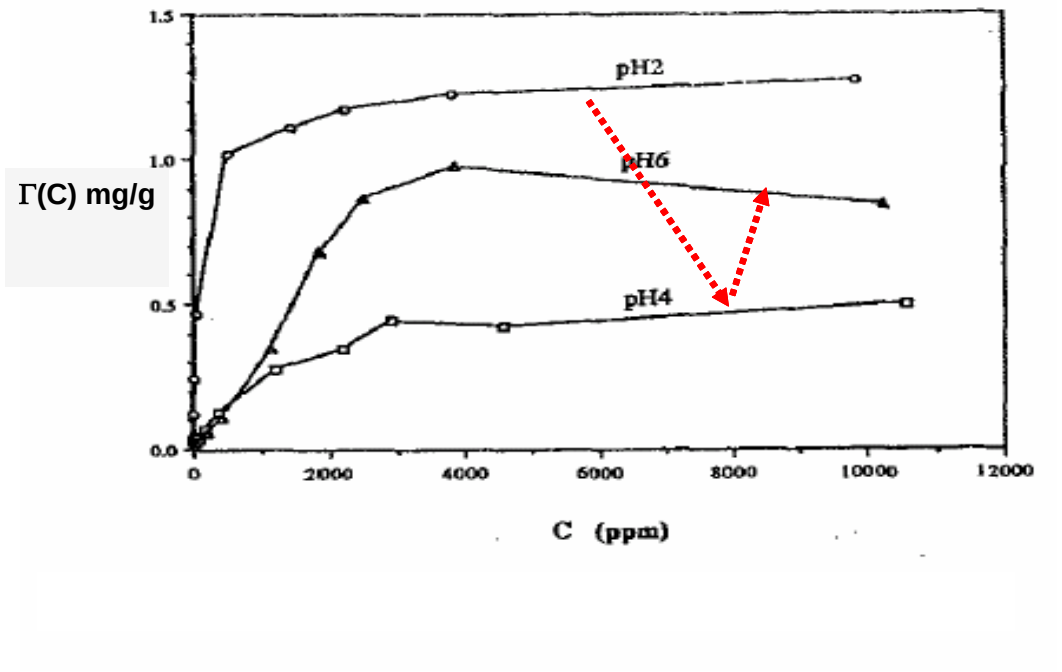

Figure A.2: Experimental static adsorption isotherms, $\Gamma(C)$, for DETPMP on crushed core material. At various pH values, 2, 4 and 6 at T = 25°C (Yuan et al, Adv. Oil. Chem., 1994).

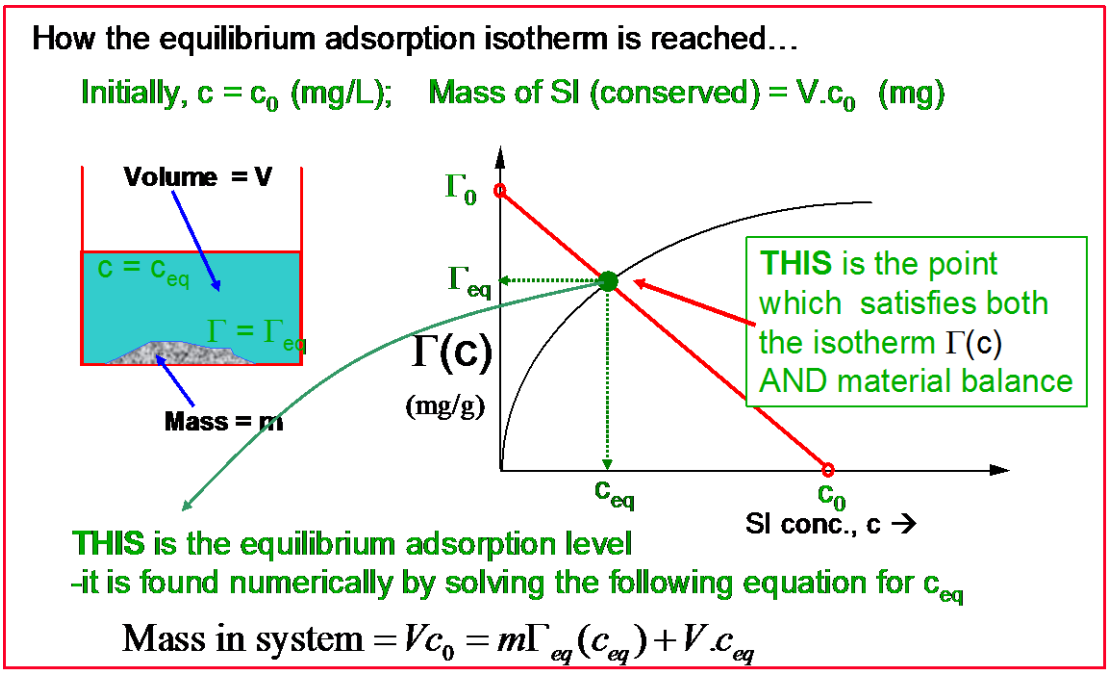

Figure A.3: Schematic showing how the static adsorption isotherm is reached as $c_0 \rightarrow c_{eq}$ such that the mass conservation is consistent with the adsorption isotherm, $\Gamma(C)$.

Numerical Examples for Adsorption: We illustrate the calculation of the equilibrium SI concentration using a numerical example where we take the Freundlich form of Γ where:

$$\Gamma_{eq}(c_{eq}) = \alpha\left(c_{eq}\right)^{\beta} \qquad \text{[c in ppm]} \tag{A.6}$$

With α = 0.021 and β = 0.73 where c is in ppm and Γ is in mg showing different /g. These parameters are not arbitrary since they relate to our experimental results which will be presented below. However, this case serves as a useful numerical example to demonstrate some of the calculations and for later use in the coupled adsorption/precipitation calculations. If the molecular weight of the SI is given by M_{SI}, then the Freundlich isotherm with molar concentration of c (M) would be:

$$\Gamma_{eq}(c_{eq}) = \alpha'\left(c_{eq}\right)^{\beta} \qquad \text{[C in M]} \tag{A.7}$$

Where $\alpha' = \left(1000 M_{SI}\right)^{\beta}.\alpha$. The Freundlich isotherm for this example is shown in Fig. A.4 and, for various values of initial concentration, c_0, we can solve Eq. (A.4) to find the equilibrium SI concentration, c_{eq}. This is illustrated by cases A, B and C in this figure where 3 values of c_0 = 2000, 1500 and 1000ppm, lead to final equilibrium values of, c_{eq} = 1493, 1094 and 705ppm. Note that by taking a series of values of 4.05, 3.24 and 2.36 mg SI/g rock, we are able to build up the points on the static adsorption isotherm as has been done for the case in Fig. A.2 above.

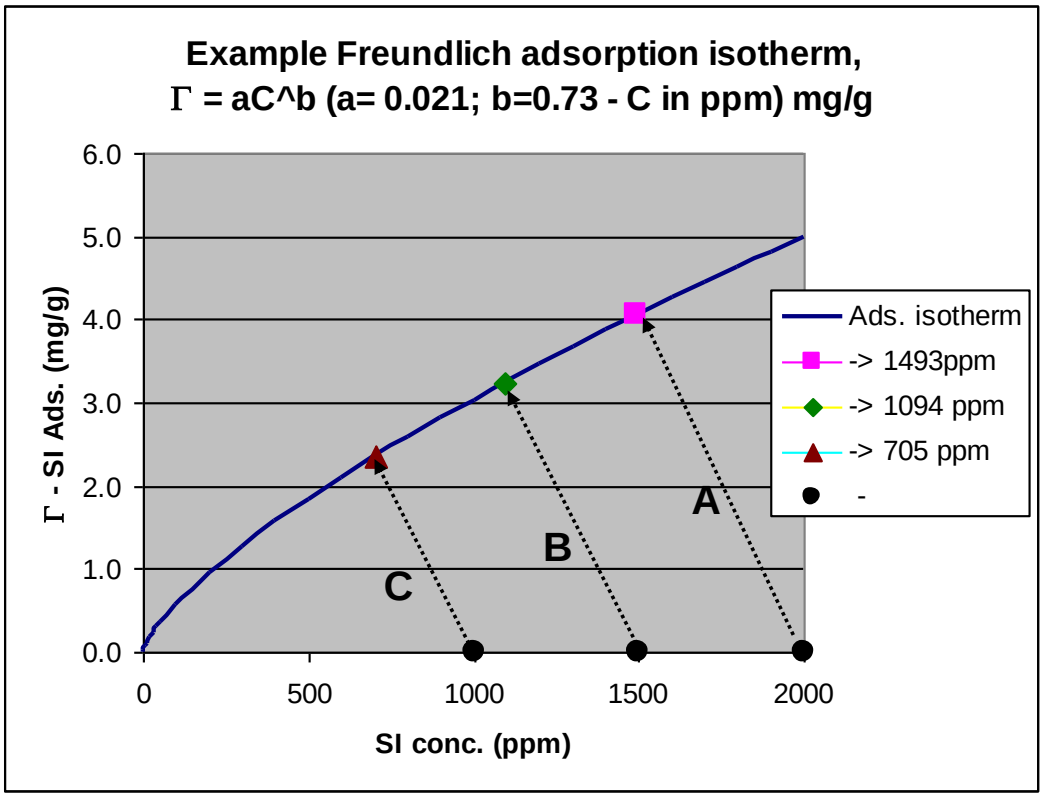

Figure A.4: The Freundlich isotherm of form, $\Gamma_{eq}(c_{eq}) = \alpha\left(c_{eq}\right)^{\beta}$, where α = 0.021 and β = 0.73 where c is in ppm and Γ is in mg/g. Cases A, B and C show the numerical calculation for initial concentrations of SI, c_0 = 2000, 1500 and 1000ppm, respectively, where the final equilibrium values are, c_{eq} = 1493, 1094 and 705ppm.

The effect of the solid mass/liquid volume ratio, (m/V), can be seen by comparing Cases C and D in Fig. A.5. Cases C and D have the same initial concentrations of SI, c_0 = 1000ppm, but they have different (m/V) ratios; Case C (m/V) = 125 and Case D (m/V) = 250. Note that, as we change (m/V) the final equilibrium point simply moves "along the isotherm". This is an important point since it will later help us to diagnose when precipitation is occurring, as explained in detail below.

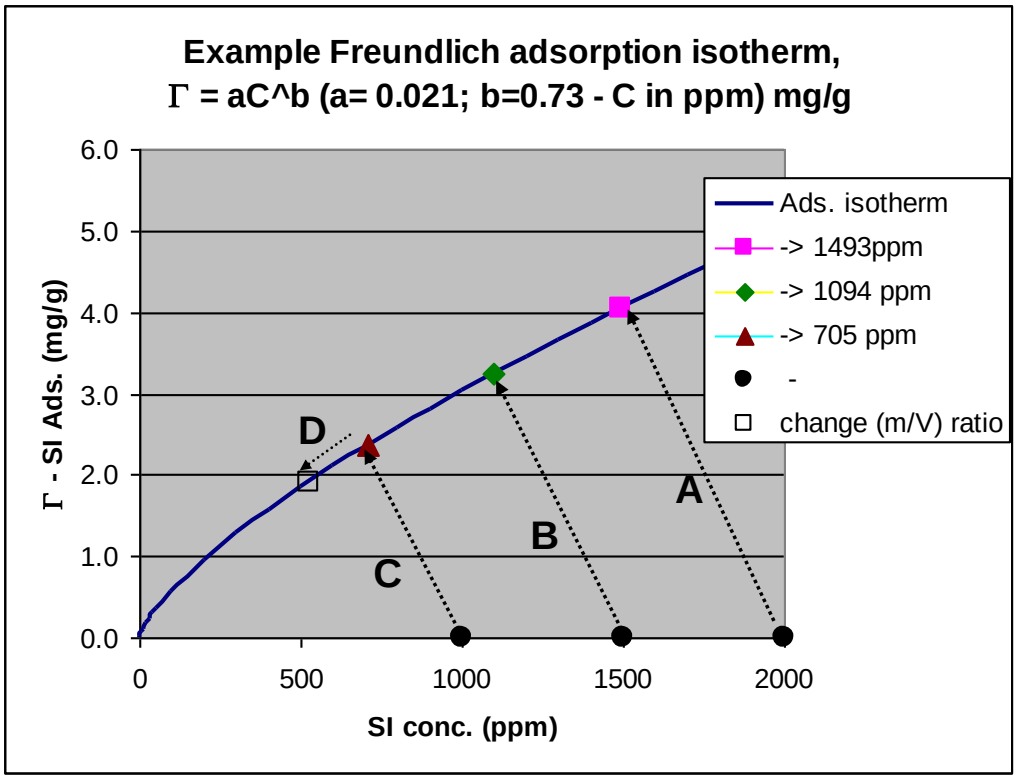

Figure A.5: The Freundlich isotherm of form, $\Gamma_{eq}(c_{eq}) = \alpha\left(c_{eq}\right)^{\beta}$, where α = 0.021 and β = 0.73 where c is in ppm and Γ is in mg/g. Case D is the same as Case C with initial concentrations of SI, c_0 = 1000ppm, but with different (m/V) ratios; Case C (m/V) = 125 and Case D (m/V) = 250.

Coupled Adsorption/Precipitation: We now extend the analysis above for pure adsorption to the case where both adsorption and precipitation can occur simultaneously. This is shown schematically in Fig. A.6 where we envisage that precipitation occurs by the formation of the calcium salt of the SI, i.e. by precipitation of SI_Ca. In general, the stoichiometry of this precipitation reaction is as follows:

$$SI + n.Ca \rightleftarrows SI\_Ca_n \qquad \text{(A.8)}$$

Where n Ca ions may bind to a single SI molecule. The solubility of this sparingly soluble salt would be described by an equilibrium solubility product, K_{sp}, of the form:

$$K_{sp} = [SI].[Ca]^n \qquad \text{(A.9)}$$

Some additional notation is introduced in Fig. A.6 as follows:

- c_{10} and c_{1f} - initial (t = 0) and final equilibrium (t→ ∞) SI Molar concs. (M);
- c_{20} and c_{2f} - initial (t = 0) and final equilibrium (t→ ∞) Ca Molar conc. (M);
- Γ – is the adsorption which depends on c_{1f}, $\Gamma = \Gamma(c_{1f})$ (mg/g);
- Π – is the precipitation process depends on both c_{1f} (SI conc.) and c_{2f} (Ca conc.) through K_{sp} as follows:
- $K_{sp} = (c_{1f}).(c_{2f})^n$ in this notation when the system is at equilibrium; units of K_{sp} → M^{n+1};
- m_p is the actual mass of precipitate which forms.

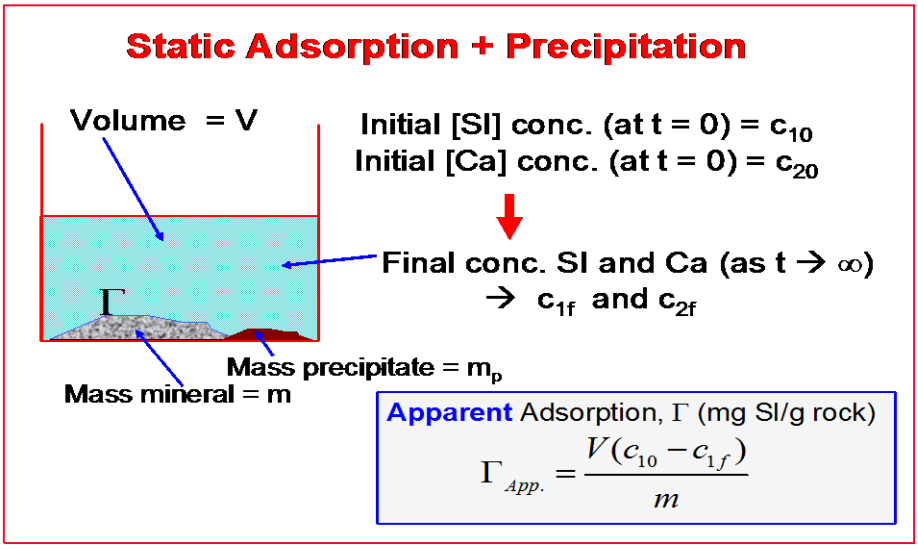

Figure A.6: Schematic showing how both coupled adsorption and precipitation can occur showing how this could be interpreted as an "apparent adsorption", $\Gamma_{App.}$

From the above quantities, we note that the initial and final values of SI concentration are c_{10} and c_{1f}. Some of this SI which is "missing" from the bulk solution is adsorbed and the remainder of it is part of the precipitate. However, if we assumed that all of this "missing" SI is adsorbed, then we would calculate an "apparent adsorption", $\Gamma_{App.}$, as follows:

$$\Gamma_{App.} = \frac{V(c_{10} - c_{1f})}{m} \tag{A.10}$$

which would clearly be an over-estimate of the actual adsorption (since some of this would be precipitate) but it is what would be seen in an actual experiment if the above formula were applied.

We now derive the main equations describing coupled adsorption/precipitation based on the view of the process discussed above and shown schematically in Fig. A.6. As before, the total masses of SI and Ca, which are conserved, are given by:

Total initial Mass of SI = $V.M_{SI}.c_{10}$

and at equilibrium (after adsorption and precipitation), then,

$$\text{Total mass of SI} = V.M_{SI}.c_{1f} + \left(\frac{m}{1000}\right).\Gamma\left(c_{1f}\right) + \phi.m_p \tag{A.11}$$

Where ϕ is the fraction of the precipitate (of formula SI_Ca_n) which is actually SI, i.e.

$$\phi = \left(\frac{M_{SI}}{M_{SI} + n.M_{Ca}}\right) \tag{A.12}$$

Note that denominator of 1000 appears in Eq. (A.11) since m. Γ is in mg and all other masses in this equation are in g. Both adsorption and precipitation are contributing to the change in SI concentration from c_{10} to c_{1f}. However, the precipitate is the only cause of the change in calcium concentration from c_{20} to c_{2f}, and since the stoichiometry is $SI + n.Ca \rightleftarrows SI\_Ca_n$, then the actual mass of precipitate must be given by:

$$m_p = \frac{V}{n}\left(c_{20} - c_{2f}\right)(M_{SI} + n.M_{SI}) \tag{A.13}$$

We can now use the above equations for ϕ and Γ (C1f) in Eq. (A.11) to obtain the following expression for the mass of SI:

Total Mass of SI =

$$V.M_{SI}.c_{1f} + \left(\frac{m}{1000}\right).\Gamma\left(c_{1f}\right) + \left(\frac{M_{SI}}{M_{SI} + n.M_{Ca}}\right).\frac{V}{n}\left(c_{20} - c_{2f}\right)\left(M_{SI} + n.M_{SI}\right) \tag{A.14}$$

Which simplifies to:

Total Mass of SI =

$$V.M_{SI}.c_{1f} + \left(\frac{m}{1000}\right).\Gamma\left(c_{1f}\right) + \left(\frac{V.M_{SI}}{n}\right)\left(c_{20} - c_{2f}\right) \tag{A.15}$$

Thus, by material balance (conservation of mass of SI), we can write:

$$V.M_{SI}.c_{10} = V.M_{SI}.c_{1f} + \left(\frac{m}{1000}\right).\Gamma\left(c_{1f}\right) + \left(\frac{M_{SI}}{n}\right)\left(c_{20} - c_{2f}\right) \tag{A.16}$$

Which can be divided through by $V.M_{SI}$ to obtain:

$$c_{10} = c_{1f} + \left(\frac{m}{V.M_{SI}1000}\right).\Gamma\left(c_{1f}\right) + \left(\frac{1}{n}\right)\left(c_{20} - c_{2f}\right) \tag{A.17}$$

The main problem with the above equation is that it has 2 unknowns, c_{1f} (SI conc.) and c_{2f} (Ca conc.), which means that it cannot be solved as written. However, we can eliminate the Ca concentration, c_{2f}, by using the solubility product equation (if there actually <u>is</u> a precipitate) for the SI_Ca_n - (i.e. $K_{sp} = \left(c_{1f}\right).\left(c_{2f}\right)^n$) to note that:

$$c_{2f} = \left(\frac{K_{sp}}{c_{1f}}\right)^{1/n}$$

Hence, this expression for c_{2f} can be substituted into Eq. (A.17) above to obtain the equation for coupled adsorption/precipitation:

$$c_{10} = c_{1f} + \left(\frac{m}{V.M_{SI}1000}\right).\Gamma\left(c_{1f}\right) + \left(\frac{1}{n}\right)\left(c_{20} - \left(\frac{K_{sp}}{c_{1f}}\right)^{1/n}\right) \quad \text{(A.18)}$$

As before, this equation can be rewritten in the final working form as:

$$F(c_{1f}) = c_{1f} + \left(\frac{m}{V.M_{SI}1000}\right).\Gamma\left(c_{1f}\right) + \left(\frac{1}{n}\right)\left(c_{20} - \left(\frac{K_{sp}}{c_{1f}}\right)^{1/n}\right) - c_{10} \quad \text{(A.19)}$$

Where, at equilibrium adsorption/precipitation, we simply have to solve this equation for c_{1f} i.e. find the root of $F(c_{1f}) = 0$. Note that this is the same equation as Eq. (5.17) for pure adsorption except for the additional coupled term describing precipitation, $\left(\frac{1}{n}\right)\left(c_{20} - \left(\frac{K_{sp}}{c_{1f}}\right)^{1/n}\right)$.

Note that Eq. (A.18) applies if (and only if) there is definitely a precipitate i.e. $\left(c_{1f}\right).\left(c_{2f}\right)^{n}$ is not less than K_{sp}. If there is no precipitate, then the substitution, $c_{2f} = \left(\frac{K_{sp}}{c_{1f}}\right)^{1/n}$, does not apply and it happens that the quantity $\left(c_{20} - \left(\frac{K_{sp}}{c_{1f}}\right)^{1/n}\right)$ < 0 which is unphysical. Hence in solving the main working Eq (A.19), we can use it for all cases of adsorption only or coupled adsorption/precipitation by setting the quantity $\left(c_{20} - \left(\frac{K_{sp}}{c_{1f}}\right)^{1/n}\right)$ to its actual value if it is ≥ 0, or to zero otherwise.

APPENDIX B: MATERIAL SAFETY DATA SHEET (MSDS)

I. DETPMP - Diethylene tetra-amine penta (methylenephosphonic acid)

II. OMTHP - Octamethylene tetra-amine hexa (methylenephosphonic acid)

III. HMDP - Hexametylene diamine tetra-methylene phosphonic acid

IV. HMTPMP - Bis(hexamethylene) tri-amine pentabis (methylene phosphonic acid)

I. HMTPMP - Bis(hexamethylene) tri-amine pentabis (methylene phosphonic acid)

Product Technical Data

BRIQUEST® 5123-45A

Phosphonate for Water Treatment Applications

August 2005
Issue No: 8

Introduction

BRIQUEST® 5123-45A is a water soluble phosphonate specifically designed for use as a multifunctional scale inhibitor in water treatment applications, where its high thermal stability, good calcium tolerance and broad spectrum activity against carbonate, sulphate and oxalate scales finds many beneficial uses[①].

Structure

BRIQUEST® 5123-45A is an aqueous solution of bishexamethylenetriamine pentakis(methylenephosphonic acid).

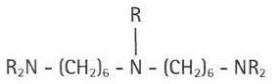

$$R_2N - (CH_2)_6 - \underset{\displaystyle R}{\underset{|}{N}} - (CH_2)_6 - NR_2 \qquad R = CH_2PO_3H_2$$

Performance Benefits

Feature	Benefit
BRIQUEST® 5123-45A exhibits enhanced thermal stability compared to conventional pentaphosphonate and is effective against carbonate and sulphate scales	Suitable for use as an alternative to pentaphosphonate in higher temperature oilfield systems
BRIQUEST® 5123-45A is particularly effective against calcium sulphate	A preferred product for use in low pH formation waters with low barium but high calcium levels
BRIQUEST® 5123-45A is an excellent inhibitor for oxalate based scales	Useful for incorporation into scale control programmes for paper and sugar processing

Applications

For oilfield squeeze treatment applications, the beneficial properties of **BRIQUEST® 5123-45A** can be further enhanced by blending with chelating agents or certain sulphonated polymers to aid in the placement of the product within the reservoir.

For conventional water treatment applications, **BRIQUEST® 5123-45A** can be blended with other phosphonate or polymeric based scale and corrosion inhibitors to give synergistic blends.

① As with all aminomethylene phosphonates, **BRIQUEST® 5123-45A** possesses antiscalent, sequestration and dispersant properties and so finds varying uses outside of water treatment applications.

Rhodia
Novecare

CHALLENGING BOUNDARIES

BRIQUEST® 5123-45A

Phosphonate for Water Treatment Applications

August 2005
Issue No: 8

Typical Properties

Appearance	-	Brown Liquid
Iron (as Fe)	-	100ppm max
Chloride (as Cl)	-	6% w/w max
Active Solids (as acid)	-	45 – 51% w/w
pH (1% w/v solution, 20°C)	-	2 max
SG (20°C)	-	1.20 – 1.26

Storage and Stability

BRIQUEST® 5123-45A is not adversely affected by freeze/thaw cycling.

Packaging

BRIQUEST® 5123-45A is available in HDHMW polythene containers and IBC's.

Rhodia Novecare Technical Services:

North America
Tel: +1 609 860 3919
Fax: +1 609 860 0076

Europe
Tel: +44 (0)121 541 3347
Fax: +44 (0)121 541 3351

Asia Pacific
Tel: +65 6775 0633
Fax: +65 6773 1641

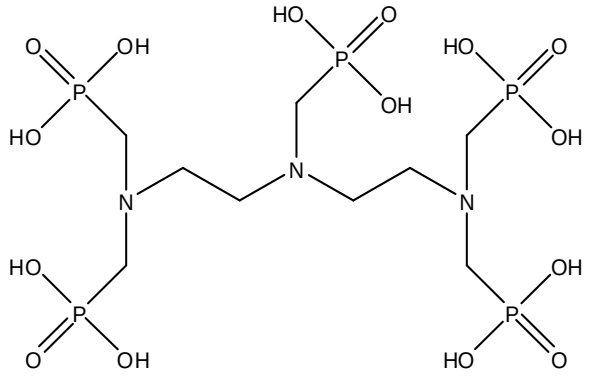

Properties	
Appearance	- Brown liquid
Iron (as Fe)	- 100ppm max
Chloride (as Cl)	- 6% w/w max
Active Solids (as acids)	- 45% w/w
pH (1% w/v soln, 20 C)	- 2 max
SG (20 C)	- 1.20 – 1.26
MWt.	- 573.25 g/mol

Table B.1: Structure and properties of DETPMP

II. OMTHP - Octamethylene tetra-amine hexa (methylenephosphonic acid)

Product Technical Data

BRIQUEST® 684-30S

Phosphonate for the Oil Industry

August 2005
Issue No: 8

Introduction

BRIQUEST® 684-30S is a water soluble phosphonate specifically developed for the oil industry, where its high thermal stability and efficacy at low pH are advantageous in squeeze treatment applications for bother carbonate and sulphate scale[①].

Structure

BRIQUEST® 684-30S is a proprietary formulation containing hexaphosphonate.

Performance Benefits

Feature	Benefit
BRIQUEST® 684-30S unlike other conventional aminomethylene phosphonates, only become protonated under strong acid conditions, eg: less than pH4	Retains its scale inhibition activity at low pH values
BRIQUEST® 684-30S exhibits a low affinity for dissolved iron	Effective in water containing high iron levels
BRIQUEST® 684-30S exhibits strong absorption properties on formation rock	Results in extended squeeze lifetimes for wells with high seawater breakthrough and moderate scaling potentials
BRIQUEST® 684-30S exhibits a reasonable tolerance towards methanol	Suitable for scale control in sub-sea deployment applications

Applications

BRIQUEST® 684-30S can be further enhanced by blending with chelating agents or certain sulphonated polymers to aid in the placement of the product within the reservoir.

① As with all aminomethylene phosphonates, **BRIQUEST® 684-30S** possesses antiscalent, sequestration and dispersant properties and so finds varying uses outside of oilfield applications.

Rhodia
Novecare

CHALLENGING BOUNDARIES

BRIQUEST® 684-30S

Phosphonate for the Oil Industry

Typical Properties

Appearance	-	Amber Liquid
Iron (as Fe)	-	Typically less than 30ppm
Chloride (as Cl)	-	Typically less than 6%
Active Solids (as acid)	-	Typically 30%
pH (1% w/v solution, 20°C)	-	Typically 6
SG (20°C)	-	Typically 1.34

Storage and Stability

BRIQUEST® 684-30S is not adversely affected by freeze/thaw cycling.

Packaging

BRIQUEST® 684-30S is available in HDHMW polythene containers, IBC's and bulk containers.

Rhodia Novecare Technical Services:

North America
Tel: +1 609 860 3919
Fax: +1 609 860 0076

Europe
Tel: +44 (0)121 541 3347
Fax: +44 (0)121 541 3351

Asia Pacific
Tel: +65 6775 0633
Fax: +65 6773 1641

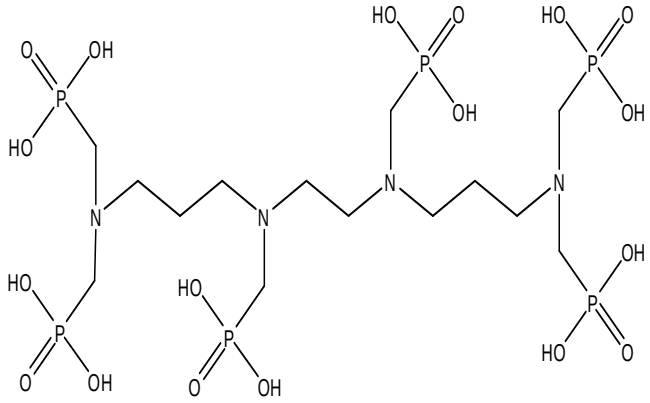

Properties	
Appearance	- Amber liquid
Iron (as Fe)	- < 30ppm
Chloride (as Cl)	- < 6%
Active Solids (as acids)	- 30% w/w
pH (1% w/v soln, 20 C)	- 2
SG (20 C)	- 1.34
MWt.	- 738.40 g/mol

Table B.2: Structure and properties of OMTHP

III. HMDP - Hexametylene diamine tetra-methylene phosphonic acid

Product Technical Data

BRIQUEST® 462-23K

Phosphonate for Water Treatment Applications

August 2005
Issue No: 7

Introduction

BRIQUEST® 462-23K is a water soluble phosphonate specifically designed for use as a multifunctional scale inhibitor in water treatment applications, where its excellent thermal stability and activity against sulphate scales finds many beneficial uses[①].

Structure

BRIQUEST® 462-23K is an aqueous solution of potassium hexamethylenediamine tetrakis (methylenephosphonate).

$R = CH_2PO_3H_2$

Performance Benefits

Feature	Benefit
BRIQUEST® 462-23K exhibits superior thermal stability (typically up to 160°C) compared to conventional phosphonates and is effective against carbonate and sulphate scales.	Suitable for use in high temperature scale control programmes.
BRIQUEST® 462-23K is particularly effective against calcium sulphate scales.	Suitable for use in systems with a high potential for calcium sulphate deposition.
BRIQUEST® 462-23K exhibits excellent compatibility with methanol.	Ideally suited for use in oilfield subsea deployment applications.

Applications

For oilfield squeeze treatment applications, the beneficial properties of **BRIQUEST® 462-23K** can be further enhanced by blending with chelating agents or certain sulphonated polymers to aid in the placement of the product within the reservoir.

For conventional water treatment applications, **BRIQUEST® 462-23K** can be blended with other phosphonate or polymeric based scale and corrosion inhibitors to give synergistic blends.

① As with all aminomethylene phosphonates, **BRIQUEST® 462-23K** possesses antiscalent, sequestration and dispersant properties and so finds varying uses outside of water treatment applications.

Rhodia
Novecare

CHALLENGING BOUNDARIES

BRIQUEST® 462-23K

Phosphonate for Water Treatment Applications

Typical Properties

Appearance	-	Clear Pale Yellow Liquid
Iron (as Fe)	-	50ppm max
Chloride (as Cl)	-	3% w/w max
Active Solids (as acid)	-	21 – 25% w/w
pH (1% w/v solution, 20°C)	-	6.5 – 7.5 max
SG (20°C)	-	1.23 – 1.29

Storage and Stability

BRIQUEST® 462-23K is not adversely affected by freeze/thaw cycling.

Packaging

BRIQUEST® 462-23K is available in HDHMW polythene containers, IBC's and bulk containers

Rhodia Novecare Technical Services:

North America
Tel: +1 609 860 3919
Fax: +1 609 860 0076

Europe
Tel: +44 (0)121 541 3347
Fax: +44 (0)121 541 3351

Asia Pacific
Tel: +65 6775 0633
Fax: +65 6773 1641

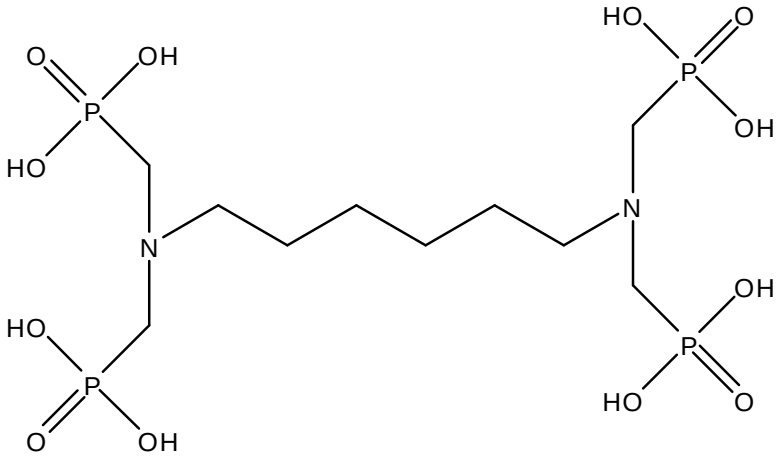

Table B.3: Structure of HMDP

IV. DETPMP - Diethylene tetra-amine penta (methylenephosphonic acid)

Product Technical Data

BRIQUEST® 543-45AS

Phosphonate for Water Treatment and Industrial Applications

August 2005
Issue No: 7
Page 1 of 2

Introduction

BRIQUEST® 543-45AS is a water soluble phosphonate specifically designed for use as a multifunctional scale inhibitor and sequestrant in water treatment and industrial applications[①].

Structure

BRIQUEST® 543-45AS is an aqueous solution of diethylenetriaminepentakis (methylenephosphonic acid).

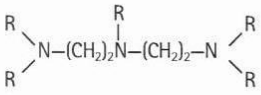

$R = CH_2PO_3H_2$

free acid structure

Performance Benefits

Feature	Benefit
BRIQUEST® 543-45AS exhibits crystal modification properties and is effective at controlling carbonate and sulphate scale	Suitable for use in scale control programmes in a range of industries, eg: oilfield, cooling towers, paper processing and reverse osmosis
BRIQUEST® 543-45AS is a superior barium sulphate inhibitor and adsorbs strongly onto sandstone and limestone	Ideally suited for use in oilfield downhole (squeeze treatment) applications
BRIQUEST® 543-45AS is an excellent sequestrant for most metal ions and especially iron and manganese	Highly effective for the stabilisation of peroxide in paper, textile and detergent related applications
BRIQUEST® 543-45AS has ANSI/NSF Standard 60 certification for use as a Reverse Osmosis (RO) antiscalent	Safe to use in scale control programmes for RO systems producing potable water

Applications

For conventional water treatment applications, **BRIQUEST® 543-45AS** can be blended with other phosphonate or polymeric based scale and corrosion inhibitors to give synergistic blends.

① As with all aminomethylene phosphonates, **BRIQUEST® 543-45AS** possesses antiscalent, sequestration and dispersant properties and so finds varying uses outside of water treatment and industrial applications.

Rhodia
Novecare

CHALLENGING BOUNDARIES

BRIQUEST® 543-45AS

Phosphonate for Water Treatment and Industrial Applications

Typical Properties

Appearance	-	Clear Amber Liquid
Iron (as Fe)	-	Typically less than 50ppm
Chloride (as Cl)	-	Typically less than 6%
pH (1% w/v solution, 20°C)	-	Typically 2
SG (20°C)	-	Typically 1.42

Storage and Stability

BRIQUEST® 543-45AS is not adversely affected by freeze/thaw cycling.

Packaging

BRIQUEST® 543-45AS is available in HDHMW polythene containers, IBC's and bulk containers.

Rhodia Novecare Technical Services:

North America
Tel: +1 609 860 3919
Fax: +1 609 860 0076

Europe
Tel: +44 (0)121 541 3347
Fax: +44 (0)121 541 3351

Asia Pacific
Tel: +65 6775 0633
Fax: +65 6773 1641

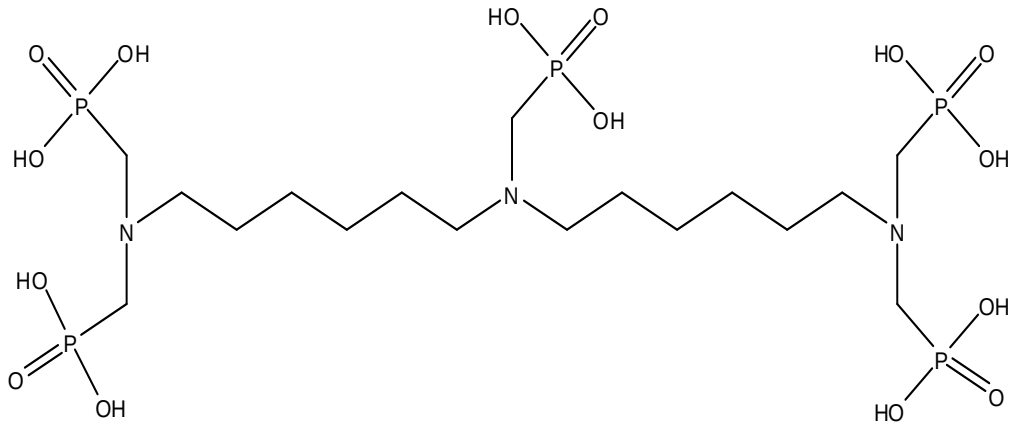

Table B.4: Structure of HMTPMP

APPENDIX C: GENERAL EQUIPMENT AND APPARATUS

I. Inductively Coupled Plasma - Optical Emission Spectroscopy (ICP-OES)

II. Environmental Scanning Electron Microscopy - Energy Dispersive X-Ray (ESEM-EDX)

III. Ultra Violet Spectrophotometer (UV)

IV. Particle Size Analyzer (PSA)

I. Inductively Coupled Plasma - Optical Emission Spectroscopy (ICP-OES)

ICP-OES is known as an effective tool for measuring ion compositions in water originating from industry as well as natural processes. In the oil and gas industry, many laboratories routinely use this technique to determine the ionic composition of oilfield brines. In this study, ICP results relating to scale inhibitor analysis were are presented, where the detection limit is within the scope of the experiments. The inhibitors that were analyzed are phosphonates, although poly-phosphino carboxylic acid (PPCA) SIs were also tested (Bedford *et al*., 1994; Christian, 1994 and Ciba-Giegy Industrial Chemicals (Now FMC Ltd., 1990). These methods had also been tested earlier between synthetic and field produced brines within the FAST group; which produced accurate results for both inhibitors, and in both type of brines (Mc Teir *et al*., 1993; Pennington, 1988). This information is essential as synthetic brines are used for all the experiments in this study.

One of the ICP spectrophotometer currently being used by the Group is described below and illustrated in Figure C.1:

Instrument Parameters:

Make: Jobin Yvon (Instruments S.A.)

Model: JY 138 Ultrace ICP Optical Emission Spectrometer with upgraded solid-state generator and software V5 (JY Ultrace 138 ICP-OES Instruction Manual)

Mode: Sequential

Analytical lines: Phosphorous at 177.441 and 214.914nm

The ICP-OES has now replaced the routine analysis once previously performed by the Atomic Absorption Spectroscopy (AAS). For these studies, the analysis for the static and non-equilibrium experiments performed within the FAST group are now analyzed by ICP (Sorbie *et al*., 1992 and Graham *et al*., 1993, 1994, 1995, 1996). These experiments require analysis for phosphonate SI, calcium, magnesium, lithium, and on occasion, iron and aluminium. Phosphonate SI analysis was performed on the ICP,

whereas poly-phosphino was conducted using wet chemical analysis which has better sensitivity and repeatability. The wavelengths and calibration standards utilized for phosphonate as well as PPCA analysis on the ICP are included. Many other elements, including barium and strontium, which are routinely analyzed for barium sulphate inhibition efficiency tests, have been analyzed within the FAST group.

The technique of ICP has the advantage of robustness with respect to solution interferences which affect many wet chemical techniques, and can therefore be used to determine residual levels of scale inhibitor in produced water (Kan *et al*., 1991). The ICP-OES is less time consuming than the wet chemical assays the calibration range/methods used have been adapted over time.

ICP is an instrumental analysis technique based on atomic emission spectrometry. The quality of its results therefore depends primarily on the quality of the spectrometer used to analyze the light emitted by the atoms in the sample introduced into the torch. ICP-OES uses inert, optically transparent Argon gas to create a high temperature plasma (up to 10,000^{o}K), generated by radio magnetic fields induced by a copper coil. Samples are introduced via an auto-sampler and nebulized into an aerosol before entering the plasma where they are excited. The atoms in the plasma emit light (photons) with characteristic wavelengths for each element. This light is recorded by one or more optical spectrometers, which provide optimum sensitivity across the full wavelength range from 160-800nm, and when calibrated against standards this technique provides a quantitative analysis of the original sample. Table C.1 presents the wavelengths and concentrations of the calibration standards that are used for different elements.

The procedures followed for each of the elements is similar. However different concentrations of calibration standards are employed for the different elements. The measurement time for each element method is 2 seconds, mode 5 is used for single point analysis and primary/secondary slits of 18/81 respectively are used. The exception to this is the PPCA analysis, which uses the Gaussian mode of 2 and primary/secondary slits of 18/15 respectively. In between samples there is a rinse time of 60sec before it returns to analyze the samples. The sampling times allow for sample introduction; 3 minutes to analyze 1 element and 5-6 minutes to analyze 4 elements.

Experimental Procedure:

1. Clean and start up the ICP. Allow to heat up for 0.5-1 hour with distilled water flowing through the machine. The rinse solution between analysis is 5% Nitric acid and flows for 60sec before moving back to the next sample.
2. Prepare the element calibration standards within the same matrix (normally synthetic SW, FW or 1% NaCl solution) that the samples have been diluted in.
3. After the heat up period, select the method to be used to analyze the samples ensuring that the same method shows in the box at the top of the analysis sheet. This ensures that the correct elements are analyzed.
4. Set up an analysis run to auto-search, auto-attenuate and auto-search again on the highest calibration standard. The next highest standard can now be auto-searched. This process is continued until all of the element containing calibration standards (not standard LOW, which is matrix solution) have been auto-searched. Once the run begins check that the peaks observed are in the middle of the wavelength window and the top standard is the full height of the screen.
5. The machine is now ready to calibrate. Set–up a run to calibrate for the elements in the selected method/matrix.
6. After calibration has been achieved, i.e. a straight line through zero, with an R square number of approximately 1, the ICP is now ready to analyze samples.
7. The samples are placed in the auto-sampler racks. Calibration standards are placed in a rack at the end of the samples. When setting up the analysis run, begin with selecting each of the standards to be analyzed as a sample, then analyze 10-12 samples before returning to the standards. Repeat this formation until all samples are analyzed, ending with a set of standards.
8. At the bottom of the sample run, add in a description of the run to help with later identification under the specific method. The analysis file is then saved onto the computer.
9. The calculated concentrations, with respect to the previous calibration, are then stored on the computer and printed out.
10. If the results for the calibration standards throughout the run have drifted from their intended concentrations, then the samples can be drift corrected.

Figure C.1: ICP-OES - JY 138 Ultrace

Element	Wavelength (nm)	Calibration (Standard)
Barium	233.527	0, 10, 25, 50
Strontium	338.071	0, 10, 25, 50
Calcium	317.933	0, 50, 200
Magnesium	279.806	0, 25, 100
Iron	259.940	0, 10, 40
Lithium	670.784	0, 5, 20
Aluminium	308.215	0, 5, 50, 250
Silicon	212.412 or 250.690	0, 5, 50, 250
Sodium	330.237 <100ppm & 589.592 >100ppm	0, 10, 100, 1000
Cobalt	237.86	0, 2, 5
Chromium	205.55	0, 2, 5
Copper	324.754 or 224.700	0, 10, 100

Nickel	221.64	0, 2, 5
Zinc	213.856 or 334.502	0, 10, 100
Molybdenum	202.03	0, 2, 5
Germanium	265.118 or 209.426	0, 10, 100
Boron	249.67	0, 10, 100
Potassium	766.490	0, 20, 100, 1000
Phosphorus - phosphonate	177.440 (0->50ppm) & 214.914 (0, 50, 500,2500)	0, 5, 50, 500, 2500
Phosphorus - PPCA	177.440 (0->50ppm) & 177.441 (0, 50, 500,2500)	0, 5, 50, 500, 2500
Lead	220.353	0, 5, 10
Tin	189.989 or 235.484	0, 10, 100
Tungsten	209.47	0, 2, 5
Sulphur	180.676	0, 5, 10 or 0, 10, 50, 250
Examples of Diluents: NaCl, DW, SW, FW, KCl/PVS, EDTA/KOH, DTPA/KOH, 5% Nitric acid and Acetic acid.		

Table C.1: ICP-OES wavelengths and calibration standards used for different elements.

II. Environmental Scanning Electron Microscopy - Energy Dispersive X-Ray (ESEM-EDX)

For this study, a Philips XL30 Environmental Scanning Electron Microscope (ESEM), with an Oxford Instruments cryo-stage, and an EDAX energy dispersive x-ray detector (EDX) was used for the analysis. These can be used to image and/or analyze virtually any substance, including wet, oily and out gassing samples that cannot be examined by more conventional SEMs (http://www.pet.hw.ac.uk/cesem/intro.htm). This is presented in Figure C.2.

An Environmental Scanning Electron Microscope (ESEM) is specifically designed to be able to examine micro-structural and ultra-structural details of samples, within a SEM chamber, in their uncoated natural state. An ESEM is able to examine wet, oily and out-gassing samples, without any form of preparation, and is able to maintain specimens within their natural state for prolonged periods within the ESEM viewing chamber. The ESEM works at low vacuum (typically 2 - 6 Torr), and utilizes a chamber gas for imaging, charge suppression and sample humidity.

ESEM is specifically suited to dynamic experimentation at the micron scale and below. ESEM technology allows for dynamic experiments involving fluids, and the possibility of imaging samples undergoing compression and tension. ESEM can therefore be regarded as a micro dynamic experimentation chamber where materials can be examined at a range of pressures, temperatures, under a variety of gases/fluids.

In simpler terms, scanning electron microscopy occurs when an electron beam is scanned across the surface of a sample. As the electrons strike the sample, a variety of signals are generated and it is the detection of these signals that produces an image or the elemental composition of a sample. There are a number of detectors that can be used under a number of different conditions, such as low or high vacuum, cryo-SEM and wet ESEM work. These detectors themselves can be split into categories depending on how they detect the sample signals. For instance, there are secondary electron detectors, solid state backscattered detectors, the environmental secondary electron detector and gaseous secondary electron detectors.

In the XL30 ESEM, the two detectors for high vacuum mode are an Everhardt-Thornley secondary electron detector and a solid state backscattered detector. Both these detectors are permanently within the chamber whereas the various environmental detectors available, all clip into the detector socket at the back of the chamber and are inserted as and when required. A summary of detectors and their suitable detection conditions are presented in Table C.2 (Philips XL30 ESEM Instruction manual).

The signals that provide the greatest amount of sample information in SEM are the secondary electrons, backscattered electrons and X-rays. The processes behind these techniques can be detailed as:

(a) Secondary electrons are emitted from the atoms occupying the top surface and are therefore able to produce a readily interpretable image of the surface,
(b) Backscattered electrons are primary beam electrons that are 'reflected' from atoms in the solid,
(c) X Spectrometry or EDX is the interaction of the primary beam with atoms in the sample that causes shell transitions, resulting in the emission of x-rays. The emitted X-rays have an energy, characteristic of the parent element. Detection and measurement of the energy permits elemental analysis (Energy Dispersive X-ray Spectroscopy or EDX). EDX can provide rapid qualitative, or with adequate standards, quantitative analysis of elemental composition with a sampling depth of 1-2 microns. X-rays may also be used to form maps or line profiles, showing the elemental distribution in a sample surface.

Before using ESEM or EDX, the user should always refer to the manufacturers instruction manual (Philips XL30 ESEM Instruction manual) and receive training before commencing work. However, a very general summary of the procedure is as follows;

a. Select the required detector.
b. Load samples into chamber.
c. Select mode – high, low, environmental and the corresponding conditions.
d. Ensure chamber is ready for use.
e. Focus the detector.

f. The SEM is now ready to image/analyse the samples.

g. When the process is finished, release the samples from the chamber.

Figure C.2: ESEM - Philips XL30 at Heriot-Watt University

Detector	Working Mode	Position
Everhardt-Thornley secondary electron	High vacuum	Permanently inside chamber
Backscattered detector	High vacuum	Permanently inside chamber, parked at back
Solid state backscattered detector	High or low vacuum (0.1 – 1.00 Torr)	Stored at back of chamber in a sleeve. To use, remove sleeve and mount under the pole piece.
Environmental secondary electron detector	Environmental 500micron detectors – P ≤ 10 Torr. 300micron detectors for higher P	Primarily SE but incorporates a substantial BSE signal. Detector is cap shaped and fits over the wet mode insert/bullet. Used in conjunction with a hook adaptor which plugs into the GSED (Gaseous SED)
Gaseous secondary electron detectors	Environmental, P ≈ 6 Torr	Fits over end of wet mode bullet/insert and clips into GSED connector at back of

	500micron wet specimens remain hydrated at P ≤ 10 Torr. 1000micron – wider field of view but P ≤ 5 Torr	chamber
Large field gaseous secondary electron detector (LF-GSED)	Low vacuum (0.1-1.00 Torr). Can be used in a water vapour atmosphere or another gas such as Nitrogen.	Contains a component of BSE. Used in conjunction with low vac/high vac bullet/insert and is plugged into the GSED connector socket at the back of ESEM chamber.
Gaseous backscattered secondary electron detector (GBSED)	Full environmental, P ≤ 10 Torr for 500micron aperture.	3 modes – SE, SE&BSE and BSE. Changes made by using pull-down 'detectors' menu. The detector must be worked at a distance of 10mm due to its size.
Bullet	High or ≤ 1 Torr low vacuum	Screwed into pole piece. It changes pumping regime of lower part of column and forms an attachment point for the various environmental and BSE detectors.
ESEM bullet	Full wet ESEM work. Low vacuum where high conical ESD detector cap is used to minimise the gas path length during EDX analysis.	Screwed into pole piece. It changes pumping regime of lower part of column and forms an attachment point for the various environmental and BSE detectors.

Table C.2: ESEM - Summary of detectors and their detection conditions

III. Ultra Violet Spectrophotometer (UV)

For this study, the UV/VIS spectrophotometer was used for the determination of sodium iodide (iodide ion) concentration in brines. This measurement was carried out in-line during sand pack characterization to measure dead volume and pore volume of the sand pack column. The instruments used for the study was the Campsec M302 (Figure C.3).

Experimental Procedure:

Sodium Iodide (iodide ion) concentrations were determined by measuring the absorbance of the sample and using a calibration curve equation to determine the concentration. The set up of the spectrophotometer to measure absorbance is detailed below:

a. Switch the instrument on using the power on switch located at the right hand side, towards the rear. Allow 15 minutes for the instrument to stabilize.
b. Set the required wavelength in nanometers (in this case is 230nm).
c. If working in the ultraviolet range (200-400nm) switch on the deuterium lamp using the UV lamp push button switch (after 30 seconds the lamp lights and the LED is illuminated) and allow up to 15 minutes for the lamp output to stabilize.
d. Set the Conc/%T/Abs control to Abs so the read-out appears in absorbance units.
e. To set the absorbance read-out to zero, place a 2 cm cuvette filled with distilled water in the cell holder and close the sample compartment lid. Use either the auto zero push button switch or 100%T control to set the absorbance to 0.

Other important points are;

Always consult the appropriate instruction manual for the specific model (Camspec M302 UV/Vis Spectrophotometer Instruction manual). The cell should be washed out with some of the sample solution, emptied and re-filled with the sample solution before the absorbance is recorded. Wash out the cell with distilled water in between analysing each sample and ensure the spectrophotometer remains at zero. It is essential that the cell is orientated in the same direction for zeroing and for every analysis.

Notes:

1. Always wipe the transparent faces of the cell with a clean tissue to remove any drops of solution,
2. Check that there are no air bubbles on the inner walls of the cell,
3. The single most important aspect of inhibitor residual assay is to ensure that all glassware is cleaned thoroughly prior to use.

These features can lead to erroneous absorbance readings.

Figure C.3: UV/Vis Spectrophotometer - Camspec M302

IV. Particle Size Analyzer (PSA)

Particle size and its distribution are important information required prior to executing static adsorption/precipitation or non-equilibrium sand pack experiments. For this study, sand, kaolinite and siderite minerals were measured before being used in the various experiments. Having a consistent size and distribution is important for the analysis as adsorption/precipitation (particularly adsorption) onto these minerals very much depends on their particle size and distribution (i.e. specific surface area). The Malvern Master Sizer MS-20 was used to measure particle size and its distribution. Refer to Figure C.4 (Malvern Master Sizer MS-20 Instruction Manual)

This machine uses the principle of laser diffraction to determine the particle size of the minerals described in Chapter 4. The technique of laser diffraction is based around the principle that particles passing through a laser beam will scatter light at an angle that is directly related to their size.

Operation Procedure:

a. Turn on the instrument. The switch is located on the back left hand side. The laser must also be switched on by turning the key adjacent to the switch.
b. Attach the appropriate lens to the flow cell. The following lens will analyze these size ranges

Lens	Size Range
300 mm	1.2 - 600 µm
100 mm	0.5 - 180 µm
45 mm	0.1 - 80 µm

c. Allow the instrument to warm up for 30 minutes.
d. Switch on the PC and select Malvern Mastersizer option (F1).
e. At the instrument parameters page type "easy" to select the "Easy" measurement mode.

f. Press F10 - Set Parameters.

g. Press the END key to change the following parameters

Presentation	- "Std"
Focal Length	- Input the lens to be used
Beam Length	- "2.2nm" is standard
Data Storage	- Facility does not work
Kill Data	- "0" always set as this

h. Press F2 (Sample details) and input sample details.

i. Introduce mobile phase into sample cell and start stirrer (set to 1/3 of max speed) so that fluid flows through the flow cell.

j. Press "a" to align the laser.

k. Press F3 (Set Zero). This sets the background level for the analysis. The mobile phase should be flowing through the cell at this point.

l. Dropwise, add dispersion to be analysed to mobile phase.

m. Press F4 (Check Sample Concentration) to assess the sample concentration and obstruction level (This value must be between 0.1 and 0.3). If below add more of the dispersion until range is reached.

n. Press F5 to measure particle size distribution.

o. The results obtained are printed out as the table detailed overleaf.

Note:

- Normally, an initial first pass measurement is made using the 300mm lens to roughly ascertain the samples distribution. Following this, an approximate particle size estimate can be made and the appropriate lens can then be used.
- Following a change in lens, the flow cell must be emptied, rinsed clean and the mobile phase is introduced to the cell. The complete procedure (from step 6 to step 15) must then be performed.

Figure C.4: Particle Size Analyzer - Malvern MS-20

REFERENCES

Bedford, C. T., Burns, P., Fallah, A., Garnham, P. J. and Barbour, W. J.: "*A new assay for phosphino carboxylate scale inhibitors at the 5ppm level*," presented at the Royal Society of Chemistry Symposium - Chemistry in the Oil Industry, held at Ambleside UK, 12-15 April 1994.

Bonnett, N, Fieler, E.R. and Hen, J.: "*Application of a Novel Squeeze Scale Inhibitor in the Beryl Field*", SPE 23107, presented at the Offshore Europe Conference held in Aberdeen, 3-6 September, 1991.

Boreng, R., Sorbie, K.S. and Yuan, M.D.: "*The Underlying Theory and Modelling of Scale Inhibitor Squeezes in Three Offshore Wells on the Norwegian Continental Shelf*", Proceedings of the Fifth International Oilfield Chemicals Symposium, Geilo, Norway, 20-23 March 1994.

Bourne, H.M., Bolton, J., Heath, S.M. and Lawless, T.A.: "*The importance of Non-Equilibrium Core Floods for the Modelling of Scale Inhibitor Squeeze Treatments*", paper presented at the Advances in Solving Oilfield Scale Problems Conference, Organised by IBC Ld., Aberdeen, 7-8 October 1992.

Boyle, M.J. and Mitchell, R.W.: "*Scale Inhibitor Problems Associated with North Sea Oil Production*", SPE8164, 1979.

Camspec M302 UV/Vis Spectrophotometer Instruction Manual.

Carlberg, B.L and Matthews, R.R.: "*Scale Control Technology - A Review*", paper for 22nd Annual S.W. Petroleum Short Course, pp. 263-270, Labbok, Texas, 17-18 April, 1975.

Carlberg, B.L. : "*Scale Inhibitor Precipitation Squeeze for Non-Carbonate Reservoirs*", SPE17008, presented at the SPE Production Technology Symposium, Lubbock, TX, 16-17 November 1987.

Carlberg, B.L.: "*Precipitation Squeeze Can Control Scale in High-Volume Wells*", Oil and Gas Journal, December 1983.

Carrell, C.D: "*The Occurence, Prevention and Treatment of Sulphate Scale in Shell Expro*", SPE16538, presented at Offshore Europe 87, Aberdeen, September 8-11, 1987.

Charleston, J.: "*Scale Removal in the Virden, Manitoba, Area*", SPE2160, presented at the 43rd Annual Fall Meeting of SPE of AIME held in Houston, Texas, 29 September - 2 October, 1968.

Chen P. and Graham G.M.: "*Examination of the Influence Flow Rate on Inhibitor Return Concentrations in Non-Equilibrium Core Flooding of Generically Different Scale Inhibitors Applied in Both Adsorption and Precipitation Treatments*." Presented at The 11th International Oil Field Chemicals Symposium, OFCS in Norway.

Christian G.D., 5th edition of Analytical Chemistry, John Wiley & Sons, Inc., 1994.

Ciba-Giegy Industrial Chemicals (Now FMC Ltd.), Product Information Bulletin: "*Bellasol S40/S45; Analytical procedure for their determination in oilfield brines,*" Manchester, January 1990. (Note: Ciba-Giegy Industrial Chemicals is now FMC Ltd.).

Cowan, J.C.: Water - Formed Scale Deposits, Gulf Publishing Co., Houston, 1976.

Durham, D.K.: "*Equations for Prediction of Scale inhibitor Return after Squeeze Treatment*", Paper SPE presented at the 1983 California Regional Meeting held in Ventura, California, March 23-25, 1983.

Flow Assurance Scale Team (FAST) Manual, Institute of Petroleum Engineering, Heriot-Watt University, 2008.

Funkhouser, G.P. and Gdanski, R.D.: "*Improved Adsorption-Isotherm Modelling for Phosphonate Scale Inhibitors*", Proceedings of the NIF International Oilfield Chemistry Symposium, Geilo, Norway, 1-4 April 2001.

Gdanski, R.D. and Funkhouser, G.P.: "*Mineralogy Driven Scale Inhibitor Squeeze Designs*", Paper SPE 94510 presented at the SPE European Formation Damage Conference held in Scheveningen, The Netherlands, 25-27 May 2005.

Gdanski, R.D. and Funkhouser, G.P.: "*Successful Model of the Kinetic release of a Phosphonate Scale Inhibitor*", Presented at the 2001 NIF International Oil Field Chemistry Symposium, Geilo, Norway, April 1-4, 2001.

Gdanski, R.D.: "*Formation Mineralogy Impacts Scale Inhibitor Squeeze Designs*", presented at the 2008 SPE Europec/EAGE Annual Conference and Exhibition held in Rome, Italy, 9-12 June 2008.

Goulding, P.S.: "*Formation Damage Arising from Barium Sulphate Scale Precipitation*", PhD thesis, Heriot-Watt University, Edinburgh, 1987.

Graham G. M., Sorbie, K. S. and Littlehales I.: "*The Accurate Detection and Assay of Oilfield Scale Inhibitors in Real Field Brines*," presented at the conference *Water Management Offshore* Organised by IBC Ltd, Marriott Hotel, Dyce, Aberdeen, 6-7 October, 1993.

Graham G. M., Sorbie, K. S., Boak, L. S., Taylor, K. and Blilie, L.A.: "*Development and Application of Accurate Detection and Assay Techniques for Oilfield Scale Inhibitors in Produced Water Samples*," SPE No. 28997, presented at the SPE International Symposium on Oilfield Chemistry, San Antonio, Texas. 14-17 February, 1994.

Graham G. M., Sorbie, K. S., Boak, L. S.: "*Development of Accurate Assay Techniques for Poly Vinyl Sulphonate (PVS) and Sulphonated Co-polymer (VS-Co) Oilfield Scale Inhibitors*," presented at NIF 6th International Oil Field Chemical Symposium, Geilo, Norway, 19-22 March, 1995.

Graham G.M., Sorbie, K.S., Johnston*, A. and Boak, L.S.: "*Complete Chemical Analysis of Produced Water by Modern Inductively Coupled Plasma Spectroscopy*

(ICP)," presented at NIF 7th International Oil Field Chemical Symposium, Geilo, Norway, 17-20 March, 1996.* Nalco Exxon Energy Chemicals.

Gregg, S.J.: The Surface Chemistry of Solids, Second Edition, Chapman & Hall Ltd., London, 1965.

Hong, S.A. and Shuler, P.J. : "*A Mathematical Model for the Scale Inhibitor Squeeze Process*," SPE16263, SPE (Production Engineering), pp.957-607, November 1998.

Hong, S.A. and Shuler, P.J.: "*A Mathematical Model for the Scale Inhibitor Squeeze Process*", SPE16263, presented at the SPE International Symposium on Oilfield Chemistry, San Antonio, TX, 4-6 February 1987.

http://www.pet.hw.ac.uk/cesem/intro.htm

Hughes, C.T. and Whittinghan, K.P.: "*The Selection of Scale Inhibitors for the Forties Field*", Paper EUR313 presented at the European Petroleum Conference held in London, England, October 25-28, 1982.

Iler, R.K.: The chemistry of Silica, A Wiley - Interscience Publication, New York, p.659, 1979.

Jakobsen, S.R., Read, P.A. and Schmidt, S.: "*Extended Scale Inhibitor Squeeze Life in pH Sensitive Sandstone Cores*", UK Corrosion 89, Blackpool, November 8-10, 1989.

Johnson, K.S.: "*Water Scaling Problems in the Oil Production Industry*", presented at the Symposium on Chemicals in Oil Industry, Royal Society of Chemistry Industrial Division, North West Region, Manchester, 1983.

Jordan M. M., Sorbie, K. S., Marulier, M. F., Taylor, K., Hourston, K. and Griffin, P.: "*Implication of Produced Water Chemistry and Formation Mineralogy on Inhibitor Adsorption/Desorption in Reservoir Sandstone and their Importance in the Correct Selection of Scale Squeeze Chemicals*." Presented at the 6th International Symposium on Chemistry in the Oil Industry, Ambleside, Cumbria, UK, 14th - 17th April, 1997.

Jordan M.M., Sorbie, K.S., Marulier, M.F., Taylor, K., Hourston, K. and Griffin, P.: "*Implication of Produced Water Chemistry and Formation Mineralogy on Inhibitor Adsorption/Desorption in Reservoir Sandstone and their Importance in the Correct Selection of Scale Squeeze Chemicals*." Presented at the 6th International Symposium on Chemistry in the Oil Industry, Ambleside, Cumbria, UK, 14th – 17th April 1997.

Jordan, M.M, Sorbie, K.S, Chen, P, Armitage, P, Hammond P and, Taylor, K.: "*The Design of Polymer and Phosphonate Scale Inhibitor Precipitation Treatments and the Importance of Precipitate Solubility in Extending Squeeze Lifetime*", SPE37275 presented at the SPE International Symposium on Oilfield Chemistry, Houston Texas, 18-21 February 1997.

JY Ultrace 138 ICP-OES Instruction Manual

Kahrwad, M., Sorbie, K.S. and Boak, L.S.: "*Coupled Adsorption/Precipitation of Scale Inhibitors: Experimental Results and Modelling*," SPE 114108, presented at the SPE International Oilfield Scale Conference, Aberdeen, UK, 28-29 May 2008.

Kan, A. T., Cao, X., Yan, X., Oddo, J.E. and Tomson, M.B.: "*The Transport of Chemical Scale Inhibitors and its Importance to the squeeze Procedure*", Paper No. 33 presented at the NACE Annual Conference and Corrosion Show held in Nashville, Tennessee, April 27-May 1, 1992.

Kan, A. T., Yan, L., Bedient, P.B., Oddo, J.E. and Tomson, M.B.: "*Sorption and Fate of Phosphonate Scale Inhibitors in the Sandstone Reservoir*", Paper SPE 21714 presented at the Production Operation Symposium held in Oklahoma, April 7-9, 1991.

Kan, A.T., Varughese, K. and Tomson, M. B.: "*Determination of Low Concentrations of Phosphonates in Brines*," SPE 21006, presented at the SPE International Symposium on Oilfield Chemistry, Anaheim, 20-22 February, 1991.

Kerver, J .K. and Morgan , F.A.: "*Corrosion Inhibitor Squeeze Technique: Laboratory Adsorption – Desorption Studies*", Journal of Materials Protection, July, 1965 P69 -77.

Kerver, J.K. and Heilhecker, J.K.: "*Scale Inhibition by the Squeeze Technique*", Journal of Canadian Petroleum Technology, 8, No. 1, pp. 15-23, January–March, 1969.

King, G.E. and Skillman, H.L. and Herring, G.D.: "*Control of Formation Damage at Prudhoe Bay, Alaska by Inhibitor Squeeze Treatment*", SPE12472, Journal Technology, pp.1019-1034, June 1985.

King, G.E. and Warden, S.L.: "*Introductory Work In Scale Inhibitor Squeeze Performance : Core Tests and Field results*", SPE18485, presented at the SPE International Symposium on Oilfield Chemistry, Houston, TX, 8-10 February 1989.

Lawless, T. A., Bourne, H. M., Heath, S. and Smith, R. N.: "*Rock/Fluid Interactions and Resulting Phase Behavior Considerations for the Scale Inhibitor Squeeze Design of Carbonate Fields*". Paper No. 53, presented at NACE Annual Conference and Corrosion Show, Baltimore, Maryland, 27th February - 4th March, 1994.

Lecourtier, J., Lee, L.T. and Chauveteau, G.: "*Adsorption of Polyacrylamides on Siliceous Mineral*", Journal of Colloid and Interface Science, vol. 47, 1990, pp.219-231.

Malandrino, A., Yuan, M.D., Sorbie, K.S. and Jordan, M.M. : "*Mechanistic Study and Modelling Of Precipitation Scale Inhibitor Squeeze Processes*", SPE29001, Proceedings of the SPE International Symposium on Oilfield Chemistry, San Antonio, TX, 14-17 February 1995.

Malvern Master Sizer MS-20 Instruction Manual

Matthews, R.R and Carlberg, B.L.: "*Scale Control Technology - A Review*", paper for 22nd Annual S.W. Petroleum Short Course, pp. 263-270, Labbok, Texas, 17-18 April, 1975.

Mazzolini, E., Bertrro, L. and Truefitt: "*Scale Prediction and Laboratory Evaluation of BaSO4 Scale Inhibitors for Seawater Flood in High Barium Environment*", SPE20894 presented at Europec 90, Hague, Netherlands, 22-24 October 1990.

McTeir, M. D. K., Ravenscroft, P. D. and Rudkin, C.: "*Modified Methods for the Determination of Polyacrylic/Phosphinopolycarboxylic Acid and Polyvinylsulphonic acid Scale Inhibitors in Oilfield Brines*," SPE 25160, presented at the SPE International Symposium on Oilfield Chemistry, New Orleans, LA, 2-5 March, 1993.

Meyers, K.O., Skillman, H.J. and Herring, G.D.: "*Control of Formation Damage at Prudhoe Bay, Alaska, by Inhibitor Squeeze Treatment*", SPE12472, Journal of Petroleum Technology, pp. 1019-1034, June 1985.

Miles, L.: "*New Well Treatment Inhibits Scale*", Oil and Gas Journal, pp. 96-99, June 1970.

MSDS from Rhodia.

Olson, J.B, Moore, D.C and Holland-Jones, N.: "*A Temperature Activated Extended Lifetime Scale Inhibitor Squeeze System*", paper No. 25 presented at the NACE Annual Conference, Nashville, TN, April 27 - May 1, 1992.

Pardue, J.E.: "*A New Scale Inhibitor for Scale Squeeze Applications*", Paper SPE21023 presented at the SPE International Symposium on Oilfield Chemistry, Anaheim, CA, 20-22 February 1991.

Pardue, J.E.: "*Results of Field Tests with a New Extended Squeeze Life Scale Inhibitor*", Paper No. 35 presented at the NACE Annual Conference and Corrosion Show held in Nashville, Tennessee, April 27-May 1, 1992.

Patton; Oilfield Water System 2nd Edition, 1977.

Payne, G.E.: "*A History of Downhole Scale Inhibition by Squeeze Treatments*", SPE 16539/1, presented at Offshore at Offshore Europe 87, Aberdeen, 8-11 September, 1987.

Pennington, J.: "*An Overview of Alternative Approaches to the Development of Monitoring Methods for Scale Inhibitors in Oil-Field Produced Waters*," Proceedings of

the 3rd International Symposium *Chemicals in the Oil Industry,* University of Manchester, 19-20 April, 1988.

Philips XL30 ESEM Instruction Manual

Poetker, R.G. and Stone, J.D.: "*Squeeze Inhibitor into Formation*", Petroleum Engineering, 1956, 28, No. 5, B-29.

Przybylinski, J.L.: "*Adsorption and Desorption Characteristic of Mineral Scale Inhibitors as related to the Design of Squeeze Treatment*," SPE 18486 presented at the 1989 SPE International Symposium on Oil-Field Chemistry, Houston, TX, 8-10 February, 1989.

Pucknell, J.: "*Oilfield Scale*", PhD thesis, Heriot-Watt University, Edinburgh, 1983.

Ray, J.M. and Fielde, M.: "*Downhole Scale Inhibition in the Beatrice Field*", Paper presented at the 3rd International Symposium on Chemicals in the Oil Industry, Royal Society of Chemistry Industrial Division, North West Region, Manchester, 19-20 April 1988.

Rogers, L.A., Varughese, K., Prestwich, S.M., Waggett, G.G., Salimi, M.H., Oddo, J.E, Street Jr., E.H. and Tomson, M.B.: "*Use of Inhibitors for Scale Control in Brine Producing Gas and Oil Well*", Journal of SPE Production Engineering, February 1990, 77-82.

Shaughnessy, C.M. and Kelly, W.E: "*EDTA Removes Formation Damage at Prudhoe Bay*", Journal of Petroleum Engineering, pp. 1783-1791, October, 1983.

Smith, C.F., Nolan III, T.J. and Crenshaw, P.L.: "*Removal and Inhibition of Calcium Sulphate Scale in Waterflood Project*", Journal of Petroleum Technology, pp. 1249-1256, November, 1968.

Smith, F.W.: "*Ion-Exchange Conditioning of Sandstones for Chemical Flooding*", Journal of Petroleum Technology, June, 1978.

Sorbie – personal communication, June 2011.

Sorbie, K. S., Yuan, M. D., Graham, G. M. and Todd, A. C.: "*Appropriate Laboratory Evaluation of Oilfield Scale Inhibitors*," presented at Advances in Solving Oilfield Scaling Problems, Organised by IBC Ltd, Aberdeen, 7-8 October 1992.

Sorbie, K.S, Todd, A.C., Thornton, A.R. and Wat, R.M.S.: "*The Interpretation and Theoretical Modelling of Inhibitor/Tracer Corefloods*", Paper SPE 20687 presented at the SPE 65th Annual Technical Conference and Exhibition of the Society of Petroleum Engineers, New Orleans, LA., 23-26 September 1990.

Sorbie, K.S, Wat, R.M.S., Todd, A.C., and McClosky, T.: "*Derivation of Scale Inhibitor Adsorption Isotherms for Oil Reservoir Squeeze Treatments*", paper presented at the 150th Annual Chemical Congress, The Royal Society of Chemistry, at Imperial College, London, 8-11 April 1991.

Sorbie, K.S. and Gdanski, R.D. : "*A Complete Theory of Scale Inhibitor Transport and Adsorption/Desorption in Squeeze Treatments*," SPE 95088, Proceedings of SPE 7th International Symposium on Oilfield Scale, Aberdeen, UK, 11-12 May 2005.

Sorbie, K.S., Jiang, P., Yuan, M.D., Chen, P., Jordan, M. and Todd, A.C.: "*The Effect of pH, Calcium and Temperature on the Adsorption of Phosphonate Inhibitor onto Consolidated and Crushed Sandstone*", Paper SPE 26605 presented at the SPE 68th Annual Technical Conference and Exhibition of the Society of Petroleum Engineers, Houston, Texas, LA, 3-6 October 1993.

Sorbie, K.S., Todd, A.C., Thornton, A.R. and Wat, R.M.S.: "*'The Interpretation and Theoretical Modelling of Inhibitor/Tracer Corefloods*", Paper SPE 20687 presented at the SPE the 65th Annual Technical Conference and Exhibition of the Society of Petroleum Engineers, New Orleans, LA, 23-26 September 1990.

Sorbie, K.S., Todd, A.C., Thornton, A.R. and Wat, R.M.S.: "*The interpretation and Theoretical Modelling of Inhibitor/Tracer Corefloods*", SPE 20687 presented at the 65th Annual Technical Conference and Exhibition of the Society of Petroleum Engineers, New Orleans, L.A. (23-26 September, 1990); SPE (Production Engineering), September 1992.

Sorbie, K.S., Wat, R.M.S. and Todd, A.C. : "*Interpretation and Theoretical Modelling of Scale Inhibitor/Tracer Corefloods,*" SPE (Production Engineering), pp.307-312, August 1992.

Sorbie, K.S., Wat, R.M.S., Todd, A.C. and McClosky, T. : "*Derivation of Scale Inhibitor Adsorption Isotherms for Sandstone Reservoirs*," Royal Society of Chemistry Publication – Chemical in the Oil Industry : Developments and Applications, edited by P.H. Ogden, 1991.

Sorbie, K.S., Yuan, M.D., Chen, P., Todd, A.C. and Wat, R.M.S. : "*The Effect of pH on the Adsorption and Transport of Phosphonate Scale Inhibitor Through Porous Media*," SPE 25165, Proceedings of the SPE International Symposium on Oilfield Chemistry, Anaheim, CA, 20-22 February 1993.

Sorbie, K.S., Yuan, M.D., Chen, P., Todd, A.C., and Wat, R.M.S.: "*The Effect of pH on the Adsorption and Transport of Phosphonate Scale Inhibitor Through Porous Media*", Paper SPE 25165 presented at the SPE International Symposium on Oilfield Chemistry, New Orleans, LA, U.S.A., March 2-5, 1993.

Sorbie, K.S., Yuan, M.D., Jordan, M.M. and Hourston, K.E.: "*Application Of A Scale Inhibitor Squeeze Model to Improve Field Squeeze Treatment Design*", SPE29001, Proceedings of the SPE European Petroleum Conference (Europec 94), London, UK, 25-27 October 1994.

Sorbie, K.S., Yuan, M.D., Todd, A.C., and Wat, R.M.S.: "*The Modelling and Design of Scale Inhibitor Squeeze Treatments in Complex Reservoirs*", Paper SPE 21024 presented at the SPE International Symposium on Oilfield Chemistry, Anaheim, CA, 20-22 February 1991.

Sorbie, K.S.: "*The Improved Design of Scale Inhibitor Squeeze Treatments*", paper presented at the Water Management Offshore Conference, Aberdeen, UK, UK, 22-23 October, 1991.

Sorbie, K.S.: "*A Genenal Coupled Kinetic Adsorption/Precipitation Transport Model for Scale Inhibitor Retention in Porous Media: I. Model Formulation*", SPE 130702, presented at the SPE International Conference on Oilfield Scale, Aberdeen, UK, 26-27 2010.

Tomson, M.B. and Rogers, L.A.: "*Use of Inhibitor for Scale Control in Brine Producing Gas and Oil Wells*", Paper SPE presented at the 61st Annual Technical Conference and Exhibition of the SPE 1986, New Orleans, LA, October 5-8, 1986.

Vazquez, O., Sorbie, K.S. and Mackay, E.J.: "*A General Coupled Kinetic Adsorption/Precipitation Transport Model for Scale Inhibitor Retention in Porous Media: II. Sensitivity Calculations and Field Predictions*", presented at the SPE International Conference on Oilfield Scale, Aberdeen, UK, 26-27 2010.

Vetter, O.J., Kandarpa, V., Schalge, A.L., Stration, M. and Veith, E.: "*Test and Evaluation Methodology for Scale Inhibitor Evaluations*", Paper SPE16295 presented at the SPE International Symposium on Oilfield Chemistry held in San Antonio, TX, February 4-6, 1987.

Vetter, O.J., Kandarpa, V.: "*Scale Inhibitor Evaluation for Oilfield and Geothermal Operation*", Paper SPE7846 presented at the 1979 SPE of AIME International Symposium on Oilfield and Geothermal Chemistry held in Houston, TX, January 22-24, 1979.

Vetter, O.J.: "*An Evaluation of Scale Inhibitors*", Journal of Petroleum Technology, August 1972.

Vetter, O.J.: "*How Barium Sulphate is Formed: An Interpretation*", Journal of Petroleum Technology, pp. 1515-1524, December 1975.

Vetter, O.J.: "*Oilfield Scale - Can We Handle It?*", Journal of Petroleum Technology, pp. 1402-1408, December 1976.

Vetter, O.J.: "*The Chemical Squeeze Process- Some New Information on Some Old Misconception*", SPE3544, Journal of Petroleum Technology, pp. 339-353, March, 1973.

Wat, R.M.S., Montgomery, H.T.R., Maclean, A.F. and Bland, I.D.: "*Squeeze Application Using a Polymer Scale Inhibitor – A Case History*", Presented at the 4th International Oilfield Chemical Symposium, Geilo, Norway, 18 – 21 April 1993.

Walter, G.L.: Water analysis Handbook, Hach Company, Loveland, Colorado, p.651, 1989.

Yuan, M.D., Sorbie, K. S.. Todd, A. C., Atkinson, L. M., Riley, H. and Gurden, S.: "*The Modeling of Adsorption and Precipitation Scale Inhibitor Squeeze Treatments in North Sea Fields*", SPE25165, presented at the SPE International Symposium on Oilfield Chemistry, New Orleans, LA, 3-5 March 1993.

Yuan, M.D.: "*Prediction of Sulphate Scaling Tendency and Investigation of Barium and Strontium Sulphate Solid Solution Scale Formation*", PhD thesis, Heriot-Watt University, Edinburgh, 1989.

Zhang, H., Mackay, E.J., Chen, P. and Sorbie, K.S. : "*Non-Equilibrium Adsorption and Precipitation of Scale Inhibitors : Corefloods and Mathematical Modelling*," SPE 64755, Proceedings of the SPE International Oil Conference and Exhibition, Beijing, China, 7-10 November 2000.